Ph.D. thesis

M-theory Perspectives on Codimension-2 Defects

Hironori Mori*

Department of Physics, Graduate School of Science, Osaka University,
Toyonaka, Osaka 560-0043, Japan

*hiromori@het.phys.sci.osaka-u.ac.jp

Abstract

In this thesis, we investigate a codimension-two defect in the supersymmetric gauge theory. The codimension-two defect is a sort of a non-local operator which has significant role to disclose various aspects in quantum field theory. The characters of this class of non-local defects are not largely uncovered in spite of many efforts to address this object. On the other hand, it has been developed that a wide variety of supersymmetric gauge theories can be descended from the six-dimensional superconformal field theory that is engineered by M-theory. The six-dimensional theory of our interest contains a self-dual string as a physical object. The specific model of the self-dual string was recently proposed as M-strings as an attempt to directly measure physical spectra in the six-dimensional theory. We mainly explore the origin of the codimension-two defect in the standpoint of M-strings and propose that such a defect can be appropriately constructed by introducing an extra M5-brane intersected with the original M5-branes in which M-strings reside. We provide strong supports for our formation of the defect by evaluating its contribution using the exact calculation scheme called the topological vertex and the elliptic genus.

Contents

1 Introduction

In high energy physics, the fundamental and essential tool is quantum field theory which has been brought to us great knowledge about the real world represented by the standard model. It also manifests powerful applications to nuclear physics and condensed matter physics, and shows novel interactions with a wide range of mathematics. Quantum field theory is built essentially by integrating the Poincaré symmetry, translations and rotations in space-time, with a few axioms (e.g. Wightman axioms and the gauge principle) and possibly internal symmetries called global (flavor) symmetries. It has been found out that, assuming the existence of a physical S-matrix, there is only one allowed extension of internal symmetries named *supersymmetry* which describes the transformation exchanging bosons and fermions. Remarkably, this is incorporated with the Poincaré symmetry in the sense that the supersymmetry algebra is closed with the Poincaré symmetry. Also, this symmetry has potential for solving long standing problems in the standard model (e.g. the naturalness problem and the unification of the gauge couplings). Further, we often encounter *conformal symmetry* under which physics enjoys the scale invariance as well as translations and rotations. The famous example equipped with conformal symmetry is a theory at the fixed point of the renormalization group (RG) flow, and a conformal field theory (CFT) could, for instance, describe critical phenomena. The integration of supersymmetry and conformal symmetry is progressing as superconformal symmetry which has been beautifully classified in [1] and can exist maximally up to six-dimensional space-time. Lately, it has been advanced that the six-dimensional superconformal field theory (SCFT) can originate a variety of quantum field theories in lower dimensions, hence, it may be regarded as the "mother" theory of quantum field theory. However, in fact, the standard notion for particle physics appears to be useless towards the six-dimensional SCFT, which will be mentioned below. To reveal the much deeper ranges of quantum field theory, we would like to study this theory using not only standard local objects but also *non-local* extended ones.

There do exist some areas in quantum field theory which we cannot simply address with ordinary local operators as elementary objects. For such a situation, non-local operators or defects play a significant role to uncover a number of the properties of quantum field theory, e.g. we can distinguish the phases in terms of their expectation values, particular spectra can be read from them, and they would give us pieces of evidence for nontrivial dualities. A representative of non-local operators is a Wilson line operator in gauge theories which can be viewed as a world-line of heavy charged particles and has a variety of applications. This is standardly defined by a gauge field A in the form

$$W_{\mathbf{R}}(\gamma) = \mathrm{Tr}_{\mathbf{R}} \mathcal{P} \exp\left(i \oint_{\gamma} A \right), \tag{1.1}$$

where $\mathbf{R}$ is a representation of a gauge group, and γ represents a certain path. This belongs to a class of "electric" operators where operators can be comprised of fundamental fields in the theory. There are counterparts which cannot be defined by elementary fields, phrased as "magnetic" operators, and behave as defects in space-time. For the case of line operators, a magnetic one is called a 't Hooft line. The expectation value of a Wilson and 't Hooft line in four dimensions, for instance, work as order parameters to parameterize the phases,

$$\begin{aligned} &\text{Area law in a Wilson line} &&\longleftrightarrow &&\text{confining phase,} \\ &\text{Area law in a 't Hooft line} &&\longleftrightarrow &&\text{Higgs phase.} \end{aligned}$$

The non-local operators are mainly classified by dimension of their support, or equivalently, codimension. We would use the latter concept in this paper since it is rather ubiquitous. When an operator has a n-dimensional support in D-dimensional space-time, we state it as an operator of codimension-d such that[1]

$$d = D - n. \tag{1.2}$$

For $D = 4$, from the codimension point of view, non-local operators are sorted as follows.

- codimension-4: usual local operators supported at a point.
- codimension-3: line operators, i.e. Wilson lines and 't Hooft lines.
- codimension-2: surface defects.
- codimension-1: domain walls, interfaces, and boundaries.

In this list, a surface defect is rather special since its codimension and dimension are the same, $d = n = 2$, which implies that the electric definition of the defect is completely dual to the magnetic one. Note that we do not mind distinction between the notions "defect" and "operator," and consistently using the former in this paper. Modern perspectives on the surface defect have been initiated in [2, 3], just as for the 't Hooft line, by studying the boundary conditions of elementary fields approaching near the defect. Then, the properties of the surface defect have been investigated through the AdS/CFT correspondence [4, 5, 6, 7, 8]. With these developments, the defect could be used as a powerful tool to test various dualities, e.g. the Alday-Gaiotto-Tachikawa (AGT) correspondence [9, 10]. Also, there are some attempts to formulate the geometrical method via knowledge carried by the defect for computing the BPS spectra of the bulk theory even if the Lagrangian description is not active for this theory [11, 12, 13, 14]. Recently, it was established for some cases [15] that

[1] In mathematical terminology, if a submanifold $\mathcal{M}$ of the D-dimensional manifold satisfies $d = D - \dim \mathcal{M}$, we say that $\mathcal{M}$ is a submanifold of codimension-d.

the contributions of the surface defect to the partition function can be evaluated in the exact way called the supersymmetric localization [16, 17, 18]. Nevertheless, many aspects of the surface defect have been not yet uncovered, e.g. its part as an order parameter is absolutely mysterious (but a suggestion were made in [19] from a geometrical viewpoint via AdS/CFT). Generically speaking, it is challenging to understand codimension-2 defects in diverse dimensions even until now. We would like to investigate this class of non-local defects in supersymmetric gauge theories.

Although a vast amount of success has been accumulated in the framework of quantum field theory, unifying quantum gravity is far from completion. The remarkable candidate to naturally integrate gravity is superstring theory in ten-dimensional space-time. There are five types of string theory allowed by theoretical consistency with physical requirements, and later it has been found [20, 21] that these five theories may be incorporated into so-called M-theory in eleven-dimensional space-time. Thus, M-theory moves into the center of attention from its discovery as the ultimate theory including quantum field theory and quantum gravity. In M-theory, we have two kinds of physical extended objects called a M2-brane and a M5-brane which have the three-dimensional and six-dimensional world-volume, respectively, and produce various extended objects termed D-branes in addition to a fundamental string in string theory. In order to understand these objects, it is relevant and necessary to find out what quantum field theories should be induced as the world-volume theories on these branes. For multiple N M2-branes, it has been suggested that the world-volume theory is possibly described by the Chen-Simons-matter theory with the $\mathrm{U}(N)_k \times \mathrm{U}(N)_{-k}$ gauge symmetry a.k.a the ABJM theory [22], where k is a Chern-Simons level. This theory is actually inherent in desired properties which the M2-brane should have.

On the other hand, the world-volume theory on multiple M5-branes has been found out to be the six-dimensional $\mathcal{N} = (2, 0)$ SCFT [23]. $\mathcal{N} = (2, 0)$ means that this theory has the maximal number, 16, of supercharges in the field theory. This can be also realized as the world-volume theory on D5-branes (six-dimensional extended objects) at the tip of ADE-type singularities in type IIB string theory [24]. This theory is described by self-dual tensionless strings [25] as physical degrees of freedom, which are originated from the boundary of the M2-brane ending on these M5-branes in M-theory. However, though the ABJM theory has been well studied, the details of the six-dimensional $(2, 0)$ SCFT are unknown mainly because it is quite hard to analyse directly the self-dual tensionless string. More precisely, there are several works to suggest the action [26, 27, 28] and equations of motion [29, 30] for the Abelian $(2, 0)$ theory (i.e. on a single M5-brane)[2], whereas even the Lagrangian description for non-Abelian $(2, 0)$ theories (i.e. on multiple M5-branes) is not found.

There is an idea to approach the six-dimensional $(2, 0)$ theory; one lets the self-dual string

[2]Recently, the Witten index of the six-dimensional $(2, 0)$ SCFT was directly computed in [31].

have small tension by separating M5-branes in one direction and extending M2-branes on that direction. The self-dual strings deformed in this way were proposed recently as M-strings [32, 33] drawn as the torus on the M5-brane in Figure 1(a). They originally studied M-strings compactified on a torus (Figure 1(a)) and really found that the partition function of M-strings could be computed by the so-called topological vertex [34, 35, 36] (indirect but rather easy to compute) and the elliptic genus [37, 38, 39] (direct but somewhat complicated). The former has been constructed as a computational tool in the topological string theory [40] and shown to be applicable to BPS state counting problems in supersymmetric gauge theories. The latter provides a quantity to capture information from the world-sheet description of M-strings. We will see how they work on the M-strings in Section 4.

Our main focus in this thesis is a codimension-2 defect in the six-dimensional $(2,0)$ theory from the M-strings point of view. Since the branes in M-theory can be intersected with each other, several types of non-local defects supported on such intersecting subspaces should be naturally defined in this theory. There are lots of developments to understand a codimension-4 defect (surface defect) in six-dimensional SCFTs associated with M-theory, e.g. [41, 42, 43, 44, 45, 46, 47, 48, 49, 50], but a codimension-2 defect may hold a more relevant role then the codimension-4 one in the context of M-strings. This is because the codimension-2 defect in the $(2,0)$ theory is only realized on the intersection of different M5-branes where the M2-branes can end on both of them. M-strings as the boundaries of these M2-branes do not exist in the $(2,0)$ theory without the defect, thus, it is expected that these M-strings carry extra degrees of freedom, which is one of our motivations. There is few attempt towards the codimension-2 defect, and this direction is highly challenging but much relevant to comprehend profound aspects of M-theory. As a conclusion in this paper, we propose the M-string configuration with an extra M5-brane (M5$'$) intersected with the original M5-brane from which the codimension-2 defect is engineered, as shown in Figure 1(b). We show that the partition function of M-strings in the presence of M5$'$ can be evaluated by the topological vertex formalism and actually contains the contribution of the defect given by a elliptic theta function as expected. This result can be confirmed from the independent calculation of the elliptic genus with additional matters. Further, based on these results, we are trying to reproduce the partition function with a codimension-2 defect directly from the framework of the open topological vertex that is still not well formulated.

The organization of the paper is as follows. In Section 2, we would collect and review shortly present knowledge for a class of codimension-2 defects in four-dimensional supersymmetric gauge theories. We prepare a basic concept and setup of M-strings in Section 3. Then, we perform how to compute the partition function of M-strings from the topological vertex and the elliptic genus in Section 4. Also, we would show the equivalence of these schemes with the simplest example. In Section 5, we explain our main result as shown in

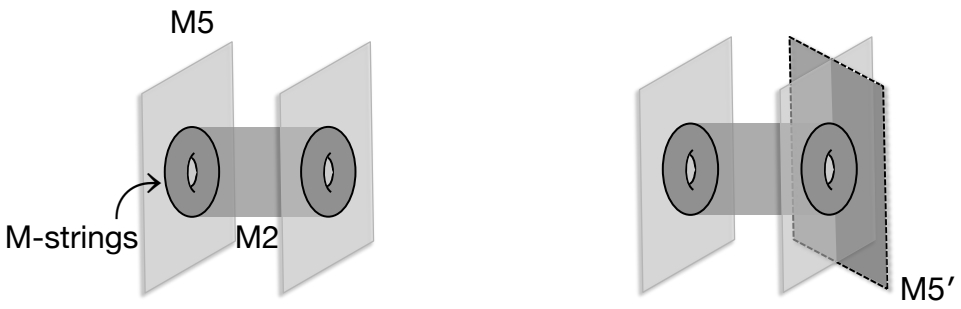

(a) M-strings without a defect

(b) M-strings with a defect

Figure 1: Our proposal for a codimension-2 defect in M-strings. (a) M-strings compactified to a torus on M5-branes which constructed in the original context [32, 33]. (b) the insertion of an extra M5-brane (M5′) to engineer a codimension-2 defect in the six-dimensional theory.

Figure 1(b). The previous two methods are still applicable and give the same answer under a suitable identification of parameters. Section 6 will be devoted to evaluate the partition function of our M-strings by directly using the open topological string and present a preliminary result. We are closing this thesis with small comments for future works in Section 7. There are three appendices to package mathematical ingredients and technical details. The convention and analysis formulae are aligned in Appendix A. The formulations and basics for the usage of the topological vertex are provided in Appendix B. Finally, Appendix C contains calculations which are skipped in the main context.

2 Surface defects in four dimensions

In this section, we would much briefly review recent developments on 4d supersymmetric gauge theories in the presence of a codimension-2 defect, i.e. a surface defect, and prepare ideas which will be applied to deriving our main result on the codimension-2 defect in Section 5. Those who would like to know more advanced topics on the surface defect are asked to read a beneficial review [19].

2.1 Current classifications

It has been found in recent studies that surface defects can be constructed in several seemingly distinct ways. The current status for them are classified as follows.

- Singular boundary conditions near the defect: The defect is basically defined as giving matter fields a specific singular behavior as approaching to it. For example, if a surface defect is located at $z = 0$, where z is a complex coordinate in $\mathbb{R}^4$, a scalar field ϕ becomes

singular as

$$\phi(z) \sim \frac{1}{z}. \tag{2.1}$$

The surface defect described by this is often referred to as a Gukov-Witten defect [2], and there are a variety of works by relying on this definition, e.g. [5, 3, 6, 7, 8, 51].

- The 2d-4d coupled system: we can consider two-dimensional degrees of freedom excited on the surface defect [52]. This 2d theory is just coupled to a 4d bulk theory, and a gauge symmetry in four dimensions should be seen as a global symmetry from the view of the 2d theory localized on the defect. A particular example is called a vortex [53, 12] as a solitonic object. Recently, another system could be investigated by means of a superconformal index [54].

- Renormalization group flow construction: given some matter field in the ultraviolet (UV) region, let its expectation value have a nontrivial spacial dependence. This expectation value triggers off a RG flow, and in the infrared (IR) scale, a defect really arises depending on the expectation value of the matter [15]. One can find great advancements on this construction, e.g. [55, 56, 57, 58, 59].

- Geometric engineering by inserting extra D-branes: it is natural to explore counterparts of surface defects in string theory and M-theory. It is naively expected that the defects are realized as the boundaries of D-branes ending on another D-branes or intersecting D-branes with each other in the geometrical way. This standpoint has been vastly tested and utilized to support dualities, e.g. the AGT correspondence [10]. Also, there is an attempt to provide a general prescription of the surface defect from M-theory [60].

These descriptions could be independently developed but actually construct the same surface defect in specific circumstances. The first and second one are considered as fundamentally equivalent in the sense that we obtain a delta function localized on a two-dimensional surface in the path integral when only 2d degrees of freedom are integrated out. Such a delta function imposes a boundary condition such as (2.1) on remaining 4d fields in the path integral. For the third one, since the flux of a vortex would be confined in a tube, we can treat with it as a string-like object and consider a 2d world-sheet theory of this string. This prescription is compatible with the second one. In this thesis, we will concentrate on the fourth point that is suitable for our purpose to discuss a codimension-2 defect in M-theory. We will also give small comments on the connection of this point with others.

2.2 Geometric engineering

The key idea to geometrically engineer the surface defect in this paper is the so-called geometric transition that relates the geometry with a brane additionally inserted into the system. We would explain this in the case of the conifold, the simplest nontrivial example of the Calabi-Yau three-fold (CY3), which is not only the starting point for generalization to other CY3's but also an essential ingredient on our main result derived in Section 5.

2.2.1 Coniforld transition

The conifold. The conifold is defined by the algebraic equation on four complex variables (x, y, u, v) of $\mathbb{C}^4$,

$$xy - uv = 0, \tag{2.2}$$

namely, a complex three-dimensional manifold. To see the topology of the conifold, it is convenient to change the variables such that

$$x = z_1 + iz_2, \qquad y = z_1 - iz_2, \qquad u = z_3 + iz_4, \qquad v = -z_3 + iz_4, \tag{2.3}$$

where $\{z_i\}_{i=1,\cdots 4} \in \mathbb{C}$, then the conifold as an algebraic manifold (2.2) is rewritten as

$$z_1^2 + z_2^2 + z_3^2 + z_4^2 = 0. \tag{2.4}$$

Further, setting $z_i = a_i + ib_i$ with $a_i, b_i \in \mathbb{R}$, the real and imaginary part of this equation become

$$\sum_{i=1}^{4} \left(a_i^2 - b_i^2\right) = 0, \qquad \sum_{i=1}^{4} a_i b_i = 0, \tag{2.5}$$

respectively. The topology that we would like to know can be easily read from those two conditions as follows. If concentrating on the slice given by

$$\sum_{i=1}^{4} \left(a_i^2 + b_i^2\right) = 2r^2, \qquad r \in \mathbb{R}, \tag{2.6}$$

then the first equation of (2.5) says

$$\sum_{i=1}^{4} a_i^2 = \sum_{i=1}^{4} b_i^2 = r^2, \tag{2.7}$$

which means that there are two three-spheres S^3's of the same radius r parametrized by $\{a_i\}$ and $\{b_i\}$. However, one set of them is restricted by imposing the second condition of (2.5). Therefore, $\{a_i\}$ span a three-sphere S^3 of radius r, while $\{b_i\}$ form a two-sphere S^2 because of the constraint (2.5). The slice (2.6) can be thought of as an S^2 fibration over S^3 at fixed

(a) Toric diagram (fiber space)

(b) Web diagram (base space)

Figure 2: The toric diagram and web diagram of the conifold. The set of labels on each top in the toric diagram is toric data which fixes the fiber structure.

r which turns out to be a trivial fibration. Moreover, the conifold shows the singularity at the point of $r = 0$ that is equivalent to $x = y = u = v = 0$ in (2.2). As a consequence, the conifold is described as the cone over $S^2 \times S^3$.

The conifold is a kind of non-compact toric CY3's. The toric geometry actually can be visualised by a toric diagram of the so-called toric data which encodes the structure of a fiber space. In addition, there exists a dual diagram to the toric diagram called the web diagram displaying the structure of a base space. The toric and web diagram of the conifold are shown in Figure 2. The tip of the cone in the conifold is now represented as the intersecting point in the web diagram.

This is as for the generic case where we must relax the singularities of CY3 by appropriately deforming the geometry. There are basically two deformations of the conifold to avoid the singularity which we will review below.

The deformed conifold. The first one is to deform the complex structure of the conifold, which is implemented in (2.2) by

$$xy - uv = \mu^2, \qquad \mu \in \mathbb{R}\backslash\{0\}. \tag{2.8}$$

Through the same reparametrization as above, the defining equations in (2.5) are slightly changed as

$$\sum_{i=1}^{4} \left(a_i^2 - b_i^2\right) = \mu^2, \qquad \sum_{i=1}^{4} a_i b_i = 0. \tag{2.9}$$

In the first condition of (2.9), the variables $\{a_i\}$ satisfy $\sum_{i=1}^4 a_i^2 \geq \mu^2$ for general a_i and b_i. In other words, the sphere of b_i shrinks as long as this inequality is saturated, $\sum_{i=1}^4 a_i^2 = \mu^2$. In addition, it can be shown that the second condition of (2.9) is topologically equal to describing the cotangent bundle T^*S^3 on S^3 of a_i. This geometry by deforming the conifold in the way (2.8) is called the deformed conifold whose topology is T^*S^3.

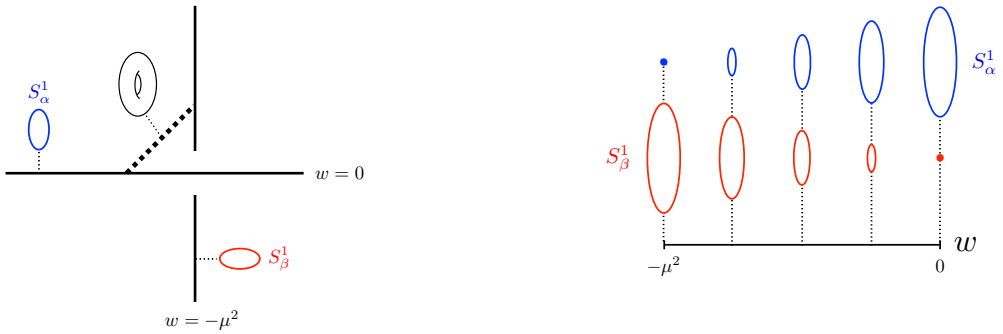

(a) Web diagram

(b) S^3 as an T^2 fibration

Figure 3: The torus fibration of the deformed conifold. The structure of the base space is drawn as (a) in which the dotted interval linking the axises of $w = 0$ and $w = -\mu^2$ is an torus fibration, that is, S^3 as shown in (b).

For our purpose, it is relevant to view the deformed conifold as its torus fibration. Getting back to the definition (2.8), one can immediately see two U(1) isometries denoted as $\mathrm{U}(1)_\alpha \times \mathrm{U}(1)_\beta$ which act on the coordinates as

$$\mathrm{U}(1)_\alpha \times \mathrm{U}(1)_\beta : (x,\, y,\, u,\, v) \mapsto (e^{i\alpha}x,\, e^{-i\alpha}y,\, e^{i\beta}u,\, e^{-i\beta}v). \tag{2.10}$$

These isometries imply that the deformed conifold has a tow-torus T^2 on which the $(0,1)$-cycle S^1_α and $(1,0)$-cycle S^1_β generate the action of $\mathrm{U}(1)_\alpha$ and $\mathrm{U}(1)_\beta$, respectively. We here should mention that the point of $x = y = 0$ is precisely the fixed point for $\mathrm{U}(1)_\alpha$, hence, S^1_α collapses at this point. Similarly, S^1_β collapses at $u = v = 0$. For the former case, the algebraic equation (2.8) is reduced to

$$uv = -\mu^2, \tag{2.11}$$

which describes a cylinder $S^1_\beta \times \mathbb{R}$. For the latter, (2.8) becomes

$$xy = \mu^2, \tag{2.12}$$

which describes another cylinder $S^1_\alpha \times \mathbb{R}$. Equivalently, if we define $w := uv$, $\mathrm{Re}(w)$ corresponds to the real axis $\mathbb{R}$ of the cylinders with the points where the 1-cycles of T^2 collapse,

$$w = -\mu^2 \quad \Leftrightarrow \quad S^1_\alpha \text{ collapses}, \tag{2.13}$$

$$w = 0 \quad \Leftrightarrow \quad S^1_\beta \text{ collapses}. \tag{2.14}$$

There is another real axis of w on which neither S^1_α nor S^1_β shrinks, namely, the torus fibration over the interval $[-\mu^2, 0]$ is realized. This is exactly the torus fibrer expression of S^3 of the

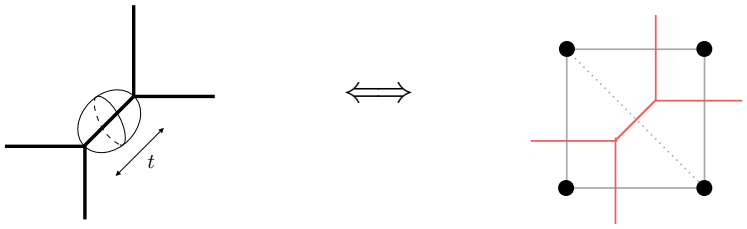

Figure 4: The web diagram of the resolved conifold. The singularity of the conifold is resolved by $\mathbb{C}\mathbf{P}^1$ of size t and related to a triangulation of the toric diagram.

radius μ here just as described in (2.9). Note that this S^3 shrinks to zero size as $\mu \to 0$ to reproduce the conifold (2.2). We sketch the web diagram of the defamed conifold with the torus structure and the torus fibration of S^3 in Figure 3.

The resolved conifold. The second deformation is associated with the Kähler structure of the conifold, and the resultant manifold is termed the resolved conifold. Let us introduce homogeneous complex coordinates (A, B) on $\mathbb{C}\mathbf{P}^1$ of the size t,

$$|A|^2 + |B|^2 = t, \qquad (A, B) \sim (\lambda A, \lambda B), \qquad (A, B) \neq (0, 0) \tag{2.15}$$

with $\lambda \in \mathbb{C}\backslash\{0\}$. We would relate (A, B) with the coordinates of the conifold by

$$Ax + Bv = 0, \qquad Au + By = 0. \tag{2.16}$$

Assuming $x \neq 0$, the first equation can be solved for A and B as

$$A = -\frac{v}{x}B, \tag{2.17}$$

then substituting this into the second equation leads to

$$xy - uv = 0, \tag{2.18}$$

which is absolutely the conifold (2.2). Although the conifold has the conical singularity at all zeros as mentioned above, the manifold defined by the algebraic equation (2.18) equipped with (2.15) can be considered as the resolution of the conifold because any (A, B) are still solutions to (2.16) even at $(x, y, u, v) = (0, 0, 0, 0)$ and consequently this point is blown up by the structure of $\mathbb{C}\mathbf{P}^1 \simeq S^2$ of the size t. That is why this geometry is named the resolved conifold. The web diagram of the resolved conifold is depicted on the left side of Figure 4. We remark that the web diagram of the resolved conifold can be obtained by a triangulation of the toric diagram of the conifold (Figure 2(a)). Given a certain triangulation on the toric diagram, the dual web diagram is produced in the way to draw a line orthogonal to each edge of the triangles. This process is demonstrated on the right side of Figure 4.

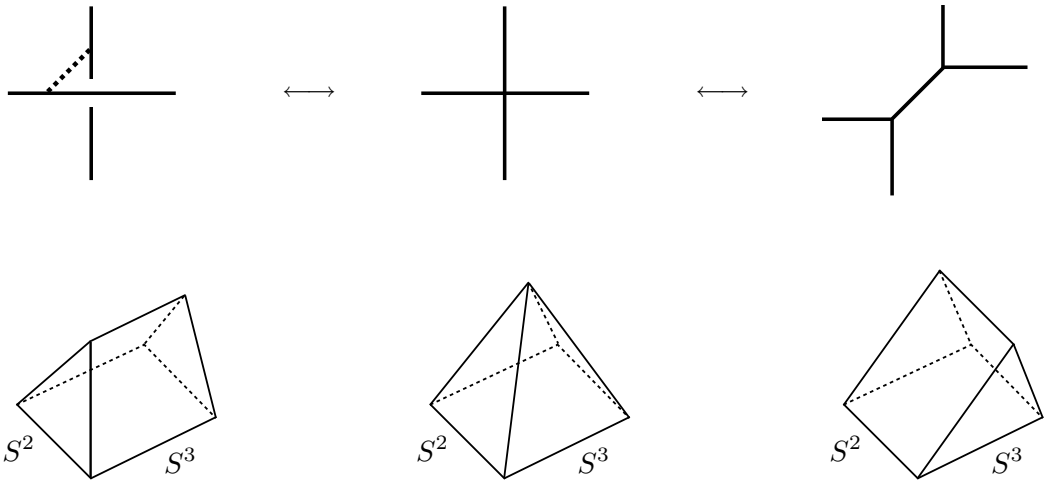

(a) deformed conifold (b) conifold (c) resolved conifold

Figure 5: The geometric transition for the conifold. The bottom line represents an associated topology for each geometry.

The conifold (Figure 5(b)) and its deformations (Figure 5(a) and 5(c)) pass through with each other by tuning the radii μ and t of S^3 and S^2, respectively, which has been originally referred to as the conifold transition [61]. This sequence has been cultivated as the geometric transition [62, 63, 64] in the context of the topological string theory.

2.2.2 Geometric transition in the topological string theory

The topological string theory [40] is a two-dimensional topological field theory on the world-sheet of a fundamental string, which is basically constructed by topological twists for a non-linear sigma model (NLSM) whose target space is CY3[3], and its partition function just counts the BPS states mapped from the string world-sheet onto CY3. There are two types of the topological string theory named A-model and B-model according to twists which make a NLSM topological with preserving supersymmetry. In this paper, our standpoint based on the web diagram is in the framework of the A-model topological string theory.

Since fundamental objects in string theory are a closed string containing gravity and an open string which ends on various D-branes, the topological string theory is formulated for both strings. It has been found [65] that the open topological string theory (i.e the world-sheet of an open string) on T^*S^3, the deformed conifold (Figure 5(a)), is equivalent to the Chern-Simons theory on S^3 with an U(N) gauge group. The dictionary of this correspondence is declared as follows. The string coupling constant g_s in string theory is

[3]This is the case of the superconformal theory.

related to the Chern-Simons level k, the coupling constant in the Chern-Simons theory, as

$$g_s = \frac{2\pi}{k+N}. \tag{2.19}$$

In addition, N corresponds to the number of D-branes wrapped on S^3 because the open string has boundaries on D-branes in the target space. On the other hand, the resolved conifold (Figure 5(b)) plays the target space of the closed topological string theory (i.e the world-sheet of a closed string).

After the establishment of this equivalence and the AdS/CFT correspondence [4], it has been conjectured [63] that the open topological string theory on the deformed conifold is dual to the closed one on the resolved conifold. Recall that the resolved conifold possesses a Kähler parameter t, the size of $\mathbb{C}\mathbf{P}^1$, to resolve the singularity of the conifold. The main statement of this conjecture is given as the relation

$$t = ig_sN \qquad \Leftrightarrow \qquad Q = q^N, \tag{2.20}$$

where $Q := e^t$ and $q := e^{ig_s}$ (in what follows, we will call Q a Kähler factor)[4]. This is geometrically interpreted as the conifold transition (Figure 5), and this duality under the relation (2.20) is referred to as the *geometric transition*, which has been proven in [66, 67]. In other words, the geometric transition couples the open topological string theory to the closed one by operating (2.20) (in this sense, often called the open/closed duality). Note that the closed topological string theory does not include any D-brane, and it appears after the geometric transition. As a result, the geometry describing the closed topological string theory is translated into a physical object, D-brane, in the open topological string theory.

The geometric transition can truly be applied to the general non-compact CY3 in the same manner as on the conifold explained above. For a generic case, a diagonal segment in the web diagram always represents $\mathbb{C}\mathbf{P}^1$ as for the resolved conifold (Figure 5(c)), while S^3 depicted as a dotted line in the deformed conifold (Figure 5(a)) is replaced by a certain 3-cycle called Lagrangian submanifold $\mathcal{L}$ in CY3. This follows on the fact that the boundary conditions keeping supersymmetry in the A-model open topological string are identical with the geometrical conditions for $\mathcal{L}$. Namely, the emergence of $\mathcal{L}$ in a web diagram ensures the existence of N D-branes on which an open string ends. Throughout this paper, we call a thick dotted line presenting $\mathcal{L}$ a Lagrangian brane. There is a case where one CY3 contains several $\mathcal{L}$'s, and specifying one of $\mathcal{L}$'s is represented by inserting a Lagrangian brane to the corresponding edge of the web diagram. Note that no Lagrangian brane is resulted from the geometric transition if $N = 0$, that is, there does not exist any D-brane. In short, we are

[4]More precisely, t is a complexified "area" of $\mathbb{C}\mathbf{P}^1$ whose real part is just a Kähler class and imaginary part is contributed from NSNS B-field. The fact that t becomes pure imaginary upon the geometric transition (2.20) implies that $\mathbb{C}\mathbf{P}^1$ shrinks but a non-zero B-field remains.

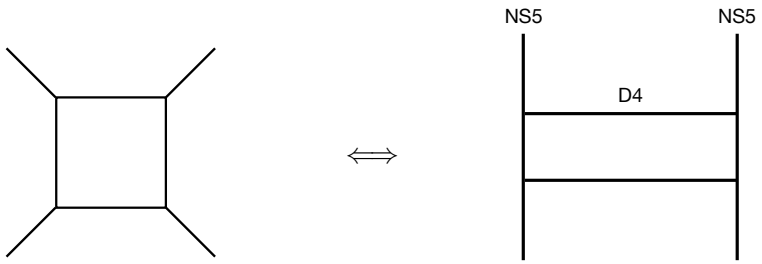

(a) Local $\mathbb{P}^1 \times \mathbb{P}^1$ (b) 4d pure gauge theory

Figure 6: The geometric engineering of the 4d $\mathcal{N} = 2$ pure gauge theory from the local $\mathbb{P}^1 \times \mathbb{P}^1$. This is in a generic point of the Coulomb branch.

working on the A-model open or closed topological string theory when the web diagram with or without a Lagrangian brane, respectively, is focused on.

Generically, if we have the set of diagonal segments attached to the same horizontal line in the web diagram, we can execute the geometric transition by taking the specialization (2.20) simultaneously but with different N_i for each diagonal segment which represents the resolution by $\mathbb{C}\mathbf{P}^1$ of the size t_i (i runs for the number of the associated segments). This situation will be shown in Section 5. In the rest of this section, we would be mainly devoted to providing the connection between the geometric transition and the surface defect.

2.2.3 Defects as Lagrangian branes

It has been proposed [68, 69] that we can geometrically engineer the surface defect as the Lagrangian brane $\mathcal{L}$ that emerges through the geometric transition. We would briefly argue this correspondence in terms of string theory.

An example which we would like to utilize for explanation is an CY3 with the web diagram of Figure 6(a) known as the local $\mathbb{P}^1 \times \mathbb{P}^1$. Remarkably, it has been discovered in [70, 71] based on much complicated discussions associated with mirror symmetry that there does exist the direct interpretation of the geometric data of CY3 expressed by the web diagram into the brane system of string theory, and vice versa. We will rely on this fact in the later sections. In the current case, the web diagram of the local $\mathbb{P}^1 \times \mathbb{P}^1$ can be mapped into the D4-branes ending on NS5-branes (NS is a shorthand for Neveu-Schwarz) in type IIA string theory (Figure 6(b)). This relation allows us to rely highly on the geometric languages to understand the dynamics of string theory. Further, the low energy dynamics on the D4-branes of this brane system generates the 4d $\mathcal{N} = 2$ pure gauge theory in a generic point of the Coulomb branch of the moduli space [72]. Namely, the 4d supersymmetric gauge theory can be engineered by the geometry thanks to the novel correspondence between the

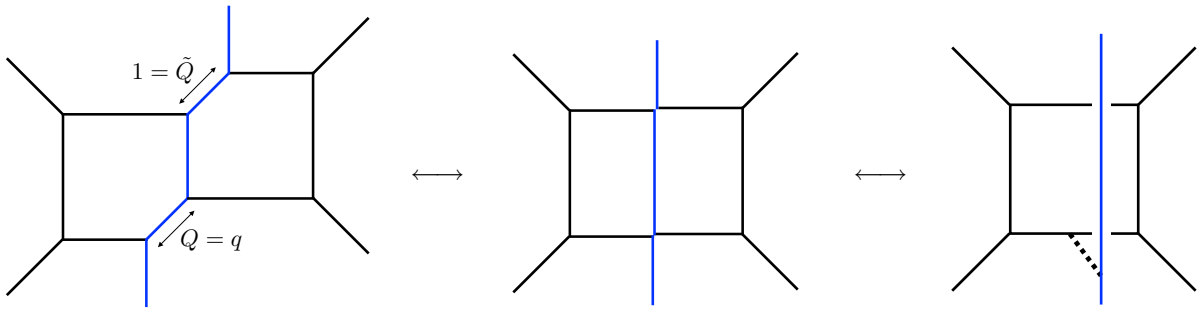

Figure 7: The geometric transition with producing a Lagrangian brane $\mathcal{L}$ (a dotted line on the right side). The middle diagram shows the singular CY3 as for the conifold.

geometry and string theory.

Let us give a rough sketch how the surface defect that particularly preserve part of supersymmetry can be inserted into the 4d theory as the Lagrangian submanifold $\mathcal{L}$ in CY3. We start with a CY3 whose web diagram is given as on the left side of Figure 7. The geometry is resolved by $\mathbb{C}\mathbf{P}^1$'s depicted as the diagonal segments along the center line of this figure in the same manner as for the resolved conifold. Let Q and $\tilde{Q}$ be Kähler factors for them in the lower and upper segment, respectively. We carry out the geometric transition for this geometry as for instance, the Kähler factors are specialized by

$$Q = q, \qquad \tilde{Q} = 1. \tag{2.21}$$

This operation means that a Lagrangian brane $\mathcal{L}$ appears to attach the bottom edge of the local $\mathbb{P}^1 \times \mathbb{P}^1$, but does not on the top edge (on the right side of Figure 7) after the transition. The consequence of the limitation (2.21) is pictorially performed in Figure 7.

Based on the correspondence of Figure 6 between the local $\mathbb{P}^1 \times \mathbb{P}^1$ and the D4-NS5 system, an extra perpendicular line in the middle of the right picture in Figure 7 is also viewed as an extra NS5-brane (NS5$'$), and the appearance of $\mathcal{L}$ is translated into a D2-brane (D2$'$) suspended between the D4-brane and the NS5$'$-brane in the top line of Figure 8. This D2$'$-brane is spanned on a two-dimensional subspace of the world-volume of the D4-brane, and it actually behaves as the surface defect from the viewpoint of the 4d theory on the D4-brane. This is the pictorial prescription to construct the surface defect from purely the geometry via the geometric transition. Moreover, we can consider the limit where the extra perpendicular line in the web diagram of Figure 8(a) is moved away at infinity, correspondingly, the NS5$'$-brane is pushed away at infinity in a certain direction. Then the D2$'$-brane is extending semi-infinitely along this direction. The basic difference between the situation with and without NS5$'$ is as follows. In the type IIA picture, open strings stretched between the D2$'$-brane and D4-brane induces the field theory degrees of freedom

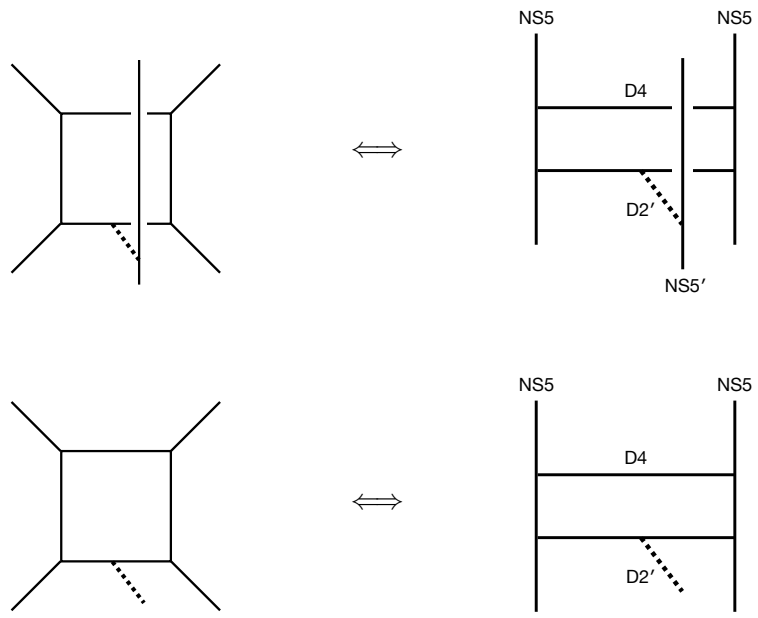

(a) Lagrangian brane (b) D2′ insertion

Figure 8: Lagrangian branes and D2-brane insertions (D2′) with a finite (upper line) and a semi-infinite extent (lower line) corresponding to the different types of surface defects in four dimensions.

on the world-volume of not only the D4-brane but also the D2′-brane. Accordingly, there is effectively a 2d supersymmetric gauge theory at the end of the D2′-brane, and its gauge coupling e^2 is proportional to the finite extent of the D2′-brane along, say, the 7 direction,

$$\frac{1}{e^2} \propto \Delta x^7. \tag{2.22}$$

The semi-infinite D2′-brane in the bottom line of Figure 8 is produced as $\Delta x^7 \to \infty$, which corresponds to the weak coupling limit of the 2d theory. Completing this limit, the effective two-dimensional theory may get superconformal symmetry since the running coupling goes away. The choice of the brane systems in Figure 8 depends on what kind of the surface defect we would like to study, but actually, the difference between them does not become important when we investigate physics independent of the 7 direction that D2′ is extending on. Indeed, the bottom situation in Figure 8 is rather suitable for us because our calculations are in the case of inserting a semi-infinite brane, and the topological vertex (Appendix B) can be straightforwardly applied to compute the partition function of the corresponding gauge theory. In this paper, we would focus on such a situation[5].

We would place brief comments on the relation of the geometric engineering with a vortex

[5]The case of the top in Figure 8 with taking certain limits has been nicely discussed in [69].

string theory. The vortex string is a solitonic object realized as a specific BPS configuration in 4d theories. This has a support of the two-dimensional subspace, and its world-volume theory is know as a 2d supersymmetric gauge theories coupled to the 4d bulk theory [12]. This fact matches with the second perspective in Section 2.1, thus, the vortex is a natural candidate to describe the surface defect. The BPS solution for the vortex actually includes a singular behavior of a gauge field near the vortex, which implies that the vortex may also be compatible with the first perspective in Section 2.1. The analysis for the surface defect in [57] is based on those viewpoints. Further, the brane system corresponding to the geometric transition in Figure 8(b) is essentially identical with the brane construction of the vortex string [12]. In other words, we would think of the vortex string description for the surface defect as the field-theoretic construction of the geometric transition.

2.3 AGT correspondence

2.3.1 Basic statements

The prominent application of the surface defect is in the 2d-4d duality known as the AGT correspondence [9]. It has originally declared relationship between the 4d $\mathcal{N}=2$ SU(2) gauge theory with four flavors and the Liouville CFT on the two-sphere, which is basically found by comparing the instanton partition function [73] of the $\mathcal{N}=2$ theory with the Liouville conformal block. After this breakthrough, it has been revealed by lots of nontrivial tests that this correspondence does hold for a much general class of the $\mathcal{N}=2$ theories called class $\mathcal{S}$ [74] and CFT's on the Riemann surface Σ with several numbers of genera and punctures. The novel point of this correspondence is that the 4d supersymmetric theory is equivalent to the 2d *non-supersymmetric* CFT.

The AGT correspondence is heuristically derived from the 6d $(2,0)$ theory compactified on a Riemann surface Σ and a four-manifold $\mathcal{M}_4 = \mathbb{R}^4_{\epsilon_1,\epsilon_2}$ or $S^4_{\epsilon_1,\epsilon_2}$,

$$\begin{array}{ccc} & \text{6d } (2,0) \text{ theory} & \\ & \text{on } \mathcal{M}_4 \times \Sigma & \\ \swarrow & & \searrow \\ \text{4d } \mathcal{N}=2 \text{ gauge theory} & & \text{2d Liouville CFT} \\ \text{on } \mathcal{M}_4 & & \text{on } \Sigma \end{array} \tag{2.23}$$

where ϵ_1 and ϵ_2 are called Ω-deformation parameters respecting two-dimensional rotations on the planes $\mathbb{R}^2_{\epsilon_1}$ and $\mathbb{R}^2_{\epsilon_2}$,

$$\mathbb{R}^4_{\epsilon_1,\epsilon_2} \simeq \mathbb{R}^2_{\epsilon_1} \times \mathbb{R}^2_{\epsilon_2}. \tag{2.24}$$

Namely, introducing the Ω-deformation parameters breaks the rotational symmetry SO(4) of $\mathbb{R}^4$ into $\mathrm{SO}(2)_{\epsilon_1} \times \mathrm{SO}(2)_{\epsilon_2}$. On the other hand, the Ω-deformation brings the effect to

regularize the divergence from the infinite volume of $\mathbb{R}^4$ so that[6]

$$\mathrm{Vol}\left(\mathbb{R}^4_{\epsilon_1,\epsilon_2}\right) = \int_{\mathbb{R}^4_{\epsilon_1,\epsilon_2}} 1 = \frac{1}{\epsilon_1\epsilon_2}, \qquad \mathrm{Vol}\left(\mathbb{R}^2_{\epsilon_1}\right) = \int_{\mathbb{R}^2_{\epsilon_1}} 1 = \frac{1}{\epsilon_1}. \tag{2.25}$$

In general, the advantage of the Ω-deformation is that we can compute the volume of the Ω-deformed manifold by only using the contributions from the fixed point of symmetries (called the Duistermaat-Heckman fixed point theorem) without struggling the entire integration. This fact lets us derive exactly the Nekrasov instanton partition function [77, 73] that is the volume integral of the instanton moduli space and plays a central role in the AGT correspondence.

Soon after the discovery of the AGT correspondence, non-local operators, i.e Wilson-'t Hooft loops and surface defects, in the 4d supersymmetric gauge theory have been incorporated in this duality [10]. We would focus on the story of the surface defect denoted as $D_{\mathfrak{t}}$ with a parameter $\mathfrak{t}$ which is the combination of the labels used in the Gukov-Witten defect [2][7]. In the original paper [10], the following brane configuration in type IIA string theory has been proposed to construct the surface defect in the AGT correspondence:

	$\overbrace{}^{\mathcal{M}_4}$									
	0	1	2	3	4	5	6	7	8	9
NS5	×	×	×	×	×	×				
D4	×	×	×	×			×			
D2′	×	×						×		

(2.26)

As shown above, the 4d $\mathcal{N} = 2$ gauge theory in question is induced on the 0123 direction of the D4-brane, and the boundary D of the D2′-brane ending on the D4-brane realizes the surface defect in that theory. This D2′-brane on the flat space keeps half of supersymmetry, and after the Ω-deformation, the surface defect as the boundary of D2′ still preserves half of supersymmetry if its support D is extended on a submanifold of $\mathcal{M}_4$ respecting the Ω-deformation, that is, $D = \mathbb{R}^2_{\epsilon_1}$ (or $\mathbb{R}^2_{\epsilon_2}$). With this brane system, they have noticed that the surface defect may be described by a certain vertex operator called the degenerate field $\Phi_{2,1}$ carrying a momentum b in the Liouville CFT,

$$\Phi_{2,1}(z) = e^{-\frac{b}{2}\phi(z)}, \tag{2.27}$$

where z represents its insertion point on Σ. The first expectation of the AGT correspondence has come from the behavior of the instanton partition function Z^{inst} in the semiclassical limit

[6] There is the so-called Duistermaat-Heckman formula [75, 76] to calculate the volume for the symplectic manifolds of even dimensions.

[7] We here do not specify the parameter $\mathfrak{t}$, but basically this parametrizes the breaking pattern of the symmetry initiated by inserting the surface defect.

$\epsilon_1\epsilon_2 \to 0$. This behavior in the presence of the surface defect can be determined from the viewpoint of the brane system (2.26),

$$Z^{\text{inst}} \sim \exp\left[-\frac{\mathcal{F}(a)}{\epsilon_1\epsilon_2} + \frac{\mathcal{W}(a,\mathfrak{t})}{\epsilon_1} + \cdots\right]. \tag{2.28}$$

The coefficient of the leading term is the Seiberg-Witten prepotential [77]. The function $\mathcal{W}(a,\mathfrak{t})$ turns out to be exactly the integral of the Seiberg-Witten differential λ_{SW} over an open path starting from some reference point p_* in the Seiberg-Witten curve,

$$\mathcal{W}(a,\mathfrak{t}) = \int_{p_*}^{p} \lambda_{\text{SW}}, \tag{2.29}$$

where the endpoint p roughly corresponds to $\mathfrak{t}$ characterizing the surface defect in the IR region. On the Liouville CFT side, the corresponding limit on the correlation function with the degenerate field can be directly evaluated as

$$Z^{\text{Liouv}} \sim \exp\left[-\frac{\mathcal{F}(a)}{\hbar^2} + \frac{\mathcal{W}(a,z)}{\hbar b} + \cdots\right], \tag{2.30}$$

where $\hbar$ is a fixed overall scale factor. The form (2.30) in the CFT perfectly agrees with (2.28) on the 4d side under identifications

$$\epsilon_1 = \hbar b, \qquad \epsilon_2 = \hbar/b \tag{2.31}$$

as originally stated in [9]. This observation strongly supports the AGT correspondence with the surface defect. We should remark that the function $\mathcal{W}(a,\mathfrak{t})$ (or $\mathcal{W}(a,z)$) cannot be seen unless the surface defect (or the degenerate field) is inserted. The emergence of this function is really a specific consequence to consider the surface defect. We shortly write down the dictionary of the AGT correspondence including the surface defect in the Table 1.

We note that there precisely are the higher-dimensional generalizations of the AGT correspondence: the 5d supersymmetric gauge theories and the theories of the q-deformed Virasoro algebra [78, 79]: the 6d supersymmetric gauge theories and the theories of the elliptic-deformed Virasoro algebra [80, 81].

2.3.2 Construction via the geometric transition

Indeed, the brane configuration in type IIA string theory (2.26) proposed for the AGT correspondence with the surface defect is identical with the brane system of Figure 8 to engineer the surface defect by the geometric transition. It has been actually pointed out [68, 69, 82, 83, 84] that there is a class of the AGT correspondence in the presence of the surface defect which can be derived in the framework of the geometric transition explained in the previous subsection. We would show a simple example of this statement.

$\mathcal{N}=2$ gauge theory		Liouville CFT
Ω-deformation parameters $\epsilon_1 : \epsilon_2$ $\mathsf{Q} = \epsilon_1 + \epsilon_2$	$\longleftrightarrow$	Liouville parameters $b : 1/b$ $\mathsf{Q} = b + 1/b$
UV gauge coupling $\tau_{\rm UV}$ $\exp\left[2\pi i \tau_{\rm UV}\right]$	$\longleftrightarrow$	Complex modulus of a tube gluing Riemann surfaces q
Mass m for an SU(2) flavor $m(\mathsf{Q}-m)$	$\longleftrightarrow$	Conformal dimension of a Liouville exponential $e^{2m\phi}$ Δ_m
Coulomb branch parameter a $a + \frac{\mathsf{Q}}{2}$	$\longleftrightarrow$	Momentum of an intermidiate primary field $e^{\alpha\tilde{\phi}}$ α
Instanton partition function $Z^{\rm inst}(a, \epsilon_1, \epsilon_2, \tau)$	$\longleftrightarrow$	Liouville conformal block $Z^{\rm Liouv}(\alpha, b, 1/b, q)$
Surface defect $D_{\mathfrak{t}}$	$\longleftrightarrow$	Degenerate primary operator at $z \in \Sigma$ $\Phi_{2,1}(z)$

Table 1: The basic dictionary of the AGT correspondence with the surface defect.

We begin with the 4d $\mathcal{N}=2$ SU(2) $\times$ SU(2) gauge theory shown as the quiver diagram in the top of Figure 9(a). Through the relation between the geometry and type IIA string theory as Figure 6, this 4d theory can be engineered by the geometry of the web diagram on the top of Figure 9(b), where thin dotted lines connecting the vertical lines indicate a subspace compactified on S^1 in the corresponding CY3. From the dictionary of the AGT correspondence, this theory is mapped into the Liouville CFT on a torus with two punctures that is often denoted as $\mathcal{T}_{2,1}$ (the top of Figure 9(c)). The connection displayed in the top line of Figure 9 has been checked by the direct computations of the Nekrasov partition function and the correlation function on the torus. Although the geometry of the web diagram in question is not toric at all, the geometric transition still consistently works. Choosing the special values of the Kähler factors on the web diagram to take the geometric transition, we obtain the web diagram with a Lagrangian brane depicted in the bottom of Figure 9(b) from which the 4d $\mathcal{N}=2$ SU(2) gauge theory with a matter in the adjoint representation

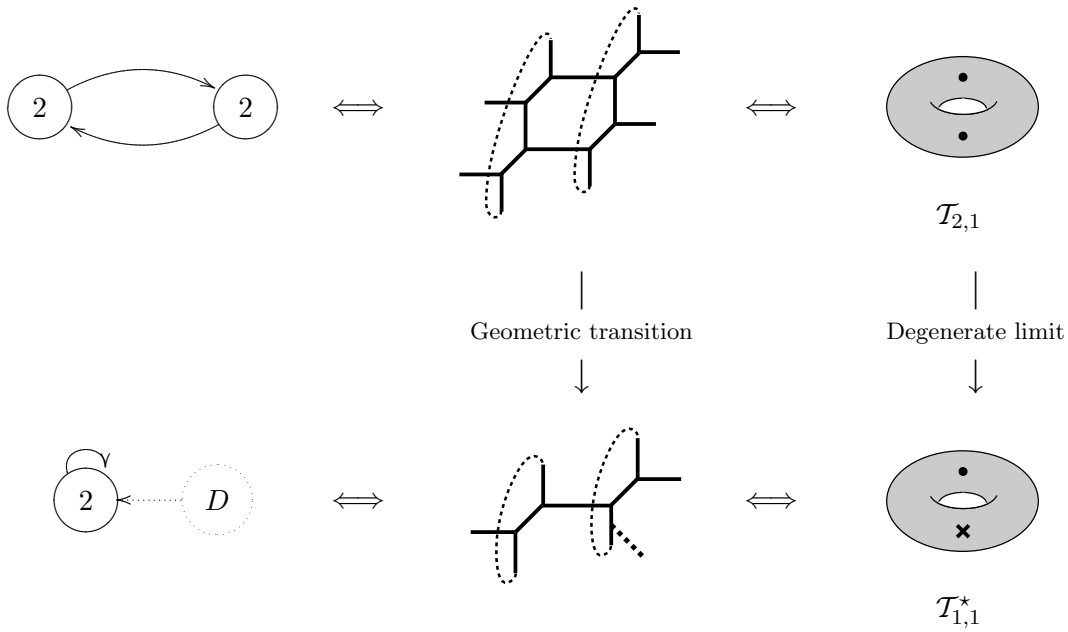

(a) 4d $\mathcal{N} = 2$ theory (b) Geometric engineering (c) Liouville CFT

Figure 9: The simplest picture of the AGT correspondence in the presence of a surface defect. (a) The 4d $\mathcal{N} = 2$ SU(2) $\times$ SU(2) quiver gauge theory (top) and $\mathcal{N} = 2$ SU(2) gauge theory with a matter in the adjoint representation (a solid line) and a surface defect D (bottom). (b) The geometric engineering of the 4d theories in (a). The surface defect as a Lagrangian brane in the bottom is generated through the geometric transition as explained in the previous subsection. (c) CFTs denoted as $\mathcal{T}_{2,1}$ and $\mathcal{T}^{\star}_{1,1}$ with a degenerate operator (a cross) which corresponds to the 4d theories in (a).

and the surface defect is engineered (the bottom of Figure 9(a)). On the CFT side, we take the corresponding limit of the associated parameters, which results in simply replacing one puncture with a degenerate operator drawn as a cross in the bottom of Figure 9(c). We would here name this CFT $\mathcal{T}^{\star}_{1,1}$. It seems surprising that only tuning the parameters changes the type of the operator in the theory, however, this phenomena can naturally be understood as the consequence of the geometric transition. The duality picture in Figure 9 has been clarified at least up to few lower levels of the expansions of the Nekrasov partition function and the CFT correlation function [82]. Remarks that the geometric transition really turns the field theories at the beginning to others. This is the basic story to derive the AGT correspondence in the presence of the surface defect from the geometric transition, and one can find other examples in the literatures.

2.4 M-theoretic realization

The AGT correspondence could be descended from the 6d $(2,0)$ theory as mentioned in (2.23), it is natural to ask a question what is the six-dimensional origin to give rise to the surface defect in the 4d $\mathcal{N}=2$ gauge theory and the degenerate field in the Liouville CFT simultaneously. Recalling that the 6d $(2,0)$ theory should be embedded into M-theory as the world-volume theory of the multiple M5-branes, the surface defect may also be engineered by the brane in M-theory. In fact, the brane configuration in type IIA string theory (2.26) can be lifted up to M-theory as follows. Both NS5 and D4-brane become M5-branes, and the D2′-brane that is inserted to make the surface defect is replaced with a M2-brane:

	$\overbrace{\quad\quad}^{\mathcal{M}_4}$						$\overbrace{\quad\quad}^{\Sigma}$				
	0	1	2	3	4	5	6	$\natural$	7	8	9
$\widetilde{\text{M5}}$	×	×	×	×	×	×					
M5	×	×	×	×			×	×			
M2	×	×							×		

(2.32)

where $\natural = 10$ stands for the eleventh direction of space-time that we will call the M-theory circle. We now put a tilde on the M5-brane ($\widetilde{\text{M5}}$) that goes down to the NS5-brane to distinguish the one down to the D4-brane. The point of this M-theory construction is that the M2-brane ends on the M5-brane and extends semi-infinitely to the 7 direction transverse to the M5-brane and the Riemann surface Σ. From the standpoint of the AGT correspondence, the boundary D of the M2-brane causes the emergence of the surface defect in the four-dimensional space-time $\mathcal{M}_4$, and the fact that the M2-brane looks a point z on Σ can induce the degenerate field $\Phi_{2,1}(z)$. Thus, we comprehend that appropriately inserting the M2-brane leads to the connection between the surface defect and the degenerate field in the AGT correspondence.

Finally, we would provide other candidates in M-theory to build the surface (codimension-2) defect in four dimensions. The defect as the boundary D of M2-brane on the M5-brane in (2.32) is codimension-4 from the viewpoint of the 6d $(2,0)$ theory and then is reduced to a codimension-2 one in the 4d $\mathcal{N}=2$ effective theory[8]. We can revive the situation with incorporating a probe M5-brane instead of the M2-brane. Since the M5-brane cannot have a boundary, we produce a codimension-4 defect in the 6d SCFT by intersecting the probe M5-brane with the multiple M5-branes on a two-dimensional subspace D and extending its other parts in $\mathbb{R}^4$ transverse to the multiple M5-branes, that is, being the point z on Σ. This M5-brane looks introducing the same surface defect as from the M2-brane above in four dimensions. The last candidate is a probe M5-brane wrapped not only on the two-dimensional subspace D but also on Σ. This turns out to be a codimension-2 defect in the

[8] See [60] for quite general (but not complete) constructions along this way.

6d $(2,0)$ theory. In six dimensions, the codimension-2 defect should be essentially distinct from the codimension-4 one, even so, they seem to originate the identical surface defect of the 4d effective theory in the IR where the size of Σ becomes relatively small to that of $\mathcal{M}_4$. This equivalence is quite of interest but not so clear for the moment, and we would not pursue this issue beyond the scope of this paper (we will comment in Section 7). These codimension-4 (M2 and M5) and codimension-2 (M5) defects are summarized as follows.

$$
\begin{array}{lccccccccc}
\text{space-time}: & \mathcal{M}_4 & \times & \Sigma & \times & \mathbb{R}^5 & & & & \\
 & \| & & \| & & \cup & & & & \\
\text{M5-brane}: & \mathcal{M}_4 & \times & \Sigma & \times & \{\text{pt}\} & \rightsquigarrow & \text{6d } \mathcal{N}=(2,0) \text{ SCFT} & \rightsquigarrow & \text{4d } \mathcal{N}=2 \text{ theory on } \mathcal{M}_4 \\
 & \cup & & \cup & & & & & & \\
\text{M2-brane}: & D & \times & \{\text{pt}\} & \times & \mathbb{R} & \rightsquigarrow & \text{codimension-4 defect} & \rightsquigarrow & \text{surface defect} \\
\text{M5-brane}: & D & \times & \{\text{pt}\} & \times & \mathbb{R}^4 & \rightsquigarrow & \text{codimension-4 defect} & \rightsquigarrow & \text{surface defect} \\
\text{M5-brane}: & D & \times & \Sigma & \times & \mathbb{R}^2 & \rightsquigarrow & \text{codimension-2 defect} & \rightsquigarrow & \text{surface defect}
\end{array}
$$

3 M-strings

3.1 Basic setup

The 6d $(2,0)$ SCFT is not considered as the standard gauge theory in the sense that this theory contains a self-dual 2-form field in a tensor multiplet, which implies that a dynamical object in this theory is not a particle but a string which we would call a self-dual string. It is known that the self-dual string should be tensionless to respect the conformal symmetry, but it is quite hard to analyze its dynamics by means of usual ways in quantum field theory. Towards understanding the self-dual string, a promising system in M-theory has been proposed by [32], which is named M-strings. The 6d $(2,0)$ SCFT naturally arises on the world-volume of the multiple M5-branes where the M2-brane can end, thus, the self-dual string is realized as the boundary of the M2-brane. In this construction, normally the self-dual string becomes tensionless since the M5-branes are on top of each other (Figure 10(a)) and the M2-branes stretched on each M5-brane do not acquire tension. In order to resolve this point, they have introduced the system where M M5-branes are slightly separated in one direction together with k_i M2-branes suspended between them[9]. The configuration is as follows:

		$\mathbb{R}^{1,1}$		$\mathbb{R}^4$					$\mathbb{R}^4$			
		0	1	2	3	4	5	6	7	8	9	$\natural$
M	M5	×	×	×	×	×	×	$\{a_i\}$				
k_i	M2	×	×					×				

(3.1)

[9] This circumstance is referred to as the tensor branch where scalars in the tensor multiplet have nonzero expectation values, as an analogue of the Coulomb branch.

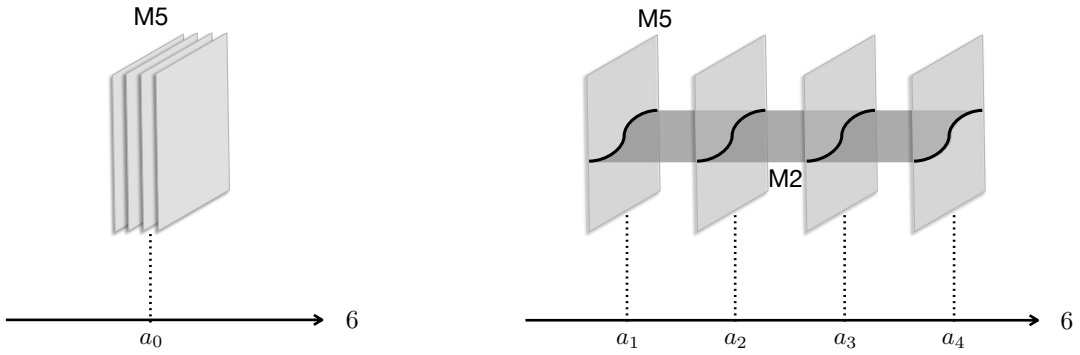

(a) Multiple M5-branes

(b) Separated M5-branes

Figure 10: (a) Self-dual tensionless strings on multiple M5-branes. (b) M-strings as self-dual strings on M5-branes separated in the 6 direction. M-strings are depicted as bold lines.

where $\natural = 10$ and $\{a_i\}_{i=1,\ldots,M}$ denote the positions of the M5-branes aligned along the 6 direction. The self-dual string as the boundary of the M2-brane in this setup is called the M-string and may capture at least partially the sector of BPS states in the 6d $(2,0)$ SCFT even though it has a small tension. We here take the flat space transverse to the M5-branes and M2-branes as a first step, and in the next subsection, we replace it with the singular background. Note that it is possible that different numbers of the M2-branes are put in each interval between the M5-branes. In a general way, for $i = 1, 2, \ldots, M-1$,

$$k_i \text{ M2-branes in the } i\text{-th interval } [a_i, a_{i+1}] \text{ of the M5-branes.}$$

Let us see supersymmetry preserved on M-strings made in the system (3.1). The six-dimensional world-volume of the M5-brane extended in the 012345 directions without the M2-brane has the superconformal group $\mathrm{OSp}(2,6|4)$ whose bosonic subgroup is

$$\mathrm{SO}(2,6) \times \mathrm{SO}(5)_R \subset \mathrm{OSp}(2,6|4). \tag{3.2}$$

Precisely, $\mathrm{SO}(2,6)$ is the conformal symmetry on the M5-brane and $\mathrm{SO}(5)_R$ is an R-symmetry corresponding to a rotational symmetry[10] of the space transverse to it in the eleven-dimensional space-time. As a result, the 6d $(2,0)$ theory on the stack of the M5-branes keeps this symmetry. For M-strings (3.1), we separate somewhat these M5-branes along the 6 direction, which means that the rotation along this direction is broken down while the $789\natural$ directions are not affected. Therefore, the original R-symmetry $\mathrm{SO}(5)_R$ is reduced to the rotational symmetry along these directions,

$$\mathrm{SO}(5)_R \to \mathrm{SO}(4)_R. \tag{3.3}$$

[10] A Spin group is often useful to characterize the supercharges as done in [32] since it is the double cover of a SO group, but this discrepancy is not essential here.

Now, we turn on the M2-branes extending the 6 direction with boundaries along the 01 directions on the M5-branes (3.1) which appears as M-strings as explained. Adding them of course breaks the Lorentz group $\mathrm{SO}(1,5) \subset \mathrm{SO}(2,6)$ into its subgroup,

$$\mathrm{SO}(1,5) \to \mathrm{SO}(1,1) \times \mathrm{SO}(4). \tag{3.4}$$

The former acts on the world-sheet of M-strings and the latter does on the space transverse to M-strings as the rotation, or equivalently, the subspace of the M5-branes on which M-strings are not wrapped. Consequently, the supercharges for preserved supersymmetry are labelled by the charge of $\mathrm{SO}(1,1)$ and the representations of $\mathrm{SO}(4) \simeq \mathrm{SU}(2)_{\mathrm{L}} \times \mathrm{SU}(2)_{\mathrm{R}}$ and $\mathrm{SO}(4)_R \simeq \widetilde{\mathrm{SU}}(2)_{\mathrm{L}} \times \widetilde{\mathrm{SU}}(2)_{\mathrm{R}}$.

Further, it can be checked how many supercharges M-strings have. What we have to do for this is to see independent components of an eleven-dimensional spinor ϵ (i.e. a 32-component spinor) as a parameter of the supersymmetry transformations. Let Γ^M ($M = 0, 1, \ldots, 9, \natural$) be eleven-dimensional gamma matrices (i.e. 32×32 matrices) satisfying

$$\Gamma^{12\cdots 9\natural} = 1, \qquad \Gamma^{M_1 M_2 \cdots M_p} := \Gamma^{M_1}\Gamma^{M_2}\cdots\Gamma^{M_p}. \tag{3.5}$$

Then, to preserve supersymmetry on the M5-brane and M2-brane requires the following conditions:

$$\begin{aligned} \Gamma^{012345}\epsilon &= \epsilon \quad \text{for the M5-brane,} \\ \Gamma^{016}\epsilon &= \epsilon \quad \text{for the M2-brane.} \end{aligned} \tag{3.6}$$

Combining these with the property (3.5) results in

$$\Gamma^{01}\epsilon = \Gamma^{2345}\epsilon = \Gamma^{789\natural}\epsilon. \tag{3.7}$$

At the beginning, there are 32 supercharges in eleven dimensions, and the presences of the M5-brane and M2-brane reduce its number to $32 \times \frac{1}{2} \times \frac{1}{2} = 8$ by imposing (3.6). In addition, the relation (3.7) tells us that the chiralities of the supercharges under $\mathrm{SO}(1,1)$, $\mathrm{SO}(4)$, and $\mathrm{SO}(4)_R$ are the same. Finally, we can conclude by using the specific forms of Γ^M that the remaining supersymmetry on the two-dimensional world-sheet of M-strings is $\mathcal{N} = (4,4)$. From above consideration, the supercharges denoted as $\mathcal{Q}_{\alpha a}$ and $\widetilde{\mathcal{Q}}_{\dot\alpha\dot a}$ are transformed under $\mathrm{SO}(1,1)$ and four $\mathrm{SU}(2)$'s as follows:

	$\mathrm{SO}(1,1)$	$\mathrm{SU}(2)_{\mathrm{L}}$	$\mathrm{SU}(2)_{\mathrm{R}}$	$\widetilde{\mathrm{SU}}(2)_{\mathrm{L}}$	$\widetilde{\mathrm{SU}}(2)_{\mathrm{R}}$
$\widetilde{\mathcal{Q}}_{\dot\alpha\dot a}$	$-\frac{1}{2}$	**1**	**2**	**1**	**2**
$\mathcal{Q}_{\alpha a}$	$+\frac{1}{2}$	**2**	**1**	**2**	**1**

(3.8)

where $\alpha, a = \pm$ for $\mathrm{SU}(2)_{\mathrm{L}}$ and $\widetilde{\mathrm{SU}}(2)_{\mathrm{L}}$, and $\dot\alpha, \dot a = \dot\pm$ for $\mathrm{SU}(2)_{\mathrm{R}}$ and $\widetilde{\mathrm{SU}}(2)_{\mathrm{R}}$, respectively. We will refer to $\widetilde{\mathcal{Q}}_{\dot\alpha\dot a}$ as left-moving supercharges and $\mathcal{Q}_{\alpha a}$ as right-moving ones. Note that

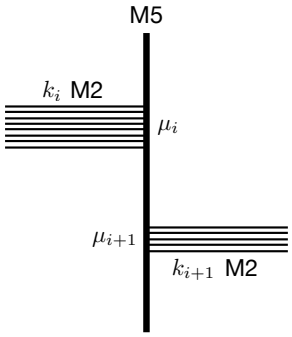

Figure 11: The M5-brane as a domain wall for the M2-branes ending on it.

the R-symmetry of the 2d $\mathcal{N} = (4, 4)$ theory is $SU(2)^3$. Thus, three of four SU(2)'s in (3.8) form really the R-symmetry, and the rest one is regarded as a global symmetry.

We would comment on the role of the M5-brane from the M2-brane point of view. For the M5-brane at the position a_{i+1} in the 6 direction, k_i M2-branes are ending on it from the left and k_{i+1} M2-branes from the right (Figure 11). It has been found [42, 85, 86, 87] that the ground states of the multiple M2-branes on the boundary are labelled by partitions μ_i (μ_{i+1}) of k_i (k_{i+1}), and the M5-brane serves as a domain wall to support the existence of such ground states. In this sense, the contribution of a single M5-brane on which M2-branes can end will be called a domain wall partition function (Section 4.2).

3.2 On Taub-NUT space

The 6d $(2, 0)$ theory arises also in type IIB string theory on the ADE-type singularity [24]. In order to make it suitable to connect M-strings with that type IIB picture, we would take the M-string configuration on the A_{N-1} singularity generated by Γ_N as the simplest extension [33],

		$\mathbb{R}^{1,1}$		$\mathbb{R}^4$					$\mathbb{R}^4/\Gamma_N \simeq \mathbb{C}^2/\Gamma_N$			
		0	1	2	3	4	5	6	7	8	9	$\natural$
M	M5	×	×	×	×	×	×	$\{a_i\}$				
k_i	M2	×	×					×				

(3.9)

where

$$\Gamma_N = \left\{ \begin{pmatrix} \gamma_n & 0 \\ 0 & \gamma_n^{-1} \end{pmatrix} \middle| \, n = 1, 2, \cdots, N-1 \right\}, \qquad \gamma_n = e^{2\pi i \frac{n}{N}}. \tag{3.10}$$

Actually, this action is $\mathbb{Z}_N$ orbifolding of which the M5-brane and M2-brane are sit on the singularity. This orbifold causes the breakdown of $(4, 4)$ supersymmetry of original M-strings

(3.1) as follows. Let (w_1, w_2) be complex coordinates on $\mathbb{R}^4 \simeq \mathbb{C}^2$ transverse to the M5-brane and M2-brane. In our case, the orbifolding Γ_N acts on this space so that

$$\Gamma_N : (w_1, w_2) \mapsto (\gamma_1 w_1, \gamma_1^{-1} w_2), \tag{3.11}$$

which precisely breaks the rotational symmetry on $\mathbb{C}^2$ and accordingly supersymmetry because the supercharges (3.8) are charged under this rotation $\widetilde{\mathrm{SU}}(2)_{\mathrm{L}} \times \widetilde{\mathrm{SU}}(2)_{\mathrm{R}}$. Nevertheless, we can preserve part of supersymmetry by embedding Γ_N into its subgroup. Here, we select the embedding $\Gamma_N \subset \widetilde{\mathrm{SU}}(2)_{\mathrm{R}}$ that, from our charge assignments (3.8), gives the action

$$\Gamma_N : (\widetilde{\mathcal{Q}}_{\dot{\alpha}+}, \widetilde{\mathcal{Q}}_{\dot{\alpha}-}, \mathcal{Q}_{\alpha+}, \mathcal{Q}_{\alpha-}) \mapsto (\gamma_1 \widetilde{\mathcal{Q}}_{\dot{\alpha}+}, \gamma_1^{-1} \widetilde{\mathcal{Q}}_{\dot{\alpha}-}, \mathcal{Q}_{\alpha+}, \mathcal{Q}_{\alpha-}). \tag{3.12}$$

Namely, the left-moving supercharges $\widetilde{\mathcal{Q}}_{\dot{\alpha}\dot{a}}$ are nontrivially transformed under Γ_N whereas the right-moving ones $\mathcal{Q}_{\alpha a}$ are invariant, in other words, M-strings on the orbifolding singularity keep $\mathcal{N} = (0, 4)$ supersymmetry as on its world-sheet theory.

From now on, we would resolve the singularity of Γ_N since it is hard to deal directly with it. The natural resolution of the A_{N-1} singularity is taken to be a Taub-NUT space which we will denote as TN_N. This space is a hyper-Kähler manifold and the geometry in the presence of the Kalza-Klein (KK) monopole whose metric is given by

$$\begin{aligned} \mathrm{d}s^2_{\mathrm{TN}} &= H \mathrm{d}\vec{x}^2 + H^{-1} \left(\mathrm{d}s + \vec{A} \cdot \mathrm{d}\vec{x} \right)^2, \\ H(\vec{x}) &= \sum_{I=1}^{N} \frac{1}{|\vec{x} - \vec{x}_I|} + \frac{1}{L^2_{\mathrm{TN}}}, \qquad \nabla H = -\nabla \times \vec{A}, \end{aligned} \tag{3.13}$$

where the coordinates $\vec{x}$ and s is a three-dimensional vector and a parameter along S^1 of the asymptotic radius L_{TN}. Thus, TN_N has in general the topology of $\mathbb{R}^3 \times S^1$. $\vec{x}_I$ for fixed I is a point called a center of TN_N where S^1 shrinks at this point. $H(\vec{x})$ should be the solution to the Laplace equation in three dimensions, and the gauge field $\vec{A}$ becomes a source of the KK monopole. The Taub-NUT space shows the A_{N-1} singularity if all centers are coincided as summarized in Table 2. Note that the naive resolution of the A_{N-1} singularity is an asymptotically locally Euclidean (ALE) space which is a specialized version of TN_N as $L_{\mathrm{TN}} \to \infty$. Indeed, the choice of either the ALE space or TN_N does not matter here because our final results do not depend on the asymptotic radius L_{TN}. We would continue discussions with the Taub-NUT space for future analysis.

It is well known that the singular limit of the Taub-NUT space can be viewed as an algebraic manifold defined locally by the equation

$$X^N + YZ = 0 \tag{3.14}$$

around the origin, that is, when all centers are collected at the origin. This is recast to our parametrization by $X = w_1 w_2$, $Y = w_1^N$, and $Z = w_2^N$. Based on this expression, we can

	metric	topology	singularity
	$\mathrm{d}s^2_{\mathrm{TN}} = H\mathrm{d}\vec{x}^2 + H^{-1}(\mathrm{d}s + \vec{A}\cdot\mathrm{d}\vec{x})^2$	$\mathbb{R}^3 \times S^1$	$\emptyset$
$\lvert\vec{x}\rvert \to \infty$	$\mathrm{d}s^2_{\mathrm{TN}} = \frac{1}{L^2_{\mathrm{TN}}}\mathrm{d}\vec{x}^2 + L^2_{\mathrm{TN}}(\mathrm{d}s + \vec{A}\cdot\mathrm{d}\vec{x})^2$	$\mathbb{R}^3 \times S^1$	$\emptyset$
$\lvert\vec{x}-\vec{x}_I\rvert \sim 0$ with $\vec{x}_J \neq \vec{x}_I$ for $\forall J$	$4\pi\mathrm{d}s^2_{\mathrm{TN}} = \frac{1}{r}\left(\mathrm{d}r^2 + r^2(\mathrm{d}\theta^2 + \sin^2\theta\mathrm{d}\phi^2)\right) + r(\mathrm{d}\psi - \cos\theta\mathrm{d}\phi) = \mathrm{d}\rho^2 + \rho^2\mathrm{d}\Omega_3^2$ $(\psi := 4\pi s,\ \rho := 2r = 2\lvert\vec{x} - \vec{x}_I\rvert)$	$\mathbb{R}^4$	$\emptyset$
$\lvert\vec{x}-\vec{x}_I\rvert \sim 0$ with $\vec{x}_J = \vec{x}_I$ for $\forall J$	$\frac{4\pi}{N}\mathrm{d}s^2_{\mathrm{TN}} = \mathrm{d}\rho^2 + \rho^2\mathrm{d}\Omega_3^2 = \mathrm{d}w_i\mathrm{d}\bar{w}_i$ $(\psi := \frac{4\pi}{N}s,\ w_{1,2} \in \mathbb{C})$	$\mathbb{C}^2/\mathbb{Z}_N$: $(w_1, w_2) \sim (\gamma_1 w_1, \gamma_1^{-1} w_2)$	A_{N-1}

Table 2: The limits of the Taub-NUT space.

immediately find the following U(1) isometries of TN_N[11]:

$$\mathrm{U}(1)_f : (w_1, w_2) \mapsto (e^{2\pi i\alpha} w_1, e^{-2\pi i\alpha} w_2), \tag{3.15}$$

$$\mathrm{U}(1)_b : (w_1, w_2) \mapsto (e^{2\pi i\alpha} w_1, e^{2\pi i\alpha} w_2). \tag{3.16}$$

Those turn out to be crucial in the next subsection to implement the torus compactification of M-strings. In what follows, we take S^1 of TN_N labeled by s to be the 7 direction in our eleven-dimensional space-time.

3.3 Torus compactification

Let us go to a further modification of M-strings in addition to replacing $\mathbb{C}^2$ with the Taub-NUT space. For practical reasons, we would employ M-strings sharing the 01 directions with the M5-branes to be compactified on a two-torus T^2 (Figure 12)[12],

		T^2		$\mathbb{R}^4_{\epsilon_1,\epsilon_2}$					TN_N			
		0	1	2	3	4	5	6	7	8	9	$\natural$
M	M5	×	×	×	×	×	×	$\{a_i\}$				
k_i	M2	×	×					×				

(3.17)

[11] The isometry is enlarged to $\mathrm{U}(1)_f \times \mathrm{SU}(2)_b$ for $N = 1$.

[12] In [88], an additional circle compactification in the M-strings system has been studied.

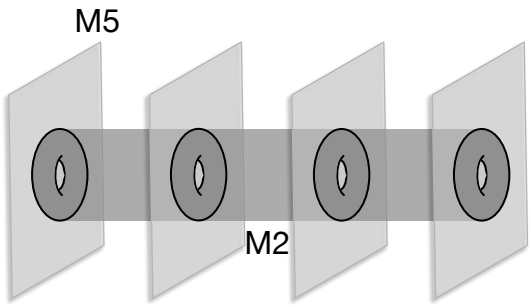

Figure 12: M-strings compactified on a torus.

and consequently the physical quantities of M-strings get the dependance on a complex modulus τ of T^2 given by

$$\tau = i\frac{R_0}{R_1}, \tag{3.18}$$

where R_0 (R_1) is a radius of the 0 (1) direction. The advantages of the torus compactification are to be able to introduce more parameters in the manner compatible with supersymmetry and make it doable to compute the partition function of M-strings from the gauge theory languages (see Section 4).

Since there are two 1-cycles on T^2, we can have the system of M-strings enriched with three parameters by twisted boundary conditions along these 1-cycles. For the 1 direction over which the 789$\natural$ directions are viewed as a fibration, the twist is denoted as $\mathrm{U}(1)_m$ called the mass deformation with a parameter m,

$$\mathrm{U}(1)_m : (w_1, w_2) \mapsto (g_m w_1, g_m^{-1} w_2), \qquad g_m = e^{2\pi i m}. \tag{3.19}$$

The reason why we name m the mass is that this parameter is identified with the mass of matter fields in the adjoint representation of the 5d quiver gauge theory (Section 4.1). Actually, the action of $\mathrm{U}(1)_m$ is similar to that of Γ_N (3.11), which implies that this action can be embedded in the same manner as for Γ_N. Hence, when taking $\mathrm{U}(1)_m \subset \widetilde{\mathrm{SU}}(2)_{\mathrm{R}}$, this acts on the supercharges as

$$\mathrm{U}(1)_m : (\widetilde{\mathcal{Q}}_{\dot{\alpha}+}, \widetilde{\mathcal{Q}}_{\dot{\alpha}-}, \mathcal{Q}_{\alpha+}, \mathcal{Q}_{\alpha-}) \mapsto (g_m \widetilde{\mathcal{Q}}_{\dot{\alpha}+}, g_m^{-1} \widetilde{\mathcal{Q}}_{\dot{\alpha}-}, \mathcal{Q}_{\alpha+}, \mathcal{Q}_{\alpha-}). \tag{3.20}$$

The right-moving supercharges are still invariant, as a result, $(0, 4)$ supersymmetry on M-strings are compatible with the mass deformation.

The possible twist along the other 1-cycle, the 0 direction, is the Ω-deformation $\mathrm{U}(1)_{\epsilon_1} \times \mathrm{U}(1)_{\epsilon_2}$ [77] that corresponds to the infrared (IR) regularizations of the 2345 directions. Note that these directions are often concentrated on as the space(-time) on which the four-dimensional supersymmetric gauge theory is defined, in particular, when we consider the

	$\mathrm{U}(1)_m$	$\mathrm{U}(1)_{\epsilon_1}$	$\mathrm{U}(1)_{\epsilon_2}$
$\widetilde{\mathcal{Q}}_{\dot{+}\dot{+}}$	$+1$	$+\frac{1}{2}$	$-\frac{1}{2}$
$\widetilde{\mathcal{Q}}_{\dot{+}\dot{-}}$	$+1$	$+\frac{1}{2}$	$-\frac{1}{2}$
$\widetilde{\mathcal{Q}}_{\dot{-}\dot{+}}$	-1	$-\frac{1}{2}$	$+\frac{1}{2}$
$\widetilde{\mathcal{Q}}_{\dot{-}\dot{-}}$	-1	$-\frac{1}{2}$	$+\frac{1}{2}$
$\mathcal{Q}_{++}$	0	0	0
$\mathcal{Q}_{+-}$	0	$+1$	$+1$
$\mathcal{Q}_{-+}$	0	-1	-1
$\mathcal{Q}_{--}$	0	0	0

Table 3: The supercharges transformed under $\mathrm{U}(1)_m$, $\mathrm{U}(1)_{\epsilon_1}$, and $\mathrm{U}(1)_{\epsilon_2}$.

torus relatively small compared with the energy scale of the theory on the 2345 directions. This is in the case of, e.g., the AGT correspondence [9] as mentioned in Section 2.3. Let (z_1, z_2) be complex coordinates on the 2345 directions, then in our situation, the action of $\mathrm{U}(1)_{\epsilon_1} \times \mathrm{U}(1)_{\epsilon_2}$ is given by

$$\begin{aligned} \mathrm{U}(1)_{\epsilon_1} \times \mathrm{U}(1)_{\epsilon_2} &: (z_1, z_2) \mapsto (e^{2\pi i \epsilon_1} z_1, e^{2\pi i \epsilon_2} z_2), \\ &: (w_1, w_2) \mapsto (g_+^{-1} w_1, g_+^{-1} w_2), \end{aligned} \tag{3.21}$$

where $g_+ := e^{\pi i(\epsilon_1+\epsilon_2)}$ and $g_- := e^{\pi i(\epsilon_1-\epsilon_2)}$. With our convention of the supercharges, this action also can be embedded into four SU(2)'s (3.8) so that

$$\begin{aligned} &(\widetilde{\mathcal{Q}}_{\dot{+}\dot{a}}, \widetilde{\mathcal{Q}}_{\dot{-}\dot{a}}, \mathcal{Q}_{+a}, \mathcal{Q}_{-a}) \mapsto (g_- \widetilde{\mathcal{Q}}_{\dot{\alpha}\dot{+}}, g_-^{-1} \widetilde{\mathcal{Q}}_{\dot{\alpha}\dot{-}}, g_+ \mathcal{Q}_{+a}, g_+^{-1} \mathcal{Q}_{-a}) && \text{when acting on } (\alpha, \dot{\alpha}), \\ &(\widetilde{\mathcal{Q}}_{\dot{\alpha}\dot{+}}, \widetilde{\mathcal{Q}}_{\dot{\alpha}\dot{-}}, \mathcal{Q}_{\alpha+}, \mathcal{Q}_{\alpha-}) \mapsto (\widetilde{\mathcal{Q}}_{\dot{\alpha}\dot{+}}, \widetilde{\mathcal{Q}}_{\dot{\alpha}\dot{-}}, g_+^{-1} \mathcal{Q}_{\alpha+}, g_+ \mathcal{Q}_{\alpha-}) && \text{when acting on } (a, \dot{a}). \end{aligned} \tag{3.22}$$

Thus, the net action unifying those is dictated by

$$\begin{aligned} \mathrm{U}(1)_{\epsilon_1} \times \mathrm{U}(1)_{\epsilon_2} &: (\widetilde{\mathcal{Q}}_{\dot{+}\dot{+}}, \widetilde{\mathcal{Q}}_{\dot{+}\dot{-}}, \widetilde{\mathcal{Q}}_{\dot{-}\dot{+}}, \widetilde{\mathcal{Q}}_{\dot{-}\dot{-}}) \mapsto (g_- \widetilde{\mathcal{Q}}_{\dot{+}\dot{+}}, g_- \widetilde{\mathcal{Q}}_{\dot{+}\dot{-}}, g_-^{-1} \widetilde{\mathcal{Q}}_{\dot{-}\dot{+}}, g_-^{-1} \widetilde{\mathcal{Q}}_{\dot{-}\dot{-}}), \\ &: (\mathcal{Q}_{++}, \mathcal{Q}_{+-}, \mathcal{Q}_{-+}, \mathcal{Q}_{--}) \mapsto (\mathcal{Q}_{++}, g_+^2 \mathcal{Q}_{+-}, g_+^{-2} \mathcal{Q}_{-+}, \mathcal{Q}_{--}). \end{aligned} \tag{3.23}$$

The fact that only $\mathcal{Q}_{++}$ and $\mathcal{Q}_{--}$ are neutral under $\mathrm{U}(1)_{\epsilon_1} \times \mathrm{U}(1)_{\epsilon_2}$ states that the Ω-deformation along the 0 direction breaks $\mathcal{N} = (0,4)$ supersymmetry to $\mathcal{N} = (0,2)$. The charges of $\mathcal{Q}_{\alpha a}$ and $\widetilde{\mathcal{Q}}_{\dot{\alpha}\dot{a}}$ under these twists are collected in Table 3. In conclusion, M-strings compactified on T^2 which are placed at the tip of the A_{N-1} singularity of the Taub-NUT space basically has $(0,4)$ supersymmetry on its world-sheet, and physical quantities with nontrivial m, ϵ_1, and ϵ_2 can only preserve $(0,2)$ supersymmetry of it.

We are closing this section with comments on two issues. The one is about the relation between the twists and the isometries of the Taub-NUT space. The mass deformation (3.19)

and the Ω-deformation (3.21) are obliviously identified with the U(1) isometries (3.15) and (3.16) of TN_N,

$$\mathrm{U}(1)_m \equiv \mathrm{U}(1)_f, \tag{3.24}$$

$$\mathrm{U}(1)_{\epsilon_1} \times \mathrm{U}(1)_{\epsilon_2} \equiv \mathrm{U}(1)_b. \tag{3.25}$$

These two isometries ensure that we can introduce two types of the twists along T^2 in the way to preserve at least $(0,2)$ supersymmetry.

The other is associated with the enhancement of supersymmetry in the case of $\mathrm{TN}_{N=1}$ where the background is flat but still has a single center of the Taub-NUT space. The non-zero values of all twist parameters still break it to $\mathcal{N}=(0,2)$ as shown above, but some of supersymmetry might be possible to recover by tuning these parameters since some supercharges get neutral under the twists (3.19) and (3.21). From the charge under these twists in Table 3, if we set $m = \pm\frac{\epsilon_1-\epsilon_2}{2}$, then two of four left-moving supercharges become invariant under the twists, thus, supersymmetry get enhanced to $\mathcal{N}=(2,2)$. On the other hand, when choosing $\epsilon_1+\epsilon_2=0$ (later called the unrefined limit), all of four right-moving supercharges do not nontrivially rotated, as a result, $\mathcal{N}=(0,4)$ arises. There is another possibility to tune parameters as $m=\pm\frac{\epsilon_1+\epsilon_2}{2}$, which naively does not give extra supersymmetry. However, it has been pointed out [32] that extra fermion zero-modes present with this tuning, and in fact, supersymmetry enlargement may occur by appropriately removing these modes. We will concretely demonstrate this phenomena in Section 4.3. If turning off all twist parameters, M-strings on TN_1 has $\mathcal{N}=(4,4)$ supersymmetry as explained in Section 3.1. These observations are summarized:

twist parameters (TN_1)	supersymmetry
$m=\epsilon_1=\epsilon_2=0$	$(4,4)$
$m=\pm\frac{\epsilon_1-\epsilon_2}{2}$	$(2,2)$
$m\neq 0,\ \epsilon_1+\epsilon_2=0$	$(0,4)$
$m=\pm\frac{\epsilon_1+\epsilon_2}{2}$	$(0,2)^*$
$m\neq 0,\ \epsilon_1\neq 0,\ \epsilon_2\neq 0$	$(0,2)$

(3.26)

where $*$ means supersymmetry enhancement due to the fermion zero-modes.

4 Partition function of M-strings

In this section, we would give the prescriptions how to compute the partition function of M-strings. As mentioned above, we do not have on hand any direct evaluation of the partition function because there is no known Lagrangian description of the 6d $(2,0)$ theory. Nevertheless, thanks to the chain of the duality, somehow indirect methods which have been developed

for decades are actually applicable to the M-strings calculations. There are basically two perspectives for the moment suitable to the M-string.

- BPS state counting: roughly, the M-string can be viewed as the BPS particle on the M5-brane world-volume $\mathbb{R}^4_{\epsilon_1,\epsilon_2}$, which turns out to be the instanton counting problem. This issue can actually be connected with the A-model topological string theory in which a partition function is exactly computed by the refined or unrefined topological vertex formulated in terms of geometry.

- 2d world-sheet theory: the 2d $\mathcal{N} = (0, 4)$ gauge theory may be induced on the world-sheet of M-strings on the Taub-NUT space. The matter contents of the world-sheet theory can be read off from string theory through the duality. As a result, we compute its partition function on T^2 as an elliptic genus by the localization technique.

The refined topological vertex is technically more powerful but conceptually rather indirect than the elliptic genus, but the fact that results obtained independently from them match clarifies the validity of these techniques for M-strings. Note that, in what follows, we call the M-theory circle a direction compactified on S^1 in eleven-dimensional space-time which becomes much small as M-theory is reduced to type IIA string theory. We will compute the partition function of M-strings from the former standpoint in Section 4.3 and the latter in Section 4.4.

4.1 BPS counting with the refined topological vertex

Let us see M-strings from the 4d plane $\mathbb{R}^4_{\epsilon_1,\epsilon_2}$ in the M5-brane at the starting point (3.17). Each collection of k_i M-strings is viewed as k_i independent points on $\mathbb{R}^4_{\epsilon_1,\epsilon_2}$. Actually, those positions of M-strings become the parameters of its moduli space. The number of real parameters of this moduli space is $4k_iN$, which is equivalent to that of k_i SU(N) instantons with a finite size [33]. Therefore, the M-string partition function can be computed as that of this instanton moduli space. With the power of dualities in string theory, we may implement this calculation by utilizing the so-called refined topological vertex in the topological string theory. To see this, in this subsection let the 1 direction be the M-theory circle. As this circle goes tiny, the M5-branes and the M2-branes wrapped on this circle are reduced to D4-branes and fundamental strings indicated as F1, respectively, in type IIA string theory[13]:

	S^1	$\mathbb{R}^4_{\epsilon_1,\epsilon_2}$					TN_N			
	0	2	3	4	5	6	7	8	9	♮
M D4	×	×	×	×	×	$\{a_i\}$				
k_i F1	×					×				

(4.1)

[13]For the moment, we assume that the mass parameter m is turned off.

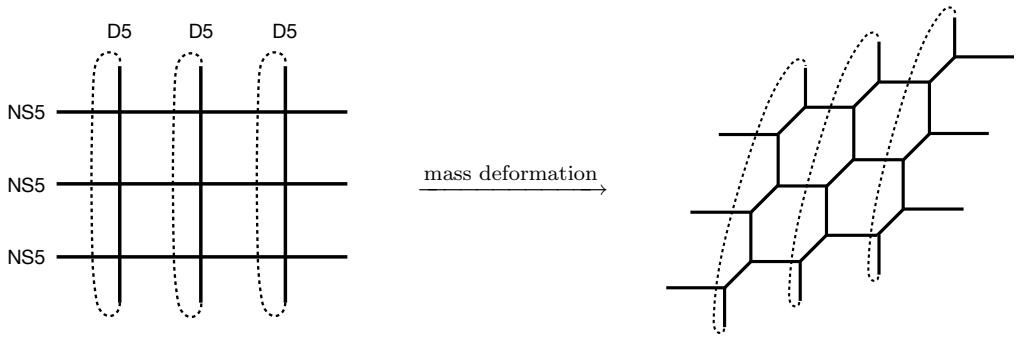

Figure 13: The (p, q)-web diagram on the 67-plane that encodes the contribution of M-strings (3.9). This is the case of $(M, N) = (3, 3)$.

In order to make it easy to find the M-theory origin, we keep the labels for the coordinates of eleven-dimensional space-time even when the ten-dimensional string theory is under consideration. This reduction of course does not affect the Tabu-NUT space.

Then, we perform T-duality along the 7 direction that is S^1 of TN_N. This T-duality brings the D4-branes into D5-branes wrapped on the 7 direction but does not change F1. Further, it is known that the dense N centers of TN_N are transformed to N NS5-branes. The resultant configuration is the following D5-NS5 system with F1's stretched between the separated D5-branes:

	S^1	$\mathbb{R}^4_{\epsilon_1,\epsilon_2}$					S^1			
	0	2	3	4	5	6	7	8	9	♮
M D5	×	×	×	×	×	$\{a_i\}$	×			
k_i F1	×					×				
N NS5	×	×	×	×	×	×				

(4.2)

This configuration projected onto the 67-plane is shown on the left side of Figure 13 where the dotted line on the D5-brane indicates that the 7 direction is compactified (as well as in Figure 9). We would restore the mass parameter m corresponding to the twisted boundary condition on the 789♮ directions. Since the D5-brane extends to the 7 direction, an Ramond-Ramond (RR) field coupled to the D5-brane has non-zero components with this direction, thus, the RR charge of the D5-brane is shifted by this twisted boundary condition when going around the 7 direction. We have to complement this shift because of the charge conservation on the D5-brane. The fact that the D5-brane is intersected with the NS5-brane allows us to absorb it into the NSNS charge of the NS5-brane. This argument is carried out by introducing the so-called (p, q)-fivebrane at the intersecting point where p and q are the NSNS and RR charge, respectively, namely, an $(1, 0)$-fivebrane is NS5 and an $(0, 1)$-fivebrane is D5. For the

current situation, the $(1,1)$-fivebrane is brought into as the diagonal line shown on the right side of Figure 13, for example, with $(M,N)=(3,3)$. This picture generically is called the (p,q)-web diagram. We here treat only with this type of the (p,q)-web diagram along the story of the M-string.

As a surprising fact, we can appropriately interpret the (p,q)-web diagram as purely a geometric object: it is just translated into a web diagram of CY3 introduced in Section 2.2.2 [89, 90, 91]. This is a prominent example that physics of string theory and the gauge theory induced on the the (p,q)-web diagram is naturally investigated in the languages of geometry. This fact also allows us to be able to evaluate the partition function of M-strings as we will see. Upon this correspondence, the mass deformation also has the natural geometrical interpretation. Getting back to the (p,q)-web diagram without the mass deformation in Figure 13, the D5-brane and the NS5-brane cross at a point on the 67-plane. This intersecting point is mapped into a singularity in the corresponding CY3, here nothing but the conifold (Section 2.2). As a result, the mass deformation at that point actually resolves the singularity of the conifold by blowing up it with $\mathbb{C}\mathbf{P}^1$ of the size m as done in Section 2.2.2. This is another reason to take the mass deformation instead of keeping full supersymmetry on the M-string.

The great success of relationship between the (p,q)-web system and CY3 provides the application of the A-model topological string theory to the gauge theory on the D5-branes under consideration. The basic ingredient of the computation in the A-model is the topological vertex [34] of which the combinatorics can produce the BPS partition function for the general CY3 with a web diagram dual to the (p,q)-web diagram in type IIB string theory. Therefore, the contribution of M-strings can be systematically evaluated by the topological vertex. Moreover, there is the *refined* version of the topological string theory called the refined topological string [35, 36] basically to incorporate the Ω-deformation parameters

$$q_1 = e^{2\pi i\epsilon_1}, \qquad q_2 = e^{-2\pi i\epsilon_2} \tag{4.3}$$

in the formulation of the topological string theory. From now on, we always say the *unrefined* topological string as the standard topological string theory to distinguish it from the refined one. Note that the refined topological string goes back to the unrefined one as taking the limit

$$q_1 = q_2 \quad \Leftrightarrow \quad \epsilon_1 + \epsilon_2 = 0. \tag{4.4}$$

Their definitions and necessary tools for the calculation are packed in Appendix B. Also, to avoid complexity, we basically note the details of calculations together in Appendix C.

4.2 Domain wall partition function

At first, to easily derive the partition function of M-strings, we write down the partition function for the domain wall (Figure 11) that corresponds to the contribution of a single M5-brane on the Taub-NUT space. More precisely, the reasons to prepare this as a building block are that, by the construction of the refined topological string, gluing the domain walls produces the web diagram for M-strings with general (M, N), and we need divide the refined topological string partition function by the domain wall partition function to drop parts come only from the KK towers of tensor multiplets in the 6d $(2, 0)$ theory and extract correctly information about M-strings. Let us denote the domain wall partition function as $Z^{\nu_1\nu_2\cdots\nu_N}_{\mu_1\mu_2\cdots\mu_N}(Q_i; q_1, q_2)$, where the parameters are defined as follows. The web diagram for the domain wall on TN_N contains a single vertical line (i.e. a single M5) with N internal diagonal segments. The vertical or diagonal internal line represents $\mathbb{C}\mathbf{P}^1$ of a Kähler parameter t_i, or equivalently, a Kähler factor Q_i,

$$Q_i = e^{2\pi i t_i}, \tag{4.5}$$

where i runs for 1 to $2N$. Since there are N external lines on both the left side and the right side, we assign Young diagrams μ_j^{T} and ν_i on the left and the right, respectively, used in the definition of the refined topological vertex (see Appendix B). Further, we define an additional Kähler factor Q_τ such that

$$e^{2\pi i\tau} = Q_\tau := \prod_{i=1}^{2N} Q_i. \tag{4.6}$$

We will identify τ with the complex modulus of the torus on which M-strings are wrapped.

4.2.1 On TN_1

As the first example, we would focus on the simplest domain wall, i.e. one M5-brane on TN_1. From string duality explained above, the associated brane system in type IIB string theory consists of one D5-brane and one NS5-brane, and the web diagram of the corresponding CY3 is depicted in Figure 14. This diagram is obtained by combining two refined topological vertex $C_{\mu\nu\rho}$ (B.8), thus, the refined topological string partition function is written as

$$Z^{\nu_1}_{\mu_1}(Q_1, Q_2; q_1, q_2) = \sum_{\rho_1,\rho_2} (-Q_1)^{|\rho_1|}(-Q_2)^{|\rho_2|} C_{\rho_2^{\mathrm{T}}\rho_1\mu_1^{\mathrm{T}}}(q_2, q_1) C_{\rho_2\rho_1^{\mathrm{T}}\nu_1}(q_1, q_2). \tag{4.7}$$

Following the definition of the refined topological vertex (B.8) and the gluing prescription in Appendix B, (4.7) can be deformed in the form of the infinite product (done in Appendix

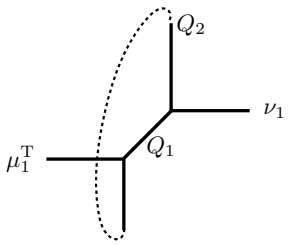

Figure 14: The domain wall corresponding to a single M5-brane on TN_1.

C.1),

$$
\begin{aligned}
&Z^{\nu_1}_{\mu_1}(Q_1,Q_2,Q_\tau;q_1,q_2)\\
&=q_1^{\frac{||\mu_1^{\mathrm{T}}||^2}{2}}q_2^{\frac{||\nu_1||^2}{2}}\widetilde{Z}_{\mu_1^{\mathrm{T}}}(q_2,q_1)\widetilde{Z}_{\nu_1}(q_1,q_2)\\
&\quad\times\prod_{n=1}^{\infty}\frac{1}{1-Q_\tau^n}\prod_{i,j,k=1}^{\infty}\left[\frac{(1-Q_2Q_\tau^{k-1}q_1^{-\mu^{\mathrm{T}}_{1,j}+i-\frac{1}{2}}q_2^{-\nu_{1,i}+j-\frac{1}{2}})(1-Q_1Q_\tau^{k-1}q_1^{-\nu^{\mathrm{T}}_{1,j}+i-\frac{1}{2}}q_2^{-\mu_{1,i}+j-\frac{1}{2}})}{(1-Q_\tau^kq_1^{-\mu^{\mathrm{T}}_{1,j}+i-1}q_2^{-\mu_{1,i}+j})(1-Q_\tau^kq_1^{-\nu^{\mathrm{T}}_{1,j}+i}q_2^{-\nu_{1,i}+j-1})}\right],
\end{aligned}
\tag{4.8}
$$

where the indices (i,j) run for all of the positions of boxes in the Young diagrams μ_1 and ν_1, and in this case,

$$
Q_\tau=Q_1Q_2. \tag{4.9}
$$

We need a further operation to derive the correct partition function of M-strings. To extract the contribution from M-strings, the factor originated purely from the degrees of freedom expect those self-dual strings should be removed. This can be achieved by the normalization that the domain wall partition function is divided by the same one with Young diagrams on the external lines being trivial, $\mu_1=\nu_1=\emptyset$. Concretely, the normalized domain wall partition function $\widehat{Z}^{\nu_1}_{\mu_1}$ is given by

$$
\begin{aligned}
&\widehat{Z}^{\nu_1}_{\mu_1}(Q_1,Q_2,Q_\tau;q_1,q_2)\\
&:=\frac{Z^{\nu_1}_{\mu_1}(Q_1,Q_2,Q_\tau;q_1,q_2)}{Z^{\emptyset}_{\emptyset}(Q_1,Q_2,Q_\tau;q_1,q_2)}\\
&=q_1^{\frac{||\mu_1^{\mathrm{T}}||^2}{2}}q_2^{\frac{||\nu_1||^2}{2}}\widetilde{Z}_{\mu_1^{\mathrm{T}}}(q_2,q_1)\widetilde{Z}_{\nu_1}(q_1,q_2)\\
&\quad\times\prod_{k=1}^{\infty}\left[\prod_{(i,j)\in\mu_1}\frac{(1-Q_2Q_\tau^{k-1}q_1^{\nu^{\mathrm{T}}_{1,j}-i+\frac{1}{2}}q_2^{\mu_{1,i}-j+\frac{1}{2}})(1-Q_1Q_\tau^{k-1}q_1^{-\nu^{\mathrm{T}}_{1,j}+i-\frac{1}{2}}q_2^{-\mu_{1,i}+j-\frac{1}{2}})}{(1-Q_\tau^kq_1^{-\mu^{\mathrm{T}}_{1,i}+j-1}q_2^{-\mu_{1,j}+i})(1-Q_\tau^kq_1^{\mu^{\mathrm{T}}_{1,i}-j}q_2^{\mu_{1,j}-i+1})}\right.\\
&\qquad\left.\times\prod_{(i,j)\in\nu_1}\frac{(1-Q_1Q_\tau^{k-1}q_1^{\mu^{\mathrm{T}}_{1,j}-i+\frac{1}{2}}q_2^{\nu_{1,i}-j+\frac{1}{2}})(1-Q_2Q_\tau^{k-1}q_1^{-\mu^{\mathrm{T}}_{1,j}+i-\frac{1}{2}}q_2^{-\nu_{1,i}+j-\frac{1}{2}})}{(1-Q_\tau^kq_1^{-\nu^{\mathrm{T}}_{1,j}+i}q_2^{-\nu_{1,i}+j-1})(1-Q_\tau^kq_1^{\nu^{\mathrm{T}}_{1,j}-i+1}q_2^{\nu_{1,i}-j})}\right].
\end{aligned}
\tag{4.10}
$$

Note that the parts independent of the Young diagrams on the external lines in (4.8) are dropped off by the normalization procedure. This is the wanted contribution of the domain wall in Figure 14.

4.2.2 On TN_2

The second example is one M5-brane on TN_2 for which the web diagram with a specific assignment of Kähler factors is shown in Figure 15. Since there are four vertices and, correspondingly, four Kähler factors, the domain wall partition function $Z^{\nu_1\nu_2}_{\mu_1\mu_2}$ in terms of the refined topological vertex is given by

$$\begin{aligned} Z^{\nu_1\nu_2}_{\mu_1\mu_2}(Q_1,Q_2,Q_3,Q_4;q_1,q_2) = &\sum_{\rho_1,\rho_2,\rho_3,\rho_4} (-Q_1)^{|\rho_1|}(-Q_2)^{|\rho_2|}(-Q_3)^{|\rho_3|}(-Q_4)^{|\rho_4|} \\ &\times C_{\rho_4^{\mathrm{T}}\rho_1\mu_1^{\mathrm{T}}}(q_2,q_1)C_{\rho_2\rho_1^{\mathrm{T}}\nu_1}(q_1,q_2)C_{\rho_2^{\mathrm{T}}\rho_3\mu_2^{\mathrm{T}}}(q_2,q_1)C_{\rho_4\rho_3^{\mathrm{T}}\nu_2}(q_1,q_2). \end{aligned} \tag{4.11}$$

We can translate the skew schur functions in the refined topological vertex into the infinite product over the Young diagrams in the same manner as for the previous case (shown in Appendix C.2). The result has also a factorized form,

$$\begin{aligned} Z^{\nu_1\nu_2}_{\mu_1\mu_2}(Q_1,Q_2,Q_3,Q_4,Q_\tau;q_1,q_2) = &\, q_1^{\frac{||\mu_1^{\mathrm{T}}||^2+||\mu_2^{\mathrm{T}}||^2}{2}} q_2^{\frac{||\nu_1||^2+||\nu_2||^2}{2}} \widetilde{Z}_{\mu_1^{\mathrm{T}}}(q_2,q_1)\widetilde{Z}_{\mu_2^{\mathrm{T}}}(q_2,q_1)\widetilde{Z}_{\nu_2}(q_1,q_2)\widetilde{Z}_{\nu_1}(q_1,q_2) \\ &\times \mathsf{Z}^{\nu_1\nu_2}_{\mu_1\mu_2}(Q_1,Q_2,Q_3,Q_4,Q_\tau;q_1,q_2), \end{aligned} \tag{4.12}$$

where $Q_\tau = Q_1Q_2Q_3Q_4$ (4.6) and the last factor collects the infinite products,

$$\begin{aligned} &\mathsf{Z}^{\nu_1\nu_2}_{\mu_1\mu_2}(Q_1,Q_2,Q_3,Q_4,Q_\tau;q_1,q_2) \\ &= \prod_{n=1}^{\infty}\frac{1}{1-Q_\tau^n}\prod_{i,j,k=1}^{\infty}\Bigg[\frac{(1-Q_2Q_3Q_4Q_\tau^{k-1}q_1^{-\mu^{\mathrm{T}}_{1,j}+i-\frac{1}{2}}q_2^{-\nu_{1,i}+j-\frac{1}{2}})(1-Q_4Q_\tau^{k-1}q_1^{-\mu^{\mathrm{T}}_{1,j}+i-\frac{1}{2}}q_2^{-\nu_{2,i}+j-\frac{1}{2}})}{(1-Q_3Q_4Q_\tau^{k-1}q_1^{-\mu^{\mathrm{T}}_{1,j}+i-1}q_2^{-\mu_{2,i}+j})(1-Q_\tau^k q_1^{-\mu^{\mathrm{T}}_{1,j}+i-1}q_2^{-\mu_{1,i}+j})} \\ &\quad\times\frac{(1-Q_2Q_\tau^{k-1}q_1^{-\mu^{\mathrm{T}}_{2,j}+i-\frac{1}{2}}q_2^{-\nu_{1,i}+j-\frac{1}{2}})(1-Q_1Q_2Q_4Q_\tau^{k-1}q_1^{-\mu^{\mathrm{T}}_{2,j}+i-\frac{1}{2}}q_2^{-\nu_{2,i}+j-\frac{1}{2}})}{(1-Q_1Q_2Q_\tau^{k-1}q_1^{-\mu^{\mathrm{T}}_{2,j}+i-1}q_2^{-\mu_{1,i}+j})(1-Q_\tau^k q_1^{-\mu^{\mathrm{T}}_{2,j}+i-1}q_2^{-\mu_{2,i}+j})} \\ &\quad\times\frac{(1-Q_1Q_\tau^{k-1}q_1^{-\nu^{\mathrm{T}}_{1,j}+i-\frac{1}{2}}q_2^{-\mu_{1,i}+j-\frac{1}{2}})(1-Q_1Q_3Q_4Q_\tau^{k-1}q_1^{-\nu^{\mathrm{T}}_{1,j}+i-\frac{1}{2}}q_2^{-\mu_{2,i}+j-\frac{1}{2}})}{(1-Q_1Q_4Q_\tau^{k-1}q_1^{-\nu^{\mathrm{T}}_{1,j}+i}q_2^{-\nu_{2,i}+j-1})(1-Q_\tau^k q_1^{-\nu^{\mathrm{T}}_{1,j}+i}q_2^{-\nu_{1,i}+j-1})} \\ &\quad\times\frac{(1-Q_1Q_2Q_3Q_\tau^{k-1}q_1^{-\nu^{\mathrm{T}}_{2,j}+i-\frac{1}{2}}q_2^{-\mu_{1,i}+j-\frac{1}{2}})(1-Q_3Q_\tau^{k-1}q_1^{-\nu^{\mathrm{T}}_{2,j}+i-\frac{1}{2}}q_2^{-\mu_{2,i}+j-\frac{1}{2}})}{(1-Q_2Q_3Q_\tau^{k-1}q_1^{-\nu^{\mathrm{T}}_{2,j}+i}q_2^{-\nu_{1,i}+j-1})(1-Q_\tau^k q_1^{-\nu^{\mathrm{T}}_{2,j}+i}q_2^{-\nu_{2,i}+j-1})}\Bigg]. \end{aligned} \tag{4.13}$$

Then, normalizing (4.13) by the one with setting $\mu_1 = \mu_2 = \nu_1 = \nu_2 = \emptyset$ results in the products of these four Young diagrams as

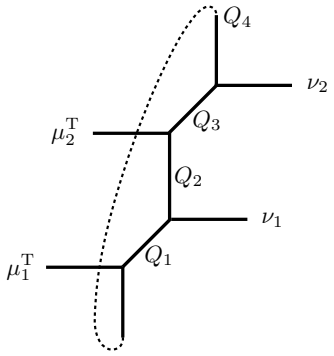

Figure 15: The domain wall corresponding to a single M5-brane on TN_2.

$$
\begin{aligned}
&\widehat{Z}^{\nu_1\nu_2}_{\mu_1\mu_2}(Q_1,Q_2,Q_3,Q_4,Q_\tau;q_1,q_2) := \frac{Z^{\nu_1\nu_2}_{\mu_1\mu_2}(Q_1,Q_2,Q_3,Q_4,Q_\tau;q_1,q_2)}{Z^{\emptyset\emptyset}_{\emptyset\emptyset}(Q_1,Q_2,Q_3,Q_4,Q_\tau;q_1,q_2)} \\
&= q_1^{\frac{||\mu_1^{\mathrm{T}}||^2+||\mu_2^{\mathrm{T}}||^2}{2}} q_2^{\frac{||\nu_1||^2+||\nu_2||^2}{2}} \widetilde{Z}_{\mu_1^{\mathrm{T}}}(q_2,q_1)\widetilde{Z}_{\mu_2^{\mathrm{T}}}(q_2,q_1)\widetilde{Z}_{\nu_1}(q_1,q_2)\widetilde{Z}_{\nu_2}(q_1,q_2) \\
&\quad\times\prod_{k=1}^{\infty}\Bigg[\prod_{(i,j)\in\mu_1}\frac{(1-Q_1Q_\tau^{k-1}q_1^{-\nu^{\mathrm{T}}_{1,j}+i-\frac{1}{2}}q_2^{-\mu_{1,i}+j-\frac{1}{2}})(1-Q_1^{-1}Q_\tau^k q_1^{\nu^{\mathrm{T}}_{1,j}-i+\frac{1}{2}}q_2^{\mu_{1,i}-j+\frac{1}{2}})}{(1-Q_\tau^k q_1^{\mu^{\mathrm{T}}_{1,j}-i}q_2^{\mu_{1,i}-j+1})(1-Q_\tau^k q_1^{-\mu^{\mathrm{T}}_{1,j}+i-1}q_2^{-\mu_{1,i}+j})} \\
&\qquad\times\frac{(1-Q_4Q_\tau^{k-1}q_1^{\nu^{\mathrm{T}}_{2,j}-i+\frac{1}{2}}q_2^{\mu_{1,i}-j+\frac{1}{2}})(1-Q_4^{-1}Q_\tau^k q_1^{-\nu^{\mathrm{T}}_{2,j}+i-\frac{1}{2}}q_2^{-\mu_{1,i}+j-\frac{1}{2}})}{(1-Q_1Q_2Q_\tau^{k-1}q_1^{-\mu^{\mathrm{T}}_{2,j}+i-1}q_2^{-\mu_{1,i}+j})(1-Q_1^{-1}Q_2^{-1}Q_\tau^k q_1^{\mu^{\mathrm{T}}_{2,j}-i}q_2^{\mu_{1,i}-j+1})} \\
&\quad\times\prod_{(i,j)\in\mu_2}\frac{(1-Q_2Q_\tau^{k-1}q_1^{\nu^{\mathrm{T}}_{1,j}-i+\frac{1}{2}}q_2^{\mu_{2,i}-j+\frac{1}{2}})(1-Q_2^{-1}Q_\tau^k q_1^{-\nu^{\mathrm{T}}_{1,j}+i-\frac{1}{2}}q_2^{-\mu_{2,i}+j-\frac{1}{2}})}{(1-Q_\tau^k q_1^{-\mu^{\mathrm{T}}_{2,j}+i-1}q_2^{-\mu_{2,i}+j})(1-Q_\tau^k q_1^{\mu^{\mathrm{T}}_{2,j}-i}q_2^{\mu_{2,i}-j+1})} \\
&\qquad\times\frac{(1-Q_3Q_\tau^{k-1}q_1^{-\nu^{\mathrm{T}}_{2,j}+i-\frac{1}{2}}q_2^{-\mu_{2,i}+j-\frac{1}{2}})(1-Q_3^{-1}Q_\tau^k q_1^{\nu^{\mathrm{T}}_{2,j}-i+\frac{1}{2}}q_2^{\mu_{2,i}-j+\frac{1}{2}})}{(1-Q_3Q_4Q_\tau^{k-1}q_1^{-\mu^{\mathrm{T}}_{1,j}+i-1}q_2^{-\mu_{2,i}+j})(1-Q_3^{-1}Q_4^{-1}Q_\tau^k q_1^{\mu^{\mathrm{T}}_{1,j}-i}q_2^{\mu_{2,i}-j+1})} \\
&\quad\times\prod_{(i,j)\in\nu_1}\frac{(1-Q_1Q_\tau^{k-1}q_1^{\mu^{\mathrm{T}}_{1,j}-i+\frac{1}{2}}q_2^{\nu_{1,i}-j+\frac{1}{2}})(1-Q_1^{-1}Q_\tau^k q_1^{-\mu^{\mathrm{T}}_{1,j}+i-\frac{1}{2}}q_2^{-\nu_{1,i}+j-\frac{1}{2}})}{(1-Q_\tau^k q_1^{-\nu^{\mathrm{T}}_{1,j}+i}q_2^{-\nu_{1,i}+j-1})(1-Q_\tau^k q_1^{\nu^{\mathrm{T}}_{1,j}-i+1}q_2^{\nu_{1,i}-j})} \\
&\qquad\times\frac{(1-Q_2Q_\tau^{k-1}q_1^{-\mu^{\mathrm{T}}_{2,j}+i-\frac{1}{2}}q_2^{-\nu_{1,i}+j-\frac{1}{2}})(1-Q_2^{-1}Q_\tau^k q_1^{\mu^{\mathrm{T}}_{2,j}-i+\frac{1}{2}}q_2^{\nu_{1,i}-j+\frac{1}{2}})}{(1-Q_2Q_3Q_\tau^{k-1}q_1^{-\nu^{\mathrm{T}}_{2,j}+i}q_2^{-\nu_{1,i}+j-1})(1-Q_2^{-1}Q_3^{-1}Q_\tau^k q_1^{\nu^{\mathrm{T}}_{2,j}-i+1}q_2^{\nu_{1,i}-j})} \\
&\quad\times\prod_{(i,j)\in\nu_2}\frac{(1-Q_3Q_\tau^{k-1}q_1^{\mu^{\mathrm{T}}_{2,j}-i+\frac{1}{2}}q_2^{\nu_{2,i}-j+\frac{1}{2}})(1-Q_3^{-1}Q_\tau^k q_1^{-\mu^{\mathrm{T}}_{2,j}+i-\frac{1}{2}}q_2^{-\nu_{2,i}+j-\frac{1}{2}})}{(1-Q_\tau^k q_1^{-\nu^{\mathrm{T}}_{2,j}+i}q_2^{-\nu_{2,i}+j-1})(1-Q_\tau^k q_1^{\nu^{\mathrm{T}}_{2,j}-i+1}q_2^{\nu_{2,i}-j})} \\
&\qquad\times\frac{(1-Q_4Q_\tau^{k-1}q_1^{-\mu^{\mathrm{T}}_{1,j}+i-\frac{1}{2}}q_2^{-\nu_{2,i}+j-\frac{1}{2}})(1-Q_4^{-1}Q_\tau^k q_1^{\mu^{\mathrm{T}}_{1,j}-i+\frac{1}{2}}q_2^{\nu_{2,i}-j+\frac{1}{2}})}{(1-Q_1Q_4Q_\tau^{k-1}q_1^{-\nu^{\mathrm{T}}_{1,j}+i}q_2^{-\nu_{2,i}+j-1})(1-Q_1^{-1}Q_4^{-1}Q_\tau^k q_1^{\nu^{\mathrm{T}}_{1,j}-i+1}q_2^{\nu_{2,i}-j})}\Bigg].
\end{aligned}
\tag{4.14}
$$

This domain wall partition function for Figure 15 will be made use of in Section 5.2 to evaluate the contribution from a codimension-2 defect to M-strings.

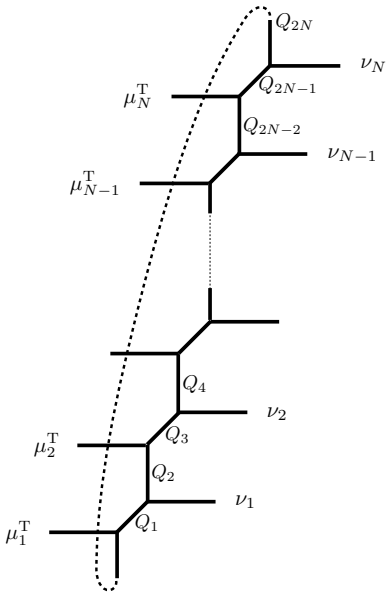

Figure 16: The domain wall corresponding to a single M5-brane on TN_N.

4.2.3 On TN_N

Finally, for general usage, we would like to write down the domain wall partition function for the web diagram with generic N shown as Figure 16. The joint of $2N$ vertices can be written in the following expression:

$$Z^{\nu_1\nu_2\cdots\nu_N}_{\mu_1\mu_2\cdots\mu_N}(Q_i;q_1,q_2)=\sum_{\{\rho_i\}}\prod_{a=1}^{N}(-Q_{2a-1})^{|\rho_{2a-1}|}(-Q_{2a})^{|\rho_{2a}|}C_{\rho^{\mathrm{T}}_{2a-2}\rho_{2a-1}\mu^{\mathrm{T}}_a}(q_2,q_1)C_{\rho_{2a}\rho^{\mathrm{T}}_{2a-1}\nu_a}(q_1,q_2), \tag{4.15}$$

where $\{\rho_i\}_{i=1,2,\cdots,2N}=\{\rho_{2a-1},\,\rho_{2a}\}_{a=1,2,\cdots,N}$ and the indices of the Kähler factors and the Young diagrams are defined modulo $2N$. We can generalize the process to deform the partition function used in the above examples, which leads to the nicely factorized form,

$$\begin{aligned}
&Z^{\nu_1\nu_2\cdots\nu_N}_{\mu_1\mu_2\cdots\mu_N}(Q_i,Q_\tau;q_1,q_2)\\
&=\left[\prod_{a=1}^{N}q_1^{\frac{||\mu_a^{\mathrm{T}}||^2}{2}}q_2^{\frac{||\nu_a||^2}{2}}\widetilde{Z}_{\mu_a^{\mathrm{T}}}(q_2,q_1)\widetilde{Z}_{\nu_a}(q_1,q_2)\right]\\
&\quad\times\prod_{a,b=1}^{N}\prod_{i,j,k=1}^{\infty}\frac{1}{(1-Q_\tau^k)}\frac{\left(1-Q_\tau^{k-1}\mathsf{Q}'_{ba}q_1^{-\mu^{\mathrm{T}}_{a,j}+i-\frac{1}{2}}q_2^{-\nu_{b,i}+j-\frac{1}{2}}\right)\left(1-Q_\tau^{k-1}\mathsf{Q}_{ab}q_1^{-\nu^{\mathrm{T}}_{b,j}+i-\frac{1}{2}}q_2^{-\mu_{a,i}+j-\frac{1}{2}}\right)}{\left(1-Q_\tau^{k-1}\widetilde{\mathsf{Q}}_{ab}q_1^{-\mu^{\mathrm{T}}_{b,j}+i-1}q_2^{-\mu_{a,i}+j}\right)\left(1-Q_\tau^{k-1}\widetilde{\mathsf{Q}}'_{ab}q_1^{-\nu^{\mathrm{T}}_{b,j}+i}q_2^{-\nu_{a,i}+j-1}\right)},
\end{aligned} \tag{4.16}$$

where Q_τ is precisely (4.6), and Q_{ab}, Q'_{ba}, $\widetilde{\mathsf{Q}}_{ab}$, and $\widetilde{\mathsf{Q}}'_{ab}$ are the products of some set of the Kähler factors, as summarized in Table 4. Note that there are simple relations, $\mathsf{Q}_{ab}\mathsf{Q}'_{ba}=Q_\tau$

	$a<b$	$a=b$	$a>b$
Q_{ab}	$\prod_{s=2a-1}^{2b-1} Q_s$	Q_{2a-1}	$\prod_{s=1}^{2b-1} Q_s \prod_{s'=2a-1}^{2N} Q_{s'}$
Q'_{ab}	$\prod_{s=2a}^{2b-2} Q_s$	$Q_\tau Q_{2a-1}^{-1}$	$\prod_{s=1}^{2b-2} Q_s \prod_{s'=2a}^{2N} Q_{s'}$
$\widetilde{\mathsf{Q}}_{ab}$	$\prod_{s=2a-1}^{2b-2} Q_s$	Q_τ	$\prod_{s=1}^{2b-2} Q_s \prod_{s'=2a-1}^{2N} Q_{s'}$
$\widetilde{\mathsf{Q}}'_{ab}$	$\prod_{s=2a}^{2b-1} Q_s$	Q_τ	$\prod_{s=1}^{2b-1} Q_s \prod_{s'=2a}^{2N} Q_{s'}$

Table 4: The products of Kähler factors.

and $Q_{2a-1}\widetilde{\mathsf{Q}}_{ab} = Q_{2b-1}\widetilde{\mathsf{Q}}'_{ab}$. We visualize which region of the consecutive Kähler factors is included in each one of Table 4 as Figure 17 and 18.

As the final step, the normalization of the domain wall partition function (4.16) for general N provides

$$\begin{aligned}
&\widehat{Z}^{\nu_1\nu_2\cdots\nu_N}_{\mu_1\mu_2\cdots\mu_N}(Q_i,Q_\tau;q_1,q_2)\\
&:=\frac{Z^{\nu_1\nu_2\cdots\nu_N}_{\mu_1\mu_2\cdots\mu_N}(Q_i,Q_\tau;q_1,q_2)}{Z^{\emptyset\emptyset\cdots\emptyset}_{\emptyset\emptyset\cdots\emptyset}(Q_i,Q_\tau;q_1,q_2)}\\
&=\left[\prod_{a=1}^{N} q^{\frac{||\mu_a^{\mathrm{T}}||^2}{2}} t^{\frac{||\nu_a||^2}{2}} \tilde{Z}_{\mu_a^{\mathrm{T}}}(q_2,q_1)\tilde{Z}_{\nu_a}(q_1,q_2)\right]\\
&\quad\times\prod_{a,b=1}^{N}\prod_{k=1}^{\infty}\prod_{(i,j)\in\mu_a}\frac{\left(1-Q_\tau^{k-1}\mathsf{Q}'_{ba}q_1^{\nu^{\mathrm{T}}_{b,j}-i+\frac{1}{2}}q_2^{\mu_{a,i}-j+\frac{1}{2}}\right)\left(1-Q_\tau^{k-1}\mathsf{Q}_{ab}q_1^{-\nu^{\mathrm{T}}_{b,j}+i-\frac{1}{2}}q_2^{-\mu_{a,i}+j-\frac{1}{2}}\right)}{\left(1-Q_\tau^{k-1}\widetilde{\mathsf{Q}}_{ba}q_1^{\mu^{\mathrm{T}}_{b,j}-i}q_2^{\mu_{a,i}-j+1}\right)\left(1-Q_\tau^{k-1}\widetilde{\mathsf{Q}}_{ab}q_1^{-\mu^{\mathrm{T}}_{b,j}+i-1}q_2^{-\mu_{a,i}+j}\right)}\\
&\qquad\times\prod_{(i,j)\in\nu_b}\frac{\left(1-Q_\tau^{k-1}\mathsf{Q}'_{ba}q_1^{-\mu^{\mathrm{T}}_{a,j}+i-\frac{1}{2}}q_2^{-\nu_{b,i}+j-\frac{1}{2}}\right)\left(1-Q_\tau^{k-1}\mathsf{Q}_{ab}q_1^{\mu^{\mathrm{T}}_{a,j}-i+\frac{1}{2}}q_2^{\nu_{b,i}-j+\frac{1}{2}}\right)}{\left(1-Q_\tau^{k-1}\widetilde{\mathsf{Q}}'_{ab}q_1^{\nu^{\mathrm{T}}_{a,j}-i+1}q_2^{\nu_{b,i}-j}\right)\left(1-Q_\tau^{k-1}\widetilde{\mathsf{Q}}'_{ba}q_1^{-\nu^{\mathrm{T}}_{a,j}+i}q_2^{-\nu_{b,i}+j-1}\right)}.
\end{aligned}\tag{4.17}$$

This is the general formula for the contributions of the domain wall, and we can also derive the general partition function of M-strings by gluing (4.17) M times which is the number of domain walls.

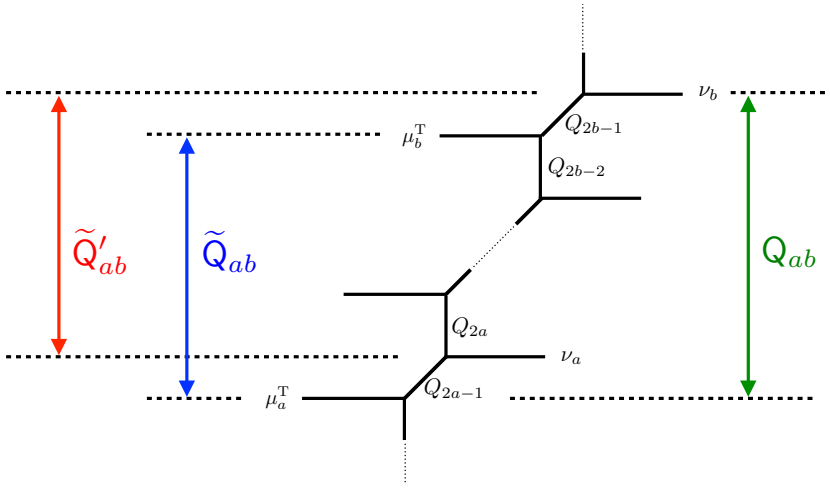

Figure 17: Q_{ab}, $\widetilde{\mathsf{Q}}_{ab}$, $\widetilde{\mathsf{Q}}'_{ab}$ for $a > b$. Each is a product of the Kähler factors in the region covered by the corresponding colored up-and-down arrow.

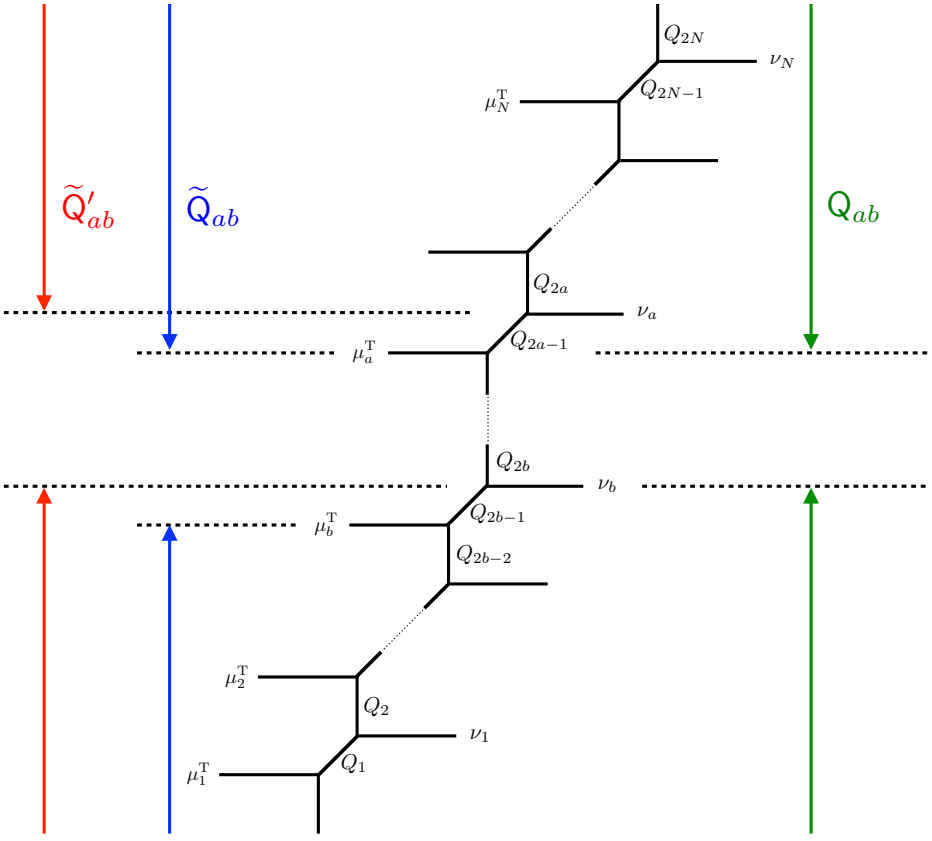

Figure 18: Q_{ab}, $\widetilde{\mathsf{Q}}_{ab}$, $\widetilde{\mathsf{Q}}'_{ab}$ for $a < b$. Each is shown in the same manner as in Figure 17.

4.3 M-string contributions

Let us turn to computing the M-string partition function that should be a quantity for the BPS states captured by M-strings on the world-volume of the M5-branes. It actually turns out that the quantity obtained simply by combining the domain wall partition functions becomes the form of a generating function $G_{(M,N)}$ of M-strings. In what follows, we will denote the partition function of k M-strings with M M5-branes on TN_N as $\mathcal{Z}_{(M,N,k)}$. As described in Appendix B, when connecting the external edges of the domain walls, we need to assign a Kähler factor Q_f and a Young diagram μ on each glued segment of the web diagram and sum over μ. Therefore, gluing the domain wall partition functions computed above provides schematically the following generating function:

$$G_{(M,N)}(Q_i, Q_f; q_1, q_2) = \sum_{k=0}^{\infty} \sum_{|\mu|=k} (-Q_f)^{|\mu|} \mathcal{Z}_{(M,N,k)}(Q_i; q_1, q_2), \tag{4.18}$$

where the summation of $|\mu| = k$ means that it is taken over possible Young diagrams with the number of boxes being k. The appearance of this sum naturally reflects the fact that the ground state of k M2-branes ending on the M5-brane is parametrized by the partitions of k as drawn in Figure 11. We will use the Kähler factor Q_f to characterize $\mathbb{C}\mathbf{P}^1$ depicted as the horizontal internal segment on the we diagram that corresponds to the finite extent of the M2-brane along the 6 direction.

Here, we introduce an additional index on Kähler factors Q_i and Young diagrams μ_a to label the number of the M5-branes so that

$$Q_{2a-1}^{(\mathfrak{a})},\ Q_{2a}^{(\mathfrak{a})},\ \mu_a^{(\mathfrak{a})} \quad \text{for } a = 1, 2, \cdots, N, \text{ and } \mathfrak{a} = 1, 2, \cdots, M. \tag{4.19}$$

From now on, we use German letters $\mathfrak{a}, \mathfrak{b}, \ldots$ for the number of the domain walls. With this convention, we arrange three conditions which have to be imposed on Kähler factors to consistently glue the domain walls.

- The only one compactification radius along the vertical axis,

$$Q_\tau = \prod_{i=1}^{2N} Q_i^{(\mathfrak{a})} = \mathsf{Q}_{ab}^{(\mathfrak{a})} \mathsf{Q}'^{(\mathfrak{a})}_{ba} \quad \text{for } \forall \mathfrak{a}. \tag{4.20}$$

- The net effect of resolving the singularities is the mass deformation,

$$e^{2\pi i m} = Q_m = \prod_{a=1}^{N} Q_{2a-1}^{(\mathfrak{a})} \quad \text{for } \forall \mathfrak{a}. \tag{4.21}$$

- For each hexagon, the total length of the compactified direction should be the same,

$$Q_{2a}^{(\mathfrak{a})} Q_{2a+1}^{(\mathfrak{a})} = Q_{2a-1}^{(\mathfrak{a}+1)} Q_{2a}^{(\mathfrak{a}+1)}. \tag{4.22}$$

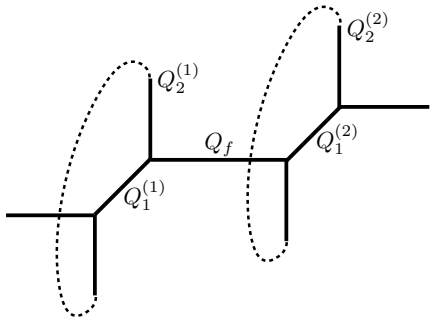

Figure 19: The web diagram corresponding to M-strings with two M5-branes on TN_1.

Note that any condition on $Q_{f,a}^{(\mathfrak{a})}$ for the horizontal internal segments does not occur. Moreover, to avoid the equations being indistinct, we define

$$\overline{Q}_i^{(\mathfrak{a})} := \left(Q_i^{(\mathfrak{a})}\right)^{-1}. \tag{4.23}$$

4.3.1 The simplest case

The simplest example to demonstrate the calculation is the M-strings with $(M,N)=(2,1)$. The corresponding web diagram is obtained as in Figure 19 by gluing two domain walls of Figure 14 with setting a Kähler factor Q_f on the line connecting them. Accordingly, we have to multiply two domain wall partition functions of (4.10) to derive the partition function of M-strings, which gives

$$\begin{aligned}
G_{(2,1)}(Q_i^{(\mathfrak{a})},Q_\tau;q_1,q_2) &= \sum_\mu (-Q_f)^{|\mu|}\widehat{Z}_\emptyset^\mu(Q_1^{(1)},Q_2^{(1)},Q_\tau;q_1,q_2)\widehat{Z}_\mu^\emptyset(Q_1^{(2)},Q_2^{(2)},Q_\tau;q_1,q_2)\\
&= \sum_\mu (-Q_f)^{|\mu|} q_1^{\frac{||\mu^{\mathrm{T}}||^2}{2}} q_2^{\frac{||\mu||^2}{2}} \widetilde{Z}_{\mu^{\mathrm{T}}}(q_2,q_1)\widetilde{Z}_\mu(q_1,q_2)\\
&\quad\times \prod_{k=1}^\infty \prod_{(i,j)\in\mu} \frac{(1-Q_1^{(1)}Q_\tau^{k-1}q_1^{-i+\frac12}q_2^{\mu_i-j+\frac12})(1-Q_2^{(1)}Q_\tau^{k-1}q_1^{i-\frac12}q_2^{-\mu_i+j-\frac12})}{(1-Q_\tau^k q_1^{-\mu_j^{\mathrm{T}}+i}q_2^{-\mu_i+j-1})(1-Q_\tau^k q_1^{\mu_j^{\mathrm{T}}-i+1}q_2^{\mu_i-j})}\\
&\qquad\times \frac{(1-Q_2^{(2)}Q_\tau^{k-1}q_1^{-i+\frac12}q_2^{\mu_i-j+\frac12})(1-Q_1^{(2)}Q_\tau^{k-1}q_1^{i-\frac12}q_2^{-\mu_i+j-\frac12})}{(1-Q_\tau^k q_1^{-\mu_j^{\mathrm{T}}+i-1}q_2^{-\mu_i+j})(1-Q_\tau^k q_1^{\mu_j^{\mathrm{T}}-i}q_2^{\mu_i-j+1})}.
\end{aligned} \tag{4.24}$$

Here note that the condition for the unique compactified radius (4.20) becomes

$$Q_\tau = Q_1^{(1)}Q_2^{(1)} = Q_1^{(2)}Q_2^{(2)}, \tag{4.25}$$

and the resolution by the mass deformation (4.21) imposes the relation

$$Q_m = Q_1^{(1)} = Q_1^{(2)}. \tag{4.26}$$

The third condition (4.22) does not occur because the web diagram of Figure 19 does not have a hexagonal loop. The existence of the infinite product over k is actually a key to recast these terms in $G_{(2,1)}$ into the elliptic theta function $\theta_1(x;Q_\tau)$ of the complex modulus Q_τ by means of the Jacobi's tuple product identity (A.56). In the following, whenever its complex modulus is Q_τ, we will use an abbreviated notation $\theta_1(x)$ unless otherwise stated. We would here perform how this recasting works and show that we can generalize it systematically to the example below. Indeed, since there is a slight difference between the numerator and denominator to generate the theta function, we would like to consider separately them.

• The numerator of (4.24): first of all, we use the relation (4.25),

$$\begin{aligned}
\mathsf{G}^{\rm num}_{(2,1)} &:= \prod_{k=1}^{\infty}\prod_{(i,j)\in\mu}\left(1-Q_1^{(1)}Q_\tau^{k-1}q_1^{-i+\frac{1}{2}}q_2^{\mu_i-j+\frac{1}{2}}\right)\left(1-Q_2^{(1)}Q_\tau^{k-1}q_1^{i-\frac{1}{2}}q_2^{-\mu_i+j-\frac{1}{2}}\right)\\
&\qquad\times\left(1-Q_2^{(2)}Q_\tau^{k-1}q_1^{-i+\frac{1}{2}}q_2^{\mu_i-j+\frac{1}{2}}\right)\left(1-Q_1^{(2)}Q_\tau^{k-1}q_1^{i-\frac{1}{2}}q_2^{-\mu_i+j-\frac{1}{2}}\right)\\
&=\prod_{k=1}^{\infty}\prod_{(i,j)\in\mu}\left(1-Q_1^{(1)}Q_\tau^{k-1}q_1^{-i+\frac{1}{2}}q_2^{\mu_i-j+\frac{1}{2}}\right)\left(1-\overline{Q}_1^{(1)}Q_\tau^{k}q_1^{i-\frac{1}{2}}q_2^{-\mu_i+j-\frac{1}{2}}\right)\\
&\qquad\times\left(1-\overline{Q}_1^{(2)}Q_\tau^{k}q_1^{-i+\frac{1}{2}}q_2^{\mu_i-j+\frac{1}{2}}\right)\left(1-Q_1^{(2)}Q_\tau^{k-1}q_1^{i-\frac{1}{2}}q_2^{-\mu_i+j-\frac{1}{2}}\right).
\end{aligned}\tag{4.27}$$

Comparing this with the definition of $\theta_1(x;p)$ of multiplicative variables (A.55), the terms coming from the same domain wall could be brought together with the infinite product of k into the Jacobi's triple product identity (A.56). With this observation, we concentrate on the factors of the first domain wall (i.e. including only $Q_a^{(1)}$),

$$\prod_{k=1}^{\infty}\left(1-Q_1^{(1)}Q_\tau^{k-1}q_1^{-i+\frac{1}{2}}q_2^{\mu_i-j+\frac{1}{2}}\right)\left(1-\overline{Q}_1^{(1)}Q_\tau^{k}q_1^{i-\frac{1}{2}}q_2^{-\mu_i+j-\frac{1}{2}}\right)=\frac{\theta_1\left(\overline{Q}_1^{(1)}q_1^{i-\frac{1}{2}}q_2^{-\mu_i+j-\frac{1}{2}}\right)}{-iQ_\tau^{\frac{1}{8}}\left(\overline{Q}_1^{(1)}q_1^{i-\frac{1}{2}}q_2^{-\mu_i+j-\frac{1}{2}}\right)^{\frac{1}{2}}(Q_\tau;Q_\tau)_\infty},\tag{4.28}$$

where $(x;p)_\infty$ is the q-Pochhammer symbol (or the q-shifted factorial) defined in (A.60). The remaining factors from the second domain wall can be straightforwardly transformed into the elliptic theta function in the same manner, hence, we have

$$\begin{aligned}
\mathsf{G}^{\rm num}_{(2,1)} &= \prod_{(i,j)\in\mu}\left(\frac{1}{iQ_\tau^{\frac{1}{8}}(Q_\tau;Q_\tau)_\infty}\right)^2\frac{\theta_1\left(\overline{Q}_1^{(1)}q_1^{i-\frac{1}{2}}q_2^{-\mu_i+j-\frac{1}{2}}\right)\theta_1\left(\overline{Q}_1^{(2)}q_1^{-i+\frac{1}{2}}q_2^{\mu_i-j+\frac{1}{2}}\right)}{\left(\overline{Q}_1^{(1)}q_1^{i-\frac{1}{2}}q_2^{-\mu_i+j-\frac{1}{2}}\right)^{\frac{1}{2}}\left(\overline{Q}_1^{(2)}q_1^{-i+\frac{1}{2}}q_2^{\mu_i-j+\frac{1}{2}}\right)^{\frac{1}{2}}}\\
&=\left(Q_1^{(1)}Q_1^{(2)}\right)^{\frac{|\mu|}{2}}\prod_{(i,j)\in\mu}\left(\frac{1}{iQ_\tau^{\frac{1}{8}}(Q_\tau;Q_\tau)_\infty}\right)^2\theta_1\left(\overline{Q}_1^{(1)}q_1^{i-\frac{1}{2}}q_2^{-\mu_i+j-\frac{1}{2}}\right)\theta_1\left(\overline{Q}_1^{(2)}q_1^{-i+\frac{1}{2}}q_2^{\mu_i-j+\frac{1}{2}}\right).
\end{aligned}\tag{4.29}$$

Note that the first factor in the product of μ that does not contain (q_1, q_2) will be simply cancelled with that of the denominator.

• The denominator of (4.24): we bring the functions $\widetilde{Z}_{\mu^{\mathrm{T}}}\widetilde{Z}_{\mu}$ together,

$$\mathsf{G}^{\mathrm{den}}_{(2,1)} := \frac{1}{\widetilde{Z}_{\mu^{\mathrm{T}}}(q_2,q_1)\widetilde{Z}_{\mu}(q_1,q_2)} \prod_{k=1}^{\infty}\prod_{(i,j)\in\mu} \underbrace{(1-Q_\tau^k q_1^{-\mu_j^{\mathrm{T}}+i} q_2^{-\mu_i+j-1})}_{\text{(1-i)}} \underbrace{(1-Q_\tau^k q_1^{\mu_j^{\mathrm{T}}-i+1} q_2^{\mu_i-j})}_{\text{(1-ii)}}$$
$$\times \underbrace{(1-Q_\tau^k q_1^{-\mu_j^{\mathrm{T}}+i-1} q_2^{-\mu_i+j})}_{\text{(2-i)}} \underbrace{(1-Q_\tau^k q_1^{\mu_j^{\mathrm{T}}-i} q_2^{\mu_i-j+1})}_{\text{(2-ii)}}, \quad (4.30)$$

where the terms labeled by (1-i), (1-ii) originally belong to the first domain wall and ones labeled by (2-i), (2-ii) to the second domain wall. The situation differs from the numerator. The factors in the first line of the infinite product cannot be directly combined into the elliptic theta function via the Jacobi's triple product identity because the powers of q_1 and q_2 do not match; we can incorporate terms which include the same power of variables. In the present case, the combination of the terms (1-ii) and (2-i) is adequate to do this, and also that of the terms (1-i) and (2-ii) is. Substituting the definition of $\widetilde{Z}_{\mu}(q_1,q_2)$ given in (B.8), the former is deformed as

$$\begin{aligned}
&\frac{1}{\widetilde{Z}_{\mu}(q_1,q_2)} \prod_{k=1}^{\infty}\prod_{(i,j)\in\mu} \underbrace{(1-Q_\tau^k q_1^{\mu_j^{\mathrm{T}}-i+1} q_2^{\mu_i-j})}_{\text{(1-ii)}} \underbrace{(1-Q_\tau^k q_1^{-\mu_j^{\mathrm{T}}+i-1} q_2^{-\mu_i+j})}_{\text{(2-i)}} \\
&= \prod_{(i,j)\in\mu} \left(1-q_1^{\mu_j^{\mathrm{T}}-i+1} q_2^{\mu_i-j}\right) \prod_{k=1}^{\infty} (1-Q_\tau^k q_1^{\mu_j^{\mathrm{T}}-i+1} q_2^{\mu_i-j})(1-Q_\tau^k q_1^{-\mu_j^{\mathrm{T}}+i-1} q_2^{-\mu_i+j}) \\
&= \prod_{(i,j)\in\mu} \prod_{k=1}^{\infty} (1-Q_\tau^{k-1} q_1^{\mu_j^{\mathrm{T}}-i+1} q_2^{\mu_i-j})(1-Q_\tau^k q_1^{-\mu_j^{\mathrm{T}}+i-1} q_2^{-\mu_i+j}) \\
&= \prod_{(i,j)\in\mu} \frac{\theta_1\left(q_1^{-\mu_j^{\mathrm{T}}+i-1} q_2^{-\mu_i+j}\right)}{-iQ_\tau^{\frac{1}{8}}\left(q_1^{-\mu_j^{\mathrm{T}}+i-1} q_2^{-\mu_i+j}\right)^{\frac{1}{2}} (Q_\tau;Q_\tau)_\infty^3},
\end{aligned} \quad (4.31)$$

Similarly, the other set of the terms (1-i), (2-ii), and $\widetilde{Z}_{\mu^{\mathrm{T}}}(q_2,q_1)$ can generate a single elliptic theta function. As a result, we obtain

$$\begin{aligned}
\mathsf{G}^{\mathrm{den}}_{(2,1)} &= \prod_{(i,j)\in\mu} \left(\frac{1}{iQ_\tau^{\frac{1}{8}}(Q_\tau;Q_\tau)_\infty^3}\right)^2 \frac{\theta_1\left(q_1^{-\mu_j^{\mathrm{T}}+i-1} q_2^{-\mu_i+j}\right)\theta_1\left(q_1^{-\mu_j^{\mathrm{T}}+i} q_2^{-\mu_i+j-1}\right)}{\left(q_1^{-\mu_j^{\mathrm{T}}+i-1} q_2^{-\mu_i+j}\right)^{\frac{1}{2}}\left(q_1^{-\mu_j^{\mathrm{T}}+i} q_2^{-\mu_i+j-1}\right)^{\frac{1}{2}}} \\
&= q_1^{\frac{||\mu^{\mathrm{T}}||^2}{2}} q_2^{\frac{||\mu||^2}{2}} \prod_{(i,j)\in\mu} \left(\frac{1}{iQ_\tau^{\frac{1}{8}}(Q_\tau;Q_\tau)_\infty^3}\right)^2 \theta_1\left(q_1^{-\mu_j^{\mathrm{T}}+i-1} q_2^{-\mu_i+j}\right)\theta_1\left(q_1^{-\mu_j^{\mathrm{T}}+i} q_2^{-\mu_i+j-1}\right),
\end{aligned} \quad (4.32)$$

where, in the last line, we used the formulae (A.4) and (A.5) to pull out the prefactors of q_1 and q_2. As we commented, the first factor independent of (q_1, q_2) in the product of μ cancels the one that appears in the numerator (4.29). We should remark that the calculation process for the denominator here happens for the general case. A term in a certain domain wall is combined with the one coming from the nearest neighbor domain wall into $\theta_1(x)$ (see details in Appendix C.4).

Now, we are in the stage to write down the partition function of M-strings. Getting $\mathsf{G}^{\rm num}_{(2,1)}$ and $\mathsf{G}^{\rm den}_{(2,1)}$ back into the generating function (4.24) leads to

$$\begin{aligned}
&G_{(2,1)}(Q_m, Q_\tau, Q_f; q_1, q_2) \\
&= \sum_\mu (-Q_f)^{|\mu|} q_1^{\frac{||\mu^{\rm T}||^2}{2}} q_2^{\frac{||\mu||^2}{2}} \frac{\mathsf{G}^{\rm num}_{(2,1)}}{\mathsf{G}^{\rm den}_{(2,1)}} \\
&= \sum_\mu \left(-Q_f \sqrt{Q_1^{(1)} Q_1^{(2)}}\right)^{|\mu|} \prod_{(i,j)\in\mu} \frac{\theta_1\left(\overline{Q}_1^{(1)} q_1^{i-\frac{1}{2}} q_2^{-\mu_i+j-\frac{1}{2}}\right) \theta_1\left(\overline{Q}_1^{(2)} q_1^{-i+\frac{1}{2}} q_2^{\mu_i-j+\frac{1}{2}}\right)}{\theta_1\left(q_1^{-\mu_j^{\rm T}+i-1} q_2^{-\mu_i+j}\right) \theta_1\left(q_1^{-\mu_j^{\rm T}+i} q_2^{-\mu_i+j-1}\right)} \\
&= \sum_\mu (-Q_f Q_m)^{|\mu|} \prod_{(i,j)\in\mu} \frac{\theta_1\left(Q_m^{-1} q_1^{i-\frac{1}{2}} q_2^{-\mu_i+j-\frac{1}{2}}\right) \theta_1\left(Q_m^{-1} q_1^{-i+\frac{1}{2}} q_2^{\mu_i-j+\frac{1}{2}}\right)}{\theta_1\left(q_1^{-\mu_j^{\rm T}+i-1} q_2^{-\mu_i+j}\right) \theta_1\left(q_1^{-\mu_j^{\rm T}+i} q_2^{-\mu_i+j-1}\right)},
\end{aligned} \tag{4.33}$$

where the condition (4.26) is put in. This is precisely the form of the generating function as (4.18). From this expression, we can simply extract the partition function of k M-strings,

$$\mathcal{Z}_{(2,1,k)}(Q_m, Q_\tau; q_1, q_2) = \sum_{|\mu|=k} \prod_{(i,j)\in\mu} \frac{\theta_1\left(Q_m^{-1} q_1^{i-\frac{1}{2}} q_2^{-\mu_i+j-\frac{1}{2}}\right) \theta_1\left(Q_m^{-1} q_1^{-i+\frac{1}{2}} q_2^{\mu_i-j+\frac{1}{2}}\right)}{\theta_1\left(q_1^{-\mu_j^{\rm T}+i-1} q_2^{-\mu_i+j}\right) \theta_1\left(q_1^{-\mu_j^{\rm T}+i} q_2^{-\mu_i+j-1}\right)}. \tag{4.34}$$

This function equipped with the theta function is expected since M-strings are now compactified on the torus T^2 and its partition function should have the elliptic property that is usually realized as the theta function as for many situations in physics. At this point, τ defined in (4.6) is smoothly identified with the complex modulus of T^2. The reason to hold this identification is roughly that the complex modulus is mapped into the size of the elliptic fibration in CY3 [32]. Although it is not really trivial that the theta function arises from the refined topological vertex, its emergence strongly supports us to correctly produce the contribution of M-strings.

The limit $m = \frac{1}{2}(\epsilon_1 + \epsilon_2)$

We would consider a certain limit on the M-string partition function to see supersymmetry enhancement as commented in the last of Section 3. At fist, by using the formula (A.12), we rewrite the numerator of (4.34) as

$$\mathcal{Z}_{(2,1,k)}(Q_m, Q_\tau; q_1, q_2) = \sum_{|\mu|=k} \prod_{(i,j)\in\mu} \frac{\theta_1\left(Q_m^{-1} q_1^{i-\frac{1}{2}} q_2^{-j+\frac{1}{2}}\right) \theta_1\left(Q_m^{-1} q_1^{-i+\frac{1}{2}} q_2^{j-\frac{1}{2}}\right)}{\theta_1\left(q_1^{-\mu_j^{\mathrm{T}}+i-1} q_2^{-\mu_i+j}\right) \theta_1\left(q_1^{-\mu_j^{\mathrm{T}}+i} q_2^{-\mu_i+j-1}\right)}. \tag{4.35}$$

Here, we concentrate on the following limit:

$$m = \frac{1}{2}(\epsilon_1 + \epsilon_2) \quad \Leftrightarrow \quad Q_m = \sqrt{\frac{q_1}{q_2}}. \tag{4.36}$$

Substituting this specialization into (4.35), we have

$$\mathcal{Z}_{(2,1,k)}(Q_\tau; q_1, q_2) = \sum_{|\mu|=k} \prod_{(i,j)\in\mu} \frac{\theta_1\left(q_1^{i-1} q_2^{-j+1}\right) \theta_1\left(q_1^{-i} q_2^{j}\right)}{\theta_1\left(q_1^{-\mu_j^{\mathrm{T}}+i-1} q_2^{-\mu_i+j}\right) \theta_1\left(q_1^{-\mu_j^{\mathrm{T}}+i} q_2^{-\mu_i+j-1}\right)}. \tag{4.37}$$

As a result, the above partition function vanishes if the Young diagram μ contains at most one box, $(i, j) = (1, 1)$ because

$$\theta_1(q_1^{i-1} q_2^{-j+1}; Q_\tau) = \theta_1(1; Q_\tau) = 0$$

for the first theta function in the numerator. This sequence is interpreted as the emergence of fermion zero-modes [32] which corresponds to an overall U(1) of U(k) and really the center of mass degree of freedom of the M-strings on the M5-branes. We need get rid of this contribution in order to still retain the nontrivial partition function. A simple treatment which does not exclude other contributions from the M-strings is to divide $\mathcal{Z}_{(2,1,k)}$ (4.37) by $\mathcal{Z}_{(2,1,1)}$ the partition function of a single M-string and then do the limit (4.36). Namely,

$$\widehat{\mathcal{Z}}_{(2,1,k)}(Q_\tau; q_1, q_2) := \left.\frac{\mathcal{Z}_{(2,1,k)}(Q_m, Q_\tau; q_1, q_2)}{\mathcal{Z}_{(2,1,1)}(Q_m, Q_\tau; q_1, q_2)}\right|_{m=\frac{1}{2}(\epsilon_1+\epsilon_2)}. \tag{4.38}$$

This gives properly the non-zero result, and it is found that this is compatible with the elliptic genus of the 2d $\mathcal{N} = (4, 4)$ SU(k) gauge theory (at least of rank $k \leq 10$) [32] that is exactly computable by the supersymmetric localization [38, 39]. This should not be U(k) since the overall U(1) is removed in (5.32). We can check quantitatively that the enlargement of supersymmetry happens due to the fermion zero-modes in the limit of the mass parameter.

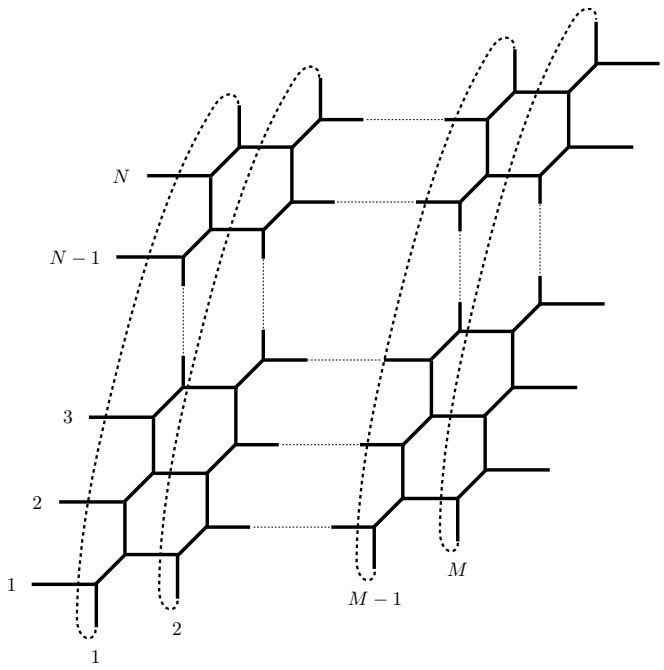

Figure 20: The web diagram corresponding to M-strings with M M5-branes on TN_N.

4.3.2 The general formula for the partition fucntion

As for the domain wall, we can compute the M-string partition function captured by the web diagram of general (M,N)[14] in Figure 20. Gluing M domain wall partition functions of (4.17) results in

$$
\begin{aligned}
&G_{(M,N)}(Q_i^{(\mathfrak{a})}, Q_\tau, Q_{f,a}^{(\mathfrak{a})}; q_1, q_2) \\
&= \sum_{\{\mu_a^{(\mathfrak{a})}\}} \left[\prod_{\mathfrak{a}=1}^{M-1}\prod_{a=1}^{N}\left(-Q_{f,a}^{(\mathfrak{a})}\right)\right] \widehat{Z}^{\mu_1^{(1)}\mu_2^{(1)}\cdots\mu_N^{(1)}}_{\emptyset\emptyset\cdots\emptyset}(Q_i^{(1)}, Q_\tau; q_1, q_2) \\
&\qquad \times \left[\prod_{\mathfrak{b}=2}^{M-1} \widehat{Z}^{\mu_1^{(\mathfrak{b})}\mu_2^{(\mathfrak{b})}\cdots\mu_N^{(\mathfrak{b})}}_{\mu_1^{(\mathfrak{b}-1)}\mu_2^{(\mathfrak{b}-1)}\cdots\mu_N^{(\mathfrak{b}-1)}}(Q_i^{(\mathfrak{b})}, Q_\tau; q_1, q_2)\right] \widehat{Z}^{\emptyset\emptyset\cdots\emptyset}_{\mu_1^{(M-1)}\mu_2^{(M-1)}\cdots\mu_N^{(M-1)}}(Q_i^{(M)}, Q_\tau; q_1, q_2),
\end{aligned}
\tag{4.39}
$$

where $\mu_a^{(\mathfrak{a})}$ and $Q_{f,a}^{(\mathfrak{a})}$ are a Young diagram and a Kähler factor, respectively, on the a-th segment from the bottom that joints the $\mathfrak{a}$-th and $(\mathfrak{a}+1)$-th domain wall. The domain wall

[14] A class of geometries with the chains of $\mathbb{C}\mathbf{P}^1$'s is known as the bubbling Calabi-Yau geometry [92, 93].

partition functions are

$$\begin{aligned}
\widehat{Z}^{\mu_1^{(1)}\mu_2^{(1)}\cdots\mu_N^{(1)}}_{\emptyset\emptyset\cdots\emptyset} &: \text{the 1st domain wall at the left end,}\\
\widehat{Z}^{\mu_1^{(\mathfrak{b})}\mu_2^{(\mathfrak{b})}\cdots\mu_N^{(\mathfrak{b})}}_{\mu_1^{(\mathfrak{b}-1)}\mu_2^{(\mathfrak{b}-1)}\cdots\mu_N^{(\mathfrak{b}-1)}} &: \text{the } \mathfrak{b}\text{-th domain wall in the middle,}\\
\widehat{Z}^{\emptyset\emptyset\cdots\emptyset}_{\mu_1^{(M-1)}\mu_2^{(M-1)}\cdots\mu_N^{(M-1)}} &: \text{the } M\text{-th domain wall at the right end.}
\end{aligned}$$

We would rewrite (4.39) in terms of the elliptic theta function by generalizing the calculation steps from (4.24) to (4.33). Because this is basically straightforward but notationally complicated, we throw details into Appendix C.4. The final result is given by

$$\begin{aligned}
&G_{(M,N)}(Q_i^{(\mathfrak{a})}, Q_\tau, Q_{f,a}^{(\mathfrak{a})}; q_1, q_2)\\
&= \sum_{\{\mu_a^{(\mathfrak{a})}\}} \prod_{\mathfrak{b}=1}^{M-1} \left[\prod_{a=1}^{N} \left(\mathfrak{Q}_{f,a}^{(\mathfrak{b})}\right)^{|\mu_a^{(\mathfrak{b})}|}\right] \left[\prod_{a,b=1}^{N} \prod_{(i,j)\in\mu_a^{(\mathfrak{b})}} \frac{\theta_1\left(\mathsf{A}_{ab}^{(\mathfrak{b})}(i,j)\right)\theta_1\left(\mathsf{B}_{ab}^{(\mathfrak{b})}(i,j)\right)}{\theta_1\left(\mathsf{C}_{ab}^{(\mathfrak{b})}(i,j)\right)\theta_1\left(\mathsf{D}_{ab}^{(\mathfrak{b})}(i,j)\right)}\right],
\end{aligned} \tag{4.40}$$

where we define for the weights in the sectors of $|\mu_a^{(\mathfrak{b})}|$,

$$\mathfrak{Q}_{f,a}^{(\mathfrak{b})} := Q_{f,a}^{(\mathfrak{b})} \left(\frac{q_2}{q_1}\right)^{\frac{N-1}{2}} \left(\prod_{b=1}^{N} Q_{2b-1}^{(\mathfrak{b})} Q_{2b-1}^{(\mathfrak{b}+1)}\right)^{\frac{1}{2}}, \tag{4.41}$$

and for the multiplicative variables of the elliptic theta function,

$$\mathsf{A}_{ab}^{(\mathfrak{b})}(i,j) := \overline{\mathsf{Q}}_{ab}^{(\mathfrak{b}+1)} q_1^{\mu_{b,j}^{(\mathfrak{b}+1)\mathrm{T}} - i + \frac{1}{2}} q_2^{\mu_{a,i}^{(\mathfrak{b})} - j + \frac{1}{2}}, \tag{4.42}$$

$$\mathsf{B}_{ab}^{(\mathfrak{b})}(i,j) := \overline{\mathsf{Q}}_{ba}^{(\mathfrak{b})} q_1^{-\mu_{b,j}^{(\mathfrak{b}-1)\mathrm{T}} + i - \frac{1}{2}} q_2^{-\mu_{a,i}^{(\mathfrak{b})} + j - \frac{1}{2}}, \tag{4.43}$$

$$\mathsf{C}_{ab}^{(\mathfrak{b})}(i,j) := \widehat{\mathsf{Q}}_{ba}^{(\mathfrak{b})} q_1^{-\mu_{b,j}^{(\mathfrak{b})\mathrm{T}} + i - 1} q_2^{-\mu_{a,i}^{(\mathfrak{b})} + j}, \tag{4.44}$$

$$\mathsf{D}_{ab}^{(\mathfrak{b})}(i,j) := \widehat{\mathsf{Q}}_{ab}^{(\mathfrak{b})} q_1^{\mu_{b,j}^{(\mathfrak{b})\mathrm{T}} - i} q_2^{\mu_{a,i}^{(\mathfrak{b})} - j + 1}, \tag{4.45}$$

with $\overline{\mathsf{Q}}_{ab}^{(\mathfrak{b})} := \left(\mathsf{Q}_{ab}^{(\mathfrak{b})}\right)^{-1}$ and

$$\widehat{\mathsf{Q}}_{ab}^{(\mathfrak{b})} = \begin{cases} 1 & \text{for } a = b, \\ \left(\widetilde{\mathsf{Q}}_{ab}^{\prime(\mathfrak{b})}\right)^{-1} & \text{for } a \neq b. \end{cases} \tag{4.46}$$

Finally, the general formula for the partition function of M-strings originated from $k_{\mathfrak{a}}$ M2-branes stretched between the $\mathfrak{a}$-th and $(\mathfrak{a}+1)$-th M5-branes on TN_N can be read as

$$\mathcal{Z}_{(M,N,\vec{k})}(Q_i^{(\mathfrak{a})}, Q_\tau; q_1, q_2) = \sum_{\sum_{a=1}^{N} |\mu_a^{(\mathfrak{a})}| = k_{\mathfrak{a}}} \prod_{\mathfrak{b}=1}^{M-1} \prod_{a,b=1}^{N} \prod_{(i,j)\in\mu_a^{(\mathfrak{b})}} \frac{\theta_1\left(\mathsf{A}_{ab}^{(\mathfrak{b})}(i,j)\right)\theta_1\left(\mathsf{B}_{ab}^{(\mathfrak{b})}(i,j)\right)}{\theta_1\left(\mathsf{C}_{ab}^{(\mathfrak{b})}(i,j)\right)\theta_1\left(\mathsf{D}_{ab}^{(\mathfrak{b})}(i,j)\right)}, \tag{4.47}$$

where $\vec{k} = (k_1, k_2, \cdots, k_{M-1})$ for $\mathfrak{a} = 1, 2, \cdots, M-1$.

4.4 Elliptic genus of the world-sheet theory

The other perspective to calculate the M-string partition function is on the world-sheet theory of M-strings. Since the M-string on TN_N keeps basically $(0,4)$ supersymmetry, its world-sheet theory could be a 2d $\mathcal{N}=(0,4)$ theory with $\mathrm{U}(k_i)$ gauge symmetries associated with the stacks of the M2-branes and several matter fields in some representations of $\mathrm{U}(k_i)$. The matter contents of this theory may not easily be read off from the world-volume of the M5-brane since we know much less the 6d SCFT[15]. Nevertheless, we can nicely pick up them from string theory as the low energy prescription of M-theory. Then, we calculate exactly the elliptic genus of the 2d theory on M-strings by the so-called supersymmetric localization [16, 17].

4.4.1 $\mathcal{N}=(0,2)$ elliptic genera

At first, we would list the formulae for the elliptic genera of 2d $\mathcal{N}=(0,2)$ supersymmetric theories. The elliptic genus [37], simply speaking, is a partition function on a torus of the complex modulus τ, or equivalently, an index on the Hilbert space of quantum mechanics. This quantity can be evaluated exactly in the path integral formalism by using the localization [54, 38, 39]. The formulae basically are written in terms of the elliptic theta function $\theta_1(z|\tau)$ (A.55). If one would know more about 2d $\mathcal{N}=(0,2)$ and $(0,4)$ theories, see e.g. [94, 95, 96, 97, 98].

The $\mathcal{N}=(0,2)$ theory consists of a vector V, a chiral Φ, and a Fermi multiplet Ψ which contain the following fields as on-shell degrees of freedom:

$\mathcal{N}=(0,2)$	scalar	fermion	gauge
vector V		λ_+	A_μ
chiral Φ	ϕ	ψ_-	
Fermi Ψ		ψ_+	

(4.48)

The elliptic genus on the Neveu-Schwarz (NS) sector[16] of the Hilbert space $\mathcal{H}$ is defined as

$$\mathcal{I}_{\mathrm{NS}}(\xi_i;\tau)=\mathrm{Tr}_{\mathcal{H}_{\mathrm{NS}}}(-1)^F p^{H_L}\bar{p}^{H_R-\frac{1}{2}J_R}\prod_i e^{2\pi i\xi_i f_i}, \tag{4.49}$$

where F is the fermion number operator, and H_{L}, H_{R} are the left-moving and right-moving Hamiltonian, respectively. J_R is the charge generator of the right-moving U(1) R-symmetry,

[15] More precisely, there is the list of multiplets in the 6d SCFT, but it is quite hard to fix the appropriate reduction to the 2d theory because we do not have any Lagrangian description which encodes interactions.

[16] In the similar way, the elliptic genus on the Ramond (R) sector is given by

$$\mathcal{I}_{\mathrm{R}}(\xi_i;\tau)=\mathrm{Tr}_{\mathcal{H}_{\mathrm{R}}}(-1)^F p^{H_L}\bar{p}^{H_R}\prod_i e^{2\pi i\xi_i f_i}.$$

and f_i are Cartan generators of a flavor symmetry. The multiplicative parameter is given by $p = e^{2\pi i\tau}$, and ξ_i corresponds to chemical potentials associated with a flavor symmetry. We now assume that the theory has one flavor symmetry, but we can easily generalize it to the case of several flavor symmetries. As an usual argument, we can choose supercharges such that the elliptic genus does not depend on $\bar{p}$. We obtain the elliptic genus by multiplying one-loop determinants $\Delta_{\text{1-loop}}$ as contributions from all multiplets in the theory of interest. The one-loop contributions of the multiplets in (4.48) are given as follows.

- The vector multiplet V with a gauge group G,

$$\Delta^{V}_{\text{1-loop}} = \left(-2\pi i\eta(\tau)^2\right)^{\text{rank}G} \prod_{\substack{\alpha\in\text{adj}\\ \alpha\neq 0}} \frac{i\theta_1(\alpha\cdot v|\tau)}{\eta(\tau)}. \tag{4.50}$$

- The chiral multiplet Φ in a representation $\mathbf{R}$,

$$\Delta^{\Phi}_{\text{1-loop}} = \prod_{\rho\in\mathbf{R}} \frac{i\eta(\tau)}{\theta_1(\rho\cdot v + f_i\xi_i|\tau)}. \tag{4.51}$$

- The Fermi multiplet Ψ in a representation $\mathbf{R}$,

$$\Delta^{\Psi}_{\text{1-loop}} = \prod_{\rho\in\mathbf{R}} \frac{i\theta_1(\rho\cdot v + f_i\xi_i|\tau)}{\eta(\tau)}, \tag{4.52}$$

where α and ρ are the elements of the root and weight of G. The function $\eta(\tau)$ is the Dedekind eta function,

$$\eta(\tau) = e^{\frac{\pi i\tau}{12}} \prod_{n=1}^{\infty} \left(1 - e^{2\pi i n\tau}\right) = p^{\frac{1}{24}}(p;p)_\infty, \tag{4.53}$$

where $(p;p)_\infty$ is the q-Pochhammer symbol (or the q-shifted factorial) given in (A.60). For instance, the elliptic genus of the $\mathrm{U}(k)$ gauge theory with one chiral and one Fermi multiplet in the fundamental representation and transformed under an $\mathrm{U}(1)_{\xi_1}$ and $\mathrm{U}(1)_{\xi_2}$ global symmetry is written as

$$\mathcal{I}(\xi) \sim \int_{\mathbb{T}} \mathrm{d}^k v \prod_{i\neq j}^{k} \theta_1(v_i - v_j) \prod_{i,j=1}^{k} \frac{\theta_1(v_i + \xi_2)}{\theta_1(v_i + \xi_1)}, \tag{4.54}$$

where we omit τ, and $\sim$ stands for the equality up to a prefactor independent of integration variables v_i which are taken in the maximal torus $\mathbb{T}$ of $\mathrm{U}(k)$. Remark that as for the refined topological vertex, we often use a convention $\mathcal{I}(\mathbf{a};p)$ with a collection of multiplicative parameters $\mathbf{a} \equiv \{a_i\}$ defined by $a_i = e^{2\pi i\xi_i}$ (i.e. the exponentiations of arguments).

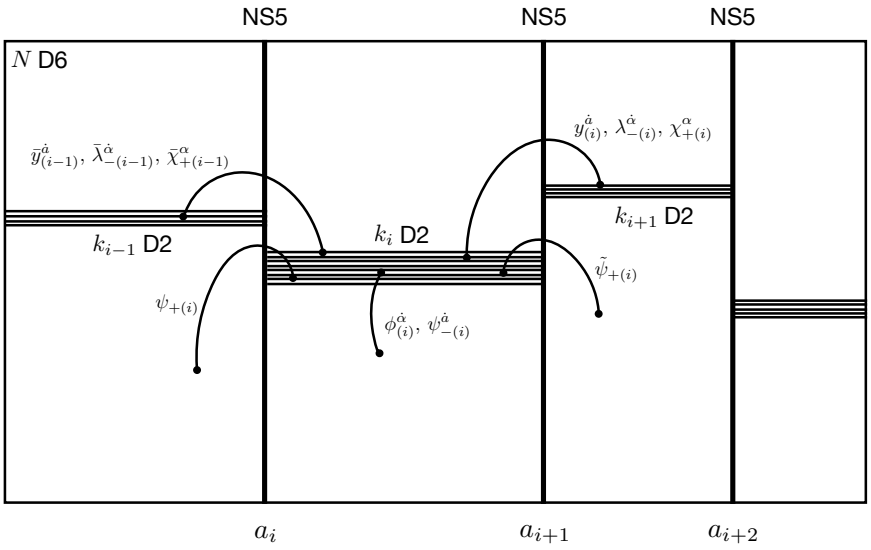

Figure 21: The D2-D6-NS5 system projected onto the 56-plane.

4.4.2 Type IIA brane system

Field contents

Let the 7 direction, S^1 of TN_N, be the M-theory circle in (3.17). As the circle shrinks, the M5-branes and the M2-branes unwrapped on this S^1 are mapped to NS5-branes and D2-branes, respectively. The centers of TN_N now are affected by this reduction to change to N D6-branes. Thus, we reach to the D2-D6-NS5 system of type IIA string theory (called the IIA brane model in [99][17]),

	T^2		$\mathbb{R}^4_{\epsilon_1,\epsilon_2}$							
	0	1	2	3	4	5	6	8	9	♮
M NS5	×	×	×	×	×	×	$\{a_i\}$			
k_i D2	×	×					×			
N D6	×	×	×	×	×	×	×			

(4.55)

We would focus on the D2-branes whose world-volume theory originally is a 3d $\mathcal{N}=2$ gauge theory. The 2d $\mathcal{N}=(0,4)$ effective theory of our interest that becomes the quiver gauge theory is obtained by reducing this 3d theory. We remark that since the multiplets of the $\mathcal{N}=(0,4)$ theory can be decomposed into these of the $\mathcal{N}=(0,2)$ theory, we list the field contents induced on the D2-branes in the languages of $\mathcal{N}=(0,2)$ as follows [99]. The gauge group of the 2d theory is $\otimes_{i=1}^{M-1}\mathrm{U}(k_i)$ that arises from open strings ending on the stacks of k_i

[17] They have mainly investigated the world-sheet theory of self-dual strings as the boundary of the ABJM theory [22] phrased as the ABJM slab and discussed its connection to the IIA brane model.

D2-branes. There are associated $(0,2)$ vector multiplets $V_{(i)}$, including gauge fields $A_{\mu(i)}$ and fermions $\lambda^{\dot\alpha\dot a}_{+(i)}$, and $(0,2)$ chiral multiplets $B_{(i)}$ in the adjoint representation which consist of scalars $b^{\alpha\dot\alpha}_{(i)}$ and fermions $\chi^{\alpha\dot a}_{-(i)}$. Further, Fermi multiplets $\Lambda_{(i)}$ which does not have the gauge fields appear:

$$\left.\begin{aligned} A_{\mu(i)},\, \lambda^{\dot\alpha\dot a}_{+(i)} &\in V_{(i)} : \text{vector} \\ b^{\alpha\dot\alpha}_{(i)},\, \chi^{\alpha\dot a}_{-(i)} &\in B_{(i)} : \text{chiral} \\ \tilde\lambda^{\dot\alpha\dot a}_{+(i)} &\in \Lambda_{(i)} : \text{Fermi} \end{aligned}\right\} \text{adjoint of } \mathrm{U}(k_i), \tag{4.56}$$

where we recycle the notation in the previous section that $\alpha, a = \pm$ for $\mathrm{SU}(2)_{\mathrm{L}}$ and $\widetilde{\mathrm{SU}}(2)_{\mathrm{L}}$, and $\dot\alpha, \dot a = \dot\pm$ for $\mathrm{SU}(2)_{\mathrm{R}}$ and $\widetilde{\mathrm{SU}}(2)_{\mathrm{R}}$, respectively. From the point of view of the D2-branes in the i-th interval $[a_i, a_{i+1}]$, the open strings stretched between the D2-branes and D6-branes give rise to chiral multiplets $\Phi_{(i)}$ in the fundamental representation $\mathbf{k}_i$, containing scalars $\phi^{\dot\alpha}_{(i)}$ and fermions $\psi^{\dot a}_{-(i)}$, and Fermi multiplets $\Psi_{(i)}$, $\tilde\Psi_{(i)}$ comprised of fermions $\psi_{+(i)}$, $\tilde\psi_{+(i)}$, respectively:

$$\left.\begin{aligned} \phi^{\dot\alpha}_{(i)},\, \psi^{\dot a}_{-(i)} &\in \Phi_{(i)} : \text{chiral} \\ \psi_{+(i)} &\in \Psi_{(i)} : \text{Fermi} \\ \tilde\psi_{+(i)} &\in \tilde\Psi_{(i)} : \text{Fermi} \end{aligned}\right\} \mathbf{k}_i \text{ of } \mathrm{U}(k_i). \tag{4.57}$$

Moreover, we actually find the open strings between the i-th and the $(i+1)$-th stacks of D2-branes, which lead to chiral multiplets $Y_{(i)}$, with scalars $y^{\dot a}_{(i)}$ and fermions $\lambda^{\dot\alpha}_{-(i)}$, and Fermi multiplets $\mathcal{X}_{(i)}$, with fermions $\chi^{\alpha}_{+(i)}$, in the bifundamental representation $(\mathbf{k}_i, \overline{\mathbf{k}}_{i+1})$:

$$\left.\begin{aligned} y^{\dot a}_{(i)},\, \lambda^{\dot\alpha}_{-(i)} &\in Y_{(i)} : \text{chiral} \\ \chi^{\alpha}_{+(i)} &\in \mathcal{X}_{(i)} : \text{Fermi} \end{aligned}\right\} (\mathbf{k}_i, \overline{\mathbf{k}}_{i+1}) \text{ of } \mathrm{U}(k_i) \times \mathrm{U}(k_{i+1}), \tag{4.58}$$

where the first entry $\mathbf{k}_i$ belongs to $\mathrm{U}(k_i)$ and the second $\overline{\mathbf{k}}_{i+1}$ to $\mathrm{U}(k_{i+1})$. We should note that there are also the fields conjugate to the above one, that is, chiral and Fermi multiplets in the bifundamental representation $(\overline{\mathbf{k}}_i, \mathbf{k}_{i+1})$ in addition to chiral and Fermi multiplets in the antifundamental representation $\overline{\mathbf{k}}_i$. The matters in (4.56)-(4.58) and their conjugate compose $(0,4)$ multiplets (see Table 5). Figure 21 shows the brane system with open strings originating these fields which are connected from the D2-branes in the i-th interval. This picture can be compared with the well-known brane system of type IIB string theory as worked in [33]. We would briefly mention this standpoint in the next subsection.

The simplest example of $(M, N) = (2, 1)$

To make discussions concrete, now we would restrict ourselves to the simplest example, $(M, N) = (2, 1)$, as in the previous subsection, and then shortly demonstrate the computation of the elliptic genus of this theory following [99]. In this case, there is only one stack of k

$\mathcal{N}=(0,4)$	$\mathcal{N}=(0,2)$	U(k)	U(1)$_m$	U(1)$_{\epsilon_1}$	U(1)$_{\epsilon_2}$
vector	vector V	adj	0	0	0
	Fermi $\tilde{\Lambda}$	adj	0	$+1$	$+1$
hyper	chiral B	adj	0	$+1$	0
	chiral $\tilde{B}$	adj	0	0	$+1$
hyper	chiral Φ	$\mathbf{k}$	0	$-\frac{1}{2}$	$-\frac{1}{2}$
	chiral $\tilde{\Phi}$	$\overline{\mathbf{k}}$	0	$-\frac{1}{2}$	$-\frac{1}{2}$
Fermi	Fermi Ψ	$\mathbf{k}$	-1	0	0
	Fermi $\tilde{\Psi}$	$\overline{\mathbf{k}}$	-1	0	0

Table 5: The matter contents of the 2d U(k) gauge theory on k D2-branes ending on $M=2$ NS5-branes and lain on $N=1$ D6-brane.

D2-branes, hence, the world-sheet theory is the $\mathcal{N}=(0,4)$ U(k) gauge theory without bifundamental fields. The matter contents are immediately read off from the above list, as summarized in Table 5 with U(1) charges under twists introduced in (3.19) and (3.21).

The elliptic genus of this theory is contributed from the $\mathcal{N}=(0,2)$ multiplets displayed in Table 5 and written in the integral form by combining their one-loop determinants given in (4.50)-(4.52),

$$\mathcal{I}_{(2,1,k)}(m,\epsilon_1,\epsilon_2;\tau) \sim \int_{\mathbb{T}} \mathrm{d}^k v \prod_{i\neq j}^{k} \theta_1(v_i-v_j) \prod_{i,j=1}^{k} \frac{\theta_1(v_i-v_j+\epsilon_1+\epsilon_2)}{\theta_1(v_i-v_j+\epsilon_1)\theta_1(v_i-v_j+\epsilon_2)} \times \prod_{i=1}^{k} \frac{\theta_1\left(v_i-m\right)\theta_1\left(-v_i-m\right)}{\theta_1\left(v_i-\frac{1}{2}\epsilon_1-\frac{1}{2}\epsilon_2\right)\theta_1\left(-v_i-\frac{1}{2}\epsilon_1-\frac{1}{2}\epsilon_2\right)}. \tag{4.59}$$

We can easily find that the integrand possesses infinitely many poles, thus, the integration contour must be carefully chosen to pick up appropriate sets of poles. The correct prescription to do this turns out to be the so-called Jeffrey-Kirwan (JK) residue [38, 39]. However, the calculation based on the JK residue seems quite intricate, hence, we would accept an alternative viewpoint called the Higgs branch localization. This idea has been introduced in studying the exact partition function on a two-sphere [100, 101][18], while the form of (4.59) is termed the Coulomb branch localization. Roughly speaking, the Coulomb branch localization is taken on the locus where a gauge field is localized on a non-trivial configuration, i.e. part of the gauge symmetry remain unbroken. The Higgs branch localization is a way to focus on the locus where matter fields are localized on a non-trivial configuration but trivial for the gauge field, which means that the gauge symmetry is completely violated and

[18]The higher dimensional versions of the Higgs branch localization also have been derived in [102, 103, 104, 105, 106, 107, 108, 109].

the integration over v_i does not occur. The final result of the Higgs branch localization is expressed by the summation over vacua in the Higgs branch of the moduli space. What we have to do is to determine BPS configurations constrained by the D-term and F-term condition that are the equations of motion for auxiliary fields. In the present situation, these conditions are found out to be

$$\begin{aligned} \phi\bar{\phi} - \bar{\tilde{\phi}}\tilde{\phi} + [b, \bar{b}] + [\tilde{b}, \bar{\tilde{b}}] + \zeta \cdot \mathbf{1}_{k\times k} = 0, \\ \phi\tilde{\phi} + [b, \tilde{b}] = 0, \end{aligned} \tag{4.60}$$

where an FI parameter ζ is turned on. Note that these are just identical with the ADHM equations for the moduli space of k U(1) instantons, which is consistent with the observation stated at the beginning in Section 4.1. The moduli space of the theory in question should be determined by (4.60) and U(k) gauge invariance. In the case of $\zeta \neq 0$ for explanation, the gauge symmetry is entirely broken by some condensed scalars. Accordingly, the theory flows to a non-linear sigma model in the IR which describes the moduli space of k U(1) instantons, and $\mathcal{I}_{(2,1,k)}$ is actually the elliptic genus of this non-linear sigma model. In the non-linear sigma model, the isometries of the target space are parametrised by m, ϵ_1, and ϵ_2, and we can incorporate them by gauging these isometries and coupling the resultant background gauge field to the theory. Especially, the target space owns a finite number of fixed points which are invariant under isometries associated with ϵ_1, ϵ_2. At each fixed point, we can sufficiently approximate the non-linear sigma model to a free theory with chiral and Fermi multiplets coupling to background fields. Therefore, the resultant elliptic genus is given by bringing the contributions from all fixed points.

With above arguments, the following formula for the elliptic genus is conjectured:

$$\begin{aligned} \mathcal{I}_{(2,1,k)}(m, \epsilon_1, \epsilon_2; \tau) = \sum_{\{u_i\}} \prod_{i,j=1}^{k} \frac{\theta_1(u_i - u_j)\,\theta_1(u_i - u_j + \epsilon_1 + \epsilon_2)}{\theta_1(u_i - u_j + \epsilon_1)\,\theta_1(u_i - u_j + \epsilon_2)} \\ \times \prod_{i=1}^{k} \frac{\theta_1(u_i - m)\,\theta_1(-u_i - m)}{\theta_1\left(u_i - \frac{1}{2}\epsilon_1 - \frac{1}{2}\epsilon_2\right)\theta_1\left(-u_i - \frac{1}{2}\epsilon_1 - \frac{1}{2}\epsilon_2\right)}, \end{aligned} \tag{4.61}$$

where the summation is taken over fixed points $\mathbf{u} := \mathrm{diag}(u_1, u_2, \cdots, u_k)$. Note that this expression still includes fermion zero-modes in the numerator of the first line and seemingly may be trivial. It is expected that these zero-modes are excluded by substituting the precise values of the fixed points. With the charge assignments read from Table 5, the fixed points of isometries generated by ϵ_1 and ϵ_2 in the target space are to be determined by

$$\begin{aligned} \mathbf{u}b - b\mathbf{u} + \epsilon_1 b = 0, \qquad & \mathbf{u}\phi + \frac{1}{2}(\epsilon_1 + \epsilon_2)\phi = 0, \\ \mathbf{u}\tilde{b} - \tilde{b}\mathbf{u} + \epsilon_2\tilde{b} = 0, \qquad & -\tilde{\phi}\mathbf{u} + \frac{1}{2}(\epsilon_1 + \epsilon_2)\tilde{\phi} = 0. \end{aligned} \tag{4.62}$$

Therefore, the fixed points $\mathbf{u}$ are described by (4.60) and the BPS conditions (4.62) as an eigenvalue problem. The way to solve these equations is well-studied mathematical problem,

for example, the solutions for $\zeta > 0$ are in a vector with k linearly independent entries given by the forms $\tilde{\phi} b^i \tilde{b}^j$ $(\phi = 0)$. It is known that those solutions can be recast into ones characterized by a Young diagram μ with k boxes as

$$(\mathbf{u})_{i,j} = \left(i - \frac{1}{2}\right)\epsilon_1 + \left(j - \frac{1}{2}\right)\epsilon_2, \tag{4.63}$$

where labels (i, j) stand for the positions of boxes in μ. A careful sight of (4.63) finds out that the fermion zero-modes in the numerator of (4.61) really are canceled by the contributions of the scalars in the denominator. Through sort of effort with nontrivial mathematical identities, we finally obtain

$$\mathcal{I}_{(2,1,k)}(m, \epsilon_1, \epsilon_2; \tau) = \sum_{|\mu|=k} \prod_{(i,j)\in\mu} \frac{\theta_1\left(-m + (i - \frac{1}{2})\epsilon_1 + (j - \frac{1}{2})\epsilon_2\right)\theta_1\left(-m - (i - \frac{1}{2})\epsilon_1 - (j - \frac{1}{2})\epsilon_2\right)}{\theta_1\left((-\mu_j^{\mathrm{T}} + i)\epsilon_1 + (\mu_i - j + 1)\epsilon_2\right)\theta_1\left((\mu_j^{\mathrm{T}} - i + 1)\epsilon_1 + (-\mu_i + j)\epsilon_2\right)}. \tag{4.64}$$

This can be seen as the elliptic genus of a free theory with $2k$ chiral and Fermi multiplets coupled to the background fields for $\mathrm{U}(1)_m$, $\mathrm{U}(1)_{\epsilon_1}$, and $\mathrm{U}(1)_{\epsilon_2}$. Remark that the number $2k$ is nothing but that of the Higgs branch in the moduli space. Rewriting this formula with multiplicative variables gives

$$\mathcal{I}_{(2,1,k)}(Q_m, Q_\tau; q_1, q_2) = \sum_{|\mu|=k} \prod_{(i,j)\in\mu} \frac{\theta_1\left(Q_m^{-1} q_1^{i-\frac{1}{2}} q_2^{-j+\frac{1}{2}}\right)\theta_1\left(Q_m^{-1} q_1^{-i+\frac{1}{2}} q_2^{j-\frac{1}{2}}\right)}{\theta_1\left(q_1^{-\mu_j^{\mathrm{T}}+i} q_2^{-\mu_i+j-1}\right)\theta_1\left(q_1^{\mu_j^{\mathrm{T}}-i+1} q_2^{\mu_i-j}\right)}. \tag{4.65}$$

This is in agreement with (4.35) up to an overall sign[19]. One can of course explicitly see the enhancement of supersymmetry with setting $m = \frac{1}{2}(\epsilon_1 + \epsilon_2)$ as for the refined topological vertex case shown in (5.32).

4.4.3 Type IIB brane system on the flat space

Finally, let us make brief comments on the brane system of type IIB string theory used mainly in [33] for approaching the world-sheet theory of the M-strings.

We would restart the argument from the IIA brane system (4.55). Taking T-duality along the 1 direction that is one of the 1-cycles of T^2 results in the following brane configuration in type IIB string theory:

[19] We are not sure that this sign is relevant for agreement. It is necessary to take a sum over k for (4.65) if we would like to compare it with the partition function $G_{(2,1)}$ (4.33) of the refined topological vertex. However, k the number of M-strings is fixed in computing the elliptic genus, and relative weights for elliptic genera in the sum of k cannot be simply determined only from the computation here.

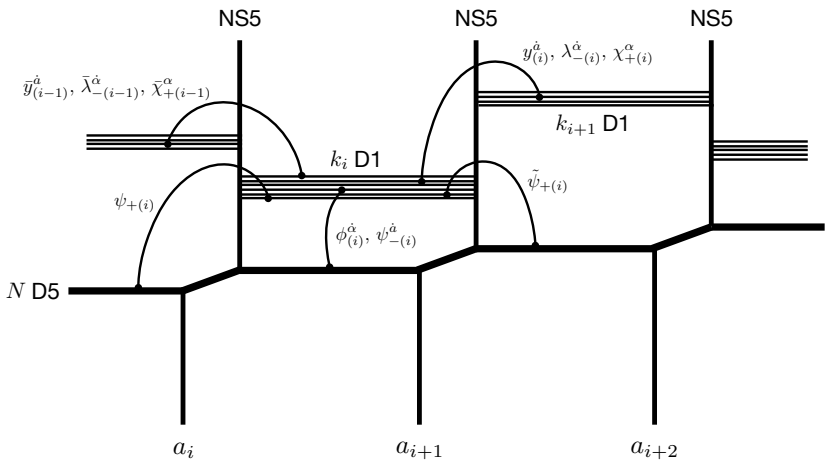

Figure 22: The D1-D5-NS5 system projected onto the 16-plane, T-dual to Figure 21.

	T^2		$\mathbb{R}^4_{\epsilon_1,\epsilon_2}$							
	0	1	2	3	4	5	6	8	9	$\natural$
M NS5	×	×	×	×	×	×	$\{a_i\}$			
k_i D1	×						×			
N D5	×		×	×	×	×	×			

(4.66)

Note that N D5-branes are on top of each other, and the mass deformation affects again the intersection of the D5-brane and the NS5-brane to introduce $(N, 1)$-fivebrane depicted as slanting lines in Figure 22. The 2d gauge theory on the D2-branes that we focused on in the previous subsection corresponds to the world-volume theory of the D1-branes. There are various open strings stretched from the D1-branes to the neighboring stacks of the D1-branes and the multiple D5-branes, and the detailed analysis of their lightest spectra concludes the same $\mathcal{N} = (0, 2)$ matter contents on the D1-branes [33] as (4.56)-(4.58) obtained from the type IIA brane system.

4.4.4 Type IIB brane system on the orbifolded space

There is another interesting brane configuration of type IIB string theory. Assuming the 6 direction is compactified in the IIA brane model (4.55), T-duality along this direction provides the D1-D5 system on TN_M:

	T^2		$\mathbb{R}^4_{\epsilon_1,\epsilon_2}$				TN_M			
	0	1	2	3	4	5	6	8	9	$\natural$
k_i D1	×	×								
N D5	×	×	×	×	×	×				

(4.67)

As explained in Section 3.2, TN_M acts on the stack of the D1-branes as $\mathbb{Z}_M$-orbifold, and the world-volume theory of the D-branes at the tip of $\mathbb{Z}_M$-orbifold becomes generically a quiver gauge theory [110]. Indeed, the current brane system (4.67) has been well studied in [111, 112] that the world-volume theory of the D1-branes turns out to be the 2d $\mathcal{N} = (0, 4)$ $\otimes_{i=1}^{M-1}\mathrm{U}(k_i)$ quiver gauge theory with fundamental chiral and Fermi multiplets, and the field contents of this theory are basically identical with these (4.56)-(4.58) in the IIA brane model except for a bifundamental chiral and Fermi multiplet [33]. The last multiplets are caused from the extra compactification of the 6 direction. On this frame, the partition function of M-strings can be considered as the elliptic genus of this 2d quiver gauge theory, and the equivalence of this elliptic genus, after removing the additional bifundamental multiplets, to the partition function by the refined topological vertex has been checked in the case of $(M, N) = (2, 1)$ [33]. These different perspectives to give the same elliptic genus play a role to justify the application of the refined topological vertex to the M-strings. We can rely on one of these duality frames in computing the M-string partition function according to our convenience.

5 M-strings with a codimension-two defect

In this section, we would explain the realization of a codimention-2 defect of the six-dimensional theory in the context of M-strings that is our main result obtained in [113]. As mentioned in Section 2.4, while the codimension-4 defect in the world-volume theory of the stack of M5-branes can be constructed by probe M2-branes ending on it or probe M5-branes intersected with it, the codimension-2 defect is only made from an intersecting M5-brane because of the matter of dimension. This construction of the codimension-2 defect is also true for the M-string system, and we will show the effects of the defect as an operator in the 6d theory and as new matter contributions onto the M-string world-sheet theory.

5.1 Brane configuration

We would concentrate on the situation of $(M, N) = (2, 1)$, i.e one collection of k M2-branes suspended between two M5-branes on TN_1. Our proposal is that a half-BPS codimension-2 defect in the 6d SCFT is produced by inserting a probe M5-brane (M5′) into the M-string configuration as follows (Figure 23):

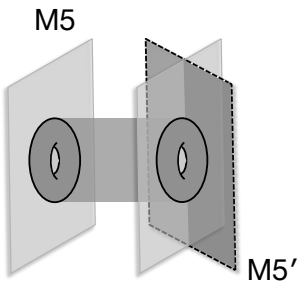

Figure 23: M-strings with a defect engineered by an intersecting M5′ (a thick gray brane).

	T^2		$\mathbb{R}^2_{\epsilon_1}$		$\mathbb{R}^2_{\epsilon_2}$			TN_1			
	0	1	2	3	4	5	6	7	8	9	$\natural$
2 M5	×	×	×	×	×	×	$\{a_i\}$				
k M2	×	×					×				
1 M5′	×	×			×	×		×	×		

(5.1)

This M5′ hits the singularity of the background, which is basically the same construction as given in [51] where the stack of the M5-branes to produce the codimension-2 (Gukov-Witten type) defect in 4d gauge theories extends to the subspace of the orbifolded space. This codimension-2 defect also can generate a surface defect in the 4d $\mathcal{N} = 2$ gauge theory belonging to the 2345 directions along which we take the twist of the Ω-deformation. In general, the introduction of non-local operators breaks part of or full supersymmetry. In fact, to preserve supersymmetry requires a condition,

$$\Gamma^{014578}\epsilon = \epsilon \quad \text{for the M5}'\text{-brane}, \tag{5.2}$$

in addition to (3.7). Therefore, $(0, 4)$ supersymmetry on M-strings is broken down to $(0, 2)$ supersymmetry, and M5′ is really a half-BPS defect.

The ingredient of our proposal is that the contribution of M5′ is calculable by the refined topological vertex and the localization. In the rest of this section, we would verify our proposal with performing the computation of its partition function. We trace again the passes for the original setup of M-strings in the previous section. On the perspective of the BPS state counting as in Section 4.1 where the M-theory circle is taken to be the 1 direction, our M-string configuration (5.1) is reduced to the following brane system of type IIA string

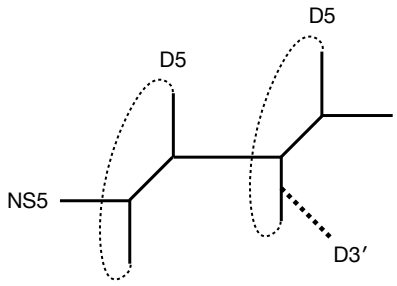

Figure 24: The D5-NS5-D3′ system that can engineer a codimension-2 defect.

theory:

	S^1	$\mathbb{R}^2_{\epsilon_1}$		$\mathbb{R}^2_{\epsilon_2}$			TN_1			
	0	2	3	4	5	6	7	8	9	$\natural$
2 D4	×	×	×	×	×	$\{a_i\}$				
k F1	×					×				
1 D4′	×			×	×		×	×		

(5.3)

Then, performing T-duality along the 7 direction results in

	S^1	$\mathbb{R}^2_{\epsilon_1}$		$\mathbb{R}^2_{\epsilon_2}$			S^1			
	0	2	3	4	5	6	7	8	9	$\natural$
2 D5	×	×	×	×	×	$\{a_i\}$	×			
k F1	×					×				
1 D3′	×			×	×			×		
1 NS5	×	×	×	×	×	×				

(5.4)

where the brane originated from the defect M5′-brane is signalled by a prime on it. The resultant D5-NS5-D3′ system is drawn in Figure 24. The insertion of M5′ makes the appearance of D3′ in the (p, q)-web diagram, and through the correspondence between the (p, q)-web and the web diagram of CY3, it is mapped into the presence of a Lagrangian brane $\mathcal{L}$. This is because the boundary condition preserving the half amount of supersymmetry in the A-model topological string theory is absolutely equivalent to the condition for $\mathcal{L}$ in CY3 as a target space. This effect may in principle be evaluated by the open topological string theory which will be argued in the next section. However, we face difficulty that for $\mathcal{L}$ on the internal segment in the web diagram, a tensor product $\mu \otimes \nu$ appears in the formula of the open topological vertex (see details in Section 6), and its calculation seems impossible to proceed at the present stage. However, we find that the geometric transition [62, 63, 64] is applicable to reproduce (5.4) and allows us to compute the partition function with avoiding this problem. Therefore, we proceed the discussion based on the geometric transition in the next subsection. We will come back this issue and try to resolve in Section 6.

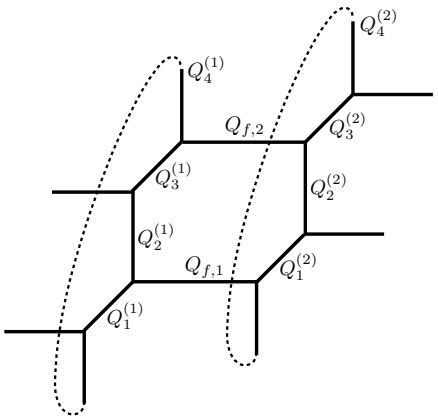

Figure 25: The web diagram connected to the (p, q)-web diagram with two D5-branes (vertical) and two NS5-branes (horizontal).

5.2 Partition function via the geometric transition

To construct the M-string system (5.1) via the geometric transition, the starting point is the web diagram corresponding to two D5-branes and two NS5-branes with the mass deformation as depicted in Figure 25, which is descended from M-strings (3.9) with $(M, N) = (2, 2)$:

	S^1	$\mathbb{R}^4_{\epsilon_1,\epsilon_2}$					S^1			
	0	2	3	4	5	6	7	8	9	♮
2 D5	×	×	×	×	×	$\{a_i\}$	×			
k F1	×					×				
2 NS5	×	×	×	×	×	×				

(5.5)

This geometry can be obtained by gluing two domain walls whose partition functions are already given in (4.14). We remark again that in consistently linking them, there are necessary conditions,

$$Q_\tau = Q_1^{(1)} Q_2^{(1)} Q_3^{(1)} Q_4^{(1)} = Q_1^{(2)} Q_2^{(2)} Q_3^{(2)} Q_4^{(2)} \tag{5.6}$$

for the compactifying radius being identical on both vertical lines, and

$$Q_2^{(1)} Q_3^{(1)} = Q_1^{(2)} Q_2^{(2)}, \qquad \text{or equivalently,} \qquad Q_4^{(1)} Q_1^{(1)} = Q_3^{(2)} Q_4^{(2)} \tag{5.7}$$

for the total length of a vertical and diagonal segment in the hexagon being equal, in addition to the relation

$$Q_m = Q_1^{(1)} Q_3^{(1)} = Q_1^{(2)} Q_3^{(2)} \tag{5.8}$$

respecting the net effect of the mass deformation by m. Its generating function with combining (5.6)-(5.8) is wrote down from the general expression (4.40) with setting $(M,N)=(2,2)$ (and the direct computation performed in Appendix C.3 for validity) as

$$
\begin{aligned}
G_{(2,2)}(Q_i^{(\mathfrak{a})},Q_\tau;q_1,q_2) = \sum_{\mu_1,\,\mu_2} &\left(-Q_{f,1}Q_1^{(2)}Q_3^{(2)}\sqrt{\frac{q_1}{q_2}}\right)^{|\mu_1|}\left(-Q_{f,2}Q_1^{(1)}Q_3^{(1)}\sqrt{\frac{q_2}{q_1}}\right)^{|\mu_2|} \\
&\times\Bigg[\prod_{(i,j)\in\mu_1}\frac{\theta_1\left(\overline{Q}_1^{(1)}\overline{Q}_3^{(1)}\overline{Q}_4^{(1)}q_1^{i-\frac{1}{2}}q_2^{-\mu_{1,i}+j-\frac{1}{2}}\right)\theta_1\left(\overline{Q}_1^{(1)}q_1^{i-\frac{1}{2}}q_2^{-\mu_{1,i}+j-\frac{1}{2}}\right)}{\theta_1\left(\overline{Q}_1^{(1)}\overline{Q}_4^{(1)}q_1^{-\mu_{2,j}^{\mathrm{T}}+i}q_2^{-\mu_{1,i}+j-1}\right)\theta_1\left(\overline{Q}_2^{(1)}\overline{Q}_3^{(1)}q_1^{\mu_{2,j}^{\mathrm{T}}-i+1}q_2^{\mu_{1,i}-j}\right)} \\
&\qquad\times\frac{\theta_1\left(\overline{Q}_1^{(2)}\overline{Q}_2^{(2)}\overline{Q}_3^{(2)}q_1^{-i+\frac{1}{2}}q_2^{\mu_{1,i}-j+\frac{1}{2}}\right)\theta_1\left(\overline{Q}_1^{(2)}q_1^{-i+\frac{1}{2}}q_2^{\mu_{1,i}-j+\frac{1}{2}}\right)}{\theta_1\left(q_1^{-\mu_{1,j}^{\mathrm{T}}+i}q_2^{-\mu_{1,i}+j-1}\right)\theta_1\left(q_1^{-\mu_{1,j}^{\mathrm{T}}+i-1}q_2^{-\mu_{1,i}+j}\right)} \\
&\times\prod_{(i,j)\in\mu_2}\frac{\theta_1\left(\overline{Q}_1^{(1)}\overline{Q}_2^{(1)}\overline{Q}_3^{(1)}q_1^{i-\frac{1}{2}}q_2^{-\mu_{2,i}+j-\frac{1}{2}}\right)\theta_1\left(\overline{Q}_3^{(1)}q_1^{i-\frac{1}{2}}q_2^{-\mu_{2,i}+j-\frac{1}{2}}\right)}{\theta_1\left(\overline{Q}_1^{(1)}\overline{Q}_4^{(1)}q_1^{\mu_{1,j}^{\mathrm{T}}-i}q_2^{\mu_{2,i}-j+1}\right)\theta_1\left(\overline{Q}_2^{(1)}\overline{Q}_3^{(1)}q_1^{-\mu_{1,j}^{\mathrm{T}}+i-1}q_2^{-\mu_{2,i}+j}\right)} \\
&\qquad\times\frac{\theta_1\left(\overline{Q}_3^{(2)}q_1^{-i+\frac{1}{2}}q_2^{\mu_{2,i}-j+\frac{1}{2}}\right)\theta_1\left(\overline{Q}_1^{(2)}\overline{Q}_3^{(2)}\overline{Q}_4^{(2)}q_1^{-i+\frac{1}{2}}q_2^{\mu_{2,i}-j+\frac{1}{2}}\right)}{\theta_1\left(q_1^{-\mu_{2,j}^{\mathrm{T}}+i}q_2^{-\mu_{2,i}+j-1}\right)\theta_1\left(q_1^{-\mu_{2,j}^{\mathrm{T}}+i-1}q_2^{-\mu_{2,i}+j}\right)}\Bigg],
\end{aligned}
\tag{5.9}
$$

where recalling our notation $\overline{Q}_i^{(\mathfrak{a})}:=\left(Q_i^{(\mathfrak{a})}\right)^{-1}$. Now, we apply the geometric transition explained in Section 2.2 to this web diagram in order to engineer the defect as a Lagrangian brane. We remark that the geometric transition for the refined case, i.e. general (q_1,q_2), is not yet entirely understood in the standard languages of geometry. Nevertheless, it has been suggested in [69] that an elementary (single) surface operator in 4d supersymmetric gauge theories on $\mathbb{R}^4_{\epsilon_1,\epsilon_2}$ can be realized as a Lagrangian brane in this way. We would extend their discussion to M-strings. As the simplest attempt, we accept the limit of the parameters,

$$
Q_1^{(1)}=\sqrt{\frac{q_1}{q_2}},\quad Q_1^{(2)}=\frac{1}{q_2}\sqrt{\frac{q_1}{q_2}}\quad\Leftrightarrow\quad \overline{Q}_1^{(1)}=\sqrt{\frac{q_2}{q_1}},\quad \overline{Q}_1^{(2)}=q_2\sqrt{\frac{q_2}{q_1}}. \tag{5.10}
$$

Note that in the unrefined limit, $q=q_1=q_2$, these are reduced to

$$
Q_1^{(1)}=1,\qquad Q_1^{(2)}=q^{-1}=e^{-ig_{\mathrm{s}}}. \tag{5.11}
$$

From the dictionary of the geometric transition (Section 2.2.2), these signify that, while no D-brane appears on the left side, a single D-brane does on the right side. In other words, there should be a Lagrangian submanifold on the right side where a D-brane can be wrapped on (Figure 26). That is why it is thought that the specialization (5.10) should work well to

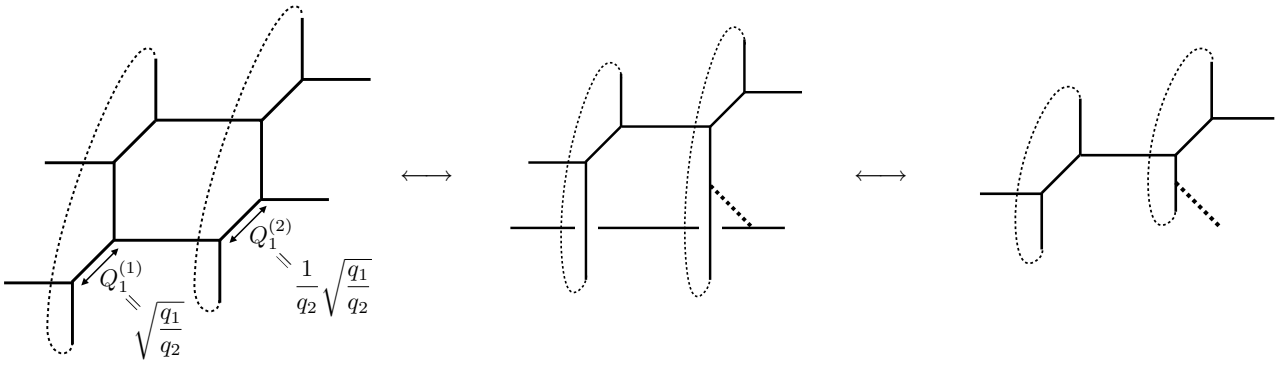

Figure 26: The web diagram with $(M, N) = (2, 2)$ (the left one) and the geometric transition to generate a Lagrangian brane represented by a dotted line on the right side.

engineer a surface defect even for the refined topological string theory. At the same time, we precisely set

$$Q_m = Q_3^{(1)} = Q_3^{(2)} \tag{5.12}$$

since the resolution caused from the mass deformation is executed by the $\mathbb{C}\mathbf{P}^1$' s of Kähler factors $Q_3^{(1)}$ and $Q_3^{(2)}$ after the geometric transition. Also note that, in this limit, the combination of (5.6) and (5.7) leads to

$$Q_1^{(1)} Q_4^{(1)} = Q_3^{(2)} Q_4^{(2)} \Rightarrow Q_4^{(1)} = \sqrt{\frac{q_2}{q_1}} Q_m Q_4^{(2)}. \tag{5.13}$$

We would denote the partition function obtained by the geometric transition as the one with $\star$ in the superscript to clearly declare the starting setup and the operation of the geometric transition. Combining (5.10)-(5.13) together into $G_{(2,2)}$ (5.9), we find that the resultant function $G^{\star}_{(2,2)}(Q_i^{(\mathfrak{a})}, Q_\tau; q_1, q_2)$ contains

$$\prod_{(i,j)\in\mu_1} \frac{\theta_1\left(\overline{Q}_3^{(1)}\overline{Q}_4^{(1)} q_1^{i-1} q_2^{-\mu_{1,i}+j}\right)\theta_1\left(q_1^{i-1} q_2^{-\mu_{1,i}+j}\right)}{\theta_1\left(\overline{Q}_4^{(1)} q_1^{-\mu_{2,j}^{\mathrm{T}}+i-\frac{1}{2}} q_2^{-\mu_{1,i}+j-\frac{1}{2}}\right)\theta_1\left(\overline{Q}_2^{(1)}\overline{Q}_3^{(1)} q_1^{\mu_{2,j}^{\mathrm{T}}-i+1} q_2^{\mu_{1,i}-j}\right)}$$
$$\times \frac{\theta_1\left(\overline{Q}_2^{(2)}\overline{Q}_3^{(2)} q_1^{-i} q_2^{\mu_{1,i}-j+2}\right)\theta_1\left(q_1^{-i} q_2^{\mu_{1,i}-j+2}\right)}{\theta_1\left(q_1^{-\mu_{1,j}^{\mathrm{T}}+i} q_2^{-\mu_{1,i}+j-1}\right)\theta_1\left(q_1^{-\mu_{1,j}^{\mathrm{T}}+i-1} q_2^{-\mu_{1,i}+j}\right)}. \tag{5.14}$$

At this point, the second factor in the first line of the numerator, $\theta_1\left(q_1^{i-1} q_2^{-\mu_{1,i}+j}; Q_\tau\right)$, vanishes even if μ_1 consists of only one box. Accordingly, we must set $\mu_1 = \emptyset$ to get the

nontrivial contribution, and then,

$$G^{\star}_{(2,2)}(Q_i^{(\mathfrak{a})},Q_\tau;q_1,q_2)=\sum_{\mu_2}\left(-Q_{f,2}Q_3^{(1)}\right)^{|\mu_2|}\prod_{(i,j)\in\mu_2}\frac{\theta_1\left(\overline{Q}_2^{(1)}\overline{Q}_3^{(1)}q_1^{i-1}q_2^{-\mu_{2,i}+j}\right)\theta_1\left(\overline{Q}_3^{(1)}q_1^{i-\frac{1}{2}}q_2^{-\mu_{2,i}+j-\frac{1}{2}}\right)}{\theta_1\left(\overline{Q}_4^{(1)}q_1^{-i-\frac{1}{2}}q_2^{\mu_{2,i}-j+\frac{3}{2}}\right)\theta_1\left(\overline{Q}_2^{(1)}\overline{Q}_3^{(1)}q_1^{i-1}q_2^{-\mu_{2,i}+j}\right)}$$
$$\times\frac{\theta_1\left(\overline{Q}_3^{(2)}q_1^{-i+\frac{1}{2}}q_2^{\mu_{2,i}-j+\frac{1}{2}}\right)\theta_1\left(\overline{Q}_3^{(2)}\overline{Q}_4^{(2)}q_1^{-i}q_2^{\mu_{2,i}-j+2}\right)}{\theta_1\left(q_1^{-\mu_{2,j}^{\mathrm{T}}+i}q_2^{-\mu_{2,i}+j-1}\right)\theta_1\left(q_1^{-\mu_{2,j}^{\mathrm{T}}+i-1}q_2^{-\mu_{2,i}+j}\right)}$$
$$=\sum_{\mu_2}\left(-Q_{f,2}Q_m\right)^{|\mu_2|}\prod_{(i,j)\in\mu_2}\frac{\theta_1\left(Q_m^{-1}q_1^{i-\frac{1}{2}}q_2^{-\mu_{2,i}+j-\frac{1}{2}}\right)\theta_1\left(Q_m^{-1}q_1^{-i+\frac{1}{2}}q_2^{\mu_{2,i}-j+\frac{1}{2}}\right)}{\theta_1\left(q_1^{-\mu_{2,j}^{\mathrm{T}}+i}q_2^{-\mu_{2,i}+j-1}\right)\theta_1\left(q_1^{-\mu_{2,j}^{\mathrm{T}}+i-1}q_2^{-\mu_{2,i}+j}\right)}$$
$$\times\frac{\theta_1\left(Q_m^{-1}\overline{Q}_4^{(2)}q_1^{-i}q_2^{\mu_{2,i}-j+2}\right)}{\theta_1\left(Q_m^{-1}\overline{Q}_4^{(2)}q_1^{-i}q_2^{\mu_{2,i}-j+1}\right)},\tag{5.15}$$

where we used (5.13) in the last line. Finally, the partition function of k M-strings is withdrawn as

$$\mathcal{Z}^{\star}_{(2,2,k)}(Q_4^{(2)},Q_m,Q_\tau;q_1,q_2)=\sum_{|\mu|=k}\prod_{(i,j)\in\mu}\frac{\theta_1\left(Q_m^{-1}q_1^{i-\frac{1}{2}}q_2^{-\mu_i+j-\frac{1}{2}}\right)\theta_1\left(Q_m^{-1}q_1^{-i+\frac{1}{2}}q_2^{\mu_i-j+\frac{1}{2}}\right)}{\theta_1\left(q_1^{-\mu_j^{\mathrm{T}}+i}q_2^{-\mu_i+j-1}\right)\theta_1\left(q_1^{-\mu_j^{\mathrm{T}}+i-1}q_2^{-\mu_i+j}\right)}$$
$$\times\frac{\theta_1\left(Q_m^{-1}\overline{Q}_4^{(2)}q_1^{-i}q_2^{\mu_i-j+2}\right)}{\theta_1\left(Q_m^{-1}\overline{Q}_4^{(2)}q_1^{-i}q_2^{\mu_i-j+1}\right)},\tag{5.16}$$

where we drop off the subscript of the Young diagram. One can notice that the first line of $\mathcal{Z}^{\star}_{(2,2,k)}$ completely agrees with the partition function $\mathcal{Z}_{(2,1,k)}$ (4.34) of M-strings without the M5′-brane. This observation can be a support for our prescription of the geometric transition with turning on two parameters (q_1,q_2). The second line of $\mathcal{Z}^{\star}_{(2,2,k)}$ should be the contributions of the M-strings attaching the M5′-brane and encode the BPS sector that might not be reached without the defect. The difference of q_2 between the numerator and the denominator is originated from the specialization (5.10), which means that our present defect is placed on the surface $\mathbb{R}^2_{\epsilon_2}\subset\mathbb{R}^4_{\epsilon_1,\epsilon_2}$ corresponding to our M5′ in (5.1). We will confirm this calculation in the next subsection from the standpoint of the world-sheet theory as before. In addition, we are discussing the properties of our defect in Section 5.4.

5.3 Partition function from the ADHM sigma model

To confirm the geometric transition and our result, we would reuse the type IIA string picture in Section 4.4.2 to compute the elliptic genus of the world-sheet theory in the presence of a

defect. Now, the M-theory circle is the 7 direction, which reduces the system (5.1) to

	T^2		$\mathbb{R}^2_{\epsilon_1}$		$\mathbb{R}^2_{\epsilon_2}$					
	0	1	2	3	4	5	6	8	9	♮
2 NS5	×	×	×	×	×	×	$\{a_i\}$			
k D2	×	×					×			
1 D4′	×	×			×	×		×		
1 D6	×	×	×	×	×	×	×			

(5.17)

From open strings stretched between k D2-branes and a D4′-brane descended from M5′, there would be an $(0,2)$ chiral multiplet Θ_{chi} and an $(0,2)$ Fermi multiplet Θ_{Fer} in the fundamental representation of $\mathrm{U}(k)$ in addition to the original multiplets in Table 5. We assume that they are accompanied with an $\mathrm{U}(1)_\xi$ global symmetry. The emergence of Θ_{chi} and Θ_{Fer} does not change the D-term and F-term constrain in (4.60), thus, the formula (4.61) is modified to simply multiply new one-loop contributions from Θ_{chi} and Θ_{Fer},

$$\mathcal{I}^\star_{(2,2,k)}(m,\epsilon_1,\epsilon_2,\xi;\tau) = \sum_{\{u_i\}}\prod_{i,j=1}^{k}\frac{\theta_1(u_i-u_j)\,\theta_1(u_i-u_j+\epsilon_1+\epsilon_2)}{\theta_1(u_i-u_j+\epsilon_1)\,\theta_1(u_i-u_j+\epsilon_2)} \times\prod_{i=1}^{k}\frac{\theta_1(u_i-m)\,\theta_1(-u_i-m)}{\theta_1\left(u_i-\frac{1}{2}\epsilon_1-\frac{1}{2}\epsilon_2\right)\theta_1\left(-u_i-\frac{1}{2}\epsilon_1-\frac{1}{2}\epsilon_2\right)}\times\frac{\theta_1(u_i+\xi-\epsilon_2)}{\theta_1(u_i+\xi)}. \tag{5.18}$$

The charge of ϵ_2 comes form the fact that the D4′-brane is extending the 45 directions, i.e. $\mathbb{R}^2_{\epsilon_2}$. Actually, this does also not affect the BPS conditions to determine fixed points, in particular the left one in the second line of (4.62). Therefore, the fixed points on the moduli space are still given by (4.63). Along the same line as to get (4.64), we conclude

$$\mathcal{I}^\star_{(2,2,k)}(m,\epsilon_1,\epsilon_2,\xi;\tau) = \sum_{|\mu|=k}\prod_{(i,j)\in\mu}\frac{\theta_1\left(-m+(i-\frac{1}{2})\epsilon_1+(j-\frac{1}{2})\epsilon_2\right)\theta_1\left(-m-(i-\frac{1}{2})\epsilon_1-(j-\frac{1}{2})\epsilon_2\right)}{\theta_1\left((-\mu_j^{\mathrm{T}}+i)\epsilon_1+(\mu_i-j+1)\epsilon_2\right)\theta_1\left((\mu_j^{\mathrm{T}}-i+1)\epsilon_1+(-\mu_i+j)\epsilon_2\right)} \times\frac{\theta_1\left((i-\frac{1}{2})\epsilon_1+(j-\frac{1}{2})\epsilon_2+\xi-\epsilon_2\right)}{\theta_1\left((i-\frac{1}{2})\epsilon_1+(j-\frac{1}{2})\epsilon_2+\xi\right)}. \tag{5.19}$$

This elliptic genus is thought of as the one of a free theory including $2k$ chiral and Fermi multiplets with additional k chiral and Fermi multiplets. In the form of multiplicative vari-

ables,

$$\mathcal{I}^{\star}_{(2,2,k)}(e^{2\pi i\xi},Q_m,Q_\tau;q_1,q_2)=\sum_{|\mu|=k}\prod_{(i,j)\in\mu}\frac{\theta_1\left(Q_m^{-1}q_1^{i-\frac{1}{2}}q_2^{-j+\frac{1}{2}}\right)\theta_1\left(Q_m^{-1}q_1^{-i+\frac{1}{2}}q_2^{j-\frac{1}{2}}\right)}{\theta_1\left(q_1^{-\mu_j^{\mathrm{T}}+i}q_2^{-\mu_i+j-1}\right)\theta_1\left(q_1^{\mu_j^{\mathrm{T}}-i+1}q_2^{\mu_i-j}\right)}\times\frac{\theta_1\left(e^{2\pi i\xi}q_1^{i-\frac{1}{2}}q_2^{-j+\frac{3}{2}}\right)}{\theta_1\left(e^{2\pi i\xi}q_1^{i-\frac{1}{2}}q_2^{-j+\frac{1}{2}}\right)}$$
$$=\sum_{|\mu|=k}\prod_{(i,j)\in\mu}\frac{\theta_1\left(Q_m^{-1}q_1^{i-\frac{1}{2}}q_2^{-j+\frac{1}{2}}\right)\theta_1\left(Q_m^{-1}q_1^{-i+\frac{1}{2}}q_2^{j-\frac{1}{2}}\right)}{\theta_1\left(q_1^{-\mu_j^{\mathrm{T}}+i}q_2^{-\mu_i+j-1}\right)\theta_1\left(q_1^{\mu_j^{\mathrm{T}}-i+1}q_2^{\mu_i-j}\right)}\times\frac{\theta_1\left(e^{-2\pi i\xi}q_1^{-i+\frac{1}{2}}q_2^{\mu_i-j+\frac{3}{2}}\right)}{\theta_1\left(e^{-2\pi i\xi}q_1^{-i+\frac{1}{2}}q_2^{\mu_i-j+\frac{1}{2}}\right)},\tag{5.20}$$

where we used (A.12) and an inversion formula (A.46) in the last line. This is exactly the same as (5.16) under the identification

$$e^{2\pi i\xi}=Q_mQ_4^{(2)}\sqrt{\frac{q_1}{q_2}}.\tag{5.21}$$

We can reproduce the result of the refined topological vertex via the geometric transition from the viewpoint of the world-sheet theory that should be the 2d $\mathcal{N}=(0,2)$ U(k) gauge theory with an extra chiral and Fermi multiplet. The validity of the refined version of the geometric transition got supported in this point.

5.4 Characteristics of the defect

In this subsection, we would like to discuss our results for the codimension-2 defect as the intersecting M5′-brane.

5.4.1 Operator interpretation in the Hilbert space of the M2-brane

Let us focus on the contribution $\mathcal{Z}_\mu^{\mathrm{defect}}$ of a codimension-2 defect in (5.16),

$$\mathcal{Z}_\mu^{\mathrm{defect}}(Q_4^{(2)},Q_m,Q_\tau;q_1,q_2)=\prod_{(i,j)\in\mu}\frac{\theta_1\left(Q_m^{-1}\overline{Q}_4^{(2)}q_1^{-i}q_2^{\mu_i-j+2}\right)}{\theta_1\left(Q_m^{-1}\overline{Q}_4^{(2)}q_1^{-i}q_2^{\mu_i-j+1}\right)}=\prod_{(i,j)\in\mu}\frac{\theta_1\left(Q_m^{-1}\overline{Q}_4^{(2)}q_1^{-i}q_2^{j+1}\right)}{\theta_1\left(Q_m^{-1}\overline{Q}_4^{(2)}q_1^{-i}q_2^{j}\right)},\tag{5.22}$$

where the formula (A.12) is used for the second equality. Following the definition of the product over the Young diagram (A.2), we can find that many theta functions are canceled

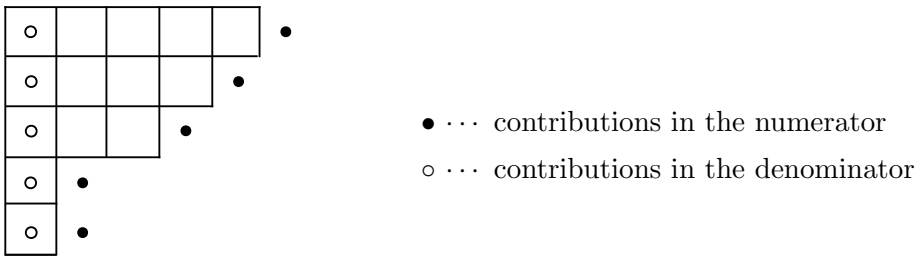

Figure 27: The action of the defect on a state in the Hilbert space of the M2-brane which labeled by a Young diagram.

out between the numerator and denominator, and this is simplified as

$$\mathcal{Z}_{\mu}^{\text{defect}}(Q_4^{(2)}, Q_m, Q_\tau; q_1, q_2) = \prod_{i=1}^{d(\mu)} \frac{\theta_1\left(Q_m^{-1}\overline{Q}_4^{(2)} q_1^{-i} q_2^{\mu_i+1}\right)}{\theta_1\left(Q_m^{-1}\overline{Q}_4^{(2)} q_1^{-i} q_2\right)}. \tag{5.23}$$

The remaining contributions here are visualized onto the Young diagram in Figure 27, where black and white dots stand for the positions of boxes contributing to the partition function in the numerator and denominator, respectively. We try to provide the interpretation to $\mathcal{Z}_{\mu}^{\text{defect}}$ as the expectation value of an operator acting on the Hilbert space of M2-branes.

One can see this Hilbert space simply as follows [32]. In the generating function of M-strings, the distances of M5-branes as domain walls and the complex modulus τ are treated as independent parameters, hence, we can consider the limit that the size of a torus of the M-string becomes sufficiently smaller than the separation of the M5-branes. The stacks of the M2-branes look like an one-dimensional system along the 6 direction. If this direction is virtually regarded as "time" in this system, the M2-branes may be described in terms of this Hilbert space with the M5-brane domain walls as operators acting on it. Then, the states of the M2-branes span this Hilbert space whose ground states $|\mu\rangle$ are labelled by a Young diagram μ, and the "Hamiltonian" is given by $H = |\mu|$. A domain wall Z on which the different numbers of the M2-branes are attached from the left and right actually acts on this Hilbert space, and the domain wall partition function $Z_{\mu_1}^{\nu_1}$ (4.8) and the generating function $G_{(2,1)}$ (4.24) of M-strings on TN_1 can be schematically written as

$$Z_{\mu_1}^{\nu_1}(Q_m, Q_\tau; q_1, q_2) = \langle \mu_1^{\mathrm{T}} | Z | \nu_1 \rangle, \tag{5.24}$$

$$G_{(2,1)}(Q_i^{(\mathfrak{a})}, Q_f, Q_\tau; q_1, q_2) = \langle 0 | Z e^{-\beta H} Z | 0 \rangle, \tag{5.25}$$

where $Q_f = e^{\beta}$, and $|\nu\rangle$ is a complete basis of the Hilbert space. Also, we can re-express our result (5.15) in the languages of this Hilbert space. Let $Z^\star$ be a domain wall with a

codimension-2 defect, then,

$$\begin{aligned} G^{\star}_{(2,2)}(Q_4^{(2)}, Q_m, Q_f, Q_\tau; q_1, q_2) &= \langle 0|Ze^{-\beta H}Z^{\star}|0\rangle \\ &= \sum_{\mu}\langle 0|Ze^{-\beta H}|\mu\rangle\langle \mu^{\mathrm{T}}|Z^{\star}|0\rangle \\ &= \sum_{\mu} e^{-\beta|\mu|}\langle 0|Z|\mu\rangle\langle \mu^{\mathrm{T}}|Z^{\star}|0\rangle. \end{aligned} \tag{5.26}$$

Therefore, the expectation value $\langle \mu^{\mathrm{T}}|Z^{\star}|0\rangle$ includes the contribution (5.23) from the defect. Note that $\langle \mu^{\mathrm{T}}|Z^{\star}|0\rangle$ contains the spectra of M-strings attaching both the domain wall and the defect, but we can easily extract the effect of the defect since its contributions are factorized. Accordingly, we can specify the action of the codimension-2 defect on a state of a certain μ shown as in Figure 27. We are seeking its physical meaning as a future work.

5.4.2 World-sheet description

In the previous subsection, we could identify the world-sheet theory of k M-strings in the presence of a codimension-2 defect with the 2d $\mathcal{N} = (0,2)$ U(k) gauge theory. Recall that this theory is comprised of the $\mathcal{N} = (0,2)$ matter contents listed in Table 5 and additionally

$$\left.\begin{array}{l} \text{A chiral multiplet } \Theta_{\text{chi}} \\ \text{A Fermi multiplet } \Theta_{\text{Fer}} \end{array}\right\} \leftarrow \text{open strings between } k \text{ D2-branes and a D4}'\text{-brane in (5.17)},$$

originated from introducing the defect. We can interpret the appearance of Θ_{chi} and Θ_{Fer} as describing the effect of the defect in the sense of two-dimensional degrees of freedom. We would like to pursue the relation between $(\Theta_{\text{chi}}, \Theta_{\text{Fer}})$ and the action of Figure 27 as the operator in the Hilbert space of the M2-branes.

Further, we assumed that Θ_{chi} and Θ_{Fer} are simultaneously rotated under the global symmetry U$(1)_\xi$, and the equivalence of the partition functions computed by two methods is valid with the identification (5.21), or equivalently,

$$\xi = m + \frac{\epsilon_1 + \epsilon_2}{2} + t_4^{(2)}, \tag{5.27}$$

where $Q_4^{(2)} = \exp(2\pi i t_4^{(2)})$ is a Kähler parameter of $\mathbb{C}\mathbf{P}^1$ associated with an internal line in the web diagram (Figure 25). We naively expect that this global symmetry is originated from the rotation in the 78-plane of (5.1) where the defect M5$'$ extends to it. This expectation is actually true because the first and second part of (5.27) are nothing but g_m (3.19) and g_+ (3.21), respectively, that are the generators of the mass and Ω-deformation acting on the 78-plane. On the other hand, the role of the final one $t_4^{(2)}$ is still mysterious. We are exploring its exact meaning in the context of M-strings.

5.4.3 Specializations of the mass and supersymmetry enhancement

For the case of TN_1 which is basically flat, the theory on M-strings has $(4,4)$ supersymmetry. The insertion of a codimension-2 defect breaks half of them, and the M-string system with the defect keeps $(2,2)$ supersymmetry. As explained in Section 3.3, physical quantities containing nontrivial twist parameters are invariant only under $(0,2)$ supersymmetry, however, this can be enlarged if we tune these parameters. Among these situations, we would pick up two of them in (3.26).

The limit $m = \frac{1}{2}(\epsilon_1 - \epsilon_2)$

The first case is the limit

$$m = \frac{1}{2}(\epsilon_1 - \epsilon_2) \quad \Leftrightarrow \quad Q_m = \sqrt{q_1 q_2}, \tag{5.28}$$

where $\mathcal{N} = (0,2)$ is enhanced to $\mathcal{N} = (2,2)$. It has been pointed out that the partition function of M-strings without the defect is reduced to a constant, that is, does not depend on the complex modulus τ, which we can directly verify. However, this phenomena does not occur in the presence of the defect. Substituting the limit (5.28) into (5.23) gives

$$\mathcal{Z}_{\mu}^{\mathrm{defect}}\Big|_{Q_m=\sqrt{q_1q_2}} = \prod_{i=1}^{d(\mu)} \frac{\theta_1\left(\overline{Q}_4^{(2)} q_1^{-i-\frac{1}{2}} q_2^{\mu_i+\frac{1}{2}}\right)}{\theta_1\left(\overline{Q}_4^{(2)} q_1^{-i-\frac{1}{2}} q_2^{\frac{1}{2}}\right)}. \tag{5.29}$$

This could capture physical states respecting $(2,2)$ supersymmetry which are completely hidden for M-strings without the defect.

The limit $m = \frac{1}{2}(\epsilon_1 + \epsilon_2)$

The second limit is the one argued in Section 4.3,

$$m = \frac{1}{2}(\epsilon_1 + \epsilon_2) \quad \Leftrightarrow \quad Q_m = \sqrt{\frac{q_1}{q_2}}. \tag{5.30}$$

Let us try if this enhancement is the case for our defect. Again using the formula (A.12), the result (5.16) becomes

$$\begin{aligned}\mathcal{Z}^{\star}_{(2,2,k)}(Q_4^{(2)}, Q_m, Q_\tau; q_1, q_2) = \sum_{|\mu|=k} \prod_{(i,j)\in\mu} & \frac{\theta_1\left(Q_m^{-1} q_1^{i-\frac{1}{2}} q_2^{-j+\frac{1}{2}}\right) \theta_1\left(Q_m^{-1} q_1^{-i+\frac{1}{2}} q_2^{j-\frac{1}{2}}\right)}{\theta_1\left(q_1^{-\mu_j^{\mathrm{T}}+i-1} q_2^{-\mu_i+j}\right) \theta_1\left(q_1^{-\mu_j^{\mathrm{T}}+i} q_2^{-\mu_i+j-1}\right)} \\ & \times \frac{\theta_1\left(Q_m^{-1}\overline{Q}_4^{(2)} q_1^{-i} q_2^{\mu_i-j+2}\right)}{\theta_1\left(Q_m^{-1}\overline{Q}_4^{(2)} q_1^{-i} q_2^{\mu_i-j+1}\right)}.\end{aligned} \tag{5.31}$$

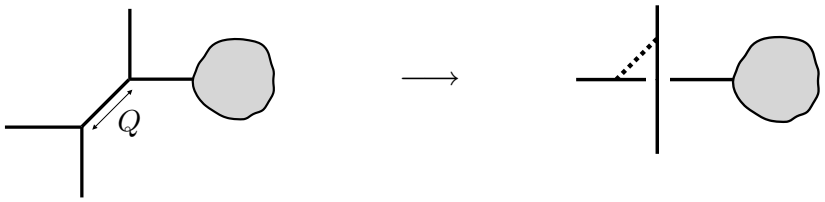

Figure 28: The geometric transition on the uncompactified web diagram, i.e. the toric CY3. The thin gray region is an arbitrary diagram which is not affected by the geometric transition.

Then, the situation is the same as in Section 4.3 where the substitution of (5.30) leads to the fermion zero-modes, thus, we expect that supersymmetry enhancement happens even in the presence of the defect. We have to remove these zero-modes corresponding to the overall U(1) part of U(k) to get a nontrivial contribution,

$$\widehat{\mathcal{Z}}^{\star}_{(2,2,k)}(Q_4^{(2)}, Q_m, Q_\tau; q_1, q_2) := \left.\frac{\mathcal{Z}^{\star}_{(2,2,k)}(Q_4^{(2)}, Q_m, Q_\tau; q_1, q_2)}{\mathcal{Z}^{\star}_{(2,2,1)}(Q_4^{(2)}, Q_m, Q_\tau; q_1, q_2)}\right|_{m=\frac{1}{2}(\epsilon_1+\epsilon_2)}, \tag{5.32}$$

where the part of a codimension-2 defect is written as

$$\prod_{\substack{(i,j)\in\mu \\ (i,j)\neq(1,1)}} \frac{\theta_1\left(\overline{Q}_4^{(2)} q_1^{-i-\frac{1}{2}} q_2^{\mu_i - j+\frac{5}{2}}\right)}{\theta_1\left(\overline{Q}_4^{(2)} q_1^{-i-\frac{1}{2}} q_2^{\mu_i - j+\frac{3}{2}}\right)}. \tag{5.33}$$

This form seems the one of a chiral multiplet in the 2d $\mathcal{N}=(2,2)$ theory, and supersymmetry might get enhanced. We would postpone a precise check of this enhancement near future.

5.4.4 Generalization of the geometric transition

More general parameter tuning for the geometric transition in the refined case has been suggested in [69] to be able to insert nonelementary surface defects in the 4d gauge theory as multiple Lagrangian branes. The natural extension of the specialization (5.10) is

$$Q_1^{(1)} = \sqrt{\frac{q_1}{q_2}}, \qquad Q_1^{(2)} = \frac{q_1^r}{q_2^s}\sqrt{\frac{q_1}{q_2}} \qquad \text{for } r, s \geq 0. \tag{5.34}$$

In [69], it has been found that the emergence of the surface defect labeled by (r, s) via the geometric transition could restrict the shape of the associated Young diagram. They considered only web diagrams without any compactification, that is, toric CY3 cases. For example of Figure 28 and the choice of the preferred direction in the refined topological vertex different from our calculation, the refined topological string partition function contains the factor

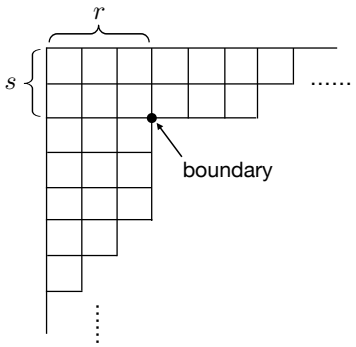

Figure 29: The zero-dimensional boundary on the Young diagram due to the surface defect.

$$\frac{1-Qq_1^{-j+\frac{1}{2}}q_2^{\mu_j^{\mathrm{T}}-i+\frac{1}{2}}}{1-Qq_1^{-j+\frac{1}{2}}q_2^{-i+\frac{1}{2}}}\to\frac{1-q_1^{r-j+1}q_2^{\mu_j^{\mathrm{T}}-s-i}}{1-q_1^{r-j+1}q_2^{-s-i}}, \tag{5.35}$$

where we implement the limitation (5.34) as

$$Q=\frac{q_1^r}{q_2^s}\sqrt{\frac{q_1}{q_2}}\qquad\text{for }\ r,s\geq 0. \tag{5.36}$$

This type of the specialization may be expected to geometrically engineer the surface defect in $\mathbb{R}^4_{\epsilon_1,\epsilon_2}$ whose support is given by

$$z_1^r z_2^s=0, \tag{5.37}$$

where z_1 and z_2 are complex coordinates on $\mathbb{R}^2_{\epsilon_1}$ and $\mathbb{R}^2_{\epsilon_2}$, respectively. One can immediately see that this factor vanishes if the conditions $j\geq r+1$ and $\mu_j^{\mathrm{T}}-i\geq s$ are simultaneously satisfied. This is because the numerator contains 0 when there is a box in some position for $j\geq r+1$ and $\mu_j^{\mathrm{T}}-i\geq s$. Thus, the insertion of this surface defect brings a zero-dimensional boundary on the Young diagram such that the nontrivial partition function picks only up the boxes of positions within

$$1\leq j\leq r\quad\text{ or }\quad 1\leq i\leq\mu_{r+1}^{\mathrm{T}}-s \tag{5.38}$$

in the Young diagram (see Figure 29). Consequently, the shape of the diagram is restricted to be hook-shaped.

Let us apply the general limitation (5.34) to our M-strings. Putting it to the generating function (5.9) gives

$$\begin{aligned}\mathcal{Z}^{\star}_{(2,2,k)}(Q_4^{(2)},Q_m,Q_\tau;q_1,q_2)=\sum_{|\mu|=k}\prod_{(i,j)\in\mu}&\frac{\theta_1\left(Q_m^{-1}q_1^{i-\frac{1}{2}}q_2^{-\mu_i+j-\frac{1}{2}}\right)\theta_1\left(Q_m^{-1}q_1^{-i+\frac{1}{2}}q_2^{\mu_i-j+\frac{1}{2}}\right)}{\theta_1\left(q_1^{-\mu_j^{\mathrm{T}}+i}q_2^{-\mu_i+j-1}\right)\theta_1\left(q_1^{-\mu_j^{\mathrm{T}}+i-1}q_2^{-\mu_i+j}\right)}\\&\times\frac{\theta_1\left(Q_m^{-1}\overline{Q}_4^{(2)}q_1^{-i-r}q_2^{\mu_i-j+1+s}\right)}{\theta_1\left(Q_m^{-1}\overline{Q}_4^{(2)}q_1^{-i}q_2^{\mu_i-j+1}\right)}.\end{aligned} \tag{5.39}$$

The above result (5.16) is the case of $(r, s) = (0, 1)$. The defect as in the second line of (5.39) does not make an effect to constraint the shape of the Young diagram (see Figure 27). From the field theory viewpoint, this discrepancy seems not to matter since the theory and also the kind of the defect under consideration in [69] basically differ from ours. On the other hand, in the standpoint of the topological vertex, this gap might be interpreted as the difference of the normalization to derive the partition function for the BPS counting. Specifically, the basic ingredient of the refined topological vertex is to select the preferred direction, but this is actually a technical artifact, hence, results naively computed by the refined topological vertex should not depend on the choice of the preferred direction (see an example in Appendix B.2). This statement is schematically given as

$$Z^{\mathrm{DGH}}\left(\right. \quad \left.\right) = Z\left(\right. \quad \left.\right), \tag{5.40}$$

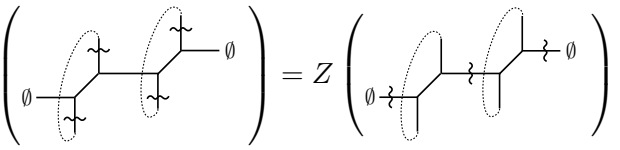

where Z^{DGH} is in the calculation scheme of [69], and a wavy line stands for the preferred direction. These need to be normalized in order to produce the partition function in the gauge theory, and for the current situation, our normalization is different from that in [69],

$$\mathcal{Z}^{\mathrm{DGH}} = Z^{\mathrm{DGH}}\left(\right. \quad \left.\right) \Big/ Z^{\mathrm{DGH}}\left(\right. \quad \left.\right), \tag{5.41}$$

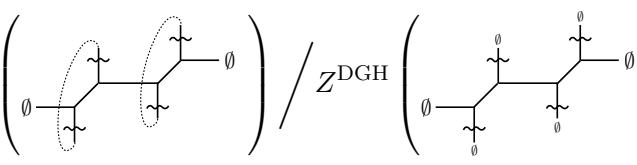

$$\mathcal{Z}_{(2,1,k)} = Z\left(\right. \quad \left.\right) \Big/ Z\left(\right. \quad \left.\right)^{2}, \tag{5.42}$$

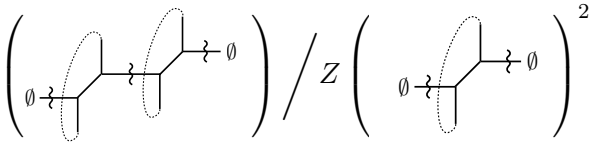

as a result, $\mathcal{Z}^{\mathrm{DGH}} \neq \mathcal{Z}_{(2,1,k)}$. The normalization is simply the scheme in the sense of the topological vertex, but the choice of it looks physically meaningful. We wonder if this is really in the case or not.

6 Defects and open topological string

In the previous section, we found that the insertion of a Lagrangian brane corresponding to a codimension-2 defect can be calculated by the refine topological vertex through the geometric transition, which is confirmed by comparing it with the elliptic genus of the M-string world-sheet theory with the defect. However, we notice that there is the situation where the geometric transition may not naively be applied to generating the Lagrangian brane. In order to overcome this point, the direct computation of the open topological vertex is necessary. We restrict ourselves to the unrefined case ($q_1 = q_2 = q$) as the first

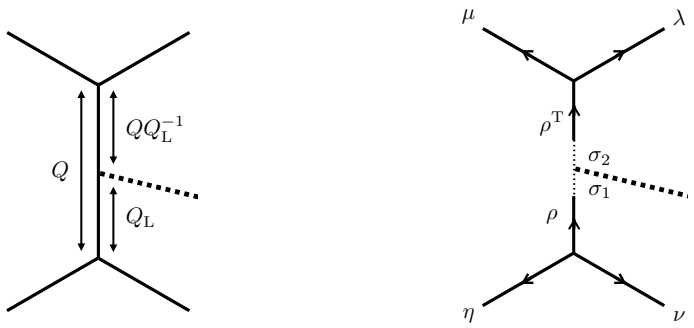

(a) Kähler factors (b) Young diagrams

Figure 30: The parameter assignments for the unrefined open topological vertex.

attempt. Since there are still ambiguities for the formalism of open topological vertex, we would fix them from our results obtained so far.

6.1 A-model open topological string

Gluing rules

We start with packaging rules to bring a Lagrangian brane into the unrefined closed topological vertex based on parameter assignments shown in Figure 30. In the topological string theory, the Lagrangian submanifold in CY3 appears as the boundary condition of an open string to preserve half of supersymmetry. This boundary condition actually is encoded into inserting a holonomy X in the context of the matrix model that is utilized to derive the formula of the topological vertex, thus, the effect of the Lagrangian brane in the web diagram is expressed to multiply the topological vertex $C_{\mu\nu\rho}$ by

$$\mathrm{Tr}_{\sigma_1^{\rm T}} X \times \mathrm{Tr}_{\sigma_2^{\rm T}} X^{-1}, \tag{6.1}$$

where, roughly speaking, the inverse of X comes from opposite orientations on the glued edges. Note that the trace is taken over the transpose of σ_1 (σ_2), which is different from the original formulation in [34]. We here would use this convention. There is an extra Kähler factor $Q_{\rm L}$ as in Figure 30(a). Also, we have to take the framing factor $\mathsf{f}_\rho(q)^{\tilde{\ell}}$ defined in (B.4), where a tilde on ℓ is used for the framing factor of the open topological vertex because, unlike the closed topological vertex, it is a free parameter for the moment. Bringing all together, the topological vertex in the presence of a Lagrangian brane of Figure 30(b) is in the following form:

$$\sum_{\rho,\sigma_1,\sigma_2} (-Q)^{|\rho|} \mathsf{f}_{\rho^{\rm T}\otimes\sigma_2}(q)^{\ell} C_{(\rho\otimes\sigma_1)\eta^{\rm T}\nu} C_{(\rho^{\rm T}\otimes\sigma_2)\lambda\mu^{\rm T}} \left(\mathsf{f}_{\rho\otimes\sigma_1}(q)^{\tilde{\ell}} Q_{\rm L}^{|\sigma_1|} \mathrm{Tr}_{\sigma_1^{\rm T}} X\right) \left(\mathsf{f}_{\rho^{\rm T}\otimes\sigma_2}(q)^{\tilde{\ell}} (QQ_{\rm L}^{-1})^{|\sigma_2|} \mathrm{Tr}_{\sigma_2^{\rm T}} X^{-1}\right). \tag{6.2}$$

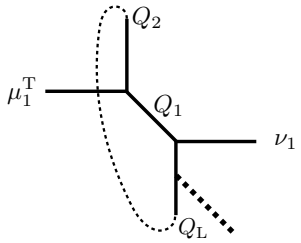

Figure 31: The domain wall on TN_1 with a Lagrangian brane.

In practice, the trace of X can be written by the Schur function,

$$\mathrm{Tr}_\sigma X = s_\sigma(\mathbf{x}), \tag{6.3}$$

where the collection $\mathbf{x} \equiv \{x_i\}$ is a set of eigenvalues of X. The simplest example as an application of the open topological vertex is given below, which is sufficient for our purpose.

The simplest web diagram with a Lagrangian brane

We demonstrate the actual computation with the web diagram in Figure 31. The partition function of the open topological string following (6.2) is given by

$$\begin{aligned} Z^{\nu_1}_{\mu_1}(Q_i, Q_{\mathrm{L}}; q) = &\sum_{\rho_1,\rho_2,\sigma_1,\sigma_2} (-Q_1)^{|\rho_1|}(-Q_2)^{|\rho_2|} C_{\rho_1^{\mathrm{T}}(\rho_2\otimes\sigma_1)\mu_1^{\mathrm{T}}}(q) C_{\rho_1(\rho_2^{\mathrm{T}}\otimes\sigma_2)\nu_1}(q) \\ &\times \left(\mathsf{f}_{\rho_2\otimes\sigma_1}(q)^\ell Q_{\mathrm{L}}^{|\sigma_1|}\mathrm{Tr}_{\sigma_1^{\mathrm{T}}} X\right)\left(\mathsf{f}_{\rho_2^{\mathrm{T}}\otimes\sigma_2}(q)^\ell (Q_2 Q_{\mathrm{L}}^{-1})^{|\sigma_2|}\mathrm{Tr}_{\sigma_2^{\mathrm{T}}} X^{-1}\right). \end{aligned} \tag{6.4}$$

Here we take an *ad hoc* value $\tilde{\ell} = 1$. A problem to proceed with the computation is to deal with the skew Schur functions possessing the tensor product of Young diagram. Fortunately, we can reduce those to the standard skew Schur functions thanks to the formula (A.37) and its definition (A.32) as follows,

$$\begin{aligned} &\sum_{\sigma_1,\sigma_2} (-Q_{\mathrm{L}})^{|\sigma_1|}(-Q_2 Q_{\mathrm{L}}^{-1})^{|\sigma_2|} s_{(\rho_2\otimes\sigma_1)/\lambda_1}(q^{-\mu_1-\mathfrak{n}}) s_{(\rho_2^{\mathrm{T}}\otimes\sigma_2)/\lambda_2}(q^{-\nu_1^{\mathrm{T}}-\mathfrak{n}}) s_{\sigma_1^{\mathrm{T}}}(x) s_{\sigma_2^{\mathrm{T}}}(x^{-1}) \\ &= \sum_{\sigma_1,\sigma_2}\left(\sum_{\gamma_1}\mathcal{N}^{\gamma_1}_{\rho_2\sigma_1} s_{\gamma_1/\lambda_1}(q^{-\mu_1-\mathfrak{n}})\right)\left(\sum_{\gamma_2}\mathcal{N}^{\gamma_2}_{\rho_2^{\mathrm{T}}\sigma_2} s_{\gamma_2/\lambda_2}(q^{-\nu_1^{\mathrm{T}}-\mathfrak{n}})\right) s_{\sigma_1^{\mathrm{T}}}(-Q_{\mathrm{L}}x) s_{\sigma_2^{\mathrm{T}}}(-Q_2 Q_{\mathrm{L}}^{-1}x^{-1}) \\ &= \sum_{\lambda_1,\lambda_2} s_{\gamma_1/\lambda_1}(q^{-\mu_1-\mathfrak{n}}) s_{\gamma_2/\lambda_2}(q^{-\nu_1^{\mathrm{T}}-\mathfrak{n}})\left(\sum_{\sigma_1}\mathcal{N}^{\gamma_1^{\mathrm{T}}}_{\rho_2^{\mathrm{T}}\sigma_1^{\mathrm{T}}} s_{\sigma_1^{\mathrm{T}}}(-Q_{\mathrm{L}}x)\right)\left(\sum_{\sigma_2}\mathcal{N}^{\gamma_2^{\mathrm{T}}}_{\rho_2\sigma_2^{\mathrm{T}}} s_{\sigma_2^{\mathrm{T}}}(-Q_2 Q_{\mathrm{L}}^{-1}x^{-1})\right) \\ &= \sum_{\lambda_1,\lambda_2} s_{\gamma_1/\lambda_1}(q^{-\mu_1-\mathfrak{n}}) s_{\gamma_2/\lambda_2}(q^{-\nu_1^{\mathrm{T}}-\mathfrak{n}}) s_{\gamma_1^{\mathrm{T}}/\rho_2^{\mathrm{T}}}(-Q_{\mathrm{L}}x) s_{\gamma_2^{\mathrm{T}}/\rho_2}(-Q_2 Q_{\mathrm{L}}^{-1}x^{-1}), \end{aligned} \tag{6.5}$$

where we use the property $\mathcal{N}^{\rho}_{\mu\nu} = \mathcal{N}^{\rho^{\mathrm{T}}}_{\mu^{\mathrm{T}}\nu^{\mathrm{T}}}$. Then, we evaluate the domain wall partition function (6.4) along the same manner for the one (4.7) without a Lagrangian brane (see

Appendix C.5 for details), and the resultant form is

$$
\begin{aligned}
Z^{\nu_1}_{\mu_1}(Q_i,Q_{\rm L};q) &= q^{\frac{1}{2}(\kappa_{\mu_1^{\rm T}}+\kappa_{\nu_1})} s_{\mu_1^{\rm T}}(q^{-\mathfrak{n}}) s_{\nu_1}(q^{-\mathfrak{n}}) \prod_{n=1}^{\infty} \frac{1}{1-Q_\tau^n} \\
&\times \prod_{i,j,k=1}^{\infty} \frac{\left(1-Q_\tau^{k-1}Q_1 q^{-\mu^{\rm T}_{1,j}+j-\nu_{1,i}+i-1}\right)\left(1-Q_\tau^{k-1}Q_2 q^{-\nu^{\rm T}_{1,j}+j-\mu_{1,i}+i-1}\right)}{\left(1-Q_\tau^{k}q^{-\mu^{\rm T}_{1,j}+j-\mu_{1,i}+i-1}\right)\left(1-Q_\tau^{k}q^{-\nu^{\rm T}_{1,j}+j-\nu_{1,i}+i-1}\right)} \\
&\times \frac{\left(1-Q_\tau^{k-1}Q_{\rm L} q^{-\mu_{1,i}+i-\frac{1}{2}}x_j\right)\left(1-Q_\tau^{k}Q_1^{-1}Q_{\rm L}^{-1}q^{-\nu^{\rm T}_{1,j}+j-\frac{1}{2}}x_i^{-1}\right)}{\left(1-Q_\tau^{k-1}Q_1Q_{\rm L} q^{-\nu_{1,i}+i-\frac{1}{2}}x_j\right)\left(1-Q_\tau^{k}Q_{\rm L}^{-1}q^{-\mu^{\rm T}_{1,j}+j-\frac{1}{2}}x_i^{-1}\right)}\left(1-Q_\tau^k x_i x_j^{-1}\right).
\end{aligned}
\tag{6.6}
$$

To use this for the comparison with the result obtained via the geometric transition in Section 5, we again normalize this partition function,

$$
\begin{aligned}
&\widehat{Z}^{\nu_1}_{\mu_1}(Q_i,Q_{\rm L};q) := \frac{Z^{\nu_1}_{\mu_1}(Q_i,Q_{\rm L};q)}{Z^{\emptyset}_{\emptyset}(Q_i,Q_{\rm L};q)} \\
&= q^{\frac{1}{2}(\kappa_{\mu_1^{\rm T}}+\kappa_{\nu_1})} s_{\mu_1^{\rm T}}(q^{-\mathfrak{n}}) s_{\nu_1}(q^{-\mathfrak{n}}) \\
&\quad\times \prod_{k=1}^{\infty}\prod_{(i,j)\in\mu_1} \frac{\left(1-Q_\tau^{k-1}Q_1 q^{\nu^{\rm T}_{1,j}-j+\mu_{1,i}-i+1}\right)\left(1-Q_\tau^{k-1}Q_2 q^{-\nu^{\rm T}_{1,j}+j-\mu_{1,i}+i-1}\right)}{\left(1-Q_\tau^{k}q^{-\mu^{\rm T}_{1,j}+j-\mu_{1,i}+i-1}\right)\left(1-Q_\tau^{k}q^{\mu^{\rm T}_{1,j}-j+\mu_{1,i}-i+1}\right)} \\
&\qquad\times \prod_{(i,j)\in\nu_1} \frac{\left(1-Q_\tau^{k-1}Q_2 q^{\mu^{\rm T}_{1,j}-j+\nu_{1,i}-i+1}\right)\left(1-Q_\tau^{k-1}Q_1 q^{-\mu^{\rm T}_{1,j}+j-\nu_{1,i}+i-1}\right)}{\left(1-Q_\tau^{k}q^{-\nu^{\rm T}_{1,j}+j-\nu_{1,i}+i-1}\right)\left(1-Q_\tau^{k}q^{\nu^{\rm T}_{1,j}-j+\nu_{1,i}-i+1}\right)} \\
&\qquad\times \prod_{i=1}^{d(\mu_1)} \frac{\left(1-Q_\tau^{k-1}Q_{\rm L} q^{-\mu_{1,i}+i-\frac{1}{2}}x_j\right)}{\left(1-Q_\tau^{k-1}Q_{\rm L} q^{i-\frac{1}{2}}x_j\right)} \prod_{i=1}^{d(\nu_1)} \frac{\left(1-Q_\tau^{k-1}Q_1Q_{\rm L} q^{i-\frac{1}{2}}x_j\right)}{\left(1-Q_\tau^{k-1}Q_1Q_{\rm L} q^{-\nu_{1,i}+i-\frac{1}{2}}x_j\right)} \\
&\qquad\times \prod_{j=1}^{\check{d}(\mu_1)} \frac{\left(1-Q_\tau^{k}Q_{\rm L}^{-1} q^{j-\frac{1}{2}}x_i^{-1}\right)}{\left(1-Q_\tau^{k}Q_{\rm L}^{-1} q^{-\mu^{\rm T}_{1,j}+j-\frac{1}{2}}x_i^{-1}\right)} \prod_{j=1}^{\check{d}(\nu_1)} \frac{\left(1-Q_\tau^{k}Q_1^{-1}Q_{\rm L}^{-1} q^{-\nu^{\rm T}_{1,j}+j-\frac{1}{2}}x_i^{-1}\right)}{\left(1-Q_\tau^{k}Q_1^{-1}Q_{\rm L}^{-1} q^{j-\frac{1}{2}}x_i^{-1}\right)},
\end{aligned}
\tag{6.7}
$$

where $d(\mu)$ and $\check{d}(\mu)$ represent the number of rows and columns, respectively, in the Young diagram μ.

6.2 Comparison to M-strings with a codimension-two defect

We would check if the above prescription of the open topological vertex correctly reproduces our results (5.16) (or equivalently (5.20)) in the previous section. We should remark that the resolution corresponding to the mass deformation (i.e. a diagonal line) on the domain wall in Figure 31 differs by ninety degrees from the one in Figure 14. These web diagrams are related by the so-called flop transition [114, 115, 116, 117]. We first introduce the concept of the flop transition and next apply it to the comparison with the M-string calculation.

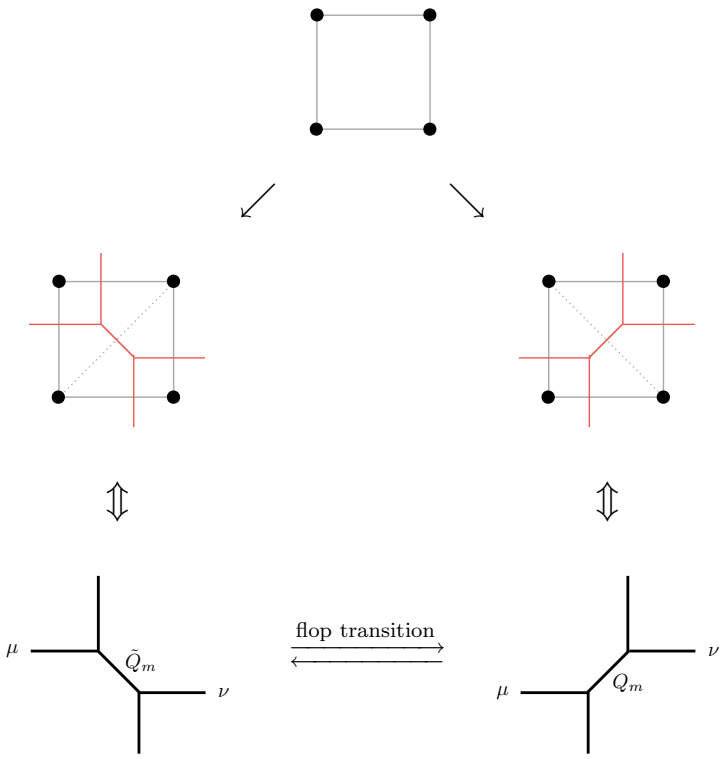

Figure 32: The flop transition in the case of the conifold.

Flop transition

The flop transition [114, 115, 116, 117] is a transformation to exchange different resolutions on web diagrams. The partition function of the topological string theory should be invariant under the flop transition, and this statement can be understood as follows. As shown in Figure 4, a web diagram with the resolution is dual to to a triangulated toric diagram. This relation is an one-to-many correspondence since the way of triangulations is not unique, namely, there are several web diagrams corresponding to one toric diagram. The different triangulations are translated into the flop transition acting on the associated web diagrams (Figure 32). However, a quantity does not depend on the choice of triangulations up to the suitable transformation of parameters. This requirement has directly been verified for the unrefined case [114, 115] and the refined case [116] with a transformation

$$\tilde{Q}_m = Q_m^{-1}. \tag{6.8}$$

Note that originally this was derived in the case of toric CY3's, and it is also found [117] that the flop transition actually works on non-toric ones corresponding to M-strings on which we are focusing in this paper. For M-strings, the following transformation is additionally

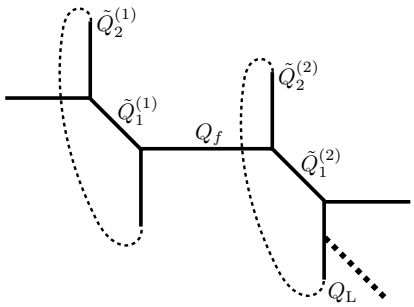

Figure 33: The web diagram with a Lagrangian brane corresponding to the M-strings of $(M,N)=(2,1)$ in the presence of M5′ up to the flop transition.

requested:

$$\tilde{Q}_\tau = Q_\tau, \tag{6.9}$$

where $\tilde{Q}_\tau$ is the complex modulus for the compactified web diagram corresponding to the one on the left side in Figure 32. At the level of the partition function $\mathcal{Z}_{(M,N,k)}$ of k M-strings, the invariance under the flop transition may be valid by accompanying the inversion formula (A.46) of $\theta_1(x;p)$ with transformations (6.8) and (6.9). The conditions on other Kähler factors can be determined recursively [117].

Comparison in the simplest case: $(M,N)=(2,1)$

Let us test whether the computation of the open topological vertex in this section is consistent with the conclusion in Section 5. First of all, we would calculate the refined topological string partition function for the web diagram in Figure 33 by the same strategy as in Section 4.1. We can immediately glue (6.7) with a domain wall partition function $\widehat{Z}^{\mu}_{\emptyset}(\tilde{Q}_i^{(1)};q)$ which does not possess a Lagrangian brane,

$$\begin{aligned}
\check{G}_{(2,1)}(\tilde{Q}_i^{(\mathfrak{a})},Q_{\rm L},Q_f;q_1,q_2) &= \sum_{\mu}(-Q_f)^{|\mu|}\widehat{Z}^{\mu}_{\emptyset}(\tilde{Q}_i^{(1)};q)\widehat{Z}^{\emptyset}_{\mu}(\tilde{Q}_i^{(2)},Q_{\rm L};q) \\
&= \sum_{\mu}\left(-Q_f\tilde{Q}_m\right)^{|\mu|}\prod_{(i,j)\in\mu}\frac{\theta_1\left(\tilde{Q}_m^{-1}q^{-i+\mu_i-j+1}\right)\theta_1\left(\tilde{Q}_m^{-1}q^{i-\mu_i+j-1}\right)}{\theta_1\left(q^{-\mu_j^{\rm T}+i-\mu_i+j-1}\right)\theta_1\left(q^{-\mu_j^{\rm T}+i-\mu_i+j-1}\right)} \\
&\quad\times\prod_{k=1}^{\infty}\prod_{i=1}^{d(\mu)}\frac{\left(1-\tilde{Q}_\tau^{k-1}Q_{\rm L}q^{-\mu_i+i-\frac{1}{2}}x\right)}{\left(1-\tilde{Q}_\tau^{k-1}Q_{\rm L}q^{i-\frac{1}{2}}x\right)}\prod_{j=1}^{\check{d}(\mu)}\frac{\left(1-\tilde{Q}_\tau^{k}Q_{\rm L}^{-1}q^{j-\frac{1}{2}}x^{-1}\right)}{\left(1-\tilde{Q}_\tau^{k}Q_{\rm L}^{-1}q^{-\mu_j^{\rm T}+j-\frac{1}{2}}x^{-1}\right)},
\end{aligned} \tag{6.10}$$

where we use a tilde on Kähler factors to distinguish the ones used in the web diagram of Figure 25 because these are primarily different. Obliviously, the contribution of the open

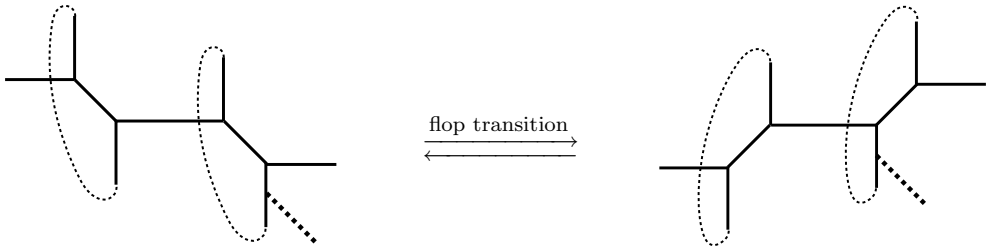

Figure 34: The flop transition transforming the web diagram used in this section into the one considered in the previous section.

topological string is extracted as

$$\check{\mathcal{Z}}^{\rm open}_{\mu}(Q_{\rm L},\tilde{Q}_\tau;q_1,q_2)=\prod_{k=1}^{\infty}\prod_{i=1}^{d(\mu)}\frac{\left(1-\tilde{Q}_\tau^{k-1}Q_{\rm L}q^{-\mu_i+i-\frac{1}{2}}x\right)}{\left(1-\tilde{Q}_\tau^{k-1}Q_{\rm L}q^{i-\frac{1}{2}}x\right)}\prod_{j=1}^{\check{d}(\mu)}\frac{\left(1-\tilde{Q}_\tau^{k}Q_{\rm L}^{-1}q^{j-\frac{1}{2}}x^{-1}\right)}{\left(1-\tilde{Q}_\tau^{k}Q_{\rm L}^{-1}q^{-\mu_j^{\rm T}+j-\frac{1}{2}}x^{-1}\right)}. \tag{6.11}$$

This form seems not to be simply formed into the elliptic theta function, but with the definition (A.2), we can actually do as follows.

$$\begin{aligned}\check{\mathcal{Z}}^{\rm open}_{\mu}(Q_{\rm L},\tilde{Q}_\tau;q_1,q_2)&=\prod_{k=1}^{\infty}\left[\prod_{i=1}^{d(\mu)}\prod_{j=1}^{\mu_i}\frac{\left(1-\tilde{Q}_\tau^{k-1}Q_{\rm L}q^{-j+i-\frac{1}{2}}x\right)}{\left(1-\tilde{Q}_\tau^{k-1}Q_{\rm L}q^{-j+i+\frac{1}{2}}x\right)}\right]\left[\prod_{j=1}^{\check{d}(\mu)}\prod_{i=1}^{\mu_j^{\rm T}}\frac{\left(1-\tilde{Q}_\tau^{k}Q_{\rm L}^{-1}q^{-i+j+\frac{1}{2}}x^{-1}\right)}{\left(1-\tilde{Q}_\tau^{k}Q_{\rm L}^{-1}q^{-i+j-\frac{1}{2}}x^{-1}\right)}\right]\\&=\prod_{k=1}^{\infty}\prod_{(i,j)\in\mu}\frac{\left(1-\tilde{Q}_\tau^{k-1}Q_{\rm L}q^{-j+i-\frac{1}{2}}x\right)}{\left(1-\tilde{Q}_\tau^{k-1}Q_{\rm L}q^{-j+i+\frac{1}{2}}x\right)}\frac{\left(1-\tilde{Q}_\tau^{k}Q_{\rm L}^{-1}q^{-i+j+\frac{1}{2}}x^{-1}\right)}{\left(1-\tilde{Q}_\tau^{k}Q_{\rm L}^{-1}q^{-i+j-\frac{1}{2}}x^{-1}\right)}\\&=q^{-|\mu|}\prod_{(i,j)\in\mu}\frac{\theta_1\left(Q_{\rm L}^{-1}q^{-i+j+\frac{1}{2}}x^{-1};\tilde{Q}_\tau\right)}{\theta_1\left(Q_{\rm L}^{-1}q^{-i+j-\frac{1}{2}}x^{-1};\tilde{Q}_\tau\right)}.\end{aligned} \tag{6.12}$$

This is essentially identical with the unrefined limit of (5.29) obtained by the geometric transition in the previous section[20], but we have to keep in mind that the equivalence between both calculations is up to the flop transition. Consequently, we conjecture the following identification with parameters used in (5.16):

$$Q_{\rm L}\equiv Q_4^{(2)},\qquad x\equiv q^{-\frac{1}{2}}. \tag{6.13}$$

We now demonstrate the flop transition to match up to the partition function obtained through the geometric transition (5.16). Upon the flop transition, the relation (6.9) gives the same elliptic theta function for both expressions, and the condition (6.8) fixes the transformation law of $Q_4^{(2)}$ [117] as

$$Q_4^{(2)}\mapsto Q_m Q_4^{(2)}. \tag{6.14}$$

[20]The weight $q^{-|\mu|}$ may be absorbed into the overall one in $\check{G}_{(2,1)}$ (6.10), but we postpone this point.

Therefore, the extra Kähler factor $Q_{\rm L}$ is transformed as

$$Q_{\rm L} \mapsto Q_m Q_4^{(2)}. \tag{6.15}$$

Finally, we can observe that the open string contribution (6.12) perfectly coincides with the result (5.16) (except for the weight factor $q^{-|\mu|}$). As a result, we suggest that the unrefined open topological vertex (6.2) is the (preliminary) correct prescription. Note that the value of $\tilde{\ell}$ here was taken for computational simplicity, and we would like to find the way to appropriately determine this as a future work.

7 Summary and outlooks

In this thesis, we constructed a codimension-2 defect in the 6d SCFT appropriately as a probe M5-brane. The physical degrees of freedom in this theory on which we focused are M-strings realized as the boundaries of M2-branes ending on slightly separated M5-branes, and we computed the partition function of M-strings in the presence of the codimension-2 defect by using the refined topological vertex and the supersymmetric localization. As main results in the paper through these calculations, we could

- find that the geometric transition to engineer the defect works for the M-string system:
- evaluate the refined topological string partition function with a Lagrangian brane in the internal segment.

In general, the codimension-2 defect in diverse dimensions are defined in a way to impose a specific singular behavior near the support of the defect on fundamental fields in the theory. However, we propose that the definite action of a class of defects realized via the geometric transition is as given in Section 5.4.1. On the other hand, the partition function of M-strings with the defect can be somewhat directly calculated from the point of view of its world-sheet theory which is read from type IIA string theory. The presence of the defect introduces an additional chiral and Fermi multiplet, which is confirmed by comparing these results under the suitable parameter identification. We believe that these results become the first step to classify codimension-2 defects in the 6d SCFT and build applications towards understanding this theory, and as mentioned in Section 5.4.2, it is an important issue to reveal the interplay of these points as a future direction.

Further, to make our computation robuster, we tried to directly apply the open topological vertex to our defect. It is found that we can avoid somehow severe problems on its usage, and the preliminary result perfectly matches with the previous calculations. We also suggest that, at least for the unrefined case, the open topological vertex used in this paper is a correct form with fixing some ambiguities for the known formulation. In closing this paper, we would shortly comment on open problems in which now we are interested.

Connection with codimension-4 defects

In the six-dimensional standpoint, the relation between a codimension-2 and codimension-4 defect is a long standing problem. As considered in this paper, the former is constructed only from an intersecting M5-brane, and the latter is basically originated from a M2-brane with the boundary on the M5-branes. They are of course distinct in M-theory, however, their discrepancy might not appear in the low energy field theory, namely, these engineer completely the same surface defect in the 4d IR theory. It has been suggested [118] that it can be interpreted as a transformation called the separation of variables connecting the Wess-Zumino-Witten (WZW) model and the Liouville theory on a Riemann surface Σ where the M5-brane is wrapped on and the M2-brane is rendered a point, respectively (see e.g. [119, 120, 121]). In the sense of the AGT correspondence, the former is in the case where the M5-brane is wrapping Σ, and the latter where the M2-brane behaves as a vertex operator. It is quite interesting to explore whether our codimension-2 defect could nontrivially confirm the statement of this framework.

Reduction to five dimensions

The codimension-2 defects in five dimensions have been investigated in [122] by making use of the geometric engineering in the (p, q)-fivebrane web diagram as we done in this paper. The 5d supersymmetric gauge theory can be realized by reducing one of spatial directions in the world-volume of the M5-branes, and for our situation, this is the limit where the 1 direction as a 1-cycle of a torus shrinks as in Section 4.1, that is, in terms of the complex modulus,

$$R_1 \to 0 \Rightarrow \tau \to i\infty. \tag{7.1}$$

In this limit, the elliptic theta function produces to the trigonometric function, which is a regular situation for the reduction of the 6d theory on a torus to the 5d theory on a circle.

Moreover, our system may be reduced to the 4d gauge theory on $\mathbb{R}_{\epsilon_1,\epsilon_2}$ as $R_0 \to 0$ (we usually need to be careful in shrinking the 0 direction that is originally the time direction, however, we naively consider this situation because here the 0 direction completely is Euclidian, not the thermal one). As commented in Section 5.1, the result is highly similar to the instanton counting problem considered in [51]. They have given the general formula for the instanton partition function in the presence of the defect and tested the AGT correspondence with several examples. We are wondering if our defect in M-strings could be the origin to describe the one studied in [51, 122].

Relation to an Y-operator

There is an effort to interpret and reformulate supersymmetric gauge theories in terms of representation theory [123] where the main idea is to think of the shape of a quiver diagram for the gauge theory as a Dynkin diagram. Then, it is conjectured that the partition function of the quiver gauge theory is dual to a character formula which is one of basic ingredients in representation theory. Also, this character has been generalized to an one-parameter family of q (unrefined) and a two-parameter family of (q_1, q_2) (refined) which are named q-character and qq-character, respectively. These parameters are ones for the Ω-deformation. On this correspondence, the so-called Y-operator Y [124, 125, 126] has a crucial role to connect them in the concrete way. Schematically, $\mathsf{Y}(x, q)$ depending basically on some fugacity x and q turns out to satisfy the difference equation

$$\langle \mathsf{Y}(x,q) \rangle + \left\langle \frac{1}{\mathsf{Y}(q^{-1}x,q)} \right\rangle + (\text{polynomial}) = 0. \tag{7.2}$$

In fact, the action of $\mathsf{Y}(x, q)$ is very similar to that of our defect expressed by the ratio of the elliptic theta functions in the sense of eigenvalues of a difference operator. We now are investigating the relation between our codimension-2 defect and the Y-operator based on the above equation.

The modular property

Because M-strings are compactified on a torus, we would expect the invariance of the M-string partition function under the $\mathrm{SL}(2, \mathbb{Z})$ transformation. However, this is not the case because $\theta_1(x; p)$ is not equipped with the modular property as mentioned in Appendix A.5. Instead, the partition function of M-strings is holomorphic with τ as expected from the formalism of the topological vertex. We can take this to be modular invariant by adding the non-holomorphic term by hand. This implies that there are holomorphic anomaly equations derived from the M-string partition function [32]. This should be true also for our M-strings with a probe M5′-brane, and it is interesting to understand the meaning of the holomorphic anomaly equation in the context of M-strings from the viewpoint of the string world-sheet.

The refined open topological vertex

The concrete formalism of the refined open topological string is still not established as far as we know. There are basically three points which must be resolved; fixing the framing factor; decomposing the tensor product of Young diagrams; two-parameter generalization of the Schur function associated with a holonomy X. An ad hoc way for first two issues is to determine these factors such that the open topological vertex computation becomes compatible with our result based on the geometric transition. On the final point, in fact,

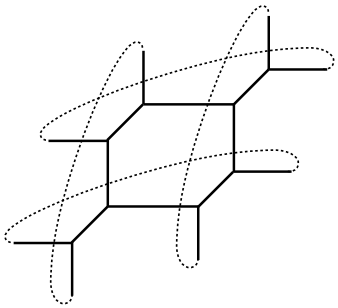

Figure 35: The web diagram with additionally compactifying the horizontal direction.

it is expected that the insertion of X written as the Schur function $s_\mu(\mathbf{x})$ in the unrefined case is replaced with the Macdonald function $P_\mu(\mathbf{x}; q_1, q_2)$ as commented in [69]. This is an absolutely analogue of the extension from the unrefined topological vertex to the refined one. We would try to test if this replacement could work by comparing it with our result.

On further compactification

There is an additionally modified version of M-strings that the 6 direction in (3.17) is also compactified, and the corresponding (p, q)-fivebrane web diagram with $(M, N) = (2, 2)$ is shown in Figure 35. The refined topological vertex still can be applied to this setup, and the M-string partition function is also evaluated as the elliptic genus [88]. However, we may not make use of the geometric transition to engineer the defect in this M-string system and need the direct calculation from the open topological vertex (Section 6) or the elliptic genus. This is another motivation to absolutely formulate the refined version of the open topological vertex, which is in turn applied to the analysis of a more general class of the codimension-2 defects. The result in Section 6 has possibility to overcome this issue.

Interpretation in matrix model and B-model

The formula of the topological vertex has been initiated from the observation of similarity between the topological string theory and the Chern-Simons matrix model [63]. This is in the unrefined case, and its refined extension is conjectured to be described by the so-called refined Chen-Simons theory. With these developments, we would like to know whether there could be a counterpart in the matrix model to our results. Further, there are some works, e.g. [68, 127], to try to translate and analyse the topological vertex results of the A-model topological string theory into the languages of the B-model. It is natural and important for us to seek the interpretation of our results in the B-model.

Acknowledgements

I am deeply grateful to Koji Hashimoto, Yutaka Hosotani, Norihiro Iizuka, Mikito Koshino, Tetsuya Onogi, and Satoshi Yamaguchi for providing great hospitality and substantial discussions to support my research in Osaka University and carefully reading this thesis, and Yuji Sugimoto for entire collaboration to be foundation of this thesis. I would like to extremely thank Takeshi Morita and Akinori Tanaka for largely enriching mathematical knowledge. I also appreciate Yasuaki Hikida, Yosuke Imamura, Katsushi Ito, Yusuke Kanayama, Tetsuji Kimura, Takahiro Nishinaka, Hongfei Shu, Shigeki Sugimoto, Seiji Terashima and Shuichi Yokoyama for giving me wonderful opportunities to communicate and discuss our results. I would like further to thank Babak Haghighat, Hirotaka Hayashi, Kazuo Hosomichi, Seok Kim, Taro Kimura, Can Kozçaz, Kazunobu Maruyoshi, Tomoki Nosaka, Masato Taki, and Wenbin Yan for helpful comments to polish up our results.

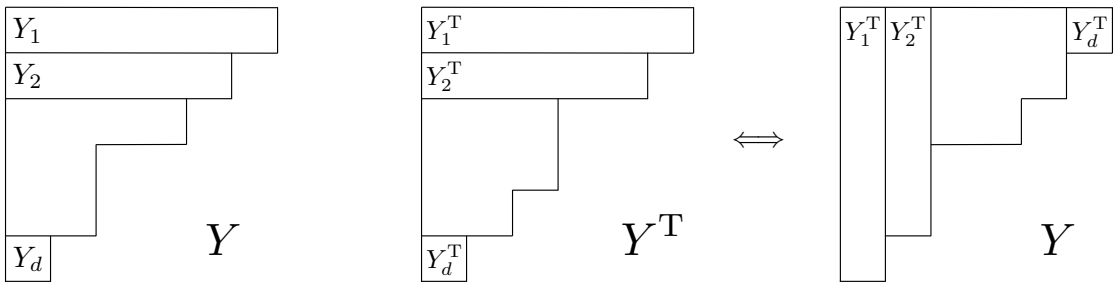

Figure 36: The sequence of the Young diagram Y and its transpose Y^{T}.

A Analysis

In this appendix, we would collect notations and formulae which play a central role in computing our main focuses.

A.1 Young diagrams

Convention

There are several ways to define the Young diagram Y. We here accept the decreasing sequence of nonnegative integers that is useful for the instanton counting,

$$\begin{aligned} Y &= \{Y_i \in \mathbb{Z}_{\geq 0} | Y_1 \geq Y_2 \geq \cdots \geq Y_d\}, \\ Y^{\mathrm{T}} &= \left\{Y_j^{\mathrm{T}} \in \mathbb{Z}_{\geq 0} | Y_j^{\mathrm{T}} = \#\{i | Y_i \geq j\}\right\}, \end{aligned} \tag{A.1}$$

where T means the transpose of the original diagram (Figure 36), and $\#\{i|Y_i \geq j\}$ represents the number of i satisfying $Y_i \geq j$. For notational simplicity, we use the following symbols:

$$|Y| = \sum_{i=1}^{d(Y)} Y_i, \quad ||Y||^2 = \sum_{i=1}^{d(Y)} Y_i^2, \quad \prod_{(i,j)\in Y} f(i,j) = \prod_{i=1}^{d(Y)} \prod_{j=1}^{Y_i} f(i,j) = \prod_{j=1}^{\check{d}(Y)} \prod_{i=1}^{Y_i^{\mathrm{T}}} f(i,j), \tag{A.2}$$

where $d(Y)$ and $\check{d}(Y)$ are the number of rows and columns, respectively, with non-zero entry in Y. Similarly, we will use $\check{d}(Y)$ for the number of columns in Y. One can immediately find that $|Y|$ is the total number of the boxes of Y and

$$|Y| = |Y^{\mathrm{T}}|, \qquad |Y \otimes W| = |Y| + |W|, \qquad d(Y^{\mathrm{T}}) = \check{d}(Y). \tag{A.3}$$

In addition, we introduce the concepts of an *arm* and a *leg* of the Young diagram. Given a box whose position is labelled by $s = (i, j)$ in the Young diagram Y, Y_i is the length of the i-th row and Y_j^{T} is the height of the j-th column as shown in Figure 36. Then, $Y_i - j$ and $Y_j^{\mathrm{T}} - i$ are to be the length of an arm and a leg, respectively, in Y (see Figure 37). Note that these values become negative when the boxes are outside Y.

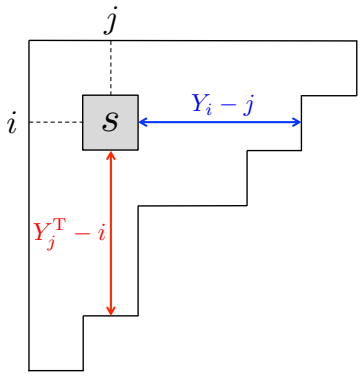

Figure 37: The length of an arm (horizontal arrow) and a leg (vertical arrow) for the box $s = (i, j)$ in Y.

Useful formulae

We enumerate formulae associated with the Young diagram which significantly utilized in the computation of the topological vertex. First, the following relations hold:

$$n(Y) := \sum_{i=1}^{d(Y)} (i-1)Y_i = \frac{1}{2}\sum_{i=1}^{d(Y)} Y_i^{\mathrm{T}}(Y_i^{\mathrm{T}} - 1) = \sum_{(i,j)\in Y} (Y_j^{\mathrm{T}} - i) = \frac{||Y^{\mathrm{T}}||^2}{2} - \frac{|Y|}{2}, \tag{A.4}$$

$$n(Y^{\mathrm{T}}) := \sum_{i=1}^{d(Y^{\mathrm{T}})} (i-1)Y_i^{\mathrm{T}} = \frac{1}{2}\sum_{i=1}^{d(Y^{\mathrm{T}})} Y_i(Y_i - 1) = \sum_{(i,j)\in Y} (Y_i - j) = \frac{||Y||^2}{2} - \frac{|Y|}{2}. \tag{A.5}$$

Next, the hock length $h(i, j)$ and the content $c(i, j)$ are defined as

$$h(i,j) = Y_i - j + Y_j^{\mathrm{T}} - i + 1, \tag{A.6}$$

$$c(i,j) = j - i, \tag{A.7}$$

which satisfy

$$\sum_{(i,j)\in Y} h(i,j) = n(Y^{\mathrm{T}}) + n(Y) + |Y|, \tag{A.8}$$

$$\kappa_Y := \sum_{(i,j)\in Y} c(i,j) = n(Y^{\mathrm{T}}) - n(Y) = \frac{||Y||^2}{2} - \frac{||Y^{\mathrm{T}}||^2}{2}. \tag{A.9}$$

Moreover, for the Young diagrams Y and W, we have

$$\sum_{(i,j)\in W} Y_j^{\mathrm{T}} = \sum_{(i,j)\in Y} W_j^{\mathrm{T}}, \tag{A.10}$$

$$\sum_{(i,j)\in Y} Y_j^{\mathrm{T}} = ||Y^{\mathrm{T}}||^2, \tag{A.11}$$

where the first one was shown in [128]. Finally, when we normalize the partition function of the refined topological string, the following formulae with the Young diagrams μ and ν is highly made use of:

$$\prod_{(i,j)\in\mu}\left(1-Qq_1^{-i+\frac{1}{2}}q_2^{\mu_i-j+\frac{1}{2}}\right)=\prod_{(i,j)\in\mu}\left(1-Qq_1^{-i+\frac{1}{2}}q_2^{j-\frac{1}{2}}\right), \tag{A.12}$$

$$\prod_{i,j=1}^{\infty}\frac{1-Qq_1^{\mu_j^{\mathrm{T}}-i+1}q_2^{\nu_i-j}}{1-Qq_1^{-i+1}q_2^{-j}}=\prod_{(i,j)\in\mu}\left(1-Qq_1^{-\nu_j^{\mathrm{T}}+i}q_2^{-\mu_i+j-1}\right)\prod_{(i,j)\in\nu}\left(1-Qq_1^{\mu_j^{\mathrm{T}}-i+1}q_2^{\nu_i-j}\right), \tag{A.13}$$

where Q is some parameter. There are expressions descended from this by limiting μ or ν,

$$\prod_{i,j=1}^{\infty}\frac{1-Qq_1^{\mu_j^{\mathrm{T}}-i}q_2^{\mu_i-j+1}}{1-Qq_1^{-i}q_2^{-j+1}}=\prod_{(i,j)\in\mu}\left(1-Qq_1^{\mu_j^{\mathrm{T}}-i}q_2^{\mu_i-j+1}\right)\left(1-Qq_1^{-\mu_j^{\mathrm{T}}+i-1}q_2^{-\mu_i+j}\right), \tag{A.14}$$

$$\prod_{i,j=1}^{\infty}\frac{1-Qq_1^{\mu_j^{\mathrm{T}}-i+\frac{1}{2}}q_2^{-j+\frac{1}{2}}}{1-Qq_1^{-i+\frac{1}{2}}q_2^{-j+\frac{1}{2}}}=\prod_{(i,j)\in\mu}\left(1-Qq_1^{i-\frac{1}{2}}q_2^{-j+\frac{1}{2}}\right), \tag{A.15}$$

$$\prod_{i,j=1}^{\infty}\frac{1-Qq_1^{-i+\frac{1}{2}}q_2^{\mu_i-j+\frac{1}{2}}}{1-Qq_1^{-i+\frac{1}{2}}q_2^{-j+\frac{1}{2}}}=\prod_{(i,j)\in\mu}\left(1-Qq_1^{-i+\frac{1}{2}}q_2^{j-\frac{1}{2}}\right), \tag{A.16}$$

or equivalently, for the convenient usage in our calculations,

$$\prod_{i,j=1}^{\infty}\frac{1-Qq_1^{-\mu_j^{\mathrm{T}}+i-\frac{1}{2}}q_2^{-\nu_i+j-\frac{1}{2}}}{1-Qq_1^{i-\frac{1}{2}}q_2^{j-\frac{1}{2}}}=\prod_{(i,j)\in\mu}\left(1-Qq_1^{\nu_j^{\mathrm{T}}-i+\frac{1}{2}}q_2^{\mu_i-j+\frac{1}{2}}\right)\prod_{(i,j)\in\nu}\left(1-Qq_1^{-\mu_j^{\mathrm{T}}+i-\frac{1}{2}}q_2^{-\nu_i+j-\frac{1}{2}}\right), \tag{A.17}$$

$$\prod_{i,j=1}^{\infty}\frac{1-Qq_1^{-\mu_j^{\mathrm{T}}+i}q_2^{-\mu_i+j-1}}{1-Qq_1^{i}q_2^{j-1}}=\prod_{(i,j)\in\mu}\left(1-Qq_1^{-\mu_j^{\mathrm{T}}+i}q_2^{-\mu_i+j-1}\right)\left(1-Qq_1^{\mu_j^{\mathrm{T}}-i+1}q_2^{\mu_i-j}\right). \tag{A.18}$$

A.2 Schur function

The main ingredient of the topological vertex (Appendix B) is the Schur function that is a kind of symmetric polynomials. The vast details about the symmetric polynomial are packaged in, e.g., [129, 130]. Let us denote the set of N variables $(x_1, x_2, \ldots, x_N)$ as x shortly. Given a representation labelled by the Young diagram Y, the Schur function is defined by

$$s_Y(x)=\frac{\det x_j^{Y_i+N-i}}{\det x_j^{N-i}}, \tag{A.19}$$

where

$$\det x_j^{Y_i+N-i} = \begin{vmatrix} x_1^{Y_1+N-1} & x_2^{Y_1+N-1} & \cdots & x_N^{Y_1+N-1} \\ x_1^{Y_2+N-2} & x_2^{Y_2+N-2} & \cdots & x_N^{Y_2+N-2} \\ \vdots & \vdots & \ddots & \vdots \\ x_1^{Y_{N-1}+1} & x_2^{Y_{N-1}+1} & \cdots & x_N^{Y_{N-1}+1} \\ x_1^{Y_N} & x_2^{Y_N} & \cdots & x_N^{Y_N} \end{vmatrix}, \tag{A.20}$$

$$\det x_j^{N-i} = \begin{vmatrix} x_1^{N-1} & x_2^{N-1} & \cdots & x_N^{N-1} \\ x_1^{N-2} & x_2^{N-2} & \cdots & x_N^{N-2} \\ \vdots & \vdots & \ddots & \vdots \\ x_1^0 & x_2^0 & \cdots & x_N^0 \end{vmatrix} = \prod_{1\le i<j\le N} (x_i - x_j) \tag{A.21}$$

for the numerator and the denominator, respectively. The denominator is nothing but the Vandermonde determinant. For examples with $N = 3$, the Schur functions for the symmetric and antisymmetric representation of two boxes are given by

$$s_{\square\square}(x) = \begin{vmatrix} x_1^4 & x_2^4 & x_3^4 \\ x_1^1 & x_2^1 & x_3^1 \\ x_1^0 & x_2^0 & x_3^0 \end{vmatrix} \Big/ \prod_{1\le i<j\le 3} (x_i - x_j) = x_1^2 + x_2^2 + x_3^2 + x_1x_2 + x_2x_3 + x_3x_1,$$

$$s_{\begin{smallmatrix}\square\\\square\end{smallmatrix}}(x) = \begin{vmatrix} x_1^3 & x_2^3 & x_3^3 \\ x_1^2 & x_2^2 & x_3^2 \\ x_1^0 & x_2^0 & x_3^0 \end{vmatrix} \Big/ \prod_{1\le i<j\le 3} (x_i - x_j) = x_1x_2 + x_2x_3 + x_3x_1.$$

The Schur function is sometimes alternatively shown by the following economical expression reflecting the symmetric character:

$$s_Y(x) = \mathrm{Tr}_Y X, \tag{A.22}$$

where the variables $x = (x_1, x_2, \dots)$ are eigenvalues of the matrix X. The Schur function satisfies the following relations:

$$s_Y(\alpha x) = \alpha^{|Y|} s_Y(x), \tag{A.23}$$

$$s_{Y\otimes W}(x) = s_Y(x) s_W(x), \tag{A.24}$$

$$s_Y(q^{\mathfrak{n}}) = q^{\frac{1}{2}\kappa_Y} s_{Y^{\mathrm{T}}}(q^{\mathfrak{n}}) = (-1)^{|Y|} s_{Y^{\mathrm{T}}}(q^{-\mathfrak{n}}), \tag{A.25}$$

$$s_Y(q^{\mathfrak{n}}) s_W(q^{\mathfrak{n}+Y}) = s_W(q^{\mathfrak{n}}) s_Y(q^{\mathfrak{n}+W}), \tag{A.26}$$

where κ_Y is defined in (A.9) and $\mathfrak{n} := -n + \frac{1}{2} = \{-\frac{1}{2}, -\frac{3}{2}, -\frac{5}{2}, \cdots\}$ $(n \in \mathbb{Z}_{>0})$, and the Cauchy formulae,

$$\sum_Y s_Y(x)s_Y(y) = \prod_{i,j\geq 1} \frac{1}{1-x_iy_j} = \exp\left[\sum_{i,j,k=1}^{\infty} \frac{1}{k} x_i^k y_j^k\right], \tag{A.27}$$

$$\sum_Y s_{Y^{\mathrm{T}}}(x)s_Y(y) = \prod_{i,j\geq 1} (1+x_iy_j) = \exp\left[-\sum_{i,j,k=1}^{\infty} \frac{(-1)^k}{k} x_i^k y_j^k\right], \tag{A.28}$$

where the sum of Y is taken over all of representations. We should remark that the Schur function can precisely become the orthogonal basis of the vector space Λ^N spanned by N-order homogeneous polynomials. In fact, let $\langle\cdot,\cdot\rangle$ be a scalar product on Λ^N (i.e. a $\mathbb{Z}_N$-valued bilinear form), then the relation (A.27) is equivalent to

$$\langle s_Y(x), s_W(x)\rangle = \delta_{YW} \quad \text{for } \forall Y, \forall W, \tag{A.29}$$

where δ_{YW} is the Kronecker delta.

A.3 Skew Schur function

There is a generalization of the Schur function called the skew Schur function $s_{Y/W}(x)$ defined by

$$\langle s_{Y/W}, s_V\rangle = \langle s_Y, s_W s_V\rangle. \tag{A.30}$$

The functions have the same argument when we omit it. Note that, by definition, the product of the Schur functions also spans Λ^N and can be re-expanded by the Schur function with some coefficients $\mathcal{N}_{YW}^V$,

$$s_Y s_W = \sum_V \mathcal{N}_{YW}^V s_V. \tag{A.31}$$

Putting this into the original definition (A.30) with orthogonality (A.29), we have

$$\begin{aligned}\langle s_{Y/W}, s_V\rangle &= \sum_R \mathcal{N}_{WV}^R \langle s_Y, s_R\rangle \\ &= \mathcal{N}_{WV}^Y \\ &= \sum_R \mathcal{N}_{WR}^Y \langle s_R, s_V\rangle,\end{aligned}$$

thus, the skew Schur function is alternatively defined as

$$s_{Y/W} = \sum_R \mathcal{N}_{WR}^Y s_R. \tag{A.32}$$

Here, the coefficients $\mathcal{N}_{WR}^{Y}$ are called Littlewood-Richardson coefficients since it counts the multiplicity of the representation parameterized by Y in the decomposition of the tensor product $W \otimes R$ and can be determined using the Littlewood-Richardson rule. The skew Schur function is reduced to the standard Schur function by setting $W = \emptyset$ in (A.30),

$$s_{Y/\emptyset}(x) = s_Y(x). \tag{A.33}$$

Similarly for the Schur function, this function satisfies the following relations:

$$s_{Y/W}(\alpha x) = \alpha^{|Y|-|W|} s_{Y/W}(x), \tag{A.34}$$

$$\sum_Y s_{Y/W}(x) s_{Y/V}(y) = \prod_{i,j\geq 1} \frac{1}{1-x_i y_j} \sum_Y s_{V/Y}(x) s_{W/Y}(y), \tag{A.35}$$

$$\sum_Y s_{Y/W^{\mathrm{T}}}(x) s_{Y^{\mathrm{T}}/V}(y) = \prod_{i,j\geq 1} (1+x_i y_j) \sum_Y s_{V^{\mathrm{T}}/Y}(x) s_{W/Y^{\mathrm{T}}}(y). \tag{A.36}$$

Furthermore, as for (A.24), by compounding the definition (A.30), (A.31), and the orthogonality (A.29),

$$\begin{aligned}
\langle s_{(Y\otimes R)/W}, s_V \rangle &= \langle s_Y s_R, s_W s_V \rangle \\
&= \sum_{P,Q} \mathcal{N}_{YR}^{P} \mathcal{N}_{WV}^{Q} \langle s_P, s_Q \rangle \\
&= \sum_{P} \mathcal{N}_{YR}^{P} \mathcal{N}_{WV}^{P} \\
&= \sum_{P,Q} \mathcal{N}_{YR}^{P} \mathcal{N}_{WQ}^{P} \langle s_Q, s_V \rangle \\
&= \sum_{P} \mathcal{N}_{YR}^{P} \langle s_{P/W}, s_V \rangle,
\end{aligned}$$

thus, we can express the skew Schur function with the tensor product of the Young diagrams as

$$s_{(Y\otimes R)/W} = \sum_P \mathcal{N}_{YR}^{P} s_{P/W}. \tag{A.37}$$

A.4 Macdonald function

The Macdonald function $P_\rho(x; q_1, q_2)$ has been introduced firstly in [130] as the two-parameter generalization of several significant symmetric functions. The Macdonald function is uniquely determined by requiring basic properties of the symmetric function, and reproducing somehow familiar symmetric functions as specializing two parameters (q_1, q_2):

(I) $P_\rho(x; q, 1) = m_\rho(x)$: the monomial symmetric function.

(II) $P_\rho(x; 1, q) = e_{\rho^{\mathrm{T}}}(x)$: the elementary symmetric function.

(III) $\lim_{q\to 1} P_\rho(x;q,q^\beta) = P_\rho^{(1/\beta)}(x)$: the Jack symmetric function.

(IV) $P_\rho(x;0,q) = P_\rho(x;q)$: the Hall-Littlewood function.

(V) $P_\rho(x;q,q) = s_\rho(x)$: the Schur function.

The explicit form of $P_\rho(x;q_1,q_2)$ is quite complicated to write down here (first few terms can be found in [35]), instead we summarize the expressions sufficient for our calculations obtained by limiting $x = q_1^{\pm\mathfrak{n}}$,

$$P_\rho(q_1^{-\mathfrak{n}};q_2,q_1) = \prod_{(i,j)\in\rho} \frac{q_1^{\rho_j^{\mathrm{T}}-i+\frac{1}{2}}}{1-q_1^{\rho_j^{\mathrm{T}}-i+1}q_2^{\rho_i-j}} \qquad \text{for } |q_1|<1, \tag{A.38}$$

$$P_\rho(q_1^{\mathfrak{n}};q_2,q_1) = \prod_{(i,j)\in\rho} \frac{-q_1^{\frac{1}{2}}q_2^{\rho_i-j}}{1-q_1^{\rho_j^{\mathrm{T}}-i+1}q_2^{\rho_i-j}} \qquad \text{for } |q_1^{-1}|<1, \tag{A.39}$$

$$P_{\rho^{\mathrm{T}}}(q_1^{-\mathfrak{n}};q_2,q_1) = \prod_{(i,j)\in\rho} \frac{-q_1^{-\frac{1}{2}}q_2^{-\rho_j^{\mathrm{T}}+i}}{1-q_1^{-\rho_i+j-1}q_2^{-\rho_j^{\mathrm{T}}-i}} \qquad \text{for } |q_1|<1, \tag{A.40}$$

$$P_{\rho^{\mathrm{T}}}(q_1^{\mathfrak{n}};q_2,q_1) = \prod_{(i,j)\in\rho} \frac{q_1^{-\rho_i+j-\frac{1}{2}}}{1-q_1^{-\rho_i+j-1}q_2^{-\rho_j^{\mathrm{T}}-i}} \qquad \text{for } |q_1^{-1}|<1. \tag{A.41}$$

A.5 Theta functions

The elliptic theta functions are defined by [131]

$$\theta_1(z|\tau) = -\sum_{n\in\mathbb{Z}} e^{\pi i\tau\left(n+\frac{1}{2}\right)^2+2\pi i\left(n+\frac{1}{2}\right)\left(z+\frac{1}{2}\right)}, \tag{A.42}$$

$$\theta_2(z|\tau) = \sum_{n\in\mathbb{Z}} e^{\pi i\tau\left(n+\frac{1}{2}\right)^2+2\pi i\left(n+\frac{1}{2}\right)z} = \theta_1\left(z+\tfrac{1}{2}\middle|\,\tau\right), \tag{A.43}$$

$$\theta_3(z|\tau) = \sum_{n\in\mathbb{Z}} e^{\pi i\tau n^2+2\pi inz} = e^{\frac{\pi i\tau}{4}+\pi iz}\theta_2\left(z+\tfrac{\tau}{2}\middle|\,\tau\right), \tag{A.44}$$

$$\theta_4(z|\tau) = \sum_{n\in\mathbb{Z}} e^{\pi i\tau n^2+2\pi in\left(z+\frac{1}{2}\right)} = \theta_3\left(z+\tfrac{1}{2}\middle|\,\tau\right), \tag{A.45}$$

where we have a variable $z\in\mathbb{C}$ and a constant $\tau\in\mathbb{C}$ whose imaginary part is positive. They satisfy inversion and periodic properties listed below which we can easily check from their definitions,

$$\theta_1(-z|\tau) = -\theta_1(z|\tau), \quad \theta_1(z+1|\tau) = -\theta_1(z|\tau), \quad \theta_1(z+\tau|\tau) = -e^{-\pi i\tau-2\pi iz}\theta_1(z|\tau), \tag{A.46}$$

$$\theta_2(-z|\tau) = \theta_2(z|\tau), \quad \theta_2(z+1|\tau) = -\theta_2(z|\tau), \quad \theta_2(z+\tau|\tau) = e^{-\pi i\tau-2\pi iz}\theta_2(z|\tau), \tag{A.47}$$

$$\theta_3(-z|\tau) = \theta_3(z|\tau), \quad \theta_3(z+1|\tau) = \theta_3(z|\tau), \quad \theta_3(z+\tau|\tau) = e^{-\pi i\tau-2\pi iz}\theta_3(z|\tau), \tag{A.48}$$

$$\theta_4(-z|\tau) = \theta_4(z|\tau), \quad \theta_4(z+1|\tau) = \theta_4(z|\tau), \quad \theta_4(z+\tau|\tau) = -e^{-\pi i\tau-2\pi iz}\theta_4(z|\tau). \tag{A.49}$$

It is also worth enumerating their modular transformations, that is, T and S transformation of $\mathrm{SL}(2,\mathbb{Z})$:

$$\theta_1(z|\tau+1) = e^{\frac{\pi i}{4}}\theta_1(z|\tau), \qquad \theta_1\left(\tfrac{z}{\tau}\middle|-\tfrac{1}{\tau}\right) = -i(-i\tau)^{\frac{1}{2}}e^{\frac{\pi i z^2}{\tau}}\theta_1(z|\tau), \tag{A.50}$$

$$\theta_2(z|\tau+1) = e^{\frac{\pi i}{4}}\theta_2(z|\tau), \qquad \theta_2\left(\tfrac{z}{\tau}\middle|-\tfrac{1}{\tau}\right) = (-i\tau)^{\frac{1}{2}}e^{\frac{\pi i z^2}{\tau}}\theta_4(z|\tau), \tag{A.51}$$

$$\theta_3(z|\tau+1) = \theta_4(z|\tau), \qquad \theta_3\left(\tfrac{z}{\tau}\middle|-\tfrac{1}{\tau}\right) = (-i\tau)^{\frac{1}{2}}e^{\frac{\pi i z^2}{\tau}}\theta_3(z|\tau), \tag{A.52}$$

$$\theta_4(z|\tau+1) = \theta_3(z|\tau), \qquad \theta_4\left(\tfrac{z}{\tau}\middle|-\tfrac{1}{\tau}\right) = (-i\tau)^{\frac{1}{2}}e^{\frac{\pi i z^2}{\tau}}\theta_2(z|\tau). \tag{A.53}$$

It is well known that the elliptic theta functions can be re-expressed in terms of the infinite product, for instance,

$$\begin{aligned}\theta_1(z|\tau) &= -ie^{\frac{\pi i\tau}{4}}e^{\pi iz}\prod_{k=1}^{\infty}\left(1-e^{2\pi ik\tau}\right)\left(1-e^{2\pi ik\tau}e^{2\pi iz}\right)\left(1-e^{2\pi i(k-1)\tau}e^{-2\pi iz}\right)\\ &= 2e^{\frac{\pi i\tau}{4}}\sin\pi z\prod_{k=1}^{\infty}\left(1-e^{2\pi ik\tau}\right)\left(1-e^{2\pi ik\tau}e^{2\pi iz}\right)\left(1-e^{2\pi ik\tau}e^{-2\pi iz}\right).\end{aligned} \tag{A.54}$$

There are other expressions $\theta_a(x;p)$ $(a=1,\ldots,4)$ for the elliptic theta functions with setting $x := e^{2\pi iz}$ and $p := e^{2\pi i\tau}$ with $|p|<1$ due to $\mathrm{Im}(\tau)>0$, e.g. for $\theta_1(z|\tau)$,

$$\theta_1(x;p) = -ip^{\frac{1}{8}}x^{\frac{1}{2}}\prod_{k=1}^{\infty}\left(1-p^k\right)\left(1-p^kx\right)\left(1-p^{k-1}x^{-1}\right), \tag{A.55}$$

which is nothing but the Jacobi's triple product identity. Further, this identity for $\theta_a(x;p)$ can be rewritten as the following useful forms:

$$\theta_1(x;p) = -ip^{\frac{1}{8}}x^{\frac{1}{2}}(p,px,x^{-1};p)_\infty, \tag{A.56}$$

$$\theta_2(x;p) = p^{\frac{1}{8}}x^{\frac{1}{2}}(p,-px,-x^{-1};p)_\infty, \tag{A.57}$$

$$\theta_3(x;p) = (p,-p^{\frac{1}{2}}x,-p^{\frac{1}{2}}x^{-1};p)_\infty, \tag{A.58}$$

$$\theta_4(x;p) = (p,p^{\frac{1}{2}}x,p^{\frac{1}{2}}x^{-1};p)_\infty, \tag{A.59}$$

where the q-Pochhammer symbol (or the q-shifted factorial) is given by

$$(x;p)_n = \begin{cases} 1 & \text{for } n=0,\\ \displaystyle\prod_{k=0}^{n-1}(1-xp^k) & \text{for } n\geq 1,\\ \displaystyle\prod_{k=1}^{-n}(1-xp^{-k})^{-1} & \text{for } n\leq -1,\end{cases} \tag{A.60}$$

and $(x;p)_\infty := \lim_{n\to\infty}(x;p)_n$ with $|p|<1$[21]. For simplicity, we use the shorthand notation

$$(x_1,x_2,\cdots,x_r;p)_n := (x_1;p)_n(x_2;p)_n\cdots(x_r;p)_n. \tag{A.61}$$

[21] As named, p is normally denoted by q, but we keep p as an elliptic variable for avoiding confusion with q in the topological vertex.

On the other hand, the theta function closely related to the elliptic theta functions is defined by

$$\theta(x;p) = \frac{1}{(p;p)_\infty} \sum_{n\in\mathbb{Z}} (-1)^n p^{\frac{1}{2}n(n-1)} x^n = (x, px^{-1}; p)_\infty, \tag{A.62}$$

which is often used in the literatures of physics[22]. This function actually fulfils the following inversion formula and difference equation:

$$\theta(x^{-1};p) = -x^{-1}\theta(x;p) = \theta(xp;p), \tag{A.63}$$

$$\theta(xp^n;p) = (-x)^{-n} p^{-\frac{n(n-1)}{2}} \theta(x;p). \tag{A.64}$$

The elliptic theta functions (A.42)-(A.45) are replaced with this theta function via the Jacobi's triple product identity,

$$\theta_1(x;p) = ip^{\frac{1}{8}} x^{-\frac{1}{2}} (p;p)_\infty \, \theta(x;p), \tag{A.65}$$

$$\theta_2(x;p) = p^{\frac{1}{8}} x^{-\frac{1}{2}} (p;p)_\infty \, \theta(-x;p), \tag{A.66}$$

$$\theta_3(x;p) = (p;p)_\infty \, \theta(-xp^{\frac{1}{2}};p), \tag{A.67}$$

$$\theta_4(x;p) = (p;p)_\infty \, \theta(xp^{\frac{1}{2}};p). \tag{A.68}$$

Eisenstein series

We have another series expansion for the elliptic theta function useful to discuss the modular property,

$$\theta_1(z;\tau) = (2\pi i z)\eta(\tau)^3 \exp\left[\sum_{k=1}^{\infty} \frac{B_{2k}}{2k\cdot(2k)!} E_{2k}(\tau)(2\pi i z)^{2k}\right], \tag{A.69}$$

where the 24th power of the Dedekind eta function $\eta(\tau)^{24} = \Delta(\tau)$, called the modular discriminant, is a modular form of the weight 12, and B_{2k} are the Bernoulli numbers defined as the coefficients of the Taylor expansion,

$$\frac{x}{e^x - 1} = \sum_{n=0}^{\infty} \frac{B_n}{n!} x^n. \tag{A.70}$$

[22]There are several notations with the symbol $\theta(x;p)$ also in the literatures of mathematics. For example,

$$\theta(x;p) = \sum_{n\in\mathbb{Z}} p^{\frac{n^2}{2}} (-x)^n = \left(p, p^{\frac{1}{2}}x, p^{\frac{1}{2}}x^{-1}; p\right)_\infty,$$

which is called the theta function of Jacobi in our paper [132] (denoted by $\theta_p(x)$ with the base p as terminology). This is absolutely identical with $\theta_4(x;p)$, and the elliptic theta functions above are frequently referred to as the theta functions of Jacobi (or Jacobi's theta functions) without distinction. Remark that some notations are basically related with each other only by redefining x.

The function $E_{2k}(\tau)$ is the Eisenstein series of the wight $2k$ defined by

$$E_{2k}(\tau) = 1 + \frac{2}{\zeta(1-2k)} \sum_{n=1}^{\infty} n^{2k-1} \frac{q^n}{1-q^n} = 1 - \frac{4k}{B_{2k}} \sum_{n=1}^{\infty} \sigma_{2k-1}(n) q^n, \tag{A.71}$$

where $\zeta(1-2k)$ is the Riemann zeta function given by $\zeta(s) = \sum_{n=1}^{\infty} n^{-s}$. In addition, $\sigma_x(n) = \sum_{d|n} d^x$ is called the divisor sum function which is the summation over the x-th power of the positive divisors of $n \in \mathbb{N}$. Precisely speaking, the Eisenstein series $E_{2k}(\tau)$ is regarded as the one by normalizing the holomorphic Eisenstein series,

$$E_{2k}(\tau) = \frac{G_{2k}(\tau)}{2\zeta(2k)}, \qquad G_{2k}(\tau) = \sum_{(m,n)\in\mathbb{Z}\setminus(0,0)} \frac{1}{(m+n\tau)^{2k}}, \tag{A.72}$$

and transformed as

$$E_{2k}\left(\frac{a\tau+b}{c\tau+d}\right) = \begin{cases} (c\tau+d)^2 E_2(\tau) - i\pi c(c\tau+d) & \text{for } k=1, \\ (c\tau+d)^{2k} E_{2k}(\tau) & \text{for } k>1, \end{cases} \tag{A.73}$$

under the modular transformation

$$\begin{pmatrix} a & b \\ c & d \end{pmatrix} \in \mathrm{SL}(2,\mathbb{Z}). \tag{A.74}$$

Therefore, $E_2(\tau)$ is *not* a modular form. To make it a modular form, we have to add a non-holomorphic term such that

$$\widehat{E}_2(\tau,\bar{\tau}) := E_2(\tau) - \frac{3}{\pi \mathrm{Im}(\tau)}, \tag{A.75}$$

then $\widehat{E}_2(\tau,\bar{\tau})$ becomes exactly a modular form of the weight 2,

$$\widehat{E}_2\left(\frac{a\tau+b}{c\tau+d}\right) = (c\tau+d)^2 \widehat{E}_2(\tau). \tag{A.76}$$

This observation actually tells us that if we exchange $E_2(\tau)$ with $\widehat{E}_2(\tau,\bar{\tau})$ in $\theta_1(z;\tau)$ (A.69), the M-strings partition function becomes *non-holomorphic* but invariant under the modular transformation acting on the twist parameters as

$$\mathrm{SL}(2,\mathbb{Z}) : (\tau, m, \epsilon_1, \epsilon_2) \mapsto \left(\frac{a\tau+b}{c\tau+d}, \frac{m}{c\tau+d}, \frac{\epsilon_1}{c\tau+d}, \frac{\epsilon_2}{c\tau+d}\right). \tag{A.77}$$

B Topological vertex

The topological vertex [34] and its refined extension [35, 36] are basic blocks to compute quantities, e.g. a free energy and Gromov-Witten invariants, in the A-model topological string theory[23]. There are a wide variety of works associated with the topological string

[23]The counterpart in the B-model topological string theory is called the topological recursion [133].

theory beyond the original geometrical perspectives, and recently it was found that this technique might be applied to condensed matter physics [134]. We would summarize the definitions of the unrefined/refined topological vertex and demonstrate how to use it to count the BPS states on Calabi-Yau three-folds (CY3's). The details of deriving the formulation and further geometrical aspects of the topological vertex are not shown here because these are not the scope of this paper, and our standpoint is to make use of it as a computational tool relying on its successful advancements in string theory and gauge theories. The readers who are interested in arguments beyond this paper[24] is asked to refer to the literatures [89, 90, 34, 91, 35, 36, 128, 138, 139, 140].

B.1 Unrefined case

The topological vertex $C_{\mu\nu\rho}(q)$ [34] is a function of q charactering the trivalent vertex of Figure 38, which is the web diagram of the simplest CY3, $\mathbb{C}^3$. A class of non-compact toric CY3's[25] basically can be described in terms of the web diagram by appropriately gluing this trivalent vertex. The indices μ, ν, and ρ there represent Young diagrams assigned on the ends of the vertex, and the directions of arrows on edges fix the Young diagrams such that we choose μ if the arrow is outgoing from the vertex and its transpose μ^{T} if the arrow is ingoing. These labels correspond to the boundary conditions of fundamental strings in the topological string theory. The topological string theory is a supersymmetric non-linear sigma model on the world-sheet of a string whose target space is CY3, and the string is wrapped on a two-dimensional subspace of CY3. Thus, the partition function of the topological string theory captures information about BPS states yielded by the string states on CY3 (more precisely, counts the holomorphic maps of the world-sheet to the target space). Through the correspondence between the web diagram of CY3 and the (p, q)-fivebrane web in string theory [89, 90, 91], the presence of the edges in the former is mapped to the corresponding D-branes where open strings can end on. Roughly, in this viewpoint, the boundary condition and the winding direction of the strings are characterized by the Young diagram and the arrow on the edge, respectively. The topological vertex $C_{\mu\nu\rho}(q)$ has been derived as

$$\begin{aligned} C_{\mu\nu\rho}(q) &= q^{\frac{1}{2}(\kappa_\nu+\kappa_\rho)} s_\rho(q^{-\mathfrak{n}}) \sum_\lambda s_{\mu^{\mathrm{T}}/\lambda}(q^{-\rho-\mathfrak{n}}) s_{\nu/\lambda}(q^{-\rho^{\mathrm{T}}-\mathfrak{n}}), \\ \kappa_\nu &:= ||\nu||^2 - ||\nu^{\mathrm{T}}||^2, \qquad \mathfrak{n} := -n + \frac{1}{2} = \left\{ -\frac{1}{2}, -\frac{3}{2}, -\frac{5}{2}, \cdots \right\} \ (n \in \mathbb{Z}_{>0}), \end{aligned} \tag{B.1}$$

where the functions used here are the Schur function (A.19) and skew Schur function (A.32). The parameter assignment of $C_{\mu\nu\rho}$ is depicted in Figure 38. There we also give vectors v

[24] For example, the topological string theory is well established only in the perturbative sense, and one of interesting directions is towards its non-perturbative definition [135, 136, 137] (and references therein).

[25] The toric manifold is a n-dimensional complex manifold equipped with n isometries which commute with each other.

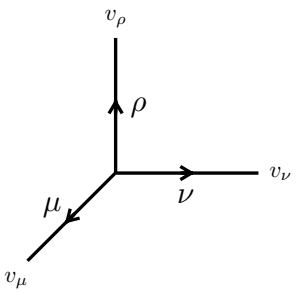

Figure 38: The definition of the unrefined topological vertex. μ, ν, and ρ are Young diagrams, and a vector v is appropriately chosen for each associated edge.

for edges to fix the so-called framing since it has been shown that the final result has an ambiguity of this framing [141]. The appropriate way to specify this framing will be provided below. For $\mathbb{C}^3$ as an example, the vectors are

$$v_\mu = (-1, -1), \qquad v_\nu = (1, 0), \qquad v_\rho = (0, 1), \tag{B.2}$$

along the directions of arrows in Figure 38. Note that the topological vertex has a non-trivial symmetry called cyclic symmetry,

$$C_{\mu\nu\rho}(q) = C_{\rho\mu\nu}(q) = C_{\nu\rho\mu}(q). \tag{B.3}$$

Next, we would like to give the prescription of gluing the topological vertex to obtain the partition function on a non-compact toric CY3 as a target space. For given two vertices, the gluing process is comprised of the following four steps:

(UR1) Fix a pair of edges to connect the vertices so that one has the outgoing arrow with a Young diagram ρ and the other has the ingoing arrow with a Young diagram ρ^{T}.

(UR2) Multiply the topological vertices (B.1) by a Kähler factor $(-Q)^{|\rho|}$ which corresponds to a Kähler parameter of $\mathbb{C}\mathbf{P}^1$ arising on a internal segment after making a joint.

(UR3) In addition to the Kähler factor, we have to include the so-called framing factor $\mathsf{f}_\rho(q)^\ell$ ($\ell \in \mathbb{Z}$) [141] given by

$$\mathsf{f}_\rho(q) = (-1)^{|\rho|} q^{-\frac{1}{2}\kappa_\rho}. \tag{B.4}$$

(UR4) Finally, take a sum over ρ allocated on the glued edge.

We should note that an exponent ℓ of the framing factor is determined as follows. One specifies vectors for the edges counterclockwise next from the glued edge on the vertices in question (Figure 39) and then take the exterior product of those vectors,

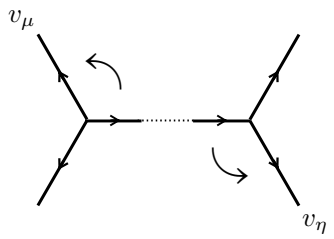

Figure 39: Our convention to determine the exponent of the framing factor.

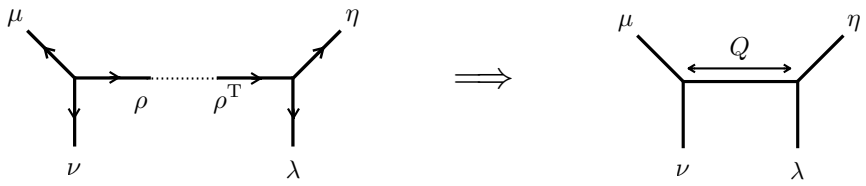

Figure 40: The web diagram of $\mathcal{O}(0) \oplus \mathcal{O}(-2) \to \mathbb{P}^1$.

$$\ell = v_\mu \wedge v_\eta = \det \begin{pmatrix} v_\mu^1 & v_\mu^2 \\ v_\eta^1 & v_\eta^2 \end{pmatrix}. \tag{B.5}$$

This value is actually what we have to use for the framing factor. We would demonstrate this below with a simple example.

Example: $\mathcal{O}(0) \oplus \mathcal{O}(-2) \to \mathbb{P}^1$**.**

We would show the way to access the topological vertex with one of the simplest CY3, $\mathcal{O}(0) \oplus \mathcal{O}(-2) \to \mathbb{P}^1$ (Figure 40). The only necessary thing is to determine an integer exponent ℓ of the framing factor. In Figure 40, we choose horizontal edges to link the vertices, and following the prescription (B.5),

$$\ell = v_\mu \wedge v_\lambda = \det \begin{pmatrix} -1 & 1 \\ 0 & -1 \end{pmatrix} = 1. \tag{B.6}$$

Combining the steps (UR1)-(UR4), the topological string partition function is written as

$$Z_{\mu\nu}^{\eta\lambda}(Q;q) = \sum_\rho (-Q)^{|\rho|} \mathsf{f}_\rho(q) C_{\mu\nu\rho}(q) C_{\lambda\eta\rho^{\mathrm{T}}}(q). \tag{B.7}$$

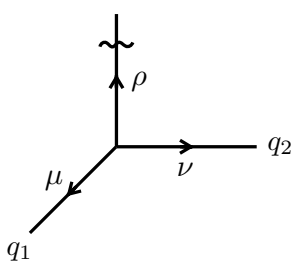

(a) Parameters and the preferred direction

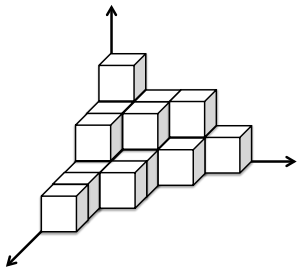

(b) 3D Young diagram

Figure 41: The definition of the refined topological vertex. The wavy line stands for the preferred direction.

B.2 Refined case

The topological vertex given in the previous subsection depends on a single parameter q, and the two parameter extension has been constructed in [35, 36, 142][26], which is called the refined topological vertex. Accordingly, the previous vertex $C_{\mu\nu\rho}(q)$ was rephrased as the unrefined topological vertex. The main purpose of this generalization is to reproduce the instanton counting with the Ω-background (ϵ_1, ϵ_2) in four-dimensional quantum field theories as well as the unrefined one does, but we should remark that it is not known whether the refined topological vertex can be interpreted consistently in the languages of geometry and string theory. Therefore, at least with the current status, we would treat it as a systematic computing method, but developing examples to justify the refined topological vertex is now making its applicable range wider and wider. The refined topological vertex $C_{\mu\nu\rho}(q_1, q_2)$ is defined as

$$C_{\mu\nu\rho}(q_1,q_2) = q_1^{-\frac{||\nu^{\mathrm{T}}||^2}{2}} q_2^{\frac{||\nu||^2+||\rho||^2}{2}} \widetilde{Z}_\rho(q_1,q_2) \sum_\lambda \left(\frac{q_2}{q_1}\right)^{\frac{|\lambda|+|\mu|-|\nu|}{2}} s_{\mu^{\mathrm{T}}/\lambda}(q_1^{-\mathfrak{n}} q_2^{-\rho}) s_{\nu/\lambda}(q_1^{-\rho^{\mathrm{T}}} q_2^{-\mathfrak{n}}),$$
$$\widetilde{Z}_\rho(q_1,q_2) = \prod_{(i,j)\in\rho} \frac{1}{1-q_1^{\rho_j^{\mathrm{T}}-i+1} q_2^{\rho_i-j}}, \qquad \mathfrak{n} := -n+\frac{1}{2} = \left\{-\frac{1}{2}, -\frac{3}{2}, \cdots\right\} \ (n \in \mathbb{Z}_{>0}). \tag{B.8}$$

The main distinction from the unrefined topological vertex is that we need to specify the *preferred direction* expressed as a wavy line in Figure 41(a). The role of the preferred direction is seen as follows. We put a Young diagram on each end, hence, the vertex can be viewed as a three-dimensional Young diagram as in Figure 41(b). This is because there now exist two parameters (q_1, q_2) corresponding to the Ω-background, and then we can distinguish the

[26] At the beginning, the formulation of the refined topological vertex has been proposed by [35] and [36] independently, and latter it was argued in [143] that they are precisely equivalent.

edges by bringing them together with the edges of the vertex like as Figure 41(a). When it is mapped into the three-dimensional Young diagram, all axises are independent, thus, we project it onto a two-dimensional slice by choosing one axis to utilize the standard method for an usual Young diagram. The choice of the slice on the three-dimensional Young diagram is implemented by the preferred direction. Upon the computation with the refined topological vertex, firstly we fix the preferred direction, secondly assign (q_1, q_2) on the remaining edges. Note that the function $\widetilde{Z}_\rho(q_1, q_2)$ is essentially the Macdonald polynomial $P_\rho(x; q_2, q_1)$ (A.38),

$$\widetilde{Z}_\rho(q_1, q_2) = q_1^{-\frac{||\rho^{\mathrm{T}}||^2}{2}} P_\rho(q_1^{-\mathfrak{n}}; q_2, q_1). \tag{B.9}$$

The refined topological vertex $C_{\mu\nu\rho}(q_1, q_2)$ in the unrefined limit $q_1 = q_2 = q$ is reduced, as required, to the unrefined one $C_{\mu\nu\rho}(q)$ due to the property (V) of the Macdonald function.

Let us turn to providing the gluing prescription for the refined topological vertex. The rule is basically the same as for the unrefined case, but there are differences come from the number of the parameters and the preferred direction. For given two refined vertices, this is achieved by the following steps:

(R1) Fix a pair of edges to connect the vertices so that one has the outgoing arrow with a Young diagram ρ and the other has the ingoing arrow with a Young diagram ρ^{T}.

(R2) Further, fix the preferred direction on one edge of the one vertex, then for the other vertex the preferred direction is chosen on the edge extending to the same axis as the previous one.

(R3) Assign parameters (q_1, q_2) on two of three edges as follows: If the preferred direction is *not* on the glued edge, these parameters are placed in the same manner as Figure 41(a) for the one vertex so that q_1 (q_2) presents on the glued edge, and then the parameters are put on the other vertex such that q_2 (q_1) resides in the glued edge: If the preferred direction *is* on the glued edge, q_1 in the one vertex and q_2 in the other vertex are set as to belong to the edges counterclockwise next from the glued edges as if the edges associated with q_1 and q_2 would be connected.

(R4) Multiply the refined topological vertices (B.8) by a Kähler factor $(-Q)^{|\rho|}$ and the framing factor $\mathsf{f}_\rho(q_1, q_2)^\ell$ ($\ell \in \mathbb{Z}$) for the refined one given by

$$\begin{cases} \mathsf{f}_\mu(q_1, q_2) = (-1)^{|\mu|} q_1^{\frac{||\mu^{\mathrm{T}}||^2}{2}} q_2^{-\frac{||\mu||^2}{2}} & \text{if the preferred direction } \textit{is} \text{ the glued edge,} \\ \tilde{\mathsf{f}}_\mu(q_1, q_2) = (-1)^{|\mu|} q_1^{\frac{||\mu^{\mathrm{T}}||^2+|\mu|}{2}} q_2^{-\frac{||\mu||^2+|\mu|}{2}} & \text{if the preferred direction is } \textit{not} \text{ the glued edge.} \end{cases} \tag{B.10}$$

(R5) Finally, take a sum over ρ allocated on the glued edge.

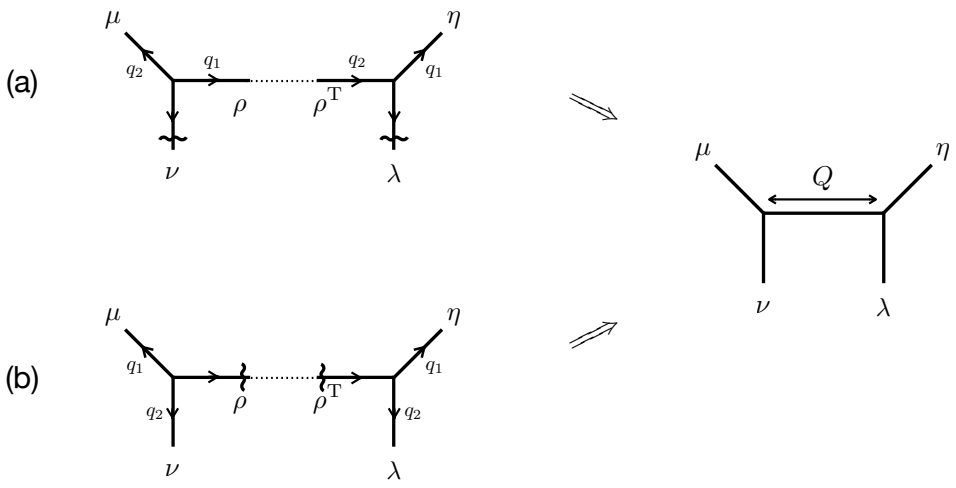

Figure 42: The web diagram of $\mathcal{O}(0)\oplus\mathcal{O}(-2)\to\mathbb{P}^1$. The preferred direction is set along the vertical line in (a) and along the horizontal glued line in (b).

The forms in (B.10) have been determined in [139, 140] by requesting the refined topological string partition function to match the superconformal index of the gauge theory engineered by the associated (p,q)-fivebrane web. We perform this procedure with $\mathcal{O}(0)\oplus\mathcal{O}(-2)\to\mathbb{P}^1$.

Example: $\mathcal{O}(0)\oplus\mathcal{O}(-2)\to\mathbb{P}^1$ revisited

There are three different ways to select the preferred direction in gluing two vertices, here we implement two of them in the refined topological vertex computation since the crucial point is whether the preferred direction is taken on the glued segment or not (Figure 42). As before, the power of the framing factor is $\ell=1$. For the case (a) in Figure 42,

$$Z^{\eta\lambda}_{\mu\nu}(Q;q_1,q_2)=\sum_{\rho}(-Q)^{|\rho|}\,\tilde{\mathsf{f}}_{\rho}(q_2,q_1)C_{\rho\mu\nu}(q_1,q_2)C_{\eta\rho^{\mathrm{T}}\lambda}(q_1,q_2). \tag{B.11}$$

For the case (b) in Figure 42 where the preferred direction is on the glued edge, following the step (R3), we assign q_1 on the edge of μ in the left vertex and q_2 on the edge of λ in the right vertex. As a result, we have

$$\check{Z}^{\eta\lambda}_{\mu\nu}(Q;q_1,q_2)=\sum_{\rho}(-Q)^{|\rho|}\,\mathsf{f}_{\rho}(q_2,q_1)C_{\mu\nu\rho}(q_1,q_2)C_{\eta\lambda\rho^{\mathrm{T}}}(q_2,q_1). \tag{B.12}$$

Independence of the choice of the preferred direction

The preferred direction is a simply artificial technique to execute the formalism of topological vertex, thus, the final results computed by the several choices of the preferred direction must be completely equivalent. This expectation leads to the infinite number of the conjectures of nontrivial mathematical identities. Indeed, one can immediately see that (B.11) looks

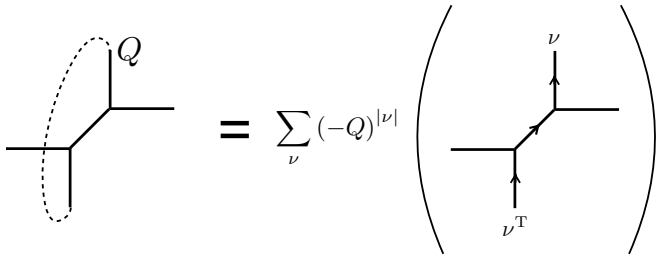

Figure 43: The compactification process in the topological vertex.

highly different from (B.12), however, equivalence between them as the independence of the preferred direction has been rigorously established in [32].

B.3 Compactification

It is a regular circumstance to consider quantum field theories on space-time with compactified directions including a class of them geometrically engineered by the brane system. This also happens for CY3 via the correspondence between its web diagram and a brane configuration in string theory, namely, the web diagram of CY3 may contain a compactified segment if the corresponding brane is wrapped on some compactified subspace. Such a situation has been firstly considered in [138], and the computation of the M-string partition function is in this framework as explained in Section 4.1. We would like here to provide the prescription of the computation with the topological vertex in the presence of the compactified direction in the web diagram. Throughout this paper, we express it as a dotted curve shown as in Figure 43. The procedure is rather simple; first we assign a Young diagram ν for the outgoing arrow and ν^{T} for the ingoing arrow; second multiplying the topological vertex by a Kähler factor $(-Q)^{|\nu|}$; third taking the sum over ν. This is quite similar to the process to glue the topological vertices but does not need the framing factor, which is depicted in Figure 43.

C Calculation details

In this appendix, we would package the details of computations which are skipped to show in the main context.

C.1 Domain wall on TN_1

Let us perform the computation of the domain wall partition function $Z^{\nu_1}_{\mu_1}$ (4.8) and the normalized one $\widehat{Z}^{\nu_1}_{\mu_1}$ (4.10) for the web diagram in Figure 44. At first, the formula of the refined topological vertex with parameter assignments as shown in Figure 44 directly gives

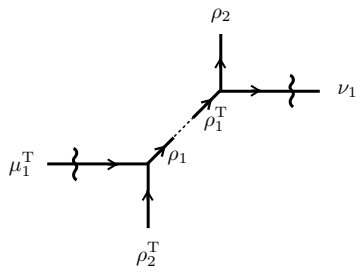

Figure 44: The parameter assignments on the web diagram for a single M5-brane on TN_1.

$$
\begin{aligned}
Z_{\mu_1}^{\nu_1}(Q_1,Q_2,Q_\tau;q_1,q_2) &= \sum_{\rho_1,\rho_2}(-Q_1)^{|\rho_1|}(-Q_2)^{|\rho_2|}C_{\rho_2^{\mathrm{T}}\rho_1\mu_1^{\mathrm{T}}}(q_2,q_1)C_{\rho_2\rho_1^{\mathrm{T}}\nu_1}(q_1,q_2) \\
&= q_1^{\frac{||\mu_1^{\mathrm{T}}||^2}{2}} q_2^{\frac{||\nu_1||^2}{2}} \widetilde{Z}_{\mu_1^{\mathrm{T}}}(q_2,q_1)\widetilde{Z}_{\nu_1}(q_1,q_2)\,\mathsf{Z}_{\mu_1}^{\nu_1},
\end{aligned}
\tag{C.1}
$$

where

$$
\begin{aligned}
\mathsf{Z}_{\mu_1}^{\nu_1} := \sum_{\rho_1,\rho_2}\sum_{\lambda_1,\lambda_2}(-Q_1)^{|\rho_1|}(-Q_2)^{|\rho_2|}\left(\frac{q_2}{q_1}\right)^{\frac{|\lambda_2|-|\lambda_1|}{2}} \\
\times s_{\rho_2/\lambda_1}\left(q_2^{-\mathfrak{n}}q_1^{-\mu_1^{\mathrm{T}}}\right)s_{\rho_1/\lambda_1}\left(q_2^{-\mu_1}q_1^{-\mathfrak{n}}\right)s_{\rho_2^{\mathrm{T}}/\lambda_2}\left(q_1^{-\mathfrak{n}}q_2^{-\nu_1}\right)s_{\rho_1^{\mathrm{T}}/\lambda_2}\left(q_1^{-\nu_1^{\mathrm{T}}}q_2^{-\mathfrak{n}}\right).
\end{aligned}
\tag{C.2}
$$

In any case of calculating the domain wall partition function, the main problem is evaluating the skew Schur functions in the factor $\mathsf{Z}_{\mu_1}^{\nu_1}$ into the infinite product by repeating the formulae (A.34)-(A.36) of the skew Schur function. For the purpose to do this and extend to the generic case, we would like to treat a slightly simple expression

$$
\widetilde{\mathsf{Z}}_{\mu_1}^{\nu_1} := \sum_{\rho_1,\rho_2}\sum_{\lambda_1,\lambda_2}A_1^{|\rho_1|}A_2^{|\rho_2|}B_1^{|\lambda_1|}B_2^{|\lambda_2|}s_{\rho_1/\lambda_1}(X_1)\,s_{\rho_1^{\mathrm{T}}/\lambda_2}(X_2)\,s_{\rho_2^{\mathrm{T}}/\lambda_2}(Y_2)\,s_{\rho_2/\lambda_1}(Y_1),
\tag{C.3}
$$

where $A_{1,2}$ and $B_{1,2}$ are just parameters and we will use

$$
C_a := A_aB_a \quad (a=1,2) \qquad \text{and} \qquad C := \prod_{a=1}^{2}C_a.
\tag{C.4}
$$

Before going to details, we note strategy to advance the deformation of $\widetilde{\mathsf{Z}}_{\mu_1}^{\nu_1}$ step by step:

(i) Use (A.34) for skew Schur functions whose Young diagrams have the same index so that coefficients A_i and B_i are combined into C_i.

(ii) Use (A.36) for the pairs of skew Schur functions with ρ_i and ρ_i^{T}.

(iii) Use (A.34) again for skew Schur functions whose Young diagrams have the same index.

(iv) Use (A.35) for the pairs of skew Schur functions with λ_i^{T}.

(v) Repeat step (i) and (ii).

(vi) Repeat step (iii) and (iv).

Note that the actual arguments of the skew Schur functions are abbreviated as, e.g., $X_1 = \{X_{1,i}\}_{i=1,2,\cdots}$. We perform the sequence from step (i) to (vi) N times, where N is the number of external lines on the left side or the right side of the web diagram. After that, we get coefficients C_i back to A_i and B_i by again (A.34), then it will be found that the summand is basically the same as $\widetilde{\mathsf{Z}}$ at the starting point but with all variables multiplied by C. Thus, we can immediately continue this $k \to \infty$ times subsequently, and then the infinite product will arise. Finally, there should be $2N^2$ terms in the numerator and denominator. Let us demonstrate this strategy to (C.3).

Step (i):

$$\begin{aligned}\widetilde{\mathsf{Z}}^{\nu_1}_{\mu_1} &= \sum_{\rho_1,\rho_2}\sum_{\lambda_1,\lambda_2} A_1^{|\rho_1|}A_2^{|\rho_2|}B_1^{|\lambda_1|}B_2^{|\lambda_2|} s_{\rho_1/\lambda_1}(X_1)\, s_{\rho_1^{\mathrm{T}}/\lambda_2}(X_2)\, s_{\rho_2^{\mathrm{T}}/\lambda_2}(Y_2)\, s_{\rho_2/\lambda_1}(Y_1) \\ &= \sum_{\rho_1,\rho_2}\sum_{\lambda_1,\lambda_2} C_1^{|\lambda_1|}C_2^{|\lambda_2|} s_{\rho_1/\lambda_1}(A_1X_1)\, s_{\rho_1^{\mathrm{T}}/\lambda_2}(X_2)\, s_{\rho_2^{\mathrm{T}}/\lambda_2}(A_2Y_2)\, s_{\rho_2/\lambda_1}(Y_1)\,.\end{aligned}$$

Step (ii):

$$\begin{aligned}\widetilde{\mathsf{Z}}^{\nu_1}_{\mu_1} &= \prod_{i,j=1}^{\infty}(1+A_1X_{1,i}X_{2,j})(1+A_2Y_{2,i}Y_{1,j}) \\ &\quad\times\sum_{\rho_1,\rho_2}\sum_{\lambda_1,\lambda_2} C_1^{|\lambda_1|}C_2^{|\lambda_2|} s_{\lambda_2^{\mathrm{T}}/\rho_1}(A_1X_1)\, s_{\lambda_1^{\mathrm{T}}/\rho_1^{\mathrm{T}}}(X_2)\, s_{\lambda_1^{\mathrm{T}}/\rho_2^{\mathrm{T}}}(A_2Y_2)\, s_{\lambda_2^{\mathrm{T}}/\rho_2}(Y_1)\,.\end{aligned}$$

Step (iii):

$$\begin{aligned}\widetilde{\mathsf{Z}}^{\nu_1}_{\mu_1} &= \prod_{i,j=1}^{\infty}(1+A_1X_{1,i}X_{2,j})(1+A_2Y_{2,i}Y_{1,j}) \\ &\quad\times\sum_{\rho_1,\rho_2}\sum_{\lambda_1,\lambda_2} C_1^{|\rho_1|}C_2^{|\rho_2|} s_{\lambda_2^{\mathrm{T}}/\rho_1}(A_1X_1)\, s_{\lambda_1^{\mathrm{T}}/\rho_1^{\mathrm{T}}}(C_1X_2)\, s_{\lambda_1^{\mathrm{T}}/\rho_2^{\mathrm{T}}}(A_2Y_2)\, s_{\lambda_2^{\mathrm{T}}/\rho_2}(C_2Y_1)\,.\end{aligned}$$

Step (iv): :

$$\begin{aligned}\widetilde{\mathsf{Z}}^{\nu_1}_{\mu_1} &= \prod_{i,j=1}^{\infty}\frac{(1+A_1X_{1,i}X_{2,j})}{(1-A_1C_2X_{1,i}Y_{1,j})}\cdot\frac{(1+A_2Y_{2,i}Y_{1,j})}{(1-A_2C_1Y_{2,i}X_{2,j})} \\ &\quad\times\sum_{\rho_1,\rho_2}\sum_{\lambda_1,\lambda_2} C_1^{|\rho_1|}C_2^{|\rho_2|} s_{\rho_2/\lambda_2^{\mathrm{T}}}(A_1X_1)\, s_{\rho_2^{\mathrm{T}}/\lambda_1^{\mathrm{T}}}(C_1X_2)\, s_{\rho_1^{\mathrm{T}}/\lambda_1^{\mathrm{T}}}(A_2Y_2)\, s_{\rho_1/\lambda_2^{\mathrm{T}}}(C_2Y_1)\,.\end{aligned}$$

Step (v):

$$\begin{aligned}
\widetilde{\mathsf{Z}}^{\nu_1}_{\mu_1} &= \prod_{i,j=1}^{\infty} \frac{(1+A_1X_{1,i}X_{2,j})}{(1-A_1C_2X_{1,i}Y_{1,j})} \cdot \frac{(1+A_2Y_{2,i}Y_{1,j})}{(1-A_2C_1Y_{2,i}X_{2,j})} \\
&\quad \times \sum_{\rho_1,\rho_2} \sum_{\lambda_1,\lambda_2} C_1^{|\lambda_1|} C_2^{|\lambda_2|} s_{\rho_2/\lambda_2^{\mathrm{T}}}(C_2A_1X_1)\, s_{\rho_2^{\mathrm{T}}/\lambda_1^{\mathrm{T}}}(C_1X_2)\, s_{\rho_1^{\mathrm{T}}/\lambda_1^{\mathrm{T}}}(C_1A_2Y_2)\, s_{\rho_1/\lambda_2^{\mathrm{T}}}(C_2Y_1) \\
&= \prod_{i,j=1}^{\infty} \frac{(1+A_1X_{1,i}X_{2,j})}{(1-A_1C_2X_{1,i}Y_{1,j})} \cdot \frac{(1+A_2Y_{2,i}Y_{1,j})}{(1-A_2C_1Y_{2,i}X_{2,j})} (1+C_2A_1X_{1,i}C_1X_{2,j})(1+C_1A_2Y_{2,i}C_2Y_{1,j}) \\
&\quad \times \sum_{\rho_1,\rho_2} \sum_{\lambda_1,\lambda_2} C_1^{|\lambda_1|} C_2^{|\lambda_2|} s_{\lambda_1/\rho_2}(C_2A_1X_1)\, s_{\lambda_2/\rho_2^{\mathrm{T}}}(C_1X_2)\, s_{\lambda_2/\rho_1^{\mathrm{T}}}(C_1A_2Y_2)\, s_{\lambda_1/\rho_1}(C_2Y_1)\,.
\end{aligned}$$

Step (vi):

$$\begin{aligned}
\widetilde{\mathsf{Z}}^{\nu_1}_{\mu_1} &= \prod_{i,j=1}^{\infty} \frac{(1+A_1X_{1,i}X_{2,j})(1+CA_1X_{1,i}X_{2,j})}{(1-A_1C_2X_{1,i}Y_{1,j})} \cdot \frac{(1+A_2Y_{2,i}Y_{1,j})(1+CA_2Y_{2,i}Y_{1,j})}{(1-A_2C_1Y_{2,i}X_{2,j})} \\
&\quad \times \sum_{\rho_1,\rho_2} \sum_{\lambda_1,\lambda_2} C_1^{|\rho_1|} C_2^{|\rho_2|} s_{\lambda_1/\rho_2}(C_2A_1X_1)\, s_{\lambda_2/\rho_2^{\mathrm{T}}}(C_1C_2X_2)\, s_{\lambda_2/\rho_1^{\mathrm{T}}}(C_1A_2Y_2)\, s_{\lambda_1/\rho_1}(C_1C_2Y_1) \\
&= \prod_{i,j=1}^{\infty} \frac{(1+A_1X_{1,i}X_{2,j})(1+CA_1X_{1,i}X_{2,j})}{(1-A_1C_2X_{1,i}Y_{1,j})(1-C_2A_1X_{1,i}CY_{1,j})} \cdot \frac{(1+A_2Y_{2,i}Y_{1,j})(1+CA_2Y_{2,i}Y_{1,j})}{(1-A_2C_1Y_{2,i}X_{2,j})(1-C_1A_2Y_{2,i}CX_{2,j})} \\
&\quad \times \sum_{\rho_1,\rho_2} \sum_{\lambda_1,\lambda_2} C_1^{|\rho_1|} C_2^{|\rho_2|} s_{\rho_1/\lambda_1}(C_2A_1X_1)\, s_{\rho_1^{\mathrm{T}}/\lambda_2}(CX_2)\, s_{\rho_2^{\mathrm{T}}/\lambda_2}(C_1A_2Y_2)\, s_{\rho_2/\lambda_1}(CY_1)\,.
\end{aligned}$$

Then, we use (A.34) to factor out coefficients $C_1^{|\rho_1|}C_2^{|\rho_2|}$ so that

$$\begin{aligned}
\widetilde{\mathsf{Z}}^{\nu_1}_{\mu_1} &= \prod_{i,j=1}^{\infty} \frac{(1+A_1X_{1,i}X_{2,j})(1+CA_1X_{1,i}X_{2,j})}{(1-A_1C_2X_{1,i}Y_{1,j})(1-C_2A_1X_{1,i}CY_{1,j})} \cdot \frac{(1+A_2Y_{2,i}Y_{1,j})(1+CA_2Y_{2,i}Y_{1,j})}{(1-A_2C_1Y_{2,i}X_{2,j})(1-C_1A_2Y_{2,i}CX_{2,j})} \\
&\quad \times \sum_{\rho_1,\rho_2} \sum_{\lambda_1,\lambda_2} A_1^{|\rho_1|} A_2^{|\rho_2|} B_1^{|\lambda_1|} B_2^{|\lambda_2|} s_{\rho_1/\lambda_1}(C_2A_1B_1X_1)\, s_{\rho_1^{\mathrm{T}}/\lambda_2}(CX_2)\, s_{\rho_2^{\mathrm{T}}/\lambda_2}(C_1A_2B_2Y_2)\, s_{\rho_2/\lambda_1}(CY_1) \\
&= \prod_{i,j=1}^{\infty} \frac{(1+A_1X_{1,i}X_{2,j})(1+A_1CX_{1,i}X_{2,j})}{(1-A_1C_2X_{1,i}Y_{1,j})(1-A_1C_2CX_{1,i}Y_{1,j})} \cdot \frac{(1+A_2Y_{2,i}Y_{1,j})(1+A_2CY_{2,i}Y_{1,j})}{(1-A_2C_1Y_{2,i}X_{2,j})(1-A_2C_1CY_{2,i}X_{2,j})} \\
&\quad \times \sum_{\rho_1,\rho_2} \sum_{\lambda_1,\lambda_2} A_1^{|\rho_1|} A_2^{|\rho_2|} B_1^{|\lambda_1|} B_2^{|\lambda_2|} s_{\rho_1/\lambda_1}(CX_1)\, s_{\rho_1^{\mathrm{T}}/\lambda_2}(CX_2)\, s_{\rho_2^{\mathrm{T}}/\lambda_2}(CY_2)\, s_{\rho_2/\lambda_1}(CY_1)\,.
\end{aligned} \tag{C.5}$$

As commented above, we have the same summand as the one at the beginning except a coefficient C in the arguments of the skew Schur functions. Accordingly, we can iterate the

sequence of step (i)-(vi) as

$$\begin{aligned}
\widetilde{\mathsf{Z}}^{\nu_1}_{\mu_1} &= \prod_{i,j=1}^{\infty} \frac{(1+A_1X_{1,i}X_{2,j})\,(1+A_1CX_{1,i}X_{2,j})}{(1-A_1C_2X_{1,i}Y_{1,j})\,(1-A_1C_2CX_{1,i}Y_{1,j})} \cdot \frac{\left(1+A_1C^2X_{1,i}X_{2,j}\right)\left(1+A_1C^3X_{1,i}X_{2,j}\right)}{(1-A_1C_2C^2X_{1,i}Y_{1,j})\,(1-A_1C_2C^3X_{1,i}Y_{1,j})} \\
&\quad \times \frac{(1+A_2Y_{2,i}Y_{1,j})\,(1+A_2CY_{2,i}Y_{1,j})}{(1-A_2C_1Y_{2,i}X_{2,j})\,(1-A_2C_1CY_{2,i}X_{2,j})} \cdot \frac{\left(1+A_2C^2Y_{2,i}Y_{1,j}\right)\left(1+A_2C^3Y_{2,i}Y_{1,j}\right)}{(1-A_2C_1C^2Y_{2,i}X_{2,j})\,(1-A_2C_1C^3Y_{2,i}X_{2,j})} \\
&\quad \times \sum_{\rho_1,\rho_2} \sum_{\lambda_1,\lambda_2} A_1^{|\rho_1|}A_2^{|\rho_2|}B_1^{|\lambda_1|}B_2^{|\lambda_2|} s_{\rho_1/\lambda_1}\left(C^2X_1\right) s_{\rho_1^{\mathrm{T}}/\lambda_2}\left(C^2X_2\right) s_{\rho_2^{\mathrm{T}}/\lambda_2}\left(C^2Y_2\right) s_{\rho_2/\lambda_1}\left(C^2Y_1\right) \\
&= \cdots\cdots \\
&= \prod_{k=1}^{\infty}\prod_{i,j=1}^{\infty} \frac{\left(1+A_1C^{k-1}X_{1,i}X_{2,j}\right)}{(1-A_1C_2C^{k-1}X_{1,i}Y_{1,j})} \cdot \frac{\left(1+A_2C^{k-1}Y_{2,i}Y_{1,j}\right)}{(1-A_2C_1C^{k-1}Y_{2,i}X_{2,j})} \lim_{k\to\infty} \widetilde{\mathsf{Z}}^{\nu_1}_{\mu_1}(C^kX_i, C^kY_i).
\end{aligned} \tag{C.6}$$

The last part does not become nontrivial unless the condition

$$|\rho_1| = |\rho_2| = |\lambda_1| = |\lambda_2| \tag{C.7}$$

is satisfied from the definition of the skew Schur function. Then, with the assumption $|C| < 1$, this factor is simplified as

$$\lim_{k\to\infty} \widetilde{\mathsf{Z}}^{\nu_1}_{\mu_1}(C^kX_i, C^kY_i) = \sum_{\sigma} C^{|\sigma|} = \prod_{n=1}^{\infty} \frac{1}{1-C^n}. \tag{C.8}$$

Thus,

$$\widetilde{\mathsf{Z}}^{\nu_1}_{\mu_1} = \prod_{n=1}^{\infty} \frac{1}{1-C^n} \prod_{i,j,k=1}^{\infty} \frac{\left(1+A_1C^{k-1}X_{1,i}X_{2,j}\right)\left(1+A_2C^{k-1}Y_{2,i}Y_{1,j}\right)}{(1-A_1C_2C^{k-1}X_{1,i}Y_{1,j})\,(1-A_2C_1C^{k-1}Y_{2,i}X_{2,j})}. \tag{C.9}$$

Getting back the original parameters identified with

$$\begin{aligned}
&A_a = -Q_a, \qquad B_1 = \sqrt{\frac{q_1}{q_2}}, \qquad B_2 = \sqrt{\frac{q_2}{q_1}}, \qquad C = Q_1Q_2 = Q_\tau, \\
&X_1 = q_2^{-\mu_1}q_1^{-\mathfrak{n}}, \qquad X_2 = q_1^{-\nu_1^{\mathrm{T}}}q_2^{-\mathfrak{n}}, \qquad Y_2 = q_1^{-\mathfrak{n}}q_2^{-\nu_1}, \qquad Y_1 = q_2^{-\mathfrak{n}}q_1^{-\mu_1^{\mathrm{T}}}
\end{aligned} \tag{C.10}$$

into the above expression, we have

$$\mathsf{Z}^{\nu_1}_{\mu_1} = \prod_{n=1}^{\infty} \frac{1}{1-Q_\tau^n} \prod_{i,j,k=1}^{\infty} \frac{\left(1-Q_2Q_\tau^{k-1}q_1^{-\mu_{1,j}^{\mathrm{T}}+i-\frac{1}{2}}q_2^{-\nu_{1,i}+j-\frac{1}{2}}\right)\left(1-Q_1Q_\tau^{k-1}q_1^{-\nu_{1,j}^{\mathrm{T}}+i-\frac{1}{2}}q_2^{-\mu_{1,i}+j-\frac{1}{2}}\right)}{\left(1-Q_\tau^kq_1^{-\nu_{1,j}^{\mathrm{T}}+i}q_2^{-\nu_{1,i}+j-1}\right)\left(1-Q_\tau^kq_1^{-\mu_{1,j}^{\mathrm{T}}+i-1}q_2^{-\mu_{1,i}+j}\right)}. \tag{C.11}$$

As a result, the final form of $Z_{\mu_1}^{\nu_1}$ can be given by

$$
\begin{aligned}
&Z_{\mu_1}^{\nu_1}(Q_1,Q_2,Q_\tau;q_1,q_2)\\
&=q_1^{\frac{||\mu_1^{\mathrm{T}}||^2}{2}}q_2^{\frac{||\nu_1||^2}{2}}\widetilde{Z}_{\mu_1^{\mathrm{T}}}(q_2,q_1)\widetilde{Z}_{\nu_1}(q_1,q_2)\\
&\quad\times\prod_{n=1}^{\infty}\frac{1}{1-Q_\tau^n}\prod_{i,j,k=1}^{\infty}\frac{\left(1-Q_2Q_\tau^{k-1}q_1^{-\mu_{1,j}^{\mathrm{T}}+i-\frac{1}{2}}q_2^{-\nu_{1,i}+j-\frac{1}{2}}\right)\left(1-Q_1Q_\tau^{k-1}q_1^{-\nu_{1,j}^{\mathrm{T}}+i-\frac{1}{2}}q_2^{-\mu_{1,i}+j-\frac{1}{2}}\right)}{\left(1-Q_\tau^kq_1^{-\nu_{1,j}^{\mathrm{T}}+i}q_2^{-\nu_{1,i}+j-1}\right)\left(1-Q_\tau^kq_1^{-\mu_{1,j}^{\mathrm{T}}+i-1}q_2^{-\mu_{1,i}+j}\right)}.
\end{aligned}
\tag{C.12}
$$

To view this as a partition function in the corresponding quantum field theory, we need to normalize this by the same function with $\mu_1=\nu_1=\emptyset$,

$$
\begin{aligned}
&\widehat{Z}_{\mu_1}^{\nu_1}(Q_1,Q_2,Q_\tau;q_1,q_2):=\frac{Z_{\mu_1}^{\nu_1}(Q_1,Q_2,Q_\tau;q_1,q_2)}{Z_{\emptyset}^{\emptyset}(Q_1,Q_2,Q_\tau;q_1,q_2)}\\
&=q_1^{\frac{||\mu_1^{\mathrm{T}}||^2}{2}}q_2^{\frac{||\nu_1||^2}{2}}\widetilde{Z}_{\mu_1^{\mathrm{T}}}(q_2,q_1)\widetilde{Z}_{\nu_1}(q_1,q_2)\\
&\quad\times\prod_{k=1}^{\infty}\left[\frac{\prod_{(i,j)\in\mu_1}\left(1-Q_2Q_\tau^{k-1}q_1^{\nu_{1,j}^{\mathrm{T}}-i+\frac{1}{2}}q_2^{\mu_{1,i}-j+\frac{1}{2}}\right)\prod_{(i,j)\in\nu_1}\left(1-Q_2Q_\tau^{-1}kq_1^{-\mu_{1,j}^{\mathrm{T}}+i-\frac{1}{2}}q_2^{-\nu_{1,i}+j-\frac{1}{2}}\right)}{\prod_{(i,j)\in\nu_1}\left(1-Q_\tau^kq_1^{-\nu_{1,j}^{\mathrm{T}}+i}t^{-\nu_{1,i}+j-1}\right)\left(1-Q_\tau^kq_1^{\nu_{1,j}^{\mathrm{T}}-i+1}t^{\nu_{1,i}-j}\right)}\right.\\
&\qquad\left.\times\frac{\prod_{(i,j)\in\mu_1}\left(1-Q_1Q_\tau^{k-1}q_1^{-\nu_{1,j}^{\mathrm{T}}+i-\frac{1}{2}}q_2^{-\mu_{1,i}+j-\frac{1}{2}}\right)\prod_{(i,j)\in\nu_1}\left(1-Q_1Q_\tau^{k-1}q_1^{\mu_{1,j}^{\mathrm{T}}-i+\frac{1}{2}}q_2^{\nu_{1,i}-j+\frac{1}{2}}\right)}{\prod_{(i,j)\in\mu_1}\left(1-Q_\tau^kq_1^{-\mu_{1,j}^{\mathrm{T}}+i-1}q_2^{-\mu_{1,i}+j}\right)\left(1-Q_\tau^kq_1^{\mu_{1,j}^{\mathrm{T}}-i}q_2^{\mu_{1,i}-j+1}\right)}\right]\\
&=q_1^{\frac{||\mu_1^{\mathrm{T}}||^2}{2}}q_2^{\frac{||\nu_1||^2}{2}}\widetilde{Z}_{\mu_1^{\mathrm{T}}}(q_2,q_1)\widetilde{Z}_{\nu_1}(q_1,q_2)\\
&\quad\times\prod_{k=1}^{\infty}\left[\prod_{(i,j)\in\mu_1}\frac{\left(1-Q_2Q_\tau^{k-1}q_1^{\nu_{1,j}^{\mathrm{T}}-i+\frac{1}{2}}q_2^{\mu_{1,i}-j+\frac{1}{2}}\right)\left(1-Q_1Q_\tau^{k-1}q_1^{-\nu_{1,j}^{\mathrm{T}}+i-\frac{1}{2}}q_2^{-\mu_{1,i}+j-\frac{1}{2}}\right)}{\left(1-Q_\tau^kq_1^{-\mu_{1,i}^{\mathrm{T}}+j-1}q_2^{-\mu_{1,j}+i}\right)\left(1-Q_\tau^kq_1^{\mu_{1,i}^{\mathrm{T}}-j}q_2^{\mu_{1,j}-i+1}\right)}\right.\\
&\qquad\left.\times\prod_{(i,j)\in\nu_1}\frac{\left(1-Q_2Q_\tau^{k-1}q_1^{-\mu_{1,j}^{\mathrm{T}}+i-\frac{1}{2}}q_2^{-\nu_{1,i}+j-\frac{1}{2}}\right)\left(1-Q_1Q_\tau^{k-1}q_1^{\mu_{1,j}^{\mathrm{T}}-i+\frac{1}{2}}q_2^{\nu_{1,i}-j+\frac{1}{2}}\right)}{\left(1-Q_\tau^kq_1^{-\nu_{1,j}^{\mathrm{T}}+i}q_2^{-\nu_{1,i}+j-1}\right)\left(1-Q_\tau^kq_1^{\nu_{1,j}^{\mathrm{T}}-i+1}q_2^{\nu_{1,i}-j}\right)}\right].
\end{aligned}
\tag{C.13}
$$

This is exactly (4.10) what we want.

C.2 Domain wall on TN_2

We here derive the domain wall partition function $Z_{\mu_1\mu_2}^{\nu_1\nu_2}$ on TN_2 with the parameter assignments shown in the web diagram of Figure 45. Gluing four refined topological vertices results in

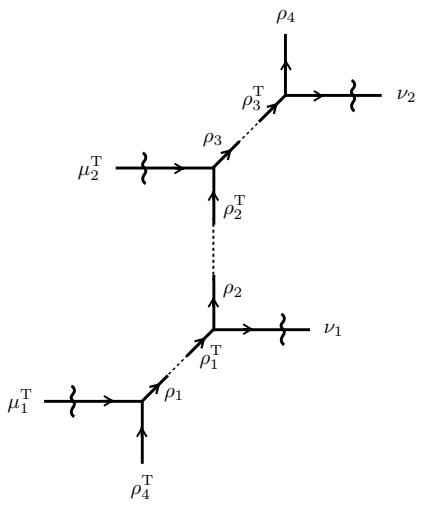

Figure 45: The parameter assignments on the web diagram for a single M5 on TN_2.

$$
\begin{aligned}
Z^{\nu_1\nu_2}_{\mu_1\mu_2}(Q_1,Q_2,Q_3,Q_4;q_1,q_2) &= \sum_{\rho_1,\rho_2,\rho_3,\rho_4} (-Q_1)^{|\rho_1|}(-Q_2)^{|\rho_2|}(-Q_3)^{|\rho_3|}(-Q_4)^{|\rho_4|} \\
&\quad \times C_{\rho_4^{\mathrm{T}}\rho_1\mu_1^{\mathrm{T}}}(q_2,q_1) C_{\rho_2\rho_1^{\mathrm{T}}\nu_1}(q_1,q_2) C_{\rho_2^{\mathrm{T}}\rho_3\mu_2^{\mathrm{T}}}(q_2,q_1) C_{\rho_4\rho_3^{\mathrm{T}}\nu_2}(q_1,q_2) \\
&= q_1^{\frac{||\mu_1^{\mathrm{T}}||^2+||\mu_2^{\mathrm{T}}||^2}{2}} q_2^{\frac{||\nu_1||^2+||\nu_2||^2}{2}} \widetilde{Z}_{\mu_1^{\mathrm{T}}}(q_2,q_1)\widetilde{Z}_{\mu_2^{\mathrm{T}}}(q_2,q_1)\widetilde{Z}_{\nu_2}(q_1,q_2)\widetilde{Z}_{\nu_1}(q_1,q_2) \\
&\quad \times \mathsf{Z}^{\nu_1\nu_2}_{\mu_1\mu_2}(Q_1,Q_2,Q_3,Q_4,Q_\tau;q_1,q_2), \qquad \text{(C.14)}
\end{aligned}
$$

where

$$
\begin{aligned}
\mathsf{Z}^{\nu_1\nu_2}_{\mu_1\mu_2} &:= \sum_{\rho_1,\rho_2,\rho_3,\rho_4} \sum_{\lambda_4,\lambda_3,\lambda_2,\lambda_1} (-Q_1)^{|\rho_1|}(-Q_2)^{|\rho_2|}(-Q_3)^{|\rho_3|}(-Q_4)^{|\rho_4|} \left(\frac{q_2}{q_1}\right)^{\frac{|\lambda_4|-|\lambda_3|+|\lambda_2|-|\lambda_1|}{2}} \\
&\quad \times s_{\rho_4/\lambda_1}\left(q_2^{-\mathfrak{n}}q_1^{-\mu_1^{\mathrm{T}}}\right) s_{\rho_1/\lambda_1}\left(q_2^{-\mu_1}q_1^{-\mathfrak{n}}\right) s_{\rho_2^{\mathrm{T}}/\lambda_2}\left(q_1^{-\mathfrak{n}}q_2^{-\nu_1}\right) s_{\rho_1^{\mathrm{T}}/\lambda_2}\left(q_1^{-\nu_1^{\mathrm{T}}}q_2^{-\mathfrak{n}}\right) \\
&\quad \times s_{\rho_2/\lambda_3}\left(q_2^{-\mathfrak{n}}q_1^{-\mu_2^{\mathrm{T}}}\right) s_{\rho_3/\lambda_3}\left(q_2^{-\mu_2}q_1^{-\mathfrak{n}}\right) s_{\rho_4^{\mathrm{T}}/\lambda_4}\left(q_1^{-\mathfrak{n}}q_2^{-\nu_2}\right) s_{\rho_3^{\mathrm{T}}/\lambda_4}\left(q_1^{-\nu_2^{\mathrm{T}}}q_2^{-\mathfrak{n}}\right). \qquad \text{(C.15)}
\end{aligned}
$$

We will again use the shorthand notation $C := \prod_{a=1}^4 A_a B_a$. As for the previous example, we define and evaluate the following general expression:

$$
\begin{aligned}
\widetilde{\mathsf{Z}}^{\nu_1\nu_2}_{\mu_1\mu_2} &:= \sum_{\rho_1,\rho_2,\rho_3,\rho_4} \sum_{\lambda_4,\lambda_3,\lambda_2,\lambda_1} A_1^{|\rho_1|}A_2^{|\rho_2|}A_3^{|\rho_3|}A_4^{|\rho_4|}B_1^{|\lambda_1|}B_2^{|\lambda_2|}B_3^{|\lambda_3|}B_4^{|\lambda_4|} \\
&\quad \times s_{\rho_1/\lambda_1}(X_1)\, s_{\rho_1^{\mathrm{T}}/\lambda_2}(X_2)\, s_{\rho_2^{\mathrm{T}}/\lambda_2}(Y_2)\, s_{\rho_2/\lambda_3}(Y_3)\, s_{\rho_3/\lambda_3}(X_3)\, s_{\rho_3^{\mathrm{T}}/\lambda_4}(X_4)\, s_{\rho_4^{\mathrm{T}}/\lambda_4}(Y_4)\, s_{\rho_4/\lambda_1}(Y_1)\,. \\
&\qquad \text{(C.16)}
\end{aligned}
$$

Again, the sequence of (i)-(vi) described in the previous section works as follows.

Step (i):

$$\begin{aligned}\widetilde{\mathsf{Z}}^{\nu_1\nu_2}_{\mu_1\mu_2} = & \sum_{\rho_1,\rho_2,\rho_3,\rho_4} \sum_{\lambda_4,\lambda_3,\lambda_2,\lambda_1} C_1^{|\rho_1|} C_2^{|\rho_2|} C_3^{|\rho_3|} C_4^{|\rho_4|} \\ & \times s_{\rho_1/\lambda_1}(A_1X_1)\, s_{\rho_1^{\mathrm{T}}/\lambda_2}(X_2)\, s_{\rho_2^{\mathrm{T}}/\lambda_2}(A_2Y_2)\, s_{\rho_2/\lambda_3}(Y_3) \\ & \times s_{\rho_3/\lambda_3}(A_3X_3)\, s_{\rho_3^{\mathrm{T}}/\lambda_4}(X_4)\, s_{\rho_4^{\mathrm{T}}/\lambda_4}(A_4Y_4)\, s_{\rho_4/\lambda_1}(Y_1)\,.\end{aligned}$$

Step (ii):

$$\begin{aligned}\widetilde{\mathsf{Z}}^{\nu_1\nu_2}_{\mu_1\mu_2} = & \prod_{i,j=1}^{\infty} (1+A_1X_{1,i}X_{2,j})(1+A_2Y_{2,i}Y_{3,j})(1+A_3X_{3,i}X_{4,j})(1+A_4Y_{4,i}Y_{1,j}) \\ & \times \sum_{\rho_1,\rho_2,\rho_3,\rho_4} \sum_{\lambda_4,\lambda_3,\lambda_2,\lambda_1} C_1^{|\rho_1|} C_2^{|\rho_2|} C_3^{|\rho_3|} C_4^{|\rho_4|} \\ & \times s_{\lambda_2^{\mathrm{T}}/\rho_1}(A_1X_1)\, s_{\lambda_1^{\mathrm{T}}/\rho_1^{\mathrm{T}}}(X_2)\, s_{\lambda_3^{\mathrm{T}}/\rho_2^{\mathrm{T}}}(A_2Y_2)\, s_{\lambda_2^{\mathrm{T}}/\rho_2}(Y_3) \\ & \times s_{\lambda_4^{\mathrm{T}}/\rho_3}(A_3X_3)\, s_{\lambda_3^{\mathrm{T}}/\rho_3^{\mathrm{T}}}(X_4)\, s_{\lambda_1^{\mathrm{T}}/\rho_4^{\mathrm{T}}}(A_4Y_4)\, s_{\lambda_4^{\mathrm{T}}/\rho_4}(Y_1)\,.\end{aligned}$$

Step (iii):

$$\begin{aligned}\widetilde{\mathsf{Z}}^{\nu_1\nu_2}_{\mu_1\mu_2} = & \prod_{i,j=1}^{\infty} (1+A_1X_{1,i}X_{2,j})(1+A_2Y_{2,i}Y_{3,j})(1+A_3X_{3,i}X_{4,j})(1+A_4Y_{4,i}Y_{1,j}) \\ & \times \sum_{\rho_1,\rho_2,\rho_3,\rho_4} \sum_{\lambda_4,\lambda_3,\lambda_2,\lambda_1} C_1^{|\lambda_1|} C_2^{|\lambda_2|} C_3^{|\lambda_3|} C_4^{|\lambda_4|} \\ & \times s_{\lambda_2^{\mathrm{T}}/\rho_1}(A_1X_1)\, s_{\lambda_1^{\mathrm{T}}/\rho_1^{\mathrm{T}}}(C_1X_2)\, s_{\lambda_3^{\mathrm{T}}/\rho_2^{\mathrm{T}}}(A_2Y_2)\, s_{\lambda_2^{\mathrm{T}}/\rho_2}(C_2Y_3) \\ & \times s_{\lambda_4^{\mathrm{T}}/\rho_3}(A_3X_3)\, s_{\lambda_3^{\mathrm{T}}/\rho_3^{\mathrm{T}}}(C_3X_4)\, s_{\lambda_1^{\mathrm{T}}/\rho_4^{\mathrm{T}}}(A_4Y_4)\, s_{\lambda_4^{\mathrm{T}}/\rho_4}(C_4Y_1)\,.\end{aligned}$$

Step (iv):

$$\begin{aligned}\widetilde{\mathsf{Z}}^{\nu_1\nu_2}_{\mu_1\mu_2} = & \prod_{i,j=1}^{\infty} \frac{(1+A_1X_{1,i}X_{2,j})(1+A_2Y_{2,i}Y_{3,j})(1+A_3X_{3,i}X_{4,j})(1+A_4Y_{4,i}Y_{1,j})}{(1-A_1C_2X_{1,i}Y_{3,j})(1-A_4C_1X_{2,i}Y_{4,j})(1-A_2C_3Y_{2,i}X_{4,j})(1-A_3C_4Y_{1,i}X_{3,j})} \\ & \times \sum_{\rho_1,\rho_2,\rho_3,\rho_4} \sum_{\lambda_4,\lambda_3,\lambda_2,\lambda_1} C_1^{|\lambda_1|} C_2^{|\lambda_2|} C_3^{|\lambda_3|} C_4^{|\lambda_4|} \\ & \times s_{\rho_2/\lambda_2^{\mathrm{T}}}(A_1X_1)\, s_{\rho_4^{\mathrm{T}}/\lambda_1^{\mathrm{T}}}(C_1X_2)\, s_{\rho_3^{\mathrm{T}}/\lambda_3^{\mathrm{T}}}(A_2Y_2)\, s_{\rho_1/\lambda_2^{\mathrm{T}}}(C_2Y_3) \\ & \times s_{\rho_4/\lambda_4^{\mathrm{T}}}(A_3X_3)\, s_{\rho_2^{\mathrm{T}}/\lambda_3^{\mathrm{T}}}(C_3X_4)\, s_{\rho_1^{\mathrm{T}}/\lambda_1^{\mathrm{T}}}(A_4Y_4)\, s_{\rho_3/\lambda_4^{\mathrm{T}}}(C_4Y_1)\,.\end{aligned}$$

Step (v):

$$
\begin{aligned}
\widetilde{\mathsf{Z}}^{\nu_1\nu_2}_{\mu_1\mu_2} &= \prod_{i,j=1}^{\infty} \frac{(1+A_1X_{1,i}X_{2,j})\,(1+A_2Y_{2,i}Y_{3,j})\,(1+A_3X_{3,i}X_{4,j})\,(1+A_4Y_{4,i}Y_{1,j})}{(1-A_1C_2X_{1,i}Y_{3,j})\,(1-A_4C_1X_{2,i}Y_{4,j})\,(1-A_2C_3Y_{2,i}X_{4,j})\,(1-A_3C_4Y_{1,i}X_{3,j})} \\
&\quad \times \sum_{\rho_1,\rho_2,\rho_3,\rho_4} \sum_{\lambda_4,\lambda_3,\lambda_2,\lambda_1} C_1^{|\rho_1|}C_2^{|\rho_2|}C_3^{|\rho_3|}C_4^{|\rho_4|} \\
&\quad \times s_{\rho_2/\lambda_2^{\mathrm{T}}}(A_1C_2X_1)\, s_{\rho_4^{\mathrm{T}}/\lambda_1^{\mathrm{T}}}(C_1X_2)\, s_{\rho_3^{\mathrm{T}}/\lambda_3^{\mathrm{T}}}(A_2C_3Y_2)\, s_{\rho_1/\lambda_2^{\mathrm{T}}}(C_2Y_3) \\
&\quad \times s_{\rho_4/\lambda_4^{\mathrm{T}}}(A_3C_4X_3)\, s_{\rho_2^{\mathrm{T}}/\lambda_3^{\mathrm{T}}}(C_3X_4)\, s_{\rho_1^{\mathrm{T}}/\lambda_1^{\mathrm{T}}}(A_4C_1Y_4)\, s_{\rho_3/\lambda_4^{\mathrm{T}}}(C_4Y_1) \\
&= \prod_{i,j=1}^{\infty} \frac{(1+A_1X_{1,i}X_{2,j})\,(1+A_2Y_{2,i}Y_{3,j})\,(1+A_3X_{3,i}X_{4,j})\,(1+A_4Y_{4,i}Y_{1,j})}{(1-A_1C_2X_{1,i}Y_{3,j})\,(1-A_4C_1X_{2,i}Y_{4,j})\,(1-A_2C_3Y_{2,i}X_{4,j})\,(1-A_3C_4Y_{1,i}X_{3,j})} \\
&\quad \times (1+A_1C_2C_3X_{1,i}X_{4,j})\,(1+A_3C_4C_1X_{3,i}X_{2,j})\,(1+A_2C_3C_4Y_{1,i}Y_{2,j})\,(1+A_4C_1C_2Y_{3,i}Y_{4,j}) \\
&\quad \times \sum_{\rho_1,\rho_2,\rho_3,\rho_4} \sum_{\lambda_4,\lambda_3,\lambda_2,\lambda_1} C_1^{|\rho_1|}C_2^{|\rho_2|}C_3^{|\rho_3|}C_4^{|\rho_4|} \\
&\quad \times s_{\lambda_3/\rho_2}(A_1C_2X_1)\, s_{\lambda_4/\rho_4^{\mathrm{T}}}(C_1X_2)\, s_{\lambda_4/\rho_3^{\mathrm{T}}}(A_2C_3Y_2)\, s_{\lambda_1/\rho_1}(C_2Y_3) \\
&\quad \times s_{\lambda_1/\rho_4}(A_3C_4X_3)\, s_{\lambda_2/\rho_2^{\mathrm{T}}}(C_3X_4)\, s_{\lambda_2/\rho_1^{\mathrm{T}}}(A_4C_1Y_4)\, s_{\lambda_3/\rho_3}(C_4Y_1)\,.
\end{aligned}
$$

Step (vi):

$$
\begin{aligned}
\widetilde{\mathsf{Z}}^{\nu_1\nu_2}_{\mu_1\mu_2} &= \prod_{i,j=1}^{\infty} \frac{(1+A_1X_{1,i}X_{2,j})\,(1+A_2Y_{2,i}Y_{3,j})\,(1+A_3X_{3,i}X_{4,j})\,(1+A_4Y_{4,i}Y_{1,j})}{(1-A_1C_2X_{1,i}Y_{3,j})\,(1-A_4C_1X_{2,i}Y_{4,j})\,(1-A_2C_3Y_{2,i}X_{4,j})\,(1-A_3C_4Y_{1,i}X_{3,j})} \\
&\quad \times (1+A_1C_2C_3X_{1,i}X_{4,j})\,(1+A_3C_4C_1X_{3,i}X_{2,j})\,(1+A_2C_3C_4Y_{1,i}Y_{2,j})\,(1+A_4C_1C_2Y_{3,i}Y_{4,j}) \\
&\quad \times \sum_{\rho_1,\rho_2,\rho_3,\rho_4} \sum_{\lambda_4,\lambda_3,\lambda_2,\lambda_1} C_1^{|\lambda_1|}C_2^{|\lambda_2|}C_3^{|\lambda_3|}C_4^{|\lambda_4|} \\
&\quad \times s_{\lambda_3/\rho_2}(A_1C_2X_1)\, s_{\lambda_4/\rho_4^{\mathrm{T}}}(C_4C_1X_2)\, s_{\lambda_4/\rho_3^{\mathrm{T}}}(A_2C_3Y_2)\, s_{\lambda_1/\rho_1}(C_1C_2Y_3) \\
&\quad \times s_{\lambda_1/\rho_4}(A_3C_4X_3)\, s_{\lambda_2/\rho_2^{\mathrm{T}}}(C_2C_3X_4)\, s_{\lambda_2/\rho_1^{\mathrm{T}}}(A_4C_1Y_4)\, s_{\lambda_3/\rho_3}(C_3C_4Y_1) \\
&= \prod_{i,j=1}^{\infty} \frac{(1+A_1X_{1,i}X_{2,j})\,(1+A_2Y_{2,i}Y_{3,j})\,(1+A_3X_{3,i}X_{4,j})\,(1+A_4Y_{4,i}Y_{1,j})}{(1-A_1C_2X_{1,i}Y_{3,j})\,(1-A_4C_1X_{2,i}Y_{4,j})\,(1-A_2C_3Y_{2,i}X_{4,j})\,(1-A_3C_4Y_{1,i}X_{3,j})} \\
&\quad \times \frac{(1+A_1C_2C_3X_{1,i}X_{4,j})\,(1+A_3C_4C_1X_{3,i}X_{2,j})\,(1+A_2C_3C_4Y_{1,i}Y_{2,j})\,(1+A_4C_1C_2Y_{3,i}Y_{4,j})}{(1-A_1C_2C_3C_4X_{1,i}Y_{1,j})\,(1-A_2C_3C_4C_1X_{2,i}Y_{2,j})\,(1-A_3C_1C_2C_4X_{3,i}Y_{3,j})\,(1-A_4C_1C_2C_3X_{4,i}Y_{4,j})} \\
&\quad \times \sum_{\rho_1,\rho_2,\rho_3,\rho_4} \sum_{\lambda_4,\lambda_3,\lambda_2,\lambda_1} C_1^{|\lambda_1|}C_2^{|\lambda_2|}C_3^{|\lambda_3|}C_4^{|\lambda_4|} \\
&\quad \times s_{\rho_3/\lambda_3}(A_1C_2X_1)\, s_{\rho_3^{\mathrm{T}}/\lambda_4}(C_4C_1X_2)\, s_{\rho_4^{\mathrm{T}}/\lambda_4}(A_2C_3Y_2)\, s_{\rho_4/\lambda_1}(C_1C_2Y_3) \\
&\quad \times s_{\rho_1/\lambda_1}(A_3C_4X_3)\, s_{\rho_1^{\mathrm{T}}/\lambda_2}(C_2C_3X_4)\, s_{\rho_2^{\mathrm{T}}/\lambda_2}(A_4C_1Y_4)\, s_{\rho_2/\lambda_3}(C_3C_4Y_1)\,.
\end{aligned}
$$

For $N=2$, we have to iterate the sequence of (i)-(vi) once more and obtain

$$
\begin{aligned}
&\widetilde{\mathsf{Z}}^{\nu_1\nu_2}_{\mu_1\mu_2} \\
&= \prod_{i,j=1}^{\infty} \frac{(1+A_1X_{1,i}X_{2,j})\,(1+A_1CX_{1,i}X_{2,j})\cdot(1+A_2Y_{2,i}Y_{3,j})\,(1+A_2CY_{2,i}Y_{3,j})}{(1-A_1C_2X_{1,i}Y_{3,j})\,(1-A_1C_2CX_{1,i}Y_{3,j})\cdot(1-A_4C_1X_{2,i}Y_{4,j})\,(1-A_4C_1CX_{2,i}Y_{4,j})} \\
&\quad\times \frac{(1+A_3X_{3,i}X_{4,j})\,(1+A_3CX_{3,i}X_{4,j})\cdot(1+A_4Y_{4,i}Y_{1,j})\,(1+A_4CY_{4,i}Y_{1,j})}{(1-A_2C_3Y_{2,i}X_{4,j})\,(1-A_2C_3CY_{2,i}X_{4,j})\cdot(1-A_3C_4Y_{1,i}X_{3,j})\,(1-A_3C_4CY_{1,i}X_{3,j})} \\
&\quad\times \frac{(1+A_1C_2C_3X_{1,i}X_{4,j})\,(1+A_1C_2C_3CX_{1,i}X_{4,j})\cdot(1+A_3C_4C_1X_{3,i}X_{2,j})\,(1+A_3C_4C_1CX_{3,i}X_{2,j})}{(1-A_1C_2C_3C_4X_{1,i}Y_{1,j})\,(1-A_1C_2C_3C_4CX_{1,i}Y_{1,j})\cdot(1-A_2C_3C_4C_1X_{2,i}Y_{2,j})\,(1-A_2C_3C_4C_1CX_{2,i}Y_{2,j})} \\
&\quad\times \frac{(1+A_2C_3C_4Y_{1,i}Y_{2,j})\,(1+A_2C_3C_4CY_{1,i}Y_{2,j})\cdot(1+A_4C_1C_2Y_{3,i}Y_{4,j})\,(1+A_4C_1C_2CY_{3,i}Y_{4,j})}{(1-A_3C_1C_2C_4X_{3,i}Y_{3,j})\,(1-A_3C_1C_2C_4CX_{3,i}Y_{3,j})\cdot(1-A_4C_1C_2C_3X_{4,i}Y_{4,j})\,(1-A_4C_1C_2C_3CX_{4,i}Y_{4,j})} \\
&\quad\times \sum_{\rho_1,\rho_2,\rho_3,\rho_4}\ \sum_{\lambda_4,\lambda_3,\lambda_2,\lambda_1} A_1^{|\rho_1|}A_2^{|\rho_2|}A_3^{|\rho_3|}A_4^{|\rho_4|}B_1^{|\lambda_1|}B_2^{|\lambda_2|}B_3^{|\lambda_3|}B_4^{|\lambda_4|} \\
&\quad\times s_{\rho_3/\lambda_3}(CX_1)\,s_{\rho_3^{\mathrm{T}}/\lambda_4}(CX_2)\,s_{\rho_4^{\mathrm{T}}/\lambda_4}(CY_2)\,s_{\rho_4/\lambda_1}(CY_3) \\
&\quad\times s_{\rho_1/\lambda_1}(CX_3)\,s_{\rho_1^{\mathrm{T}}/\lambda_2}(CX_4)\,s_{\rho_2^{\mathrm{T}}/\lambda_2}(CY_4)\,s_{\rho_2/\lambda_3}(CY_1)\,. \qquad \text{(C.17)}
\end{aligned}
$$

We put this expression into the last three lines sequentially infinite times, then, this expression is simply written in the form of the infinite product,

$$
\begin{aligned}
\widetilde{\mathsf{Z}}^{\nu_1\nu_2}_{\mu_1\mu_2} = \prod_{n=1}^{\infty}\frac{1}{1-C^n}\prod_{k=1}^{\infty}\prod_{i,j=1}^{\infty}
&\frac{\left(1+A_1C^{k-1}X_{1,i}X_{2,j}\right)\cdot\left(1+A_2C^{k-1}Y_{2,i}Y_{3,j}\right)}{(1-A_1C_2C^{k-1}X_{1,i}Y_{3,j})\cdot(1-A_4C_1C^{k-1}X_{2,i}Y_{4,j})} \\
&\times\frac{\left(1+A_3C^{k-1}X_{3,i}X_{4,j}\right)\cdot\left(1+A_4C^{k-1}Y_{4,i}Y_{1,j}\right)}{(1-A_2C_3C^{k-1}Y_{2,i}X_{4,j})\cdot(1-A_3C_4C^{k-1}Y_{1,i}X_{3,j})} \\
&\times\frac{\left(1+A_1C_2C_3C^{k-1}X_{1,i}X_{4,j}\right)\cdot\left(1+A_3C_4C_1C^{k-1}X_{3,i}X_{2,j}\right)}{(1-A_1C_2C_3C_4C^{k-1}X_{1,i}Y_{1,j})\cdot(1-A_2C_3C_4C_1C^{k-1}X_{2,i}Y_{2,j})} \\
&\times\frac{\left(1+A_2C_3C_4C^{k-1}Y_{1,i}Y_{2,j}\right)\cdot\left(1+A_4C_1C_2C^{k-1}Y_{3,i}Y_{4,j}\right)}{(1-A_3C_1C_2C_4C^{k-1}X_{3,i}Y_{3,j})\cdot(1-A_4C_1C_2C_3C^{k-1}X_{4,i}Y_{4,j})}, \qquad \text{(C.18)}
\end{aligned}
$$

where we use

$$
\lim_{k\to\infty}\widetilde{\mathsf{Z}}^{\nu_1\nu_2}_{\mu_1\mu_2}(C^kX_i,C^kY_i)=\prod_{n=1}^{\infty}\frac{1}{1-C^n}. \qquad \text{(C.19)}
$$

For our purpose to get $\mathsf{Z}^{\nu_1\nu_2}_{\mu_1\mu_2}$, substituting the original parameters identified with

$$
\begin{aligned}
&A_a=-Q_a, && B_1=B_3=\sqrt{\frac{q_1}{q_2}}, && B_2=B_4=\sqrt{\frac{q_2}{q_1}}, && C=Q_\tau, \\
&X_1=q_2^{-\mu_1}q_1^{-\mathfrak{n}}, && X_2=q_1^{-\nu_1^{\mathrm{T}}}q_2^{-\mathfrak{n}}, && X_3=q_2^{-\mu_2}q_1^{-\mathfrak{n}}, && X_4=q_1^{-\nu_2^{\mathrm{T}}}q_2^{-\mathfrak{n}}, \\
&Y_1=q_2^{-\mathfrak{n}}q_1^{-\mu_1^{\mathrm{T}}}, && Y_2=q_1^{-\mathfrak{n}}q_2^{-\nu_1}, && Y_3=q_2^{-\mathfrak{n}}q_1^{-\mu_2^{\mathrm{T}}}, && Y_4=q_1^{-\mathfrak{n}}q_2^{-\nu_2}
\end{aligned}
$$

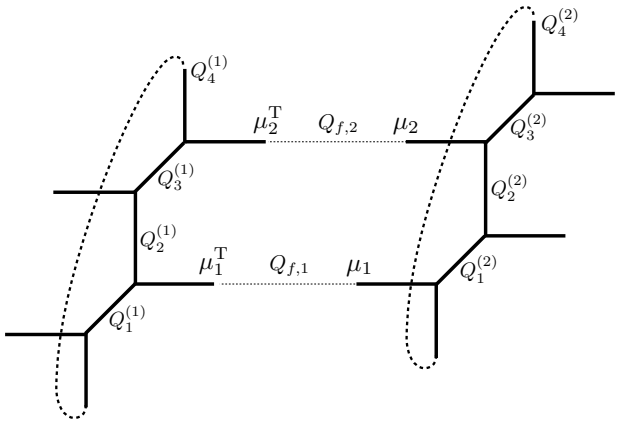

Figure 46: The web diagram obtained by gluing two domain walls on TN_2.

into (C.18) leads to

$$
\begin{aligned}
&\mathsf{Z}^{\nu_1\nu_2}_{\mu_1\mu_2}(Q_1,Q_2,Q_3,Q_4,Q_\tau;q_1,q_2)\\
&=\prod_{n=1}^{\infty}\frac{1}{1-Q_\tau^n}\prod_{i,j,k=1}^{\infty}\Bigg[\frac{(1-Q_2Q_3Q_4Q_\tau^{k-1}q_1^{-\mu^{\mathrm{T}}_{1,j}+i-\frac{1}{2}}q_2^{-\nu_{1,i}+j-\frac{1}{2}})(1-Q_4Q_\tau^{k-1}q_1^{-\mu^{\mathrm{T}}_{1,j}+i-\frac{1}{2}}q_2^{-\nu_{2,i}+j-\frac{1}{2}})}{(1-Q_3Q_4Q_\tau^{k-1}q_1^{-\mu^{\mathrm{T}}_{1,j}+i-1}q_2^{-\mu_{2,i}+j})(1-Q_\tau^{k}q_1^{-\mu^{\mathrm{T}}_{1,j}+i-1}q_2^{-\mu_{1,i}+j})}\\
&\qquad\times\frac{(1-Q_2Q_\tau^{k-1}q_1^{-\mu^{\mathrm{T}}_{2,j}+i-\frac{1}{2}}q_2^{-\nu_{1,i}+j-\frac{1}{2}})(1-Q_1Q_2Q_4Q_\tau^{k-1}q_1^{-\mu^{\mathrm{T}}_{2,j}+i-\frac{1}{2}}q_2^{-\nu_{2,i}+j-\frac{1}{2}})}{(1-Q_1Q_2Q_\tau^{k-1}q_1^{-\mu^{\mathrm{T}}_{2,j}+i-1}q_2^{-\mu_{1,i}+j})(1-Q_\tau^{k}q_1^{-\mu^{\mathrm{T}}_{2,j}+i-1}q_2^{-\mu_{2,i}+j})}\\
&\qquad\times\frac{(1-Q_1Q_\tau^{k-1}q_1^{-\nu^{\mathrm{T}}_{1,j}+i-\frac{1}{2}}q_2^{-\mu_{1,i}+j-\frac{1}{2}})(1-Q_1Q_3Q_4Q_\tau^{k-1}q_1^{-\nu^{\mathrm{T}}_{1,j}+i-\frac{1}{2}}q_2^{-\mu_{2,i}+j-\frac{1}{2}})}{(1-Q_1Q_4Q_\tau^{k-1}q_1^{-\nu^{\mathrm{T}}_{1,j}+i}q_2^{-\nu_{2,i}+j-1})(1-Q_\tau^{k}q_1^{-\nu^{\mathrm{T}}_{1,j}+i}q_2^{-\nu_{1,i}+j-1})}\\
&\qquad\times\frac{(1-Q_1Q_2Q_3Q_\tau^{k-1}q_1^{-\nu^{\mathrm{T}}_{2,j}+i-\frac{1}{2}}q_2^{-\mu_{1,i}+j-\frac{1}{2}})(1-Q_3Q_\tau^{k-1}q_1^{-\nu^{\mathrm{T}}_{2,j}+i-\frac{1}{2}}q_2^{-\mu_{2,i}+j-\frac{1}{2}})}{(1-Q_2Q_3Q_\tau^{k-1}q_1^{-\nu^{\mathrm{T}}_{2,j}+i}q_2^{-\nu_{1,i}+j-1})(1-Q_\tau^{k}q_1^{-\nu^{\mathrm{T}}_{2,j}+i}q_2^{-\nu_{2,i}+j-1})}\Bigg],
\end{aligned}
\tag{C.20}
$$

thus, we can produce (4.13).

C.3 Generating function on TN_2

For consistency, we would directly reach the generating function $G_{(2,2)}$ (5.9) that is necessary as the starting point of our main arguments in Section 5.2. This is obtained by gluing two domain wall partition functions (C.20) as shown in Figure 46,

$$
\begin{aligned}
&G_{(2,2)}(Q_i^{(\mathfrak{a})}, Q_\tau; q_1, q_2) \\
&= \sum_{\mu_1,\mu_2} (-Q_{f_2})^{|\mu_2|}(-Q_{f_1})^{|\mu_1|} \widehat{Z}^{\mu_1\mu_2}_{\emptyset\emptyset}(Q_i^{(1)}, Q_\tau; q_1, q_2)\widehat{Z}^{\emptyset\emptyset}_{\mu_1\mu_2}(Q_i^{(2)}, Q_\tau; q_1, q_2) \\
&= \sum_{\mu_1,\mu_2} (-Q_{f_2})^{|\mu_2|}(-Q_{f_1})^{|\mu_1|} q_1^{\frac{||\mu_1^{\mathrm{T}}||^2+||\mu_2^{\mathrm{T}}||^2}{2}} q_2^{\frac{||\mu_1||^2+||\mu_2||^2}{2}} \widetilde{Z}_{\mu_2^{\mathrm{T}}}(q_2, q_1)\widetilde{Z}_{\mu_1^{\mathrm{T}}}(q_2, q_1)\widetilde{Z}_{\mu_2}(q_1, q_2)\widetilde{Z}_{\mu_1}(q_1, q_2) \\
&\quad \times \prod_{k=1}^{\infty} \Bigg[\prod_{(i,j)\in\mu_1} \frac{(1-Q_2^{(1)}Q_\tau^{k-1}q_1^{i-\frac{1}{2}}q_2^{-\mu_{1,i}+j-\frac{1}{2}})(1-\overline{Q}_2^{(1)}Q_\tau^k q_1^{-i+\frac{1}{2}}q_2^{\mu_{1,i}-j+\frac{1}{2}})}{\underbrace{(1-Q_2^{(1)}Q_3^{(1)}Q_\tau^{k-1}q_1^{-\mu_{2,j}^{\mathrm{T}}+i}q_2^{-\mu_{1,i}+j-1})}_{\text{(1-i)}}(1-\overline{Q}_2^{(1)}\overline{Q}_3^{(1)}Q_\tau^k q_1^{\mu_{2,j}^{\mathrm{T}}-i+1}q_2^{\mu_{1,i}-j})} \\
&\qquad \times \frac{(1-Q_1^{(1)}Q_\tau^{k-1}q_1^{-i+\frac{1}{2}}q_2^{\mu_{1,i}-j+\frac{1}{2}})(1-\overline{Q}_1^{(1)}Q_\tau^k q_1^{i-\frac{1}{2}}q_2^{-\mu_{1,i}+j-\frac{1}{2}})}{\underbrace{(1-Q_\tau^k q_1^{-\mu_{1,j}^{\mathrm{T}}+i}q_2^{-\mu_{1,i}+j-1})}_{\text{(1-ii)}}(1-Q_\tau^k q_1^{\mu_{1,j}^{\mathrm{T}}-i+1}q_2^{\mu_{1,i}-j})} \\
&\quad \times \prod_{(i,j)\in\mu_2} \frac{(1-Q_4^{(1)}Q_\tau^{k-1}q_1^{i-\frac{1}{2}}t^{-\mu_{2,i}+j-\frac{1}{2}})(1-\overline{Q}_4^{(1)}Q_\tau^k q_1^{-i+\frac{1}{2}}t^{\mu_{2,i}-j+\frac{1}{2}})}{(1-Q_1^{(1)}Q_4^{(1)}Q_\tau^{k-1}q_1^{-\mu_{1,j}^{\mathrm{T}}+i}q_2^{-\mu_{2,i}+j-1})(1-\overline{Q}_1^{(1)}\overline{Q}_4^{(1)}Q_\tau^k q_1^{\mu_{1,j}^{\mathrm{T}}-i+1}q_2^{\mu_{2,i}-j})} \\
&\qquad \times \frac{(1-Q_3^{(1)}Q_\tau^{k-1}q_1^{-i+\frac{1}{2}}q_2^{\mu_{2,i}-j+\frac{1}{2}})(1-\overline{Q}_3^{(1)}Q_\tau^k q_1^{i-\frac{1}{2}}q_2^{-\mu_{2,i}+j-\frac{1}{2}})}{(1-Q_\tau^k q_1^{-\mu_{2,j}^{\mathrm{T}}+i}q_2^{-\mu_{2,i}+j-1})(1-Q_\tau^k q_1^{\mu_{2,j}^{\mathrm{T}}-i+1}q_2^{\mu_{2,i}-j})} \Bigg] \\
&\quad \times \Bigg[\prod_{(i,j)\in\mu_1} \frac{(1-Q_4^{(2)}Q_\tau^{k-1}q_1^{-i+\frac{1}{2}}q_2^{\mu_{1,i}-j+\frac{1}{2}})(1-\overline{Q}_4^{(2)}Q_\tau^k q_1^{i-\frac{1}{2}}q_2^{-\mu_{1,i}+j-\frac{1}{2}})}{(1-Q_1^{(2)}Q_2^{(2)}Q_\tau^{k-1}q_1^{-\mu_{2,j}^{\mathrm{T}}+i-1}q_2^{-\mu_{1,i}+j})\underbrace{(1-\overline{Q}_1^{(2)}\overline{Q}_2^{(2)}Q_\tau^k q_1^{\mu_{2,j}^{\mathrm{T}}-i}q_2^{\mu_{1,i}-j+1})}_{\text{(2-i)}}} \\
&\qquad \times \frac{(1-Q_1^{(2)}Q_\tau^{k-1}q_1^{i-\frac{1}{2}}q_2^{-\mu_{1,i}+j-\frac{1}{2}})(1-\overline{Q}_1^{(2)}Q_\tau^k q_1^{-i+\frac{1}{2}}q_2^{\mu_{1,i}-j+\frac{1}{2}})}{(1-Q_\tau^k q_1^{-\mu_{1,j}^{\mathrm{T}}+i-1}q_2^{-\mu_{1,i}+j})\underbrace{(1-Q_\tau^k q_1^{\mu_{1,j}^{\mathrm{T}}-i}q_2^{\mu_{1,i}-j+1})}_{\text{(2-ii)}}} \\
&\quad \times \prod_{(i,j)\in\mu_2} \frac{(1-Q_3^{(2)}Q_\tau^{k-1}q_1^{i-\frac{1}{2}}q_2^{-\mu_{2,i}+j-\frac{1}{2}})(1-\overline{Q}_3^{(2)}Q_\tau^k q_1^{-i+\frac{1}{2}}q_2^{\mu_{2,i}-j+\frac{1}{2}})}{(1-Q_3^{(2)}Q_4^{(2)}Q_\tau^{k-1}q_1^{-\mu_{1,j}^{\mathrm{T}}+i-1}q_2^{-\mu_{2,i}+j})(1-\overline{Q}_3^{(2)}\overline{Q}_4^{(2)}Q_\tau^k q_1^{\mu_{1,j}^{\mathrm{T}}-i}q_2^{\mu_{2,i}-j+1})} \\
&\qquad \times \frac{(1-Q_2^{(2)}Q_\tau^{k-1}q_1^{-i+\frac{1}{2}}q_2^{\mu_{2,i}-j+\frac{1}{2}})(1-\overline{Q}_2^{(2)}Q_\tau^k q_1^{i-\frac{1}{2}}q_2^{-\mu_{2,i}+j-\frac{1}{2}})}{(1-Q_\tau^k q_1^{-\mu_{2,j}^{\mathrm{T}}+i-1}q_2^{-\mu_{2,i}+j})(1-Q_\tau^k q_1^{\mu_{2,j}^{\mathrm{T}}-i}q_2^{\mu_{2,i}-j+1})} \Bigg].
\end{aligned}
\tag{C.21}
$$

Because the deforming process into the elliptic theta function is different between the numerator and denominator, we concentrate separately on them.

• The numerator of (C.21): We can naively combine factors from the same domain wall into $\theta_1(x;p)$. For instance, picking up the first line in the first bracket that belongs to the first

(left) domain wall in Figure 46, then we have

$$
\begin{aligned}
&(1-Q_2^{(1)}Q_\tau^{k-1}q_1^{i-\frac{1}{2}}q_2^{-\mu_{1,i}+j-\frac{1}{2}})(1-\overline{Q}_2^{(1)}Q_\tau^{k}q_1^{-i+\frac{1}{2}}q_2^{\mu_{1,i}-j+\frac{1}{2}})\\
&=(1-\overline{Q}_1^{(1)}\overline{Q}_3^{(1)}\overline{Q}_4^{(1)}Q_\tau^{k}q_1^{i-\frac{1}{2}}q_2^{-\mu_{1,i}+j-\frac{1}{2}})(1-Q_1^{(1)}Q_3^{(1)}Q_4^{(1)}Q_\tau^{k-1}q_1^{-i+\frac{1}{2}}q_2^{\mu_{1,i}-j+\frac{1}{2}})\\
&=\frac{\theta_1\left(\overline{Q}_1^{(1)}\overline{Q}_3^{(1)}\overline{Q}_4^{(1)}q_1^{i-\frac{1}{2}}q_2^{-\mu_{1,i}+j-\frac{1}{2}}\right)}{-iQ_\tau^{\frac{1}{8}}(Q_\tau;Q_\tau)_\infty\sqrt{\overline{Q}_1^{(1)}\overline{Q}_3^{(1)}\overline{Q}_4^{(1)}q_1^{i-\frac{1}{2}}q_2^{-\mu_{1,i}+j-\frac{1}{2}}}},
\end{aligned}
\tag{C.22}
$$

where we use $Q_\tau=Q_1^{(1)}Q_2^{(1)}Q_3^{(1)}Q_4^{(1)}$ with the convention $\overline{Q}_1^{(1)}=\left(Q_1^{(1)}\right)^{-1}$. Similarly, other parts can be recast into $\theta_1(x;p)$, and we gather them together,

$$
\begin{aligned}
\mathsf{G}^{\text{num}}_{(2,2)\mu_1}=\prod_{(i,j)\in\mu_1}Q_1^{(1)}Q_1^{(2)}\sqrt{Q_3^{(1)}Q_4^{(1)}Q_2^{(2)}Q_3^{(2)}}&\times\theta_1\left(\overline{Q}_1^{(1)}\overline{Q}_3^{(1)}\overline{Q}_4^{(1)}q_1^{i-\frac{1}{2}}q_2^{-\mu_{1,i}+j-\frac{1}{2}}\right)\theta_1\left(\overline{Q}_1^{(1)}q_1^{i-\frac{1}{2}}q_2^{-\mu_{1,i}+j-\frac{1}{2}}\right)\\
&\times\theta_1\left(\overline{Q}_1^{(2)}\overline{Q}_2^{(2)}\overline{Q}_3^{(2)}q_1^{-i+\frac{1}{2}}q_2^{\mu_{1,i}-j+\frac{1}{2}}\right)\theta_1\left(\overline{Q}_1^{(2)}q_1^{-i+\frac{1}{2}}q_2^{\mu_{1,i}-j+\frac{1}{2}}\right),
\end{aligned}
\tag{C.23}
$$

where we omit constant factors depending only on Q_τ since these are canceled out by the ones in the denominator. Along this way, we can obtain the similar expression $\mathsf{G}^{\text{num}}_{(2,2)\mu_2}$ for the μ_2 sector.

• The denominator of (C.21): Unlike the numerator, factors from a certain domain wall are formed together with ones from the next domain wall into $\theta_1(x;p)$. There are two groups to make a pair. The first group does not need to incorporate the function $\widetilde{Z}_\mu(q_1,q_2)$ with itself. For example, the terms labeled by (1-i) and (2-i) are combined as

$$
\begin{aligned}
&\prod_{k=1}^{\infty}(1-Q_2^{(1)}Q_3^{(1)}Q_\tau^{k-1}q_1^{-\mu_{2,j}^{\mathrm{T}}+i}q_2^{-\mu_{1,i}+j-1})(1-\overline{Q}_1^{(2)}\overline{Q}_2^{(2)}Q_\tau^{k}q_1^{\mu_{2,j}^{\mathrm{T}}-i}q_2^{\mu_{1,i}-j+1})\\
&=\prod_{k=1}^{\infty}(1-\overline{Q}_1^{(1)}\overline{Q}_4^{(1)}Q_\tau^{k-1}q_1^{-\mu_{2,j}^{\mathrm{T}}+i}q_2^{-\mu_{1,i}+j-1})(1-Q_1^{(1)}Q_4^{(1)}Q_\tau^{k}q_1^{\mu_{2,j}^{\mathrm{T}}-i}q_2^{\mu_{1,i}-j+1})\\
&=\frac{\theta_1\left(\overline{Q}_1^{(1)}\overline{Q}_4^{(1)}q_1^{-\mu_{2,j}^{\mathrm{T}}+i}q_2^{-\mu_{1,i}+j-1}\right)}{-iQ_\tau^{\frac{1}{8}}(Q_\tau;Q_\tau)_\infty\sqrt{\overline{Q}_1^{(1)}\overline{Q}_4^{(1)}q_1^{-\mu_{2,j}^{\mathrm{T}}+i}q_2^{-\mu_{1,i}+j-1}}}.
\end{aligned}
\tag{C.24}
$$

On the other hand, the second group is requested to bring the function $\widetilde{Z}_\mu(q_1,q_2)$ such as,

for the pair of (1-ii) and (2-ii),

$$\begin{aligned}
&\frac{1}{\widetilde{Z}_{\mu_1^{\mathrm{T}}}(q_2,q_1)}\prod_{k=1}^{\infty}(1-Q_\tau^k q_1^{-\mu_{1,j}^{\mathrm{T}}+i}q_2^{-\mu_{1,i}+j-1})(1-Q_\tau^k q_1^{\mu_{1,j}^{\mathrm{T}}-i}q_2^{\mu_{1,i}-j+1})\\
&=\prod_{k=1}^{\infty}(1-Q_\tau^{k+1} q_1^{-\mu_{1,j}^{\mathrm{T}}+i}q_2^{-\mu_{1,i}+j-1})(1-Q_\tau^k q_1^{\mu_{1,j}^{\mathrm{T}}-i}q_2^{\mu_{1,i}-j+1})\\
&=\frac{\theta_1\left(q_1^{-\mu_{1,j}^{\mathrm{T}}+i}q_2^{-\mu_{1,i}+j-1}\right)}{iQ_\tau^{-\frac{1}{8}}(Q_\tau;Q_\tau)_\infty\sqrt{q_1^{-\mu_{1,j}^{\mathrm{T}}+i}q_2^{-\mu_{1,i}+j-1}}}.
\end{aligned}\tag{C.25}$$

We can divide the remaining parts into those two groups and apply the same deformation as above, and consequently, in the μ_1 sector,

$$\begin{aligned}
\mathsf{G}^{\mathrm{den}}_{(2,2)\mu_1}=\prod_{(i,j)\in\mu_1}q_1^{\mu_{1,j}^{\mathrm{T}}-i}q_2^{\mu_{1,i}-j+1}\sqrt{Q_1^{(1)}Q_2^{(1)}Q_3^{(1)}Q_4^{(1)}}\times\theta_1\left(q_1^{-\mu_{1,j}^{\mathrm{T}}+i}q_2^{-\mu_{1,i}+j-1}\right)\theta_1\left(q_1^{-\mu_{1,j}^{\mathrm{T}}+i-1}q_2^{-\mu_{1,i}+j}\right)\\
\times\theta_1\left(\overline{Q}_1^{(1)}\overline{Q}_4^{(1)}q_1^{-\mu_{2,j}^{\mathrm{T}}+i}q_2^{-\mu_{1,i}+j-1}\right)\theta_1\left(\overline{Q}_2^{(1)}\overline{Q}_3^{(1)}q_1^{\mu_{2,j}^{\mathrm{T}}-i+1}q_2^{\mu_{1,i}-j}\right).
\end{aligned}\tag{C.26}$$

We can also generate the similar expression $\mathsf{G}^{\mathrm{den}}_{(2,2)\mu_2}$ for the μ_2 sector.

Finally, collecting them together with using the relations (5.7) and (5.8) results in

$$\begin{aligned}
G_{(2,2)}(Q_i^{(\mathfrak{a})},Q_\tau;q_1,q_2)&=\sum_{\mu_1,\mu_2}(-Q_{f_2})^{|\mu_2|}(-Q_{f_1})^{|\mu_1|}q_1^{\frac{||\mu_1^{\mathrm{T}}||^2+||\mu_2^{\mathrm{T}}||^2}{2}}q_2^{\frac{||\mu_1||^2+||\mu_2||^2}{2}}\frac{\mathsf{G}^{\mathrm{num}}_{(2,2)\mu_1}}{\mathsf{G}^{\mathrm{den}}_{(2,2)\mu_1}}\cdot\frac{\mathsf{G}^{\mathrm{num}}_{(2,2)\mu_2}}{\mathsf{G}^{\mathrm{den}}_{(2,2)\mu_2}}\\
&=\sum_{\mu_1,\,\mu_2}\left(-Q_{f,1}Q_1^{(2)}Q_3^{(2)}\sqrt{\frac{q_1}{q_2}}\right)^{|\mu_1|}\left(-Q_{f,2}Q_1^{(1)}Q_3^{(1)}\sqrt{\frac{q_2}{q_1}}\right)^{|\mu_2|}\\
&\times\left[\prod_{(i,j)\in\mu_1}\frac{\theta_1\left(\overline{Q}_1^{(1)}\overline{Q}_3^{(1)}\overline{Q}_4^{(1)}q_1^{i-\frac{1}{2}}q_2^{-\mu_{1,i}+j-\frac{1}{2}}\right)\theta_1\left(\overline{Q}_1^{(1)}q_1^{i-\frac{1}{2}}q_2^{-\mu_{1,i}+j-\frac{1}{2}}\right)}{\theta_1\left(\overline{Q}_1^{(1)}\overline{Q}_4^{(1)}q_1^{-\mu_{2,j}^{\mathrm{T}}+i}q_2^{-\mu_{1,i}+j-1}\right)\theta_1\left(\overline{Q}_2^{(1)}\overline{Q}_3^{(1)}q_1^{\mu_{2,j}^{\mathrm{T}}-i+1}q_2^{\mu_{1,i}-j}\right)}\right.\\
&\qquad\times\frac{\theta_1\left(\overline{Q}_1^{(2)}\overline{Q}_2^{(2)}\overline{Q}_3^{(2)}q_1^{-i+\frac{1}{2}}q_2^{\mu_{1,i}-j+\frac{1}{2}}\right)\theta_1\left(\overline{Q}_1^{(2)}q_1^{-i+\frac{1}{2}}q_2^{\mu_{1,i}-j+\frac{1}{2}}\right)}{\theta_1\left(q_1^{-\mu_{1,j}^{\mathrm{T}}+i}q_2^{-\mu_{1,i}+j-1}\right)\theta_1\left(q_1^{-\mu_{1,j}^{\mathrm{T}}+i-1}q_2^{-\mu_{1,i}+j}\right)}\\
&\times\prod_{(i,j)\in\mu_2}\frac{\theta_1\left(\overline{Q}_1^{(1)}\overline{Q}_2^{(1)}\overline{Q}_3^{(1)}q_1^{i-\frac{1}{2}}q_2^{-\mu_{2,i}+j-\frac{1}{2}}\right)\theta_1\left(\overline{Q}_3^{(1)}q_1^{i-\frac{1}{2}}q_2^{-\mu_{2,i}+j-\frac{1}{2}}\right)}{\theta_1\left(\overline{Q}_1^{(1)}\overline{Q}_4^{(1)}q_1^{\mu_{1,j}^{\mathrm{T}}-i}q_2^{\mu_{2,i}-j+1}\right)\theta_1\left(\overline{Q}_2^{(1)}\overline{Q}_3^{(1)}q_1^{-\mu_{1,j}^{\mathrm{T}}+i-1}q_2^{-\mu_{2,i}+j}\right)}\\
&\qquad\left.\times\frac{\theta_1\left(\overline{Q}_3^{(2)}q_1^{-i+\frac{1}{2}}q_2^{\mu_{2,i}-j+\frac{1}{2}}\right)\theta_1\left(\overline{Q}_1^{(2)}\overline{Q}_3^{(2)}\overline{Q}_4^{(2)}q_1^{-i+\frac{1}{2}}q_2^{\mu_{2,i}-j+\frac{1}{2}}\right)}{\theta_1\left(q_1^{-\mu_{2,j}^{\mathrm{T}}+i}q_2^{-\mu_{2,i}+j-1}\right)\theta_1\left(q_1^{-\mu_{2,j}^{\mathrm{T}}+i-1}q_2^{-\mu_{2,i}+j}\right)}\right].
\end{aligned}\tag{C.27}$$

We can verify the generating function $G_{(2,2)}$ (5.9).

C.4 Generating function on TN_N

Let us apply the procedure described in the previous subsection to deriving the generating function $G_{(M,N)}$ on general TN_N written in Section 4.3.2. Recall the form obtained by gluing M domain walls,

$$
\begin{aligned}
&G_{(M,N)}(Q_i^{(\mathfrak{a})}, Q_\tau, Q_{f,a}^{(\mathfrak{a})}; q_1, q_2) \\
&= \sum_{\{\mu_a^{(\mathfrak{a})}\}} \left[\prod_{\mathfrak{a}=1}^{M-1} \prod_{a=1}^{N} \left(-Q_{f,a}^{(\mathfrak{a})}\right)^{|\mu_a^{(\mathfrak{a})}|} \right] \widehat{Z}^{\mu_1^{(1)}\mu_2^{(1)}\cdots\mu_N^{(1)}}_{\emptyset\emptyset\cdots\emptyset}(Q_i^{(1)}, Q_\tau; q_1, q_2) \\
&\quad \times \left[\prod_{\mathfrak{b}=2}^{M-1} \widehat{Z}^{\mu_1^{(\mathfrak{b})}\mu_2^{(\mathfrak{b})}\cdots\mu_N^{(\mathfrak{b})}}_{\mu_1^{(\mathfrak{b}-1)}\mu_2^{(\mathfrak{b}-1)}\cdots\mu_N^{(\mathfrak{b}-1)}}(Q_i^{(\mathfrak{b})}, Q_\tau; q_1, q_2) \right] \widehat{Z}^{\emptyset\emptyset\cdots\emptyset}_{\mu_1^{(M-1)}\mu_2^{(M-1)}\cdots\mu_N^{(M-1)}}(Q_i^{(M)}, Q_\tau; q_1, q_2).
\end{aligned}
\tag{C.28}
$$

Let us pick up the $\mathfrak{b}$-th and $(\mathfrak{b}+1)$-th domain wall from (C.28),

$$
\begin{aligned}
&\widehat{Z}^{\mu_1^{(\mathfrak{b})}\mu_2^{(\mathfrak{b})}\cdots\mu_N^{(\mathfrak{b})}}_{\mu_1^{(\mathfrak{b}-1)}\mu_2^{(\mathfrak{b}-1)}\cdots\mu_N^{(\mathfrak{b}-1)}} \times \widehat{Z}^{\mu_1^{(\mathfrak{b}+1)}\mu_2^{(\mathfrak{b}+1)}\cdots\mu_N^{(\mathfrak{b}+1)}}_{\mu_1^{(\mathfrak{b})}\mu_2^{(\mathfrak{b})}\cdots\mu_N^{(\mathfrak{b})}} \\
&= \left[\prod_{a=1}^{N} q_1^{\frac{||\mu_a^{(\mathfrak{b}-1)\mathrm{T}}||^2}{2}} q_2^{\frac{||\mu_a^{(\mathfrak{b})}||^2}{2}} \widetilde{Z}_{\mu_a^{(\mathfrak{b}-1)\mathrm{T}}}(q_2, q_1) \widetilde{Z}_{\mu_a^{(\mathfrak{b})}}(q_1, q_2) \cdot q_1^{\frac{||\mu_a^{(\mathfrak{b})\mathrm{T}}||^2}{2}} q_2^{\frac{||\mu_a^{(\mathfrak{b}+1)}||^2}{2}} \widetilde{Z}_{\mu_a^{(\mathfrak{b})\mathrm{T}}}(q_2, q_1) \widetilde{Z}_{\mu_a^{(\mathfrak{b}+1)}}(q_1, q_2) \right] \\
&\quad \times \prod_{a,b=1}^{N} \prod_{k=1}^{\infty} \left[\prod_{(i,j)\in\mu_a^{(\mathfrak{b}-1)}} \frac{\left(1 - Q_\tau^{k-1} \mathsf{Q}'^{(\mathfrak{b})}_{ba} q_1^{\mu_{b,j}^{(\mathfrak{b})\mathrm{T}} - i + \frac{1}{2}} q_2^{\mu_{a,i}^{(\mathfrak{b}-1)} - j + \frac{1}{2}}\right)\left(1 - Q_\tau^{k-1} \mathsf{Q}^{(\mathfrak{b})}_{ab} q_1^{-\mu_{b,j}^{(\mathfrak{b})\mathrm{T}} + i - \frac{1}{2}} q_2^{-\mu_{a,i}^{(\mathfrak{b}-1)} + j - \frac{1}{2}}\right)}{\left(1 - Q_\tau^{k-1} \widetilde{\mathsf{Q}}^{(\mathfrak{b})}_{ba} q_1^{\mu_{b,j}^{(\mathfrak{b}-1)\mathrm{T}} - i} q_2^{\mu_{a,i}^{(\mathfrak{b}-1)} - j + 1}\right)\left(1 - Q_\tau^{k-1} \widetilde{\mathsf{Q}}^{(\mathfrak{b})}_{ab} q_1^{-\mu_{b,j}^{(\mathfrak{b}-1)\mathrm{T}} + i - 1} q_2^{-\mu_{a,i}^{(\mathfrak{b}-1)} + j}\right)} \right. \\
&\qquad \left. \times \prod_{(i,j)\in\mu_b^{(\mathfrak{b})}} \frac{\left(1 - Q_\tau^{k-1} \mathsf{Q}'^{(\mathfrak{b})}_{ba} q_1^{-\mu_{a,j}^{(\mathfrak{b}-1)\mathrm{T}} + i - \frac{1}{2}} q_2^{-\mu_{b,i}^{(\mathfrak{b})} + j - \frac{1}{2}}\right)\left(1 - Q_\tau^{k-1} \mathsf{Q}^{(\mathfrak{b})}_{ab} q_1^{\mu_{a,j}^{(\mathfrak{b}-1)\mathrm{T}} - i + \frac{1}{2}} q_2^{\nu_{b,i}^{(\mathfrak{b})} - j + \frac{1}{2}}\right)}{\left(1 - Q_\tau^{k-1} \widetilde{\mathsf{Q}}'^{(\mathfrak{b})}_{ab} q_1^{\mu_{a,j}^{(\mathfrak{b})\mathrm{T}} - i + 1} q_2^{\mu_{b,i}^{(\mathfrak{b})} - j}\right)\left(1 - Q_\tau^{k-1} \widetilde{\mathsf{Q}}'^{(\mathfrak{b})}_{ba} q_1^{-\mu_{a,j}^{(\mathfrak{b})\mathrm{T}} + i} q_2^{-\mu_{b,i}^{(\mathfrak{b})} + j - 1}\right)} \right] \\
&\quad \times \left[\prod_{(i,j)\in\mu_a^{(\mathfrak{b})}} \frac{\left(1 - Q_\tau^{k-1} \mathsf{Q}'^{(\mathfrak{b}+1)}_{ba} q_1^{\mu_{b,j}^{(\mathfrak{b}+1)\mathrm{T}} - i + \frac{1}{2}} q_2^{\mu_{a,i}^{(\mathfrak{b})} - j + \frac{1}{2}}\right)\left(1 - Q_\tau^{k-1} \mathsf{Q}^{(\mathfrak{b}+1)}_{ab} q_1^{-\mu_{b,j}^{(\mathfrak{b}+1)\mathrm{T}} + i - \frac{1}{2}} q_2^{-\mu_{a,i}^{(\mathfrak{b})} + j - \frac{1}{2}}\right)}{\left(1 - Q_\tau^{k-1} \widetilde{\mathsf{Q}}^{(\mathfrak{b}+1)}_{ba} q_1^{\mu_{b,j}^{(\mathfrak{b})\mathrm{T}} - i} q_2^{\mu_{a,i}^{(\mathfrak{b})} - j + 1}\right)\left(1 - Q_\tau^{k-1} \widetilde{\mathsf{Q}}^{(\mathfrak{b}+1)}_{ab} q_1^{-\mu_{b,j}^{(\mathfrak{b})\mathrm{T}} + i - 1} q_2^{-\mu_{a,i}^{(\mathfrak{b})} + j}\right)} \right. \\
&\qquad \left. \times \prod_{(i,j)\in\mu_b^{(\mathfrak{b}+1)}} \frac{\left(1 - Q_\tau^{k-1} \mathsf{Q}'^{(\mathfrak{b}+1)}_{ba} q_1^{-\mu_{a,j}^{(\mathfrak{b})\mathrm{T}} + i - \frac{1}{2}} q_2^{-\mu_{b,i}^{(\mathfrak{b}+1)} + j - \frac{1}{2}}\right)\left(1 - Q_\tau^{k-1} \mathsf{Q}^{(\mathfrak{b}+1)}_{ab} q_1^{\mu_{a,j}^{(\mathfrak{b})\mathrm{T}} - i + \frac{1}{2}} q_2^{\mu_{b,i}^{(\mathfrak{b}+1)} - j + \frac{1}{2}}\right)}{\left(1 - Q_\tau^{k-1} \widetilde{\mathsf{Q}}'^{(\mathfrak{b}+1)}_{ab} q_1^{\mu_{a,j}^{(\mathfrak{b}+1)\mathrm{T}} - i + 1} q_2^{\mu_{b,i}^{(\mathfrak{b}=1)} - j}\right)\left(1 - Q_\tau^{k-1} \widetilde{\mathsf{Q}}'^{(\mathfrak{b}+1)}_{ba} q_1^{-\mu_{a,j}^{(\mathfrak{b}+1)\mathrm{T}} + i} q_2^{-\mu_{b,i}^{(\mathfrak{b}+1)} + j - 1}\right)} \right].
\end{aligned}
\tag{C.29}
$$

Both include the contributions of the $\mathfrak{b}$-th domain wall encoded into the products of $\mu_a^{(\mathfrak{b})}$, and it is enough to concentrate on this sector,

$$\begin{aligned}\frac{\mathsf{G}^{\rm num}_{(M,N,\mathfrak{b})}}{\mathsf{G}^{\rm den}_{(M,N,\mathfrak{b})}} :=& \left[\prod_{a=1}^{N} q_1^{\frac{||\mu_a^{(\mathfrak{b})\mathrm{T}}||^2}{2}} q_2^{\frac{||\mu_a^{(\mathfrak{b})}||^2}{2}} \widetilde{Z}_{\mu_a^{(\mathfrak{b})\mathrm{T}}}(q_2,q_1)\widetilde{Z}_{\mu_a^{(\mathfrak{b})}}(q_1,q_2)\right] \\ &\times \prod_{a,b=1}^{N}\prod_{(i,j)\in\mu_a^{(\mathfrak{b})}} \frac{\left(1-Q_\tau^{k-1}\mathsf{Q}'^{(\mathfrak{b})}_{ab} q_1^{-\mu_{b,j}^{(\mathfrak{b}-1)\mathrm{T}}+i-\frac{1}{2}} q_2^{-\mu_{a,i}^{(\mathfrak{b})}+j-\frac{1}{2}}\right)\left(1-Q_\tau^{k-1}\mathsf{Q}^{(\mathfrak{b})}_{ba} q_1^{\mu_{b,j}^{(\mathfrak{b}-1)\mathrm{T}}-i+\frac{1}{2}} q_2^{\nu_{a,i}^{(\mathfrak{b})}-j+\frac{1}{2}}\right)}{\underbrace{\left(1-Q_\tau^{k-1}\widetilde{\mathsf{Q}}'^{(\mathfrak{b})}_{ba} q_1^{\mu_{b,j}^{(\mathfrak{b})\mathrm{T}}-i+1} q_2^{\mu_{a,i}^{(\mathfrak{b})}-j}\right)}_{\text{(1-i)}}\underbrace{\left(1-Q_\tau^{k-1}\widetilde{\mathsf{Q}}'^{(\mathfrak{b})}_{ab} q_1^{-\mu_{b,j}^{(\mathfrak{b})\mathrm{T}}+i} q_2^{-\mu_{a,i}^{(\mathfrak{b})}+j-1}\right)}_{\text{(1-ii)}}} \\ &\times \frac{\left(1-Q_\tau^{k-1}\mathsf{Q}'^{(\mathfrak{b}+1)}_{ba} q_1^{\mu_{b,j}^{(\mathfrak{b}+1)\mathrm{T}}-i+\frac{1}{2}} q_2^{\mu_{a,i}^{(\mathfrak{b})}-j+\frac{1}{2}}\right)\left(1-Q_\tau^{k-1}\mathsf{Q}^{(\mathfrak{b}+1)}_{ab} q_1^{-\mu_{b,j}^{(\mathfrak{b}+1)\mathrm{T}}+i-\frac{1}{2}} q_2^{-\mu_{a,i}^{(\mathfrak{b})}+j-\frac{1}{2}}\right)}{\underbrace{\left(1-Q_\tau^{k-1}\widetilde{\mathsf{Q}}^{(\mathfrak{b}+1)}_{ba} q_1^{\mu_{b,j}^{(\mathfrak{b})\mathrm{T}}-i} q_2^{\mu_{a,i}^{(\mathfrak{b})}-j+1}\right)}_{\text{(2-ii)}}\underbrace{\left(1-Q_\tau^{k-1}\widetilde{\mathsf{Q}}^{(\mathfrak{b}+1)}_{ab} q_1^{-\mu_{b,j}^{(\mathfrak{b})\mathrm{T}}+i-1} q_2^{-\mu_{a,i}^{(\mathfrak{b})}+j}\right)}_{\text{(2-i)}}},\end{aligned} \tag{C.30}$$

where the first and second line in the product of $\mu_a^{(\mathfrak{b})}$ come from the $\mathfrak{b}$-th and $(\mathfrak{b}+1)$-th domain wall, respectively. We can transform independently these in the numerator $\mathsf{G}^{\rm num}_{(M,N,\mathfrak{b})}$ and denominator $\mathsf{G}^{\rm den}_{(M,N,\mathfrak{b})}$ into the elliptic theta function $\theta_1(x;p)$ as follows.

• The numerator of (C.30): As done in Section 4.3 and Appendix C.3, the factors sit in the same domain wall can be combined into $\theta_1(x;p)$. This is rather easily implemented by defining

$$\mathsf{A}^{(\mathfrak{b})}_{ab}(i,j) := \overline{\mathsf{Q}}^{(\mathfrak{b}+1)}_{ab} q_1^{\mu_{b,j}^{(\mathfrak{b}+1)\mathrm{T}}-i+\frac{1}{2}} q_2^{\mu_{a,i}^{(\mathfrak{b})}-j+\frac{1}{2}}, \tag{C.31}$$

$$\mathsf{B}^{(\mathfrak{b})}_{ab}(i,j) := \overline{\mathsf{Q}}^{(\mathfrak{b})}_{ba} q_1^{-\mu_{b,j}^{(\mathfrak{b}-1)\mathrm{T}}+i-\frac{1}{2}} q_2^{-\mu_{a,i}^{(\mathfrak{b})}+j-\frac{1}{2}}, \tag{C.32}$$

then, we have

$$\begin{aligned}&\prod_{a,b=1}^{N}\prod_{k=1}^{\infty}\prod_{(i,j)\in\mu_a^{(\mathfrak{b})}}\left(1-Q_\tau^k\mathsf{A}^{(\mathfrak{b})}_{ab}(i,j)\right)\left(1-Q_\tau^{k-1}\overline{\mathsf{A}}^{(\mathfrak{b})}_{ab}(i,j)\right)\left(1-Q_\tau^k\mathsf{B}^{(\mathfrak{b})}_{ab}(i,j)\right)\left(1-Q_\tau^{k-1}\overline{\mathsf{B}}^{(\mathfrak{b})}_{ab}(i,j)\right) \\ &\sim \prod_{a,b=1}^{N}\prod_{(i,j)\in\mu_a^{(\mathfrak{b})}}\frac{\theta_1\left(\mathsf{A}^{(\mathfrak{b})}_{ab}(i,j)\right)}{\sqrt{\mathsf{A}^{(\mathfrak{b})}_{ab}(i,j)}}\frac{\theta_1\left(\mathsf{B}^{(\mathfrak{b})}_{ab}(i,j)\right)}{\sqrt{\mathsf{B}^{(\mathfrak{b})}_{ab}(i,j)}} \\ &= \prod_{a,b=1}^{N}\prod_{(i,j)\in\mu_a^{(\mathfrak{b})}}\sqrt{\frac{\mathsf{Q}^{(\mathfrak{b}+1)}_{ab}\mathsf{Q}^{(\mathfrak{b})}_{ba}}{q_1^{\mu_{b,j}^{(\mathfrak{b}+1)\mathrm{T}}-\mu_{b,j}^{(\mathfrak{b}-1)\mathrm{T}}}}}\theta_1\left(\mathsf{A}^{(\mathfrak{b})}_{ab}(i,j)\right)\theta_1\left(\mathsf{B}^{(\mathfrak{b})}_{ab}(i,j)\right),\end{aligned} \tag{C.33}$$

where $\overline{\mathsf{A}}^{(\mathfrak{b})}_{ab}(i,j) := \left(\mathsf{A}^{(\mathfrak{b})}_{ab}(i,j)\right)^{-1}$, and $\sim$ stands for the equality up to factors depending only on Q_τ which will be canceled out in the final step. From the definition in Table 4, the

prefactor of Kähler parameters is simplified as

$$\mathsf{Q}_{ab}^{(\mathfrak{b}+1)}\mathsf{Q}_{ba}^{(\mathfrak{b})} = \begin{cases} Q_{2b-1}^{(\mathfrak{b})}Q_{2b-1}^{(\mathfrak{b}+1)} & \text{for } a = b, \\ Q_\tau Q_{2b-1}^{(\mathfrak{b})}Q_{2b-1}^{(\mathfrak{b}+1)} & \text{for } a \neq b. \end{cases} \tag{C.34}$$

Moreover, the denominator in the square root will be also canceled out after the joint of all domain walls. To see this, using the relation, $\sum_{(i,j)\in W} Y_j^{\mathrm{T}} = \sum_{(i,j)\in Y} W_j^{\mathrm{T}}$,

$$\begin{aligned} &\prod_{a,b=1}^{N} \prod_{(i,j)\in\mu_a^{(\mathfrak{b})}} q_1^{\mu_{b,j}^{(\mathfrak{b}+1)\mathrm{T}}} q_1^{-\mu_{b,j}^{(\mathfrak{b}-1)\mathrm{T}}} \prod_{(i,j)\in\mu_a^{(\mathfrak{b}+1)}} q_1^{\mu_{b,j}^{(\mathfrak{b}+2)\mathrm{T}}} q_1^{-\mu_{b,j}^{(\mathfrak{b})\mathrm{T}}} \\ &= \prod_{a,b=1}^{N} \prod_{(i,j)\in\mu_b^{(\mathfrak{b}+1)}} q_1^{\mu_{a,j}^{(\mathfrak{b})\mathrm{T}}} \prod_{(i,j)\in\mu_a^{(\mathfrak{b})}} q_1^{-\mu_{b,j}^{(\mathfrak{b}-1)\mathrm{T}}} \prod_{(i,j)\in\mu_a^{(\mathfrak{b}+1)}} q_1^{\mu_{b,j}^{(\mathfrak{b}+2)\mathrm{T}}} q_1^{-\mu_{b,j}^{(\mathfrak{b})\mathrm{T}}} \\ &= \prod_{a,b=1}^{N} \prod_{(i,j)\in\mu_a^{(\mathfrak{b})}} q_1^{-\mu_{b,j}^{(\mathfrak{b}-1)\mathrm{T}}} \prod_{(i,j)\in\mu_a^{(\mathfrak{b}+1)}} q_1^{\mu_{b,j}^{(\mathfrak{b}+2)\mathrm{T}}}. \end{aligned} \tag{C.35}$$

The same cancellation happens for the rests by gluing all domain walls. Therefore, the actual contributions of the numerator is given by

$$\mathsf{G}^{\mathrm{num}}_{(M,N,\mathfrak{b})} = \prod_{a,b=1}^{N} \prod_{(i,j)\in\mu_a^{(\mathfrak{b})}} \sqrt{\mathsf{Q}_{ab}^{(\mathfrak{b}+1)}\mathsf{Q}_{ba}^{(\mathfrak{b})}}\,\theta_1\left(\mathsf{A}_{ab}^{(\mathfrak{b})}(i,j)\right)\theta_1\left(\mathsf{B}_{ab}^{(\mathfrak{b})}(i,j)\right). \tag{C.36}$$

• The denominator of (C.30): As for the numerator, it is convenient to define

$$\mathsf{C}_{ab}^{(\mathfrak{b})}(i,j) := \widehat{\mathsf{Q}}_{ba}^{(\mathfrak{b})} q_1^{-\mu_{b,j}^{(\mathfrak{b})\mathrm{T}}+i-1} q_2^{-\mu_{a,i}^{(\mathfrak{b})}+j} \qquad \text{for the terms (1-i) and (2-i) in (C.30)}, \tag{C.37}$$

$$\mathsf{D}_{ab}^{(\mathfrak{b})}(i,j) := \widehat{\mathsf{Q}}_{ab}^{(\mathfrak{b})} q_1^{\mu_{b,j}^{(\mathfrak{b})\mathrm{T}}-i} q_2^{\mu_{a,i}^{(\mathfrak{b})}-j+1} \qquad \text{for the terms (1-ii) and (2-ii) in (C.30)}, \tag{C.38}$$

with a normalized notation for the specific product of Kähler factors,

$$\widehat{\mathsf{Q}}_{ab}^{(\mathfrak{b})} = \begin{cases} 1 & \text{for } a = b, \\ \left(\widetilde{\mathsf{Q}}_{ab}^{\prime(\mathfrak{b})}\right)^{-1} & \text{for } a \neq b. \end{cases} \tag{C.39}$$

These factors do not contain any Kähler factor if $a = b$ and, hence, should be incorporated with the functions $\widetilde{Z}_{\mu_a^{(\mathfrak{b})\mathrm{T}}}(q_2,q_1)\widetilde{Z}_{\mu_a^{(\mathfrak{b})}}(q_1,q_2)$. With its definition (B.8), the denominator for

$a=b$ becomes

$$\begin{aligned}
&\prod_{a=1}^{N}\prod_{k=1}^{\infty}\prod_{(i,j)\in\mu_a^{(\mathfrak{b})}}\frac{1}{\widetilde{Z}_{\mu_a^{(\mathfrak{b})}}(q_1,q_2)}\left(1-Q_\tau^k q_1^{\mu_{a,j}^{(\mathfrak{b})\mathrm{T}}-i+1}q_2^{\mu_{a,i}^{(\mathfrak{b})}-j}\right)\left(1-Q_\tau^k q_1^{-\mu_{a,j}^{(\mathfrak{b})\mathrm{T}}+i-1}q_2^{-\mu_{a,i}^{(\mathfrak{b})}+j}\right)\\
&\qquad\times\frac{1}{\widetilde{Z}_{\mu_a^{(\mathfrak{b})\mathrm{T}}}(q_2,q_1)}\left(1-Q_\tau^k q_1^{-\mu_{a,j}^{(\mathfrak{b})\mathrm{T}}+i}q_2^{-\mu_{a,i}^{(\mathfrak{b})}+j-1}\right)\left(1-Q_\tau^k q_1^{\mu_{a,j}^{(\mathfrak{b})\mathrm{T}}-i}q_2^{\mu_{a,i}^{(\mathfrak{b})}-j+1}\right)\\
&=\prod_{a=1}^{N}\prod_{k=1}^{\infty}\prod_{(i,j)\in\mu_a^{(\mathfrak{b})}}\left(1-Q_\tau^{k-1} q_1^{\mu_{a,j}^{(\mathfrak{b})\mathrm{T}}-i+1}q_2^{\mu_{a,i}^{(\mathfrak{b})}-j}\right)\left(1-Q_\tau^k q_1^{-\mu_{a,j}^{(\mathfrak{b})\mathrm{T}}+i-1}q_2^{-\mu_{a,i}^{(\mathfrak{b})}+j}\right)\\
&\qquad\times\left(1-Q_\tau^k q_1^{-\mu_{a,j}^{(\mathfrak{b})\mathrm{T}}+i}q_2^{-\mu_{a,i}^{(\mathfrak{b})}+j-1}\right)\left(1-Q_\tau^{k-1} q_1^{\mu_{a,j}^{(\mathfrak{b})\mathrm{T}}-i}q_2^{\mu_{a,i}^{(\mathfrak{b})}-j+1}\right)\\
&\sim\prod_{a=1}^{N}\prod_{(i,j)\in\mu_a^{(\mathfrak{b})}}\frac{\theta_1\left(\mathsf{C}_{aa}^{(\mathfrak{b})}(i,j)\right)}{\sqrt{q_1^{-\mu_{a,j}^{(\mathfrak{b})\mathrm{T}}+i-1}q_2^{-\mu_{a,i}^{(\mathfrak{b})}+j}}}\frac{\theta_1\left(\overline{\mathsf{D}}_{aa}^{(\mathfrak{b})}(i,j)\right)}{\sqrt{q_1^{-\mu_{a,j}^{(\mathfrak{b})\mathrm{T}}+i}q_2^{-\mu_{a,i}^{(\mathfrak{b})}+j-1}}}\\
&=\prod_{a=1}^{N}\prod_{(i,j)\in\mu_a^{(\mathfrak{b})}}(-1)q_1^{\mu_{a,j}^{(\mathfrak{b})\mathrm{T}}-i+\frac{1}{2}}q_2^{\mu_{a,i}^{(\mathfrak{b})}-j+\frac{1}{2}}\theta_1\left(\mathsf{C}_{aa}^{(\mathfrak{b})}(i,j)\right)\theta_1\left(\mathsf{D}_{aa}^{(\mathfrak{b})}(i,j)\right)\\
&=\prod_{a=1}^{N}(-1)^{|\mu_a^{(\mathfrak{b})}|}q_1^{\frac{1}{2}||\mu_a^{(\mathfrak{b})\mathrm{T}}||^2}q_2^{\frac{1}{2}||\mu_a^{(\mathfrak{b})}||^2}\prod_{(i,j)\in\mu_a^{(\mathfrak{b})}}\theta_1\left(\mathsf{C}_{aa}^{(\mathfrak{b})}(i,j)\right)\theta_1\left(\mathsf{D}_{aa}^{(\mathfrak{b})}(i,j)\right),
\end{aligned}\tag{C.40}$$

where $\overline{\mathsf{D}}_{aa}^{(\mathfrak{b})}(i,j)=\left(\mathsf{D}_{aa}^{(\mathfrak{b})}(i,j)\right)^{-1}$. On the other hand, the contributions from $a\neq b$ are deformed as

$$\begin{aligned}
&\prod_{a\neq b}^{N}\prod_{k=1}^{\infty}\prod_{(i,j)\in\mu_a^{(\mathfrak{b})}}\left(1-Q_\tau^{k-1}\widetilde{\mathsf{Q}}_{ab}^{\prime(\mathfrak{b})}q_1^{\mu_{b,j}^{(\mathfrak{b})\mathrm{T}}-i+1}q_2^{\mu_{a,i}^{(\mathfrak{b})}-j}\right)\left(1-Q_\tau^{k-1}\widetilde{\mathsf{Q}}_{ba}^{(\mathfrak{b})}q_1^{-\mu_{b,j}^{(\mathfrak{b})\mathrm{T}}+i-1}q_2^{-\mu_{a,i}^{(\mathfrak{b})}+j}\right)\\
&\qquad\times\left(1-Q_\tau^{k-1}\widetilde{\mathsf{Q}}_{ba}^{\prime(\mathfrak{b})}q_1^{-\mu_{b,j}^{(\mathfrak{b})\mathrm{T}}+i}q_2^{-\mu_{a,i}^{(\mathfrak{b})}+j-1}\right)\left(1-Q_\tau^{k-1}\widetilde{\mathsf{Q}}_{ab}^{(\mathfrak{b})}q_1^{\mu_{b,j}^{(\mathfrak{b})\mathrm{T}}-i}q_2^{\mu_{a,i}^{(\mathfrak{b})}-j+1}\right)\\
&=\prod_{a\neq b}^{N}\prod_{(i,j)\in\mu_a^{(\mathfrak{b})}}\frac{\theta_1\left(\mathsf{C}_{ab}^{(\mathfrak{b})}(i,j)\right)}{\sqrt{\mathsf{C}_{ab}^{(\mathfrak{b})}(i,j)}}\frac{\theta_1\left(\mathsf{D}_{ab}^{(\mathfrak{b})}(i,j)\right)}{\sqrt{\mathsf{D}_{ab}^{(\mathfrak{b})}(i,j)}}\\
&=\prod_{a\neq b}^{N}\left(\frac{q_1}{q_2}\right)^{\frac{1}{2}|\mu_a^{(\mathfrak{b})}|}\prod_{(i,j)\in\mu_a^{(\mathfrak{b})}}\frac{1}{\sqrt{\widehat{\mathsf{Q}}_{ba}^{(\mathfrak{b})}\widehat{\mathsf{Q}}_{ab}^{(\mathfrak{b})}}}\theta_1\left(\mathsf{C}_{ab}^{(\mathfrak{b})}(i,j)\right)\theta_1\left(\mathsf{D}_{ab}^{(\mathfrak{b})}(i,j)\right)\\
&=\prod_{a=1}^{N}\left(\frac{q_1}{q_2}\right)^{\frac{N-1}{2}|\mu_a^{(\mathfrak{b})}|}\prod_{a\neq b}^{N}\prod_{(i,j)\in\mu_a^{(\mathfrak{b})}}\frac{1}{\sqrt{\widehat{\mathsf{Q}}_{ba}^{(\mathfrak{b})}\widehat{\mathsf{Q}}_{ab}^{(\mathfrak{b})}}}\theta_1\left(\mathsf{C}_{ab}^{(\mathfrak{b})}(i,j)\right)\theta_1\left(\mathsf{D}_{ab}^{(\mathfrak{b})}(i,j)\right).
\end{aligned}\tag{C.41}$$

Combining (C.40) and (C.41) together provides the denominator contribution as

$$\mathsf{G}^{\rm den}_{(M,N,\mathfrak{b})} = \prod_{a=1}^{N}(-1)^{|\mu_a^{(\mathfrak{b})}|} q_1^{\frac{1}{2}||\mu_a^{(\mathfrak{b})\mathrm{T}}||^2} q_2^{\frac{1}{2}||\mu_a^{(\mathfrak{b})}||^2} \left(\frac{q_1}{q_2}\right)^{\frac{N-1}{2}|\mu_a^{(\mathfrak{b})}|} \times \prod_{a,b=1}^{N}\prod_{(i,j)\in\mu_a^{(\mathfrak{b})}} \frac{1}{\sqrt{\widehat{\mathsf{Q}}_{ba}^{(\mathfrak{b})}\widehat{\mathsf{Q}}_{ab}^{(\mathfrak{b})}}}\theta_1\left(\mathsf{C}_{ab}^{(\mathfrak{b})}(i,j)\right)\theta_1\left(\mathsf{D}_{ab}^{(\mathfrak{b})}(i,j)\right). \tag{C.42}$$

Then, as gluing M domain walls, the partition function of a single domain wall is written from (C.36) and (C.42) by

$$\begin{aligned}\frac{\mathsf{G}^{\rm num}_{(M,N,\mathfrak{b})}}{\mathsf{G}^{\rm den}_{(M,N,\mathfrak{b})}} &= \prod_{a=1}^{N} q_1^{\frac{1}{2}||\mu_a^{(\mathfrak{b})\mathrm{T}}||^2} q_2^{\frac{1}{2}||\mu_a^{(\mathfrak{b})}||^2}\cdot(-1)^{|\mu_a^{(\mathfrak{b})}|} q_1^{-\frac{1}{2}||\mu_a^{(\mathfrak{b})\mathrm{T}}||^2} q_2^{-\frac{1}{2}||\mu_a^{(\mathfrak{b})}||^2}\left(\frac{q_2}{q_1}\right)^{\frac{N-1}{2}|\mu_a^{(\mathfrak{b})}|} \\ &\quad\times\prod_{a,b=1}^{N}\prod_{(i,j)\in\mu_a^{(\mathfrak{b})}}\sqrt{\mathsf{Q}_{ab}^{(\mathfrak{b}+1)}\mathsf{Q}_{ba}^{(\mathfrak{b})}\widehat{\mathsf{Q}}_{ba}^{(\mathfrak{b})}\widehat{\mathsf{Q}}_{ab}^{(\mathfrak{b})}}\frac{\theta_1\left(\mathsf{A}_{ab}^{(\mathfrak{b})}(i,j)\right)\theta_1\left(\mathsf{B}_{ab}^{(\mathfrak{b})}(i,j)\right)}{\theta_1\left(\mathsf{C}_{ab}^{(\mathfrak{b})}(i,j)\right)\theta_1\left(\mathsf{D}_{ab}^{(\mathfrak{b})}(i,j)\right)} \\ &= \prod_{a=1}^{N}(-1)^{|\mu_a^{(\mathfrak{b})}|}\left(\frac{q_2}{q_1}\right)^{\frac{N-1}{2}|\mu_a^{(\mathfrak{b})}|}\left(\prod_{b=1}^{N}Q_{2b-1}^{(\mathfrak{b})}Q_{2b-1}^{(\mathfrak{b}+1)}\right)^{\frac{1}{2}|\mu_a^{(\mathfrak{b})}|} \\ &\quad\times\prod_{a,b=1}^{N}\prod_{(i,j)\in\mu_a^{(\mathfrak{b})}}\frac{\theta_1\left(\mathsf{A}_{ab}^{(\mathfrak{b})}(i,j)\right)\theta_1\left(\mathsf{B}_{ab}^{(\mathfrak{b})}(i,j)\right)}{\theta_1\left(\mathsf{C}_{ab}^{(\mathfrak{b})}(i,j)\right)\theta_1\left(\mathsf{D}_{ab}^{(\mathfrak{b})}(i,j)\right)}.\end{aligned} \tag{C.43}$$

Finally, we can simplify the generic generating function (C.28) as the ratio of the elliptic theta functions,

$$\begin{aligned}G_{(M,N)}(Q_i^{(\mathfrak{a})},Q_\tau,Q_{f,a}^{(\mathfrak{a})};q_1,q_2) &= \sum_{\{\mu_a^{(\mathfrak{a})}\}}\prod_{\mathfrak{b}=1}^{M-1}\left[\left\{\prod_{a=1}^{N}\left(-Q_{f,a}^{(\mathfrak{b})}\right)^{|\mu_a^{(\mathfrak{b})}|}\right\}\frac{\mathsf{G}^{\rm num}_{(M,N,\mathfrak{b})}}{\mathsf{G}^{\rm den}_{(M,N,\mathfrak{b})}}\right] \\ &= \sum_{\{\mu_a^{(\mathfrak{a})}\}}\prod_{\mathfrak{b}=1}^{M-1}\left[\prod_{a=1}^{N}\left(\mathfrak{Q}_{f,a}^{(\mathfrak{b})}\right)^{|\mu_a^{(\mathfrak{b})}|}\right]\left[\prod_{a,b=1}^{N}\prod_{(i,j)\in\mu_a^{(\mathfrak{b})}}\frac{\theta_1\left(\mathsf{A}_{ab}^{(\mathfrak{b})}(i,j)\right)\theta_1\left(\mathsf{B}_{ab}^{(\mathfrak{b})}(i,j)\right)}{\theta_1\left(\mathsf{C}_{ab}^{(\mathfrak{b})}(i,j)\right)\theta_1\left(\mathsf{D}_{ab}^{(\mathfrak{b})}(i,j)\right)}\right],\end{aligned} \tag{C.44}$$

where we define

$$\mathfrak{Q}_{f,a}^{(\mathfrak{b})} := Q_{f,a}^{(\mathfrak{b})}\left(\frac{q_2}{q_1}\right)^{\frac{N-1}{2}}\left(\prod_{b=1}^{N}Q_{2b-1}^{(\mathfrak{b})}Q_{2b-1}^{(\mathfrak{b}+1)}\right)^{\frac{1}{2}}. \tag{C.45}$$

C.5 Unrefined open topological vertex for the domain wall on TN_1

In this subsection, the domain wall partition function on TN_1 with a Lagrangian brane $Z^{\nu_1}_{\mu_1}(Q_i,Q_{\rm L};q)$ (6.6) is concretely derived by the formalism of the unrefined open topological

string (6.2). The starting point with $\tilde{\ell}=1$ is

$$Z^{\nu_1}_{\mu_1}(Q_i,Q_{\rm L};q)=\sum_{\rho_1,\rho_2,\sigma_1,\sigma_2}(-Q_1)^{|\rho_1|}(-Q_2)^{|\rho_2|}C_{\rho_1^{\rm T}(\rho_2\otimes\sigma_1)\mu_1^{\rm T}}(q)C_{\rho_1(\rho_2^{\rm T}\otimes\sigma_2)\nu_1}(q)$$
$$\times\left(\mathsf{f}_{\rho_2\otimes\sigma_1}(q)Q_{\rm L}^{|\sigma_1|}{\rm Tr}_{\sigma_1^{\rm T}}X\right)\left(\mathsf{f}_{\rho_2^{\rm T}\otimes\sigma_2}(q)(Q_2Q_{\rm L}^{-1})^{|\sigma_2|}{\rm Tr}_{\sigma_2^{\rm T}}X^{-1}\right). \tag{C.46}$$

Putting the formulae of the unrefined topological vertex (B.1) and (6.5) into it leads to

$$Z^{\nu_1}_{\mu_1}(Q_i,Q_{\rm L};q)=q^{\frac{1}{2}(\kappa_{\mu_1^{\rm T}}+\kappa_{\nu_1})}s_{\mu_1^{\rm T}}(q^{-\mathfrak{n}})s_{\nu_1}(q^{-\mathfrak{n}})\,\check{\mathsf{Z}}^{\nu_1}_{\mu_1}, \tag{C.47}$$

where

$$\check{\mathsf{Z}}^{\nu_1}_{\mu_1}=\sum_{\rho_1,\rho_2,\gamma_1,\gamma_2,\lambda_1,\lambda_2}(-Q_1)^{|\rho_1|}(-Q_2)^{|\rho_2|}$$
$$\times s_{\rho_1/\lambda_1}(q^{-\mu_1^{\rm T}-\mathfrak{n}})s_{\rho_1^{\rm T}/\lambda_2}(q^{-\nu_1-\mathfrak{n}})s_{\gamma_1/\lambda_1}(q^{-\mu_1-\mathfrak{n}})s_{\gamma_2/\lambda_2}(q^{-\nu_1^{\rm T}-\mathfrak{n}})s_{\gamma_1^{\rm T}/\rho_2^{\rm T}}(-Q_{\rm L}x)s_{\gamma_2^{\rm T}/\rho_2}(-Q_2Q_{\rm L}^{-1}x^{-1}). \tag{C.48}$$

The main differences from the closed topological string in Appendix C.1 are the number of the skew Schur functions and Young diagrams over which we take the summations. As before, let us consider an useful form,

$$\widetilde{\check{\mathsf{Z}}}^{\nu_1}_{\mu_1}=\sum_{\rho_1,\rho_2,\gamma_1,\gamma_2,\lambda_1,\lambda_2}(-Q_1)^{|\rho_1|}(-Q_2)^{|\rho_2|}$$
$$\times s_{\rho_1/\lambda_1}(X_1)s_{\rho_1^{\rm T}/\lambda_2}(X_2)s_{\gamma_1/\lambda_1}(Y_1)s_{\gamma_1^{\rm T}/\rho_2^{\rm T}}(Y_2)s_{\gamma_2/\lambda_2}(Z_1)s_{\gamma_2^{\rm T}/\rho_2}(Z_2). \tag{C.49}$$

The strategy is basically the same as for the previous cases, but we would carefully trace the computational process. First of all, using (A.34) to the skew Schur function with ρ_1,

$$\widetilde{\check{\mathsf{Z}}}^{\nu_1}_{\mu_1}=\sum_{\rho_1,\rho_2,\gamma_1,\gamma_2,\lambda_1,\lambda_2}(-Q_1)^{|\lambda_1|}(-Q_2)^{|\rho_2|}$$
$$\times s_{\rho_1/\lambda_1}(-Q_1X_1)s_{\rho_1^{\rm T}/\lambda_2}(X_2)s_{\gamma_1/\lambda_1}(Y_1)s_{\gamma_1^{\rm T}/\rho_2^{\rm T}}(Y_2)s_{\gamma_2/\lambda_2}(Z_1)s_{\gamma_2^{\rm T}/\rho_2}(Z_2). \tag{C.50}$$

Next, applying the formula (A.36),

$$\widetilde{\check{\mathsf{Z}}}^{\nu_1}_{\mu_1}=\prod_{i,j=1}^{\infty}(1-Q_1X_{1,i}X_{2,j})(1+Y_{1,i}Y_{2,j})(1+Z_{1,i}Z_{2,j})$$
$$\times\sum_{\rho_1,\rho_2,\gamma_1,\gamma_2,\lambda_1,\lambda_2}(-Q_1)^{|\lambda_1|}(-Q_2)^{|\rho_2|}$$
$$\times s_{\lambda_2^{\rm T}/\rho_1}(-Q_1X_1)s_{\lambda_1^{\rm T}/\rho_1^{\rm T}}(X_2)s_{\rho_2/\gamma_1}(Y_1)s_{\lambda_1^{\rm T}/\gamma_1^{\rm T}}(Y_2)s_{\rho_2^{\rm T}/\gamma_2}(Z_1)s_{\lambda_2^{\rm T}/\gamma_2^{\rm T}}(Z_2).$$

Then, again using (A.34) to the skew Schur functions whose Young diagrams have the same number,

$$\begin{aligned}\widetilde{\widetilde{\mathsf{Z}}}^{\nu_1}_{\mu_1} &= \prod_{i,j=1}^{\infty}(1-Q_1X_{1,i}X_{2,j})(1+Y_{1,i}Y_{2,j})(1+Z_{1,i}Z_{2,j})\\ &\times\sum_{\rho_1,\rho_2,\gamma_1,\gamma_2,\lambda_1,\lambda_2}(-Q_1)^{|\gamma_1|}(-Q_2)^{|\gamma_2|}\\ &\times s_{\lambda_2^{\mathrm{T}}/\rho_1}(-Q_1X_1)s_{\lambda_1^{\mathrm{T}}/\rho_1^{\mathrm{T}}}(X_2)s_{\rho_2/\gamma_1}(Y_1)s_{\lambda_1^{\mathrm{T}}/\gamma_1^{\mathrm{T}}}(-Q_1Y_2)s_{\rho_2^{\mathrm{T}}/\gamma_2}(-Q_2Z_1)s_{\lambda_2^{\mathrm{T}}/\gamma_2^{\mathrm{T}}}(Z_2).\end{aligned}$$

We can now employ the formula (A.35) in addition to (A.36),

$$\begin{aligned}\widetilde{\widetilde{\mathsf{Z}}}^{\nu_1}_{\mu_1} &= \prod_{i,j=1}^{\infty}(1-Q_1X_{1,i}X_{2,j})(1+Y_{1,i}Y_{2,j})(1+Z_{1,i}Z_{2,j})\frac{(1-Q_2Y_{1,i}Z_{1,j})}{(1+Q_1X_{1,i}Z_{2,j})(1+Q_1X_{2,i}Y_{2,j})}\\ &\times\sum_{\rho_1,\rho_2,\gamma_1,\gamma_2,\lambda_1,\lambda_2}(-Q_1)^{|\gamma_1|}(-Q_2)^{|\gamma_2|}\\ &\times s_{\gamma_2^{\mathrm{T}}/\lambda_2^{\mathrm{T}}}(-Q_1X_1)s_{\gamma_1^{\mathrm{T}}/\lambda_1^{\mathrm{T}}}(X_2)s_{\gamma_2^{\mathrm{T}}/\rho_2}(Y_1)s_{\rho_1^{\mathrm{T}}/\lambda_1^{\mathrm{T}}}(-Q_1Y_2)s_{\gamma_1^{\mathrm{T}}/\rho_2^{\mathrm{T}}}(-Q_2Z_1)s_{\rho_1/\lambda_2^{\mathrm{T}}}(Z_2).\end{aligned}$$

Further, applying (A.34)-(A.36) leads to

$$\begin{aligned}\widetilde{\widetilde{\mathsf{Z}}}^{\nu_1}_{\mu_1} &= \prod_{i,j=1}^{\infty}\frac{(1-Q_1X_{1,i}X_{2,j})(1+Y_{1,i}Y_{2,j})(1+Z_{1,i}Z_{2,j})(1-Q_2Y_{1,i}Z_{1,j})}{(1+Q_1X_{1,i}Z_{2,j})(1+Q_1X_{2,i}Y_{2,j})}\frac{(1-Q_1Y_{2,i}Z_{2,j})}{(1-Q_\tau X_{1,i}Y_{1,j})(1-Q_\tau X_{2,i}Z_{1,j})}\\ &\times\sum_{\rho_1,\rho_2,\gamma_1,\gamma_2,\lambda_1,\lambda_2}(-Q_1)^{|\lambda_1|}(-Q_2)^{|\lambda_2|}\\ &\times s_{\rho_2/\gamma_2^{\mathrm{T}}}(Q_\tau X_1)s_{\rho_2^{\mathrm{T}}/\gamma_1^{\mathrm{T}}}(-Q_1X_2)s_{\lambda_2^{\mathrm{T}}/\gamma_2^{\mathrm{T}}}(Y_1)s_{\lambda_2/\rho_1^{\mathrm{T}}}(-Q_1Y_2)s_{\lambda_1^{\mathrm{T}}/\gamma_1^{\mathrm{T}}}(-Q_2Z_1)s_{\lambda_1/\rho_1}(Z_2),\end{aligned}$$

and this settles down by using (A.34) once more,

$$\begin{aligned}\widetilde{\widetilde{\mathsf{Z}}}^{\nu_1}_{\mu_1} &= \prod_{i,j=1}^{\infty}\frac{(1-Q_1X_{1,i}X_{2,j})(1+Y_{1,i}Y_{2,j})(1+Z_{1,i}Z_{2,j})(1-Q_2Y_{1,i}Z_{1,j})(1-Q_1Y_{2,i}Z_{2,j})}{(1+Q_1X_{1,i}Z_{2,j})(1+Q_1X_{2,i}Y_{2,j})(1-Q_\tau X_{1,i}Y_{1,j})(1-Q_\tau X_{2,i}Z_{1,j})}\\ &\times\sum_{\rho_1,\rho_2,\gamma_1,\gamma_2,\lambda_1,\lambda_2}(-Q_1)^{|\rho_1|}(-Q_2)^{|\gamma_2|}\\ &\times s_{\rho_2/\gamma_2^{\mathrm{T}}}(Q_\tau X_1)s_{\rho_2^{\mathrm{T}}/\gamma_1^{\mathrm{T}}}(-Q_1X_2)s_{\lambda_2^{\mathrm{T}}/\gamma_2^{\mathrm{T}}}(-Q_2Y_1)s_{\lambda_2/\rho_1^{\mathrm{T}}}(-Q_1Y_2)s_{\lambda_1^{\mathrm{T}}/\gamma_1^{\mathrm{T}}}(-Q_2Z_1)s_{\lambda_1/\rho_1}(-Q_1Z_2).\end{aligned}\tag{C.51}$$

This looks like the form of (C.50) but not identical, and we repeat the sequence from (C.50) to (C.51) once again. The result is given by

$$\begin{aligned}\widetilde{\check{\mathsf{Z}}}^{\nu_1}_{\mu_1} &= \prod_{i,j=1}^{\infty} \frac{(1-Q_1X_{1,i}X_{2,j})\,(1-Q_1Q_\tau X_{1,i}X_{2,j})}{(1+Q_1X_{1,i}Z_{2,j})\,(1+Q_1Q_\tau X_{1,i}Z_{2,j})} \frac{(1+Y_{1,i}Y_{2,j})\,(1+Q_\tau Y_{1,i}Y_{2,j})}{(1+Q_1X_{2,i}Y_{2,j})\,(1+Q_1Q_\tau X_{2,i}Y_{2,j})} \\ &\times \frac{(1-Q_2Y_{1,i}Z_{1,j})\,(1-Q_2Q_\tau Y_{1,i}Z_{1,j})}{(1-Q_\tau X_{1,i}Y_{1,j})\,(1-Q_\tau^2X_{1,i}Y_{1,i})} \frac{(1+Z_{1,i}Z_{2,j})\,(1+Q_\tau Z_{1,i}Z_{2,j})}{(1-Q_\tau X_{2,i}Z_{1,j})\,(1-Q_\tau^2X_{2,i}Z_{1,j})} \\ &\times (1-Q_1Y_{2,i}Z_{2,j})\,(1-Q_1Q_\tau Y_{2,i}Z_{2,j}) \sum_{\rho_1,\rho_2,\gamma_1,\gamma_2,\lambda_1,\lambda_2} (-Q_1)^{|\rho_1|}(-Q_2)^{|\rho_2|} \\ &\times s_{\rho_1/\lambda_1}(Q_\tau X_1)s_{\rho_1^{\mathrm{T}}/\lambda_2}(Q_\tau X_2)s_{\gamma_1/\lambda_1}(Q_\tau Y_1)s_{\gamma_1^{\mathrm{T}}/\rho_2^{\mathrm{T}}}(Q_\tau Y_2)s_{\gamma_2/\lambda_2}(Q_\tau Z_1)s_{\gamma_2^{\mathrm{T}}/\rho_2}(Q_\tau Z_2).\end{aligned} \tag{C.52}$$

We get to the same alignment of the skew Schur functions as in (6.6) except a factor Q_τ in the arguments. Iterating this sequence infinite times produces the following infinite products:

$$\begin{aligned}\widetilde{\check{\mathsf{Z}}}^{\nu_1}_{\mu_1} &= \prod_{n=1}^{\infty} \frac{1}{1-Q_\tau^n} \prod_{i,j,k=1}^{\infty} \frac{\left(1-Q_1Q_\tau^{k-1}X_{1,i}X_{2,j}\right)}{\left(1+Q_1Q_\tau^{k-1}X_{1,i}Z_{2,j}\right)} \frac{\left(1+Q_\tau^{k-1}Y_{1,i}Y_{2,j}\right)}{\left(1+Q_1Q_\tau^{k-1}X_{2,i}Y_{2,j}\right)} \\ &\times \frac{\left(1-Q_2Q_\tau^{k-1}Y_{1,i}Z_{1,j}\right)}{(1-Q_\tau^kX_{1,i}Y_{1,j})} \frac{\left(1-Q_1Q_\tau^{k-1}Y_{2,i}Z_{2,j}\right)}{(1-Q_\tau^kX_{2,i}Z_{1,j})} \left(1+Q_\tau^{k-1}Z_{1,i}Z_{2,j}\right),\end{aligned} \tag{C.53}$$

where we again employ the fact

$$\lim_{k\to\infty} \mathsf{Z}^{\nu_1}_{\mu_1^{\mathrm{T}}}(Q_\tau^kX_i, Q_\tau^kY_i, Q_\tau^kZ_i) = \prod_{n=1}^{\infty} \frac{1}{1-Q_\tau^n} \quad \text{for } |Q_\tau|<1. \tag{C.54}$$

Here, replacing the parameters with the original variables as

$$\begin{aligned} &X_1 = q^{-\mu_1^{\mathrm{T}}-\mathfrak{n}}, && Y_1 = q^{-\mu_1-\mathfrak{n}}, && Z_1 = q^{-\nu_1^{\mathrm{T}}-\mathfrak{n}}, \\ &X_2 = q^{-\nu_1-\mathfrak{n}}, && Y_2 = -Q_{\mathrm{L}}x, && Z_2 = -Q_2Q_{\mathrm{L}}^{-1}x^{-1}, \end{aligned} \tag{C.55}$$

brings $\widetilde{\check{\mathsf{Z}}}^{\nu_1}_{\mu_1}$ back to $\check{\mathsf{Z}}^{\nu_1}_{\mu_1^{\mathrm{T}}}$,

$$\begin{aligned}\check{\mathsf{Z}}^{\nu_1}_{\mu_1^{\mathrm{T}}} &= \prod_{n=1}^{\infty} \frac{1}{1-Q_\tau^n} \prod_{i,j,k=1}^{\infty} \frac{\left(1-Q_\tau^{k-1}Q_1q^{-\mu_{1,j}^{\mathrm{T}}+j-\nu_{1,i}+i-1}\right)\left(1-Q_\tau^{k-1}Q_2q^{-\nu_{1,j}^{\mathrm{T}}+j-\mu_{1,i}+i-1}\right)}{\left(1-Q_\tau^kq^{-\mu_{1,j}^{\mathrm{T}}+j-\mu_{1,i}+i-1}\right)\left(1-Q_\tau^kq^{-\nu_{1,j}^{\mathrm{T}}+j-\nu_{1,i}+i-1}\right)} \\ &\times \frac{\left(1-Q_\tau^{k-1}Q_{\mathrm{L}}q^{-\mu_{1,i}+i-\frac{1}{2}}x_j\right)\left(1-Q_\tau^kQ_1^{-1}Q_{\mathrm{L}}^{-1}q^{-\nu_{1,j}^{\mathrm{T}}+j-\frac{1}{2}}x_i^{-1}\right)}{\left(1-Q_\tau^{k-1}Q_1Q_{\mathrm{L}}q^{-\nu_{1,i}+i-\frac{1}{2}}x_j\right)\left(1-Q_\tau^kQ_{\mathrm{L}}^{-1}q^{-\mu_{1,j}^{\mathrm{T}}+j-\frac{1}{2}}x_i^{-1}\right)} \left(1-Q_\tau^kx_ix_j^{-1}\right).\end{aligned} \tag{C.56}$$

As a result, we can obtain the domain wall partition function with a Lagrangian brane using the open topological vertex,

$$
\begin{aligned}
Z^{\nu_1}_{\mu_1}(Q_i, Q_{\rm L}; q) = q^{\frac{1}{2}(\kappa_{\mu_1^{\rm T}}+\kappa_{\nu_1})} s_{\mu_1^{\rm T}}(q^{-\mathfrak{n}}) s_{\nu_1}(q^{-\mathfrak{n}}) \prod_{n=1}^{\infty} \frac{1}{1-Q_\tau^n} \\
\times \prod_{i,j,k=1}^{\infty} \frac{\left(1-Q_\tau^{k-1} Q_1 q^{-\mu^{\rm T}_{1,j}+j-\nu_{1,i}+i-1}\right)\left(1-Q_\tau^{k-1} Q_2 q^{-\nu^{\rm T}_{1,j}+j-\mu_{1,i}+i-1}\right)}{\left(1-Q_\tau^{k} q^{-\mu^{\rm T}_{1,j}+j-\mu_{1,i}+i-1}\right)\left(1-Q_\tau^{k} q^{-\nu^{\rm T}_{1,j}+j-\nu_{1,i}+i-1}\right)} \\
\times \frac{\left(1-Q_\tau^{k-1} Q_{\rm L} q^{-\mu_{1,i}+i-\frac{1}{2}} x_j\right)\left(1-Q_\tau^{k} Q_1^{-1} Q_{\rm L}^{-1} q^{-\nu^{\rm T}_{1,j}+j-\frac{1}{2}} x_i^{-1}\right)}{\left(1-Q_\tau^{k-1} Q_1 Q_{\rm L} q^{-\nu_{1,i}+i-\frac{1}{2}} x_j\right)\left(1-Q_\tau^{k} Q_{\rm L}^{-1} q^{-\mu^{\rm T}_{1,j}+j-\frac{1}{2}} x_i^{-1}\right)} \left(1-Q_\tau^k x_i x_j^{-1}\right).
\end{aligned}
\tag{C.57}
$$

References

[1] W. Nahm, "Supersymmetries and their Representations," *Nucl.Phys.* **B135** (1978) 149.

[2] S. Gukov and E. Witten, "Gauge Theory, Ramification, And The Geometric Langlands Program," arXiv:hep-th/0612073 [hep-th].

[3] S. Gukov and E. Witten, "Rigid Surface Operators," *Adv. Theor. Math. Phys.* **14** no. 1, (2010) 87–178, arXiv:0804.1561 [hep-th].

[4] J. M. Maldacena, "The Large N limit of superconformal field theories and supergravity," *Adv.Theor.Math.Phys.* **2** (1998) 231–252, arXiv:hep-th/9711200 [hep-th].

[5] J. Gomis and S. Matsuura, "Bubbling surface operators and S-duality," *JHEP* **06** (2007) 025, arXiv:0704.1657 [hep-th].

[6] N. Drukker, J. Gomis, and S. Matsuura, "Probing N=4 SYM With Surface Operators," *JHEP* **10** (2008) 048, arXiv:0805.4199 [hep-th].

[7] E. Koh and S. Yamaguchi, "Holography of BPS surface operators," *JHEP* **02** (2009) 012, arXiv:0812.1420 [hep-th].

[8] E. Koh and S. Yamaguchi, "Surface operators in the Klebanov-Witten theory," *JHEP* **06** (2009) 070, arXiv:0904.1460 [hep-th].

[9] L. F. Alday, D. Gaiotto, and Y. Tachikawa, "Liouville Correlation Functions from Four-dimensional Gauge Theories," *Lett. Math. Phys.* **91** (2010) 167–197, arXiv:0906.3219 [hep-th].

[10] L. F. Alday, D. Gaiotto, S. Gukov, Y. Tachikawa, and H. Verlinde, "Loop and surface operators in N=2 gauge theory and Liouville modular geometry," *JHEP* **01** (2010) 113, arXiv:0909.0945 [hep-th].

[11] M. Shifman and A. Yung, "NonAbelian string junctions as confined monopoles," *Phys. Rev.* **D70** (2004) 045004, arXiv:hep-th/0403149 [hep-th].

[12] A. Hanany and D. Tong, "Vortex strings and four-dimensional gauge dynamics," *JHEP* **0404** (2004) 066, arXiv:hep-th/0403158 [hep-th].

[13] D. Gaiotto, G. W. Moore, and A. Neitzke, "Wall-Crossing in Coupled 2d-4d Systems," *JHEP* **12** (2012) 082, arXiv:1103.2598 [hep-th].

[14] D. Gaiotto, G. W. Moore, and A. Neitzke, "Spectral networks," *Annales Henri Poincare* **14** (2013) 1643–1731, arXiv:1204.4824 [hep-th].

[15] D. Gaiotto, L. Rastelli, and S. S. Razamat, "Bootstrapping the superconformal index with surface defects," *JHEP* **1301** (2013) 022, arXiv:1207.3577 [hep-th].

[16] V. Pestun, "Localization of gauge theory on a four-sphere and supersymmetric Wilson loops," *Commun.Math.Phys.* **313** (2012) 71–129, arXiv:0712.2824 [hep-th].

[17] A. Kapustin, B. Willett, and I. Yaakov, "Exact Results for Wilson Loops in Superconformal Chern-Simons Theories with Matter," *JHEP* **1003** (2010) 089, arXiv:0909.4559 [hep-th].

[18] N. Hama, K. Hosomichi, and S. Lee, "SUSY Gauge Theories on Squashed Three-Spheres," *JHEP* **1105** (2011) 014, arXiv:1102.4716 [hep-th].

[19] S. Gukov, "Surface Operators," arXiv:1412.7127 [hep-th].

[20] C. Hull and P. Townsend, "Unity of superstring dualities," *Nucl.Phys.* **B438** (1995) 109–137, arXiv:hep-th/9410167 [hep-th].

[21] E. Witten, "String theory dynamics in various dimensions," *Nucl.Phys.* **B443** (1995) 85–126, arXiv:hep-th/9503124 [hep-th].

[22] O. Aharony, O. Bergman, D. L. Jafferis, and J. Maldacena, "N=6 superconformal Chern-Simons-matter theories, M2-branes and their gravity duals," *JHEP* **10** (2008) 091, arXiv:0806.1218 [hep-th].

[23] A. Strominger, "Open p-branes," *Phys.Lett.* **B383** (1996) 44–47, arXiv:hep-th/9512059 [hep-th].

[24] E. Witten, "Some comments on string dynamics," arXiv:hep-th/9507121 [hep-th].

[25] O. J. Ganor, "Six-dimensional tensionless strings in the large N limit," *Nucl.Phys.* **B489** (1997) 95–121, arXiv:hep-th/9605201 [hep-th].

[26] P. Pasti, D. P. Sorokin, and M. Tonin, "Covariant action for a D = 11 five-brane with the chiral field," *Phys.Lett.* **B398** (1997) 41–46, arXiv:hep-th/9701037 [hep-th].

[27] I. A. Bandos, K. Lechner, A. Nurmagambetov, P. Pasti, D. P. Sorokin, and M. Tonin, "Covariant action for the superfive-brane of M theory," *Phys.Rev.Lett.* **78** (1997) 4332–4334, arXiv:hep-th/9701149 [hep-th].

[28] I. A. Bandos, K. Lechner, A. Nurmagambetov, P. Pasti, D. P. Sorokin, and M. Tonin, "On the equivalence of different formulations of the M theory five-brane," *Phys.Lett.* **B408** (1997) 135–141, arXiv:hep-th/9703127 [hep-th].

[29] I. Bandos, "On Lagrangian approach to self-dual gauge fields in spacetime of nontrivial topology," *JHEP* **08** (2014) 048, arXiv:1406.5185 [hep-th].

[30] H. Isono, "Note on the self-duality of gauge fields in topologically nontrivial spacetime," *PTEP* **2014** no. 9, (2014) 093B05, arXiv:1406.6023 [hep-th].

[31] D. Bak and A. Gustavsson, "Witten indices of abelian M5 brane on $\mathbb{R} \times S^5$," arXiv:1610.06255 [hep-th].

[32] B. Haghighat, A. Iqbal, C. Kozçaz, G. Lockhart, and C. Vafa, "M-Strings," *Commun. Math. Phys.* **334** no. 2, (2015) 779–842, arXiv:1305.6322 [hep-th].

[33] B. Haghighat, C. Kozcaz, G. Lockhart, and C. Vafa, "On orbifolds of M-strings," *Phys. Rev.* **D89** no. 4, (2014) 046003, arXiv:1310.1185 [hep-th].

[34] M. Aganagic, A. Klemm, M. Marino, and C. Vafa, "The Topological vertex," *Commun. Math. Phys.* **254** (2005) 425–478, arXiv:hep-th/0305132 [hep-th].

[35] H. Awata and H. Kanno, "Instanton counting, Macdonald functions and the moduli space of D-branes," *JHEP* **05** (2005) 039, arXiv:hep-th/0502061 [hep-th].

[36] A. Iqbal, C. Kozcaz, and C. Vafa, "The Refined topological vertex," *JHEP* **10** (2009) 069, arXiv:hep-th/0701156 [hep-th].

[37] E. Witten, "Elliptic Genera and Quantum Field Theory," *Commun. Math. Phys.* **109** (1987) 525.

[38] F. Benini, R. Eager, K. Hori, and Y. Tachikawa, "Elliptic genera of two-dimensional N=2 gauge theories with rank-one gauge groups," *Lett. Math. Phys.* **104** (2014) 465–493, arXiv:1305.0533 [hep-th].

[39] F. Benini, R. Eager, K. Hori, and Y. Tachikawa, "Elliptic Genera of 2d $\mathcal{N} = 2$ Gauge Theories," *Commun.Math.Phys.* **333** no. 3, (2015) 1241–1286, arXiv:1308.4896 [hep-th].

[40] E. Witten, "Topological sigma models," *Communications in Mathematical Physics* **118** no. 3, (1988) 411–449.

[41] D. E. Berenstein, R. Corrado, W. Fischler, and J. M. Maldacena, "The Operator product expansion for Wilson loops and surfaces in the large N limit," *Phys. Rev.* **D59** (1999) 105023, arXiv:hep-th/9809188 [hep-th].

[42] H. Lin, O. Lunin, and J. M. Maldacena, "Bubbling AdS space and 1/2 BPS geometries," *JHEP* **10** (2004) 025, arXiv:hep-th/0409174 [hep-th].

[43] O. Lunin, "1/2-BPS states in M theory and defects in the dual CFTs," *JHEP* **10** (2007) 014, arXiv:0704.3442 [hep-th].

[44] B. Chen, W. He, J.-B. Wu, and L. Zhang, "M5-branes and Wilson Surfaces," *JHEP* **08** (2007) 067, arXiv:0707.3978 [hep-th].

[45] B. Chen, C.-Y. Liu, and J.-B. Wu, "Operator Product Expansion of Wilson surfaces from M5-branes," *JHEP* **01** (2008) 007, arXiv:0711.2194 [hep-th].

[46] B. Chen and J.-B. Wu, "Wilson-Polyakov surfaces and M-theory branes," *JHEP* **05** (2008) 046, arXiv:0802.2173 [hep-th].

[47] E. D'Hoker, J. Estes, M. Gutperle, and D. Krym, "Exact Half-BPS Flux Solutions in M-theory. I: Local Solutions," *JHEP* **08** (2008) 028, arXiv:0806.0605 [hep-th].

[48] E. D'Hoker, J. Estes, M. Gutperle, and D. Krym, "Exact Half-BPS Flux Solutions in M-theory II: Global solutions asymptotic to AdS(7) x S**4," *JHEP* **12** (2008) 044, arXiv:0810.4647 [hep-th].

[49] D. Young, "Wilson Loops in Five-Dimensional Super-Yang-Mills," *JHEP* **02** (2012) 052, arXiv:1112.3309 [hep-th].

[50] H. Mori and S. Yamaguchi, "M5-branes and Wilson surfaces in AdS_7/CFT_6 correspondence," *Phys. Rev.* **D90** no. 2, (2014) 026005, arXiv:1404.0930 [hep-th].

[51] H. Kanno and Y. Tachikawa, "Instanton counting with a surface operator and the chain-saw quiver," *JHEP* **06** (2011) 119, arXiv:1105.0357 [hep-th].

[52] D. Gaiotto, "Surface Operators in N = 2 4d Gauge Theories," *JHEP* **11** (2012) 090, arXiv:0911.1316 [hep-th].

[53] A. Hanany and D. Tong, "Vortices, instantons and branes," *JHEP* **07** (2003) 037, arXiv:hep-th/0306150 [hep-th].

[54] A. Gadde and S. Gukov, "2d Index and Surface operators," *JHEP* **1403** (2014) 080, arXiv:1305.0266 [hep-th].

[55] M. Bullimore, M. Fluder, L. Hollands, and P. Richmond, "The superconformal index and an elliptic algebra of surface defects," *JHEP* **1410** (2014) 62, arXiv:1401.3379 [hep-th].

[56] D. Gaiotto and S. S. Razamat, "$\mathcal{N} = 1$ theories of class $\mathcal{S}_k$," *JHEP* **07** (2015) 073, arXiv:1503.05159 [hep-th].

[57] H.-Y. Chen and H.-Y. Chen, "Heterotic Surface Defects and Dualities from 2d/4d Indices," *JHEP* **10** (2014) 004, arXiv:1407.4587 [hep-th].

[58] K. Maruyoshi and J. Yagi, "Surface defects as transfer matrices," arXiv:1606.01041 [hep-th].

[59] Y. Ito and Y. Yoshida, "Superconformal index with surface defects for class $\mathcal{S}_k$," arXiv:1606.01653 [hep-th].

[60] J. Gomis and B. Le Floch, "M2-brane surface operators and gauge theory dualities in Toda," arXiv:1407.1852 [hep-th].

[61] P. Candelas and X. C. de la Ossa, "Comments on Conifolds," *Nucl. Phys.* **B342** (1990) 246–268.

[62] R. Gopakumar and C. Vafa, "M theory and topological strings. 1.," arXiv:hep-th/9809187 [hep-th].

[63] R. Gopakumar and C. Vafa, "On the gauge theory / geometry correspondence," *Adv. Theor. Math. Phys.* **3** (1999) 1415–1443, arXiv:hep-th/9811131 [hep-th].

[64] R. Gopakumar and C. Vafa, "M theory and topological strings. 2.," arXiv:hep-th/9812127 [hep-th].

[65] E. Witten, "Chern-Simons gauge theory as a string theory," *Prog. Math.* **133** (1995) 637–678, arXiv:hep-th/9207094 [hep-th].

[66] C. Vafa, "Superstrings and topological strings at large N," *J. Math. Phys.* **42** (2001) 2798–2817, arXiv:hep-th/0008142 [hep-th].

[67] H. Ooguri and C. Vafa, "World sheet derivation of a large N duality," *Nucl. Phys.* **B641** (2002) 3–34, arXiv:hep-th/0205297 [hep-th].

[68] C. Kozcaz, S. Pasquetti, and N. Wyllard, "A & B model approaches to surface operators and Toda theories," *JHEP* **08** (2010) 042, arXiv:1004.2025 [hep-th].

[69] T. Dimofte, S. Gukov, and L. Hollands, "Vortex Counting and Lagrangian 3-manifolds," *Lett. Math. Phys.* **98** (2011) 225–287, arXiv:1006.0977 [hep-th].

[70] P. Candelas, X. C. De La Ossa, P. S. Green, and L. Parkes, "A Pair of Calabi-Yau manifolds as an exactly soluble superconformal theory," *Nucl. Phys.* **B359** (1991) 21–74.

[71] K. Hori and C. Vafa, "Mirror symmetry," arXiv:hep-th/0002222 [hep-th].

[72] E. Witten, "Solutions of four-dimensional field theories via M theory," *Nucl.Phys.* **B500** (1997) 3–42, arXiv:hep-th/9703166 [hep-th].

[73] N. Nekrasov and A. Okounkov, "Seiberg-Witten theory and random partitions," arXiv:hep-th/0306238 [hep-th].

[74] D. Gaiotto, "N=2 dualities," *JHEP* **08** (2012) 034, arXiv:0904.2715 [hep-th].

[75] J. J. Duistermaat and G. J. Heckman, "On the variation in the cohomology of the symplectic form of the reduced phase space," *Inventiones mathematicae* **69** no. 2, (1982) 259–268.

[76] M. Atiyah and R. Bott, "The moment map and equivariant cohomology," *Topology* **23** no. 1, (1984) 1 – 28.

[77] N. A. Nekrasov, "Seiberg-Witten prepotential from instanton counting," *Adv. Theor. Math. Phys.* **7** (2004) 831–864, arXiv:hep-th/0206161 [hep-th].

[78] H. Awata and Y. Yamada, "Five-dimensional AGT Conjecture and the Deformed Virasoro Algebra," *JHEP* **01** (2010) 125, arXiv:0910.4431 [hep-th].

[79] H. Awata and Y. Yamada, "Five-dimensional AGT Relation and the Deformed beta-ensemble," *Prog. Theor. Phys.* **124** (2010) 227–262, arXiv:1004.5122 [hep-th].

[80] A. Iqbal, C. Kozcaz, and S.-T. Yau, "Elliptic Virasoro Conformal Blocks," arXiv:1511.00458 [hep-th].

[81] F. Nieri, "An elliptic Virasoro symmetry in 6d," arXiv:1511.00574 [hep-th].

[82] M. Taki, "Surface Operator, Bubbling Calabi-Yau and AGT Relation," *JHEP* **07** (2011) 047, arXiv:1007.2524 [hep-th].

[83] H. Awata, H. Fuji, H. Kanno, M. Manabe, and Y. Yamada, "Localization with a Surface Operator, Irregular Conformal Blocks and Open Topological String," *Adv. Theor. Math. Phys.* **16** no. 3, (2012) 725–804, arXiv:1008.0574 [hep-th].

[84] G. Bonelli, A. Tanzini, and J. Zhao, "Vertices, Vortices and Interacting Surface Operators," *JHEP* **06** (2012) 178, arXiv:1102.0184 [hep-th].

[85] J. Gomis, D. Rodriguez-Gomez, M. Van Raamsdonk, and H. Verlinde, "A Massive Study of M2-brane Proposals," *JHEP* **09** (2008) 113, arXiv:0807.1074 [hep-th].

[86] D. S. Berman, M. J. Perry, E. Sezgin, and D. C. Thompson, "Boundary Conditions for Interacting Membranes," *JHEP* **04** (2010) 025, arXiv:0912.3504 [hep-th].

[87] H.-C. Kim and S. Kim, "Supersymmetric vacua of mass-deformed M2-brane theory," *Nucl. Phys.* **B839** (2010) 96–111, arXiv:1001.3153 [hep-th].

[88] S. Hohenegger and A. Iqbal, "M-strings, elliptic genera and $\mathcal{N} = 4$ string amplitudes," *Fortsch. Phys.* **62** (2014) 155–206, arXiv:1310.1325 [hep-th].

[89] O. Aharony, A. Hanany, and B. Kol, "Webs of (p,q) five-branes, five-dimensional field theories and grid diagrams," *JHEP* **01** (1998) 002, arXiv:hep-th/9710116 [hep-th].

[90] N. C. Leung and C. Vafa, "Branes and toric geometry," *Adv. Theor. Math. Phys.* **2** (1998) 91–118, arXiv:hep-th/9711013 [hep-th].

[91] T. J. Hollowood, A. Iqbal, and C. Vafa, "Matrix models, geometric engineering and elliptic genera," *JHEP* **03** (2008) 069, arXiv:hep-th/0310272 [hep-th].

[92] J. Gomis and T. Okuda, "Wilson loops, geometric transitions and bubbling Calabi-Yau's," *JHEP* **02** (2007) 083, arXiv:hep-th/0612190 [hep-th].

[93] J. Gomis and T. Okuda, "D-branes as a Bubbling Calabi-Yau," *JHEP* **07** (2007) 005, arXiv:0704.3080 [hep-th].

[94] E. Witten, "Phases of N=2 theories in two-dimensions," *Nucl. Phys.* **B403** (1993) 159–222, arXiv:hep-th/9301042 [hep-th].

[95] M. Edalati and D. Tong, "Heterotic Vortex Strings," *JHEP* **05** (2007) 005, arXiv:hep-th/0703045 [HEP-TH].

[96] A. Gadde, S. Gukov, and P. Putrov, "(0, 2) trialities," *JHEP* **03** (2014) 076, arXiv:1310.0818 [hep-th].

[97] D. Tong, "The holographic dual of $AdS_3 \times S^3 \times S^3 \times S^1$," *JHEP* **04** (2014) 193, arXiv:1402.5135 [hep-th].

[98] P. Putrov, J. Song, and W. Yan, "(0,4) dualities," *JHEP* **03** (2016) 185, arXiv:1505.07110 [hep-th].

[99] K. Hosomichi and S. Lee, "Self-dual Strings and 2D SYM," *JHEP* **01** (2015) 076, arXiv:1406.1802 [hep-th].

[100] F. Benini and S. Cremonesi, "Partition functions of N=(2,2) gauge theories on S^2 and vortices," arXiv:1206.2356 [hep-th].

[101] N. Doroud, J. Gomis, B. Le Floch, and S. Lee, "Exact Results in D=2 Supersymmetric Gauge Theories," *JHEP* **1305** (2013) 093, arXiv:1206.2606 [hep-th].

[102] H.-Y. Chen, H.-Y. Chen, and J.-K. Ho, "Connecting Mirror Symmetry in 3d and 2d via Localization," *Int. J. Mod. Phys.* **A29** no. 32, (2014) 1530004, arXiv:1312.2361 [hep-th].

[103] M. Fujitsuka, M. Honda, and Y. Yoshida, "Higgs branch localization of 3d $\mathcal{N} = 2$ theories," *PTEP* **2014** no. 12, (2014) 123B02, arXiv:1312.3627 [hep-th].

[104] F. Benini and W. Peelaers, "Higgs branch localization in three dimensions," *JHEP* **05** (2014) 030, arXiv:1312.6078 [hep-th].

[105] Y. Yoshida, "Factorization of 4d N=1 superconformal index," arXiv:1403.0891 [hep-th].

[106] W. Peelaers, "Higgs branch localization of $\mathcal{N} = 1$ theories on S^3 x S^1," *JHEP* **08** (2014) 060, arXiv:1403.2711 [hep-th].

[107] Y. Pan, "5d Higgs Branch Localization, Seiberg-Witten Equations and Contact Geometry," *JHEP* **01** (2015) 145, arXiv:1406.5236 [hep-th].

[108] H.-Y. Chen and T.-H. Tsai, "On Higgs branch localization of Seiberg-Witten theories on an ellipsoid," *PTEP* **2016** no. 1, (2016) 013B09, arXiv:1506.04390 [hep-th].

[109] Y. Pan and W. Peelaers, "Ellipsoid partition function from Seiberg-Witten monopoles," *JHEP* **10** (2015) 183, arXiv:1508.07329 [hep-th].

[110] M. R. Douglas and G. W. Moore, "D-branes, quivers, and ALE instantons," arXiv:hep-th/9603167 [hep-th].

[111] M. R. Douglas, "Gauge fields and D-branes," *J. Geom. Phys.* **28** (1998) 255–262, arXiv:hep-th/9604198 [hep-th].

[112] K. Okuyama, "D1-D5 on ALE space," *JHEP* **12** (2005) 042, arXiv:hep-th/0510195 [hep-th].

[113] H. Mori and Y. Sugimoto, "Surface Operators from M-strings," arXiv:1608.02849 [hep-th].

[114] A. Iqbal and A.-K. Kashani-Poor, "The Vertex on a strip," *Adv. Theor. Math. Phys.* **10** no. 3, (2006) 317–343, arXiv:hep-th/0410174 [hep-th].

[115] Y. Konishi and S. Minabe, "Flop invariance of the topological vertex," *Int. J. Math.* **19** (2008) 27–45, arXiv:math/0601352 [math-ag].

[116] M. Taki, "Flop Invariance of Refined Topological Vertex and Link Homologies," arXiv:0805.0336 [hep-th].

[117] Y. Sugimoto, "The Enhancement of Supersymmetry in M-strings," *Int. J. Mod. Phys.* **A31** no. 16, (2016) 1650088, arXiv:1508.02125 [hep-th].

[118] E. Frenkel, S. Gukov, and J. Teschner, "Surface Operators and Separation of Variables," *JHEP* **01** (2016) 179, arXiv:1506.07508 [hep-th].

[119] E. K. Sklyanin, "Separation of variables in the Gaudin model," *J. Sov. Math.* **47** (1989) 2473–2488.

[120] E. Frenkel, "Affine algebras, Langlands duality and Bethe ansatz," in *Mathematical physics. Proceedings, 11th International Congress, Paris, France, July 18-22, 1994*. 1995. arXiv:q-alg/9506003 [q-alg].

[121] A. V. Stoyanovsky, "A relation between the knizhnik-zamolodchikov and belavin-polyakov-zamolodchikov systems of partial differential equations," arXiv:math-ph/0012013 [math-ph].

[122] D. Gaiotto and H.-C. Kim, "Surface defects and instanton partition functions," *JHEP* **10** (2016) 012, arXiv:1412.2781 [hep-th].

[123] N. Nekrasov, "BPS/CFT correspondence: non-perturbative Dyson-Schwinger equations and qq-characters," *JHEP* **03** (2016) 181, arXiv:1512.05388 [hep-th].

[124] T. Kimura and V. Pestun, "Quiver W-algebras," arXiv:1512.08533 [hep-th].

[125] H.-C. Kim, "Line defects and 5d instanton partition functions," *JHEP* **03** (2016) 199, arXiv:1601.06841 [hep-th].

[126] T. Kimura and V. Pestun, "Quiver elliptic W-algebras," arXiv:1608.04651 [hep-th].

[127] B. Haghighat and W. Yan, "M-strings in thermodynamic limit: Seiberg-Witten geometry," arXiv:1607.07873 [hep-th].

[128] M. Taki, "Refined Topological Vertex and Instanton Counting," *JHEP* **03** (2008) 048, arXiv:0710.1776 [hep-th].

[129] P. Di Francesco, P. Mathieu, and D. Senechal, *Conformal Field Theory*. Graduate Texts in Contemporary Physics. Springer-Verlag, New York, 1997.

[130] I. Macdonald, *Symmetric Functions and Hall Polynomials*. Oxford mathematical monographs. Clarendon Press, 1998.

[131] E. T. Whittaker and G. N. Watson, *A course of modern analysis : an introduction to the general theory of infinite processes and of analytic functions : with an account of the principal transcendental functions*. Cambridge University Press, 4th ed., 1927.

[132] H. Mori and T. Morita, "Summation formulae for the bilateral basic hypergeometric series ${}_1\psi_1(a;b;q,z)$," arXiv:1603.06657 [math.CA].

[133] B. Eynard and N. Orantin, "Invariants of algebraic curves and topological expansion," *Commun. Num. Theor. Phys.* **1** (2007) 347–452, arXiv:math-ph/0702045 [math-ph].

[134] Y. Hatsuda, H. Katsura, and Y. Tachikawa, "Hofstadter ' s butterfly in quantum geometry," *New J. Phys.* **18** no. 10, (2016) 103023, arXiv:1606.01894 [hep-th].

[135] Y. Hatsuda, S. Moriyama, and K. Okuyama, "Instanton Effects in ABJM Theory from Fermi Gas Approach," *JHEP* **01** (2013) 158, arXiv:1211.1251 [hep-th].

[136] Y. Hatsuda, M. Marino, S. Moriyama, and K. Okuyama, "Non-perturbative effects and the refined topological string," *JHEP* **09** (2014) 168, arXiv:1306.1734 [hep-th].

[137] Y. Sugimoto, "Geometric transition in the nonperturbative topological string," *Phys. Rev.* **D94** no. 5, (2016) 055010, arXiv:1607.01534 [hep-th].

[138] A. Iqbal, C. Kozcaz, and K. Shabbir, "Refined Topological Vertex, Cylindric Partitions and the U(1) Adjoint Theory," *Nucl. Phys.* **B838** (2010) 422–457, arXiv:0803.2260 [hep-th].

[139] L. Bao, V. Mitev, E. Pomoni, M. Taki, and F. Yagi, "Non-Lagrangian Theories from Brane Junctions," *JHEP* **01** (2014) 175, arXiv:1310.3841 [hep-th].

[140] H. Hayashi, H.-C. Kim, and T. Nishinaka, "Topological strings and 5d T_N partition functions," *JHEP* **06** (2014) 014, arXiv:1310.3854 [hep-th].

[141] M. Aganagic, A. Klemm, and C. Vafa, "Disk instantons, mirror symmetry and the duality web," *Z. Naturforsch.* **A57** (2002) 1–28, arXiv:hep-th/0105045 [hep-th].

[142] H. Awata and H. Kanno, "Refined BPS state counting from Nekrasov's formula and Macdonald functions," *Int. J. Mod. Phys.* **A24** (2009) 2253–2306, arXiv:0805.0191 [hep-th].

[143] H. Awata, B. Feigin, and J. Shiraishi, "Quantum Algebraic Approach to Refined Topological Vertex," *JHEP* **03** (2012) 041, arXiv:1112.6074 [hep-th].